

DEVELOPMENT OF AN INTEGRATED COMPUTATIONAL TOOL FOR  
DESIGN AND ANALYSIS OF COMPOSITE TURBINE BLADES UNDER OCEAN  
CURRENT LOADING

by

Fang Zhou

A Dissertation Submitted to the Faculty of  
College of Engineering and Computer Science  
in Partial Fulfillment of the Requirements for the Degree of  
Doctor of Philosophy

Florida Atlantic University

Boca Raton, FL

August 2013

Copyright by Fang Zhou 2013

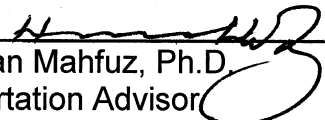
DEVELOPMENT OF AN INTEGRATED COMPUTATIONAL TOOL FOR DESIGN  
AND ANALYSIS OF COMPOSITE TURBINE BLADES UNDER OCEAN  
CURRENT LOADING

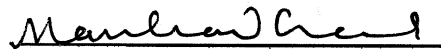
by

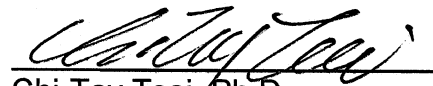
Fang Zhou

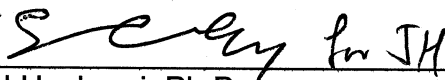
This dissertation was prepared under the direction of the candidate's dissertation advisor, Dr. Hassan Mahfuz, Department of Ocean and Mechanical Engineering, and has been approved by the members of his supervisory committee. It was submitted to the faculty of the College of Engineering and Computer Science and was accepted in partial fulfillment of the requirements for the degree of Doctor of Philosophy.

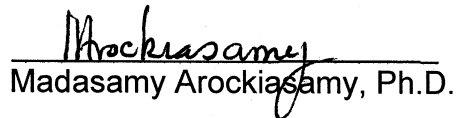
SUPERVISORY COMMITTEE:

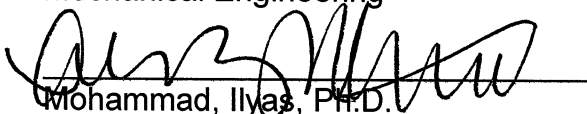
  
Hassan Mahfuz, Ph.D.  
Dissertation Advisor

  
Manhar Dhanak, Ph.D.

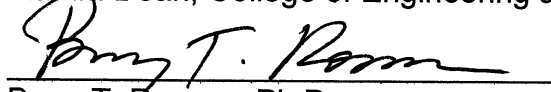
  
Chi-Tay Tsai, Ph.D.

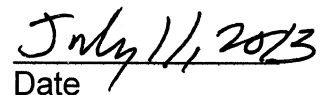
  
Javad Hashemi, Ph.D.  
Chair, Department of Ocean and  
Mechanical Engineering

  
Madasamy Arockiasamy, Ph.D.

  
Mohammad, Ilyas, Ph.D.  
Interim Dean, College of Engineering and Computer Science

  
James H. VanZwieten Jr, Ph.D.

  
Barry T. Rosson, Ph.D.  
Dean, Graduate College

  
Date

## ACKNOWLEDGEMENTS

I would like to express my deepest appreciation and gratitude to my dissertation advisor, Dr. Hassan Mahfuz, for his excellent guidance and support through this dissertation study. Without his help and tireless instruction, this work would not have been possible. I am also sincerely grateful to all of my committee members: Dr. Manhar Dhanak, Dr. Chi-Tay Tsai, Dr. Madasamy Arockiasamy and Dr. James H. VanZwieten Jr. for their help and valuable advices on my research.

I would like to express my sincere thanks to the Southeast National Marine Renewable Energy Center (SNMREC) for supporting this research.

Finally, I am especially to my family especially my lovely wife and daughter. I appreciate their support and encouragement during my pursuit of the Doctorate.

## ABSTRACT

Author: Fang Zhou

Title: Development of an Integrated Computational Tool for Design and Analysis of Composite Turbine Blades under Ocean Current Loading

Institution: Florida Atlantic University

Dissertation Advisor: Dr. Hassan Mahfuz

Degree: Doctor of Philosophy

Year: 2013

A computational tool has been developed by integrating National Renewable Energy Laboratory (NREL) codes, Sandia National Laboratories' NuMAD, and ANSYS to investigate a horizontal axis composite ocean current turbine. The study focused on the design, analysis, and life prediction of composite blade considering random ocean current, cyclic rotation, and hurricane-driven ocean current. A structural model for a horizontal axis FAU research OCT blade was developed. Following NREL codes were used: PreCom, BModes, ModeShape, AeroDyn and FAST. PreComp was used to compute section properties of the OCT blade. BModes and ModeShape calculated the mode shapes of the blade. Hydrodynamic loading on the OCT blade was calculated by modifying the inputs to AeroDyn and FAST. These codes were then used to obtain the dynamic

response of the blade, including blade tip displacement, normal force ( $F_N$ ) and tangential force ( $F_T$ ), flap and edge bending moment distribution with respect to blade rotation. In the next step, a model was developed using NuMAD and it was used as an input file to ANSYS. Loads ( $F_N$ ,  $F_T$ ) applied to ANSYS model to perform the static and buckling analysis. It identified the regions of high stresses in the blade. Fatigue life was then predicted based on the stresses at the critical locations. Bending moment time histories were converted to stress-time histories and Goodman diagram was used to calculate life at various stress levels and ratios. Actual number of cycle was computed from the velocity-time histogram as obtained from experimental data. This allowed calculation of damage, and fatigue life of the blade was predicted using Palmgren-Miner's rule for cumulative fatigue.

The OCT blade, when submerged in sea water, experiences buoyancy forces which is not accounted in NREL codes. A procedure was therefore developed to calculate buoyancy effect and adjusted the gravitational acceleration input "g" to run it on FAST. Since OCT blades rotate under water, inertia due to accelerating fluid was also considered as added mass in this investigation. This was implemented by considering an added mass coefficient. The procedures have enabled accurate determination of blade tip deflections and bending moment histories for fatigue analysis.

DEVELOPMENT OF AN INTEGRATED COMPUTATIONAL TOOL FOR  
DESIGN AND ANALYSIS OF COMPOSITE TURBINE BLADES UNDER OCEAN  
CURRENT LOADING

LIST OF FIGURES .....	x
LIST OF TABLES .....	xv
CHAPTER 1. INTRODUCTION .....	1
1.1 Gulf Stream for MHK Energy .....	1
1.2 MHK Turbine Design.....	4
1.3 Research Problem .....	5
CHAPTER 2. LITERATURE REVIEW .....	7
2.1 Introduction .....	7
2.2 Momentum Theory and Betz limit .....	7
2.3 Angular Momentum Theory.....	11
2.4 Lift force, Drag force and Non-dimensional Parameters .....	13
2.5 Blade Element Theory and Blade Element Momentum Theory .....	16
2.6 NREL's Key Wind Turbine Codes .....	20
CHAPTER 3. MODELING AND NUMERICAL SIMULATION OF OCEAN CURRENT TURBINE BLADE.....	26
3.1 Overall Design and Analysis Scheme .....	26

3.2 OCT Blades Modeling and Analysis with NREL Codes .....	27
3.2.1 OCT Blade Design.....	27
3.2.2 Blade Layup Definition.....	32
3.2.3 Blade Structural Properties.....	35
3.2.4 OCT Blade Mode shapes .....	40
3.2.5 Blade Hydrodynamic Loading.....	43
3.2.6 FAST with AeroDyn Model .....	45
3.2.6.1 FAST and AeroDyn Theory .....	45
3.2.6.2 OCT Blades Modeling with FAST and AeroDyn .....	51
3.2.6.3 OCT Blades Modeling Results and Discussion .....	55
3.2.6.4 Comparison of FAST Results and CFD Results .....	59
3.3 OCT Blades Modeling with Sandia’s NuMAD Codes .....	61
3.4 Modeling OCT Blade Using NREL Codes, NuMAD, and ANSYS .....	70
CHAPTER 4. RESULTS AND DISCUSSION -- SIMULATION UNDER HYDRODYNAMICS LOADS.....	72
4.1 Load cases assumptions.....	72
4.2 Safety Factors for OCT .....	77
4.3 Ultimate loads on OCT blades .....	81
4.3.1 Maximum regular cross-flow current.....	81
4.3.2 Extreme storm conditions .....	82
4.3.3 Ekman Solution for wind-driven current.....	82
4.3.4 Deterministic Ultimate load for OCT Blade .....	88
4.4 OCT Blade Static Analysis .....	88



4.5 Buckling Evaluation.....	94
4.6 Fatigue Analysis.....	98
CHAPTER 5. SUMMARY AND FUTURE WORK.....	110
5.1 Summary.....	110
5.2 Future Work .....	112
APPENDIXES .....	114
A. PreComp Files.....	114
B. BModes Files.....	128
C. AeroDyn Files.....	130
D. FAST Files.....	160
E. NuMAD Files .....	171
REFERENCES.....	181

## LIST OF FIGURES

Figure 1.1 The Gulf Stream .....	1
Figure 1.2 The Florida Current .....	2
Figure 1.3 The maximum, average, and minimum ocean current speed .....	3
Figure 2.1 Actuator disc model of an OCT rotor (Jonkman 2003).....	7
Figure 2.2 Wake rotation (Jonkman 2003).....	11
Figure 2.3 Annular stream tube .....	11
Figure 2.4 Pressure and shear stress acting on an airfoil (Jonkman 2003).....	14
Figure 2.5 Definition of lift, drag and pitching moment .....	15
Figure 2.6 A blade element sweeps out an annular (Burton et al. 2001).....	17
Figure 2.7 Blade element velocities (Burton et al. 2001).....	17
Figure 2.8 Blade element forces (Burton et al. 2001).....	19
Figure 2.9 NREL's key wind turbine codes.....	20
Figure 2.10 Example of composites layup at a typical blade section (Bir2005).....	21
Figure 2.11 Technical approach for computation of beam coupled modes in BModes (Bir 2005).....	22
Figure 2.12 BEM discretization in AeroDyn (Laino 2001).....	23
Figure 2.13 Layout of a conventional, upwind, three-bladed turbine (Jonkman 2005).....	24

Figure 2.14 Blade schematic after all stations and shear webs have been defined (Laird 2009).....	25
Figure 3.1 Flow diagram: Modeling and analyzing OCT blade using NREL codes, NuMAD and ANSYS.....	26
Figure 3.2 Flow diagram: Modeling and analyzing OCT blade using NREL codes.....	27
Figure 3.3 Histogram of the current speed at a depth of 25 m measured by the SNMREC at 30 minute intervals over a period of 13 months.....	28
Figure 3.4 Example power curve for a stall-regulated turbine and definition of the fitness function and its quantities of interest (Sale 2009).....	30
Figure 3.5 An ocean current turbine designed and developed by the SNMREC.....	31
Figure 3.6 Layup of composites at the blade section.....	34
Figure 3.7 Reference axes for section properties in PreComp (Bir 2005).....	36
Figure 3.8 OCT blade flap and edge mode shapes .....	43
Figure 3.9 Corrected coefficients of the FX77_W_16 hydrofoil.....	45
Figure 3.10 Local blade element velocities and flow angles (Moriarty 2005).....	47
Figure 3.11 Local blade element forces (Moriarty 2005).....	48
Figure 3.12 FAST and AeroDyn input and output files (Jonkman 2003).....	53
Figure 3.13 Cross-section view of a blade element indicating $F_N$ , $F_T$ , and $M_P$ (Moriarty 2005).....	54

Figure 3.14 Flap/Edge bending moment of blade root at 0.5 m/s current speed.....	55
Figure 3.15 Flap/Edge bending moment of blade root at 1.5 m/s current Speed.....	56
Figure 3.16 Flap/Edge bending moment of blade root at 2.5 m/s current speed.....	56
Figure 3.17 The normal and tangential force of each blade elements distributions calculated using FAST output at ocean current 2.5 m/s.....	57
Figure 3.18 Variation of root flapwise and edgewise bending moment with ocean current speed.....	57
Figure 3.19 Variation of root flapwise and edgewise shear with ocean current speed.....	58
Figure 3.20 Materials and composites interface in NuMAD.....	62
Figure 3.21 The delineation points at blade station.....	64
Figure 3.22 Final blade schematic representation after all stations and web have been added and modified.....	64
Figure 3.23 Blade data check display for a successful OCT blade definition.....	67
Figure 3.24 Blade property distributions (Laird 2009).....	67
Figure 3.25 OCT blade mode shapes extracted by NuMAD.....	69
Figure 3.26 Distribution of flap stiffness generated by PreComp and NuMAD.....	69

Figure 3.27 Distribution of edge stiffness generated byPreComp and NuMAD.....	70
Figure 3.28 SHELL281 element geometry (ANSYS 2010).....	71
Figure 3.29 Finished ANSYS blade model.....	71
Figure 4.1 Ekman current generated by wind (Oceanworld 2004).....	86
Figure 4.2 The ultimate loads applied at nearby nodes along the blade’s pitch axis of blade FE model in ANSYS.....	91
Figure 4.3 Bending stress along the blade span.....	92
Figure 4.4 The maximum and minimum of stress at blade root.....	93
Figure 4.5 The lowest buckling mode at 50% span.....	96
Figure 4.6 Second buckling mode at 46% span.....	96
Figure 4.7 Third buckling mode at 15-33% span.....	97
Figure 4.8 Adding core foam and reinforcement materials for all strength and stability criteria (HyperSizer 2010).....	98
Figure 4.9 Blade coordinate system in FAST (Jonkman 2005).....	100
Figure 4.10 Stress-time history of X2 point in blade root section at ocean current 2.5 m/s.....	102
Figure 4.11 Stress-time history of X8 point in blade root section at ocean current 2.5 m/s.....	102
Figure 4.12 Stress evaluations of 10 points for blade root section at 2.5 m/s ocean current speed using Equations (4.17) and (4.18).....	103

Figure 4.13 ANSYS stress results of blade root section at 2.5 m/s	
current speed .....	103
Figure 4.14 DOE/MSU Composite Material Fatigue Database: Constant	
life diagrams for materials QQ1 (DOE/MSU 2008).....	105
Figure 4.15 Stress-time history of X8 point in blade root section	
at ocean current 1.5 m/s.....	107

## LIST OF TABLES

Table 3.1 Rotor design characteristics .....	31
Table 3.2 OCT blade geometric properties and hydrofoils .....	32
Table 3.3 Material properties for blade design.....	33
Table 3.4 Composite layup of OCT blade.....	35
Table 3.5 Blade structural properties computed by PreComp.....	37
Table 3.6 Buoyancy of Blade.....	38
Table 3.7 Added mass and all mass along the blade span.....	41
Table 3.8 Airfoil ( hydrofoil)-date input file- fx77_01486_14.....	50
Table 3.9 Ratio of net blade gravity to total mass along the blade span.....	52
Table 3.10 Effect of added mass coefficients.....	59
Table 3.11 Drag (Normal force) and moment (edgewise) results of 1.6 m radius rotor at 1.5 m/s current speed from CFD and NREL's WT_Perf (Borghini 2012).....	60
Table 3.12 Power results of 1.6 m radius rotor at 1.5 m/s current speed from CFD and BEM (NREL's WT_Perf) (Borghini 2012).....	60
Table 3.13 Results of FAST, CFD, and WT_Perf at 1.5 m/s current speed.....	60
Table 3.14 Blade properties extracted by NuMAD.....	68
Table 4.1 Load groups to be considered for design of ocean current turbines (GL 2005).....	75

Table 4.2 Partial safety factors for loads $\gamma_F$ (GL 2005).....	78
Table 4.3 Partial safety factors for OCT blade.....	80
Table 4.4 Normal force ( $F_N$ ), Tangential force ( $F_T$ ) and Ultimate loads.....	89
Table 4.5 Stresses at blade root computed by ANSYS at the ultimate loads.....	91
Table 4.6 Blade tip deflection results of FAST and ANSYS at speed 3.5 m/s.....	93
Table 4.7 List of principal buckling modes.....	97
Table 4.8 Blade tip deflection results of FAST and ANSYS at speed 2.5 m/s.....	104
Table 4.9 Miner' fatigue damage results at X8 (33% chord) point of root section for one year.....	109



## CHAPTER 1. INTRODUCTION

### 1.1 Gulf Stream for MHK Energy

Ocean current is continually on the move. The movement of ocean water current represents a significant amount of marine hydrokinetic (MHK) energy. Ocean current energy has the potential of producing an enormous amount of new renewable energy around the world. Ocean currents can power the world. The total worldwide power in ocean currents has been estimated to be about 5,000 GW (DOI 2006).

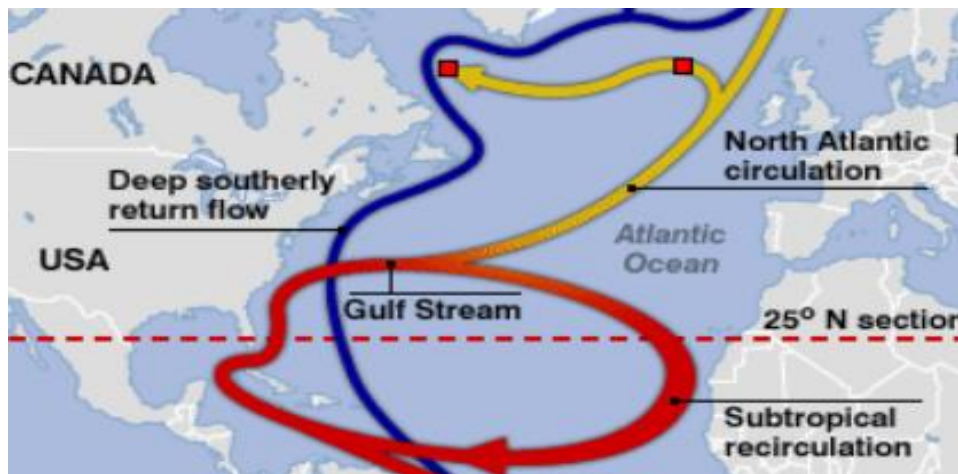


Figure 1.1 The Gulf Stream

The Gulf Stream is a powerful, warm, Atlantic ocean current. It begins at the tip of Florida, and follows the eastern coastlines of the United States before crossing the Atlantic Ocean. The Gulf Stream is typically 100 kilometers wide

and about 1,000 meters deep. The current velocity is fastest near the surface, with the maximum speed typically about 2.5 meters per second. The Gulf Stream represents a major renewable energy resource for the U.S. A technology report from the US Department of the Interior (DOI) states: "It has been estimated that capturing just 1/1,000th of the available energy from the Gulf Stream, which has 21,000 times more energy than Niagara Falls in a flow of water that is 50 times the total flow of all the world's freshwater rivers, would supply Florida with 35% of its electrical needs." (DOI 2006)

The Florida Current, which flows through the Florida Straits (Figure 1.2), is the southernmost part of the Gulf Stream. The relatively constant extractable energy density near the surface of the Florida Straits Current is about 1 kW/m<sup>2</sup> of flow area (DOI 2006). The United States and other countries are constantly pursuing ocean current energy. However, ocean current energy is at an early stage of development. There are no commercial devices currently operating to capture ocean current energy.

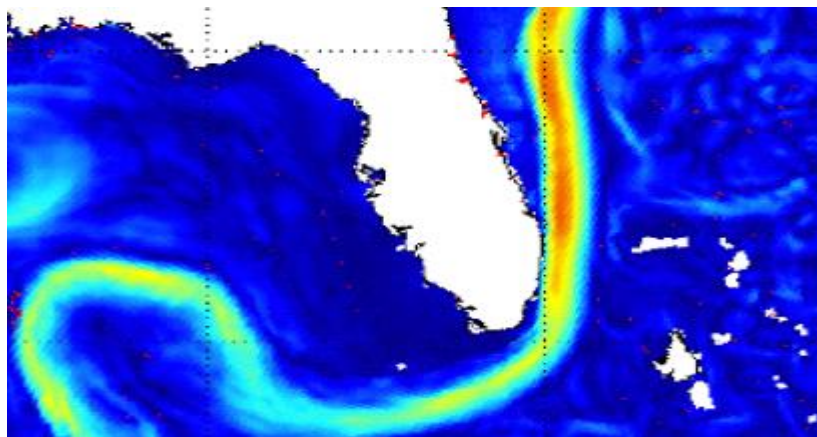


Figure 1.2 The Florida Current

The Florida Current off of the southern and eastern shores of Florida represents 20% of the Gulf Stream and North Atlantic Gyre, and has significant hydrokinetic energy available in its moving water and density structures. The Southeast National Marine Renewable Energy Center (SNMREC) at Florida Atlantic University has been established to pursue research and technologies that will aid industry in harnessing the vast ocean energy resources off the coast of Florida. Nearly 2 years of measurements taken near the core of the Florida Current offshore Ft. Lauderdale, Florida show that the mean current speed near the surface is nearly 1.7 m/s, with a maximum current speed of 2.5 m/s, and can exceed 1 m/s, even at depths of up to 150 m (Driscoll 2008).

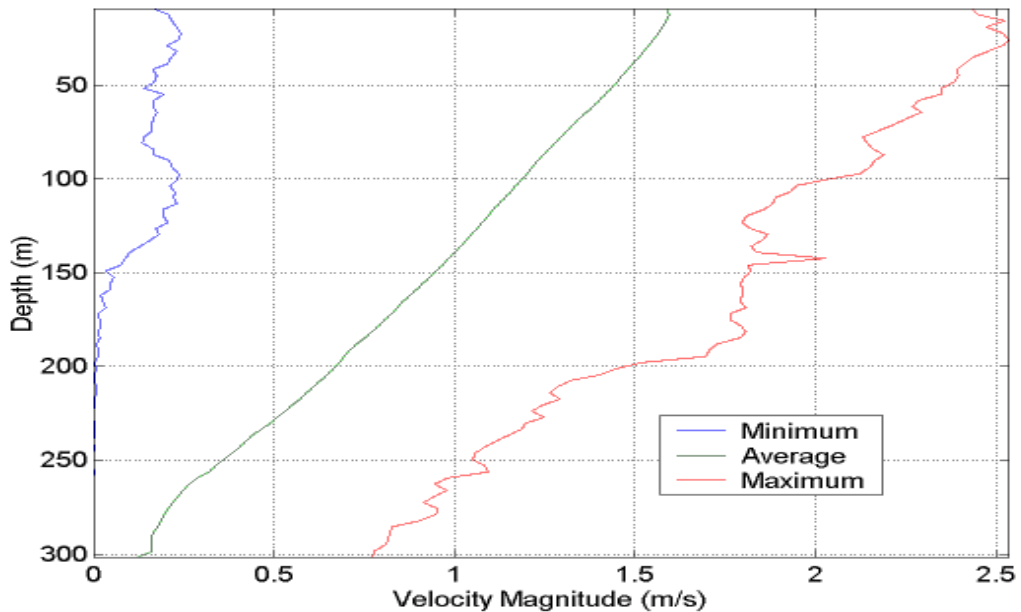


Figure 1.3 The maximum, average, and minimum ocean current speed measured offshore Ft. Lauderdale, FL over a period of nearly 2 years. Velocity measurements were made at 15 minute intervals with a 75 kHz ADCP by SNMREC (Driscoll 2008)

## 1.2 MHK Turbine Design

A MHK turbine is very similar to wind turbine except that they operate in two different fluids. A wind turbine is a device that converts kinetic energy from the wind into electricity power. During the past couple of years, wind energy has become the fastest-growing new energy source. The U.S. Department of Energy's (DOE) National Renewable Energy Laboratory (NREL) has sponsored the development, verification, and validation of various computer codes for analysis of wind turbine. These codes, called HARP\_Opt, PreComp, BModes, AirfoilPrep, AeroDyn, and FAST, are used for modeling both two- and three-bladed, horizontal-axis wind turbines.

Kinetic energy contained in flowing fluid is proportional to their density and the cube of their velocity. Ocean current speeds are generally lower than wind speeds. But ocean water is about 835 times denser than wind. As with wind turbines, submerged ocean current turbines (OCT) can capture kinetic energy from the movement of the marine current as it passes the rotor blades to generate electric power.

Energy can be extracted from the ocean currents using submerged OCT that are similar in function to wind turbines. An OCT operates on many of the same principles as wind turbines and shares similar design features. Because of the similarities between wind turbines and OCTs, these codes can be adapted for rotor modeling for OCT.

The idea in this dissertation is to use NREL design codes for the composites

ocean OCT blades. However, the higher density of water and randomness of ocean conditions make the loading on an OCT more complex and significantly different than on wind turbines. In this dissertation, NREL codes are combined with commercial codes to model and analyze a horizontal axis experimental OCT to be deployed in the Florida Current. The analysis includes a comprehensive fatigue analysis, structural design, load distributions, boundary conditions, and materials for OCT blades.

### **1.3 Research Problem**

Ocean current turbines are designed for optimized operation for a given set of environmental conditions. Good hydrodynamic design of OCT blades would increase the power extracted from the ocean current. At the same time, OCT blades must be able to withstand the expected normal ocean current loads and the loads caused by extreme loading such as hurricanes. Hence, another important issue is accurate prediction of the loads on the OCT blade due to a variable set of environmental conditions.

The ability to predict the hydrodynamic performance of an ocean current turbine is essential to the design of the turbine. Methodologies are also needed to predict and evaluate the hydrodynamic and operational performances of the ocean current turbines especially under random ocean current loading. Although much has been done with wind turbine, the technology for OCT is still evolving. There are fundamental differences in the design and operation of OCT that that

require further research.

One objective of this dissertation is to increase the modeling capability of the NREL wind turbine codes for the analysis of composite OCT blades. The second purpose of this study is to assess fatigue loading arising from ocean current and come up with procedure to predict useful life of OCT blades.

In order to perform stress and buckling analysis, an ANSYS finite element blade model was created using NuMAD, a turbine blade modeling software developed by Sandia National Laboratories. ANSYS was run to determine static deformations, stresses and buckling loads.

## **Approach**

The following approaches were undertaken:

- Model and analyze OCT blade using NREL codes with appropriate modifications
- Include NuMAD in the modeling to interface with ANSYS
- Couple NREL codes with ANASYS via NuMAD
- Perform blade failure analysis -- predict ultimate loads on OCT blades under various ocean conditions
- Perform blade fatigue analysis -- predicting fatigue life

## CHAPTER 2. LITERATURE REVIEW

### 2.1 Introduction

Energy can be extracted from the ocean currents using submerged horizontal-axis OCT that are similar in function to wind turbines. In order to better understand OCT and the research problem, in this chapter a brief description of the major theoretical concepts and NREL's wind codes used in this work is given.

### 2.2 Momentum Theory and Betz limit

A simple actuator disc model, generally attributed to Betz (1926), can be used to determine the power from an ideal turbine rotor, the thrust of the water current on the ideal rotor, and the effect of the rotor operation on the local current field. This model is based on a momentum theory developed over 100 years ago to predict the performance of ship propellers.

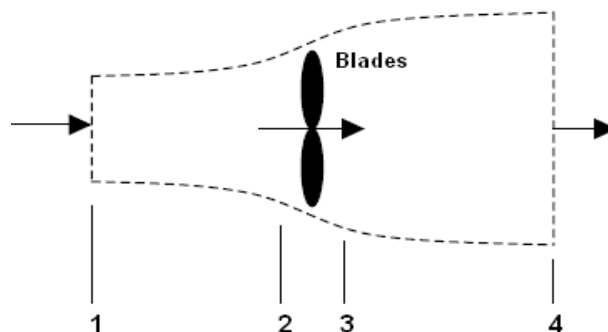


Figure 2.1 Actuator disc model of an OCT rotor (Jonkman 2003)

An ocean current turbine is a device extracting kinetic energy from the water current. This actuator disc model (Figure 2.1) has a number of simplifying assumptions. Rotor is modeled as an actuator disk which adds momentum and energy to the flow:

Flow is incompressible, inviscid, irrotational.

Flow is steady, homogenous and fixed in one direction.

Flow is one-dimensional, and uniform through the rotor disk, and in the far wake.

There is no swirl in the wake.

In Figure 2.1, Station 1 is upstream from the turbine, station 2 is right before the blades, station 3 just after, and station 4 is far downstream. As the water passes the rotor disc and convert its kinetic energy into rotor power, the water must slow down. The mass of water which passes through a given cross section in a unit length of time is  $\rho AU$ , where  $\rho$  is the water density,  $A$  is the cross-sectional area and  $U$  is the flow velocity. The mass flow rate must be the same at any location along the stream-tube. (Jonkman 2003)

$$\rho V_1 A_1 = \rho V_2 A_2 = \rho V_3 A_3 = \rho V_4 A_4 \quad (2.1)$$

According to the assumption, steady-state, incompressible, homogenous flow,  $V_2$  is equal to  $V_3$ ,  $A_2$  is equal to  $A_3$  and the static pressure  $p_1 = p_4$ .

Apply the Bernoulli's equation:

$$p_1 + \frac{1}{2} \rho V_1^2 = p_2 + \frac{1}{2} \rho V_2^2 \quad (2.2)$$

*and*



$$p_3 + \frac{1}{2} \rho V_3^2 = p_4 + \frac{1}{2} \rho V_4^2 \quad (2.3)$$

After some algebra:

$$p_2 - p_3 = \frac{1}{2} \rho (V_1^2 - V_4^2) \quad (2.4)$$

The thrust force at the rotor disc,  $T$ , is the differential pressure between stations 2 and 3 times the disc area:

$$T = (p_2 - p_3) A_2 = \frac{1}{2} \rho A_2 (V_1^2 - V_4^2) \quad (2.5)$$

Also, the thrust force is equal and opposite to the rate of change of momentum of the flow stream. For steady state flow,  $m = \rho V_1 A_1 = \rho V_2 A_2 = \rho V_3 A_3 = \rho V_4 A_4$ , where  $m$  is the mass flow rate.

$$T = m (V_1 - V_4) = \rho V_2 A_2 (V_1 - V_4) \quad (2.6)$$

Equating Equations (2.5) and (2.6), one obtains:

$$V_2 = \frac{V_1 + V_4}{2}$$

Define the axial induction factor as:

$$a = \frac{V_1 - V_2}{V_1} \quad (2.7)$$

It can also be shown that:

$$V_2 = V_1 (1 - a)$$

and

$$V_4 = V_1 (1 - 2a) \quad (2.8)$$

Substituting for  $V_4$  from Equation (2.8), Equation (2.6) can be rewritten as:

$$T = \frac{1}{2} \rho A V_1^2 4a(1-a) \quad (2.9)$$

The power extracted from the water by the rotor,  $P$ , is the product of the thrust,  $T$ , and velocity of water at the rotor plane,  $V_2$ , from Equation (2.7)

$$P(\text{Power}) = TV_2 = \frac{1}{2} \rho A V_1^3 4a(1-a)^2 \quad (2.10)$$

A power coefficient,  $C_P$ , is then defined as

$$C_P = \frac{P}{\frac{1}{2} \rho A V_1^3} = 4a(1-a)^2 \quad (2.11)$$

The maximum value of  $C_P$  occurs when

$$\frac{dC_P}{da} = 4(1-a)(1-3a) = 0 \quad (2.12)$$

Which gives a value of  $a = 1/3$ ,

Hence,

$$C_{P_{\max}} = \frac{16}{27} = 0.593 \quad (2.13)$$

The maximum achievable value of the power coefficient is known as the Betz limit. This is the maximum theoretically possible rotor power coefficient.

### 2.3 Angular Momentum Theory

In a similar manner as above we looked at the angular momentum. Consider the rotating annular stream tube shown in Figure 2.2. Four stations are shown in the Figure 2.3. Station 1 is upstream from the turbine, station 2 is right before the blades, station 3 just after, and station 4 is far downstream. Between 2 and 3 the rotation of the turbine imparts a rotation onto the blade wake. (Jonkman 2003)

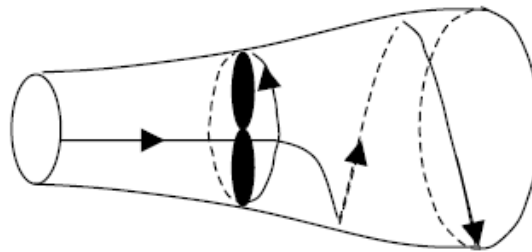


Figure 2.2 Wake rotation (Jonkman 2003)

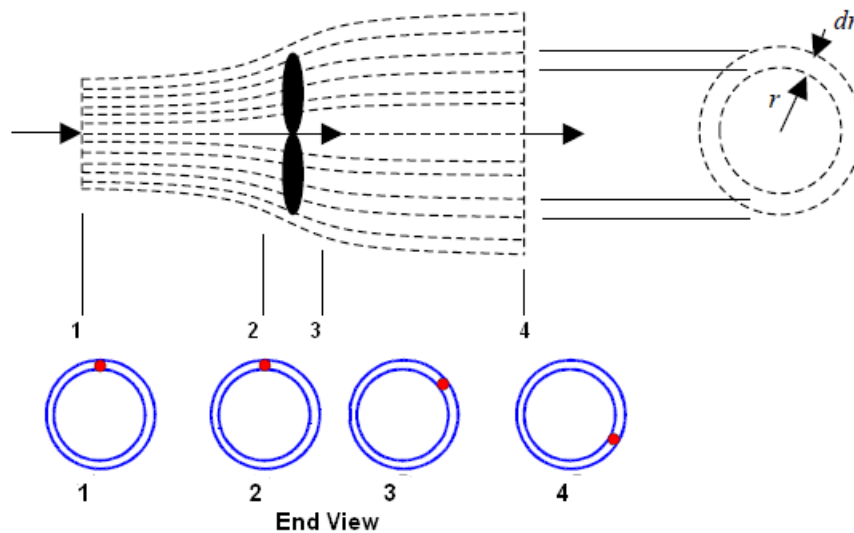


Figure 2.3 Annular stream tube

Consider the conservation of angular momentum in this annular stream tube. The flow behind the rotor will rotate in the opposite direction as the rotor in reaction to the flow imparting torque on the rotor as shown in Figure 2.2. The blade wake rotates with an angular velocity  $\omega$  and the blades rotate with an angular velocity of  $\Omega$ .

An angular induction factor,  $a'$ , is customarily defined as:

$$a' = \frac{\omega}{\Omega} \quad (2.14)$$

There is no stream ahead of the rotor according to the assumption of the conservation of angular momentum.

$$\omega_1 = \omega_2 = 0 \quad (2.15)$$

$\omega$  is the average value of the angular velocity just upwind and downwind of the rotor:

$$\omega = \frac{\omega_2 + \omega_3}{2} = \frac{0 + \omega_3}{2} \quad (2.16)$$

$$\text{or: } \omega_3 = 2\omega = 2a'\Omega$$

$$\omega = a'\Omega \quad (2.17)$$

Moment of Inertia ( $I$ ) of an annular ring (axis of rotation) is

$$I = mr^2 \quad (2.18)$$

where  $m$  is the flow mass,  $r$  is radius.

Angular Moment ( $L$ ) is,

$$L = I\omega = mr^2\omega \quad (2.19)$$

The definition of torque (Q) is:

$$Q = \frac{dL}{dt} = \frac{dI\omega_3}{dt} = \frac{d(mr^2\omega_3)}{dt} = r^2\omega_3 \frac{dm}{dt} \quad (2.20)$$

$$\frac{dm}{dt} = dAV_3 = \rho 2\pi r dr V_3 \quad (2.21)$$

By combining Equations (2.20) and (2.21), the differential torque of a blade element is:

$$dQ = r^2 \omega_3 \rho 2\pi r dr V_3 \quad (2.22)$$

$$V_3 = V_2 = V_1 (1 - a) = V (1 - a) \quad (2.23)$$

Substituting Equations (2.17) and (2.23) to (2.22), the differential torque of a blade element is:

$$dQ = \rho V_1 \Omega r^2 4(1 - a)a' \pi r dr \quad (2.24)$$

According to Equation (2.9), the differential rotor thrust of a blade element,

$$dT = \frac{1}{2} \rho dA_3 V_1^2 4a(1 - a) \quad (2.25)$$

$$dA_3 = 2\pi r dr \quad (2.26)$$

Replacing Equation (2.26) to (2.25), the differential thrust of a blade element is:

$$dT = \rho V_1^2 4a(1 - a) \pi r dr \quad (2.27)$$

## 2.4 Lift force, Drag force and Non-dimensional Parameters

In fluid dynamics, Bernoulli's principle states that for an inviscid flow, an increase in the speed of the fluid occurs simultaneously with a decrease in pressure or a decrease in the fluid's potential energy.

The forces exerted on an object by fluid as it flows over the object are due to pressure and viscous stresses. In Figure 2.4, the pressure on the upper surface of an airfoil is less than that of the incoming flow stream and effectively “sucks” the airfoil upward (normal to the incoming flow stream). By contrast, the pressure on the lower surface of the airfoil is greater than that of the incoming flow stream and effectively “pushes” the airfoil upward (normal to the incoming flow stream). This pressure difference and viscous stress distribution around a typical airfoil results in an upwards lift force, drag force and pitching moment. (Jonkman 2003)

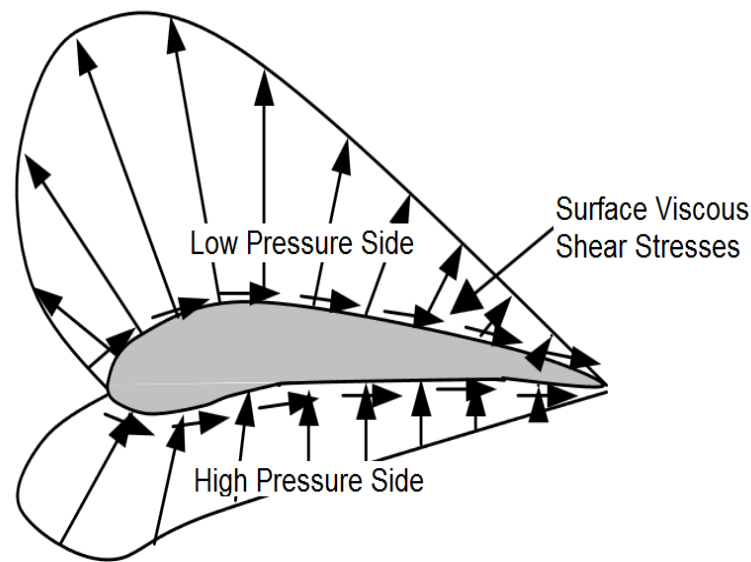


Figure 2.4 Pressure and shear stress acting on an airfoil (Jonkman 2003)

As shown in Figure 2.5, the resultant of all of these pressure and viscous stress is usually resolved into two forces and moment that act along the chord at a distance of quarter chord from the airfoil leading edge. Lift force is the

component of net force that is perpendicular to the oncoming flow direction. Drag force is the component of the surface force parallel to the flow direction. The effective moment, known as the pitching moment, is usually defined about an axis normal to the airfoil cross-section, located at quarter of the distance from the leading edge to the trailing edge of the airfoil.

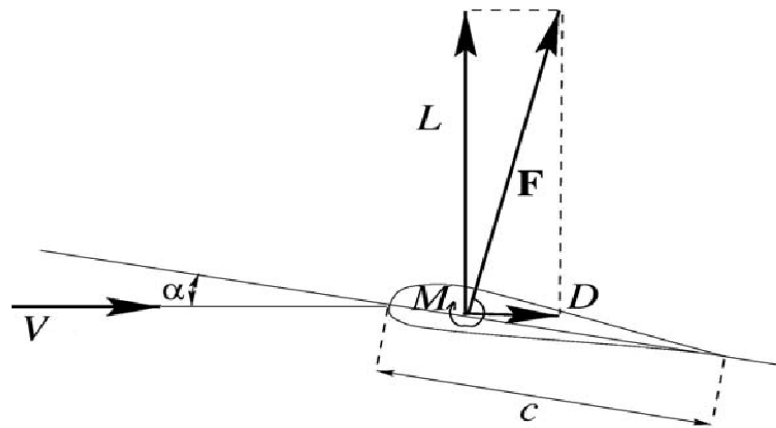


Figure 2.5 Definition of lift, drag and pitching moment

Lift force ( $L$ ), drag force ( $D$ ) and pitching moment ( $M_p$ ) are often expressed in terms of the lift coefficient ( $C_L$ ), drag coefficient ( $C_D$ ) and pitching moment coefficient ( $C_M$ ) as

$$L = \frac{1}{2} \rho V^2 c C_L \quad (2.28)$$

$$D = \frac{1}{2} \rho V^2 c C_D \quad (2.29)$$

$$M = \frac{1}{2} \rho V^2 c^2 C_M \quad (2.30)$$

where  $\rho$  is the fluid density,  $V$  is the fluid flow velocity and  $c$  is the chord length of the aerofoil.

The lift, drag and pitching moment coefficients are dimensionless numbers. In general, the lift, drag, and pitching moment coefficients are a function of the body shape, Reynolds number and angle of attack.

Reynolds number is the most important non-dimensional parameter for defining the characteristics of fluid flow conditions. Reynolds number ( $Re$ ) is defined as:

$$Re = \frac{UL}{\nu} = \frac{\rho UL}{\mu} = \frac{\text{Inertial force}}{\text{Viscous force}} \quad (2.31)$$

where  $\rho$  is the fluid density,  $\mu$  is fluid viscosity,  $\nu = \mu/\rho$  is the kinematic viscosity, and  $U$  and  $L$  are a velocity and length that characterize the scale of the flow. For fluid flowing over an immersed airfoil, these might be the incoming flow velocity and chord length of the airfoil.

## 2.5 Blade Element Theory and Blade Element Momentum Theory

Blade element theory (BET) is a mathematical process originally developed to determine the behavior of propellers. It involves breaking a blade down into several small parts then determining the forces on each of these small blade elements. As shown in Figure 2.6, the blade is assumed to be divided into  $N$  elements.



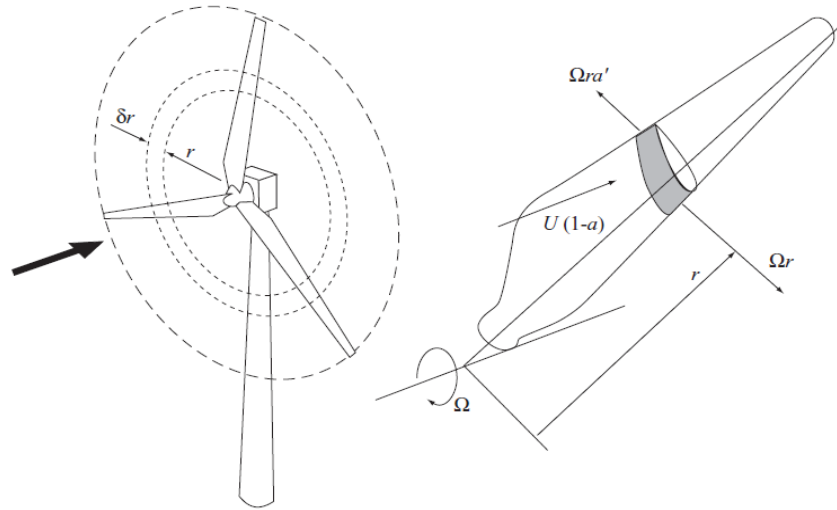


Figure 2.6 A blade element sweeps out an annular (Burton et al. 2001)

Blade element theory relies on two key assumptions:

- There are no hydrodynamic interactions between different blade elements.
- The forces exerted on the blade elements by the flow stream are solely determined by the lift and drag coefficients of the blade element hydrofoil shape.

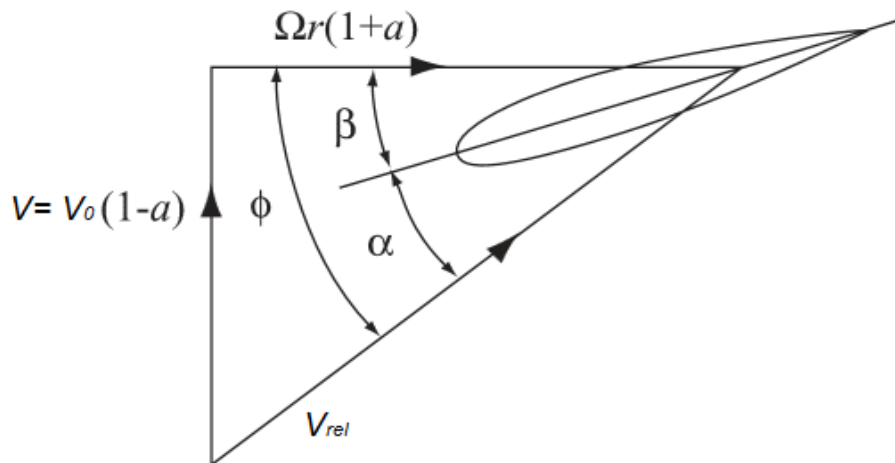


Figure 2.7 Blade element velocities (Burton et al. 2001)

In Figure 2.7,  $V$  is the axial inflow velocity at the rotor plane.  $\Omega r$  is the inflow velocity caused by the rotation of the blade.  $\omega r$  is the inflow velocity caused by wake rotation at the rotor plane (Jonkman 2003).

$$\Omega r + (\omega/2)r = \Omega r + \Omega a' r = \Omega r(1 + a') \quad (2.32)$$

The velocity of the inflowing flow stream relative to the blade element,  $V_{rel}$  is found to be:

$$V_{rel} = \sqrt{[V_0(1-a)]^2 + [\Omega r(1+a')]^2} \quad (2.33)$$

The lift force  $L$ , and drag  $D$  force per unit length on the blade element can be found from Equations (2.28) and (2.29):

$$L = \frac{1}{2} \rho V_{rel} c C_l \quad (2.34)$$

and

$$D = \frac{1}{2} \rho V_{rel} c C_d \quad (2.35)$$

As an alternative to the lift and drag forces, the normal force is the component of the net force acting normal to the chord line and the tangential force is the component of the net force acting parallel to the chord line. For a given flow condition, the relationships between the lift and drag forces and the normal and tangential forces are purely vectorial as determined by the angle of attack of the incoming flow stream. The angle of attack,  $\alpha$  is defined as the angle between the incoming flow stream and the chord line of the airfoil. These

characteristics are shown in Figure 2.8 (Jonkman 2003).

The relationships between the resultant forces are (Jonkman 2003):

$$\text{Normal Force} = \text{Lift Force} \times \cos(\alpha) + \text{Drag Force} \times \sin(\alpha) \quad (2.36)$$

and

$$\text{Tangential Force} = \text{Lift Force} \times \sin(\alpha) - \text{Drag Force} \times \cos(\alpha) \quad (2.37)$$

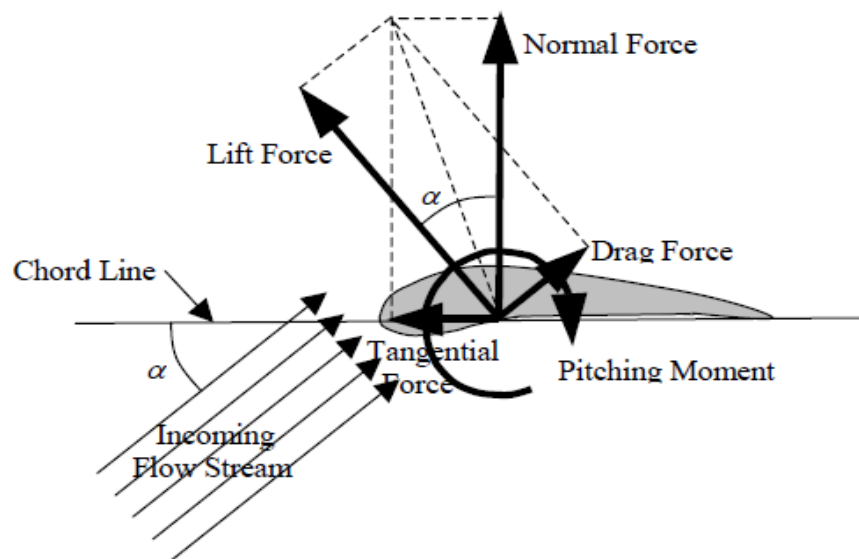


Figure 2.8 Resultant forces exerted on an airfoil (Jonkman 2003)

## 2.6 NREL's Key Wind Turbine Codes

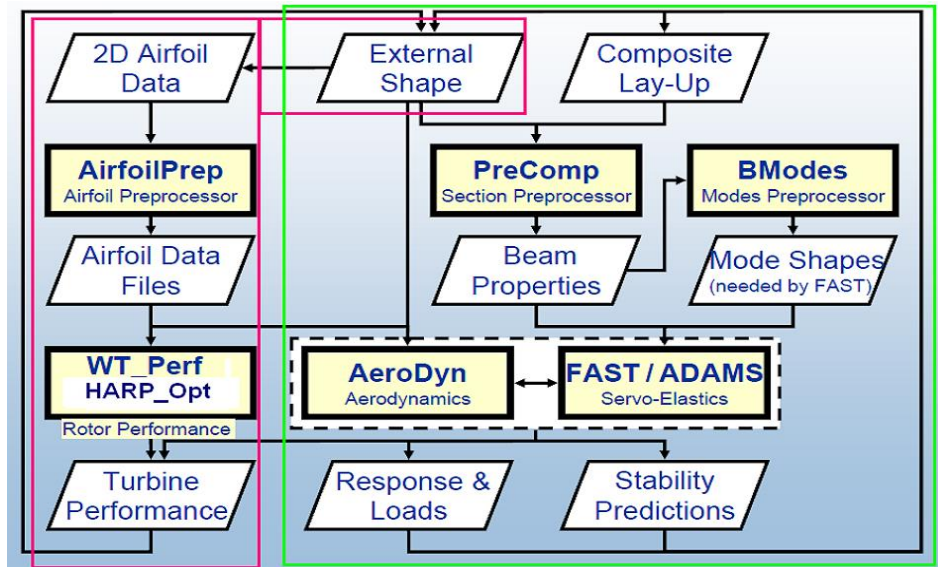


Figure 2.9 NREL's key wind turbine codes (Jonkman 2009)

### NREL's HARP\_Opt program

The HARP\_Opt (Horizontal Axis Rotor Performance Optimization) code utilizes a multiple objective genetic algorithm and blade-element momentum (BEM) theory flow model to design horizontal-axis wind and hydrokinetic turbine rotors. HARP\_Opt evaluates the airfoil (hydrofoil) shape of the blade, predicts rotor performance, and calculates the optimal blade shape (twist, chord, and airfoil/hydrofoil distributions) and optimal control of the rotor speed and blade pitch. The HARP\_Opt code is designed to be user friendly, and is operated using a graphical user interface (GUI) and easy to manipulate text input files. Output from the HARP\_Opt code is summarized in automatically generated Excel spreadsheets and text files. (Sale 2010)

## NREL's PreComp program

PreComp (Pre-processor for computing Composite blade structural properties) was developed to compute the stiffness and inertial properties of a composite blade's cross sections given their geometry and material layup. It also computes the cross-coupled stiffness, principal axes, and coordinates of the shear-center for a given section (Bir 2005). All wind turbine aeroelastic codes, such as FAST, need such properties to model the major flexible components—blades, tower, and drivetrain shaft.

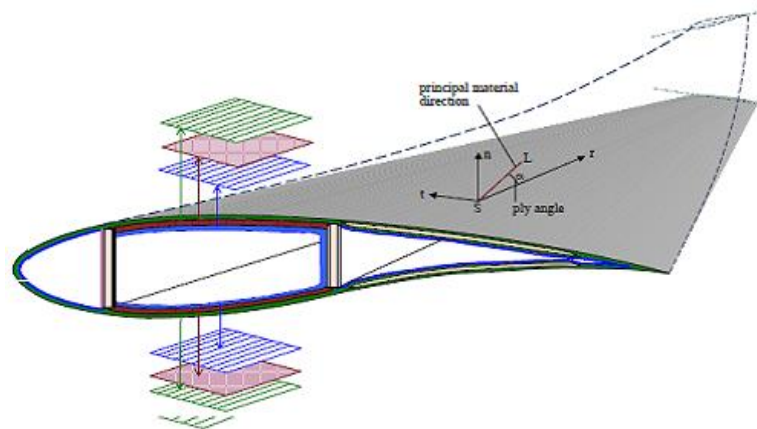


Figure 2.10 Example of composites layup at a typical blade section (Bir 2005)

PreComp assumes that the blade is fabricated with composite laminates and consists of an outer shell with internal spar webs, which is the most common construction method for modern composite blades. The cross-sectional analysis method allows for simplification and speedy results. Each cross-section is divided into sectors along the blade edge, for each of which the lamina stack is of constant thickness. Figure 2.10 shows the layup of a cross section defined through sectors along its periphery and the laminas schedule for each sector.

## NREL's BModes

BModes is a finite-element code that provides coupled modes for a turbine blade or a tower. Both the blade, rotating or non-rotating, and the tower can have arbitrary distribution of structural properties along their length. BModes is a code developed primarily to provide mode shapes for FAST, using a FEM approach. The blade is idealized as an Euler-Bernoulli beam that undergoes flap bending, lag bending, elastic twist, and axial deflection. BModes provides the modes for both the blades and the tower in the turbine system. The input files include the RPM, turbine radius, hub radius, section properties, and section property multipliers. The BModes output file contains the frequencies of blade modes, as well as maximum displacement and slope data. (Bir 2005)

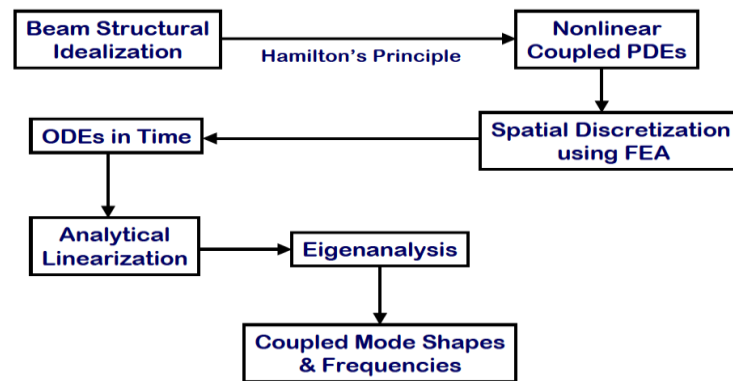


Figure 2.11 Technical approach for computation of beam coupled modes in BModes (Bir 2005)

## NREL's AeroDyn

AeroDyn is an aerodynamics software written to perform the aerodynamic calculations for aero-elastic simulations of horizontal axis wind turbine

configurations, and calculates the aerodynamic lift, drag, and pitching moment of airfoil sections along the wind turbine blades under varying conditions. AeroDyn contains two wake models: the blade element momentum (BEM) theory and the generalized dynamic wake theory. Although AeroDyn is not a standalone program – it is integrated into FAST – it has its own separate input files. The main input file first allows the user to choose between several models for various calculations: dynamic stall, inflow, induction factor, tip-loss, and hub-loss. Additionally, the user is allowed to enter tower-specific data and has the option of using the aerodynamic pitching moment model. The next part of the input file allows the user to choose which wind file is to be used, and to set the wind viscosity and density. (Laino 2001)

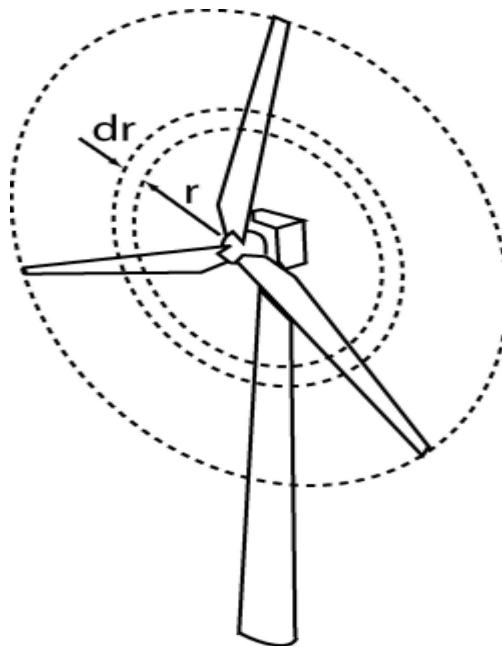
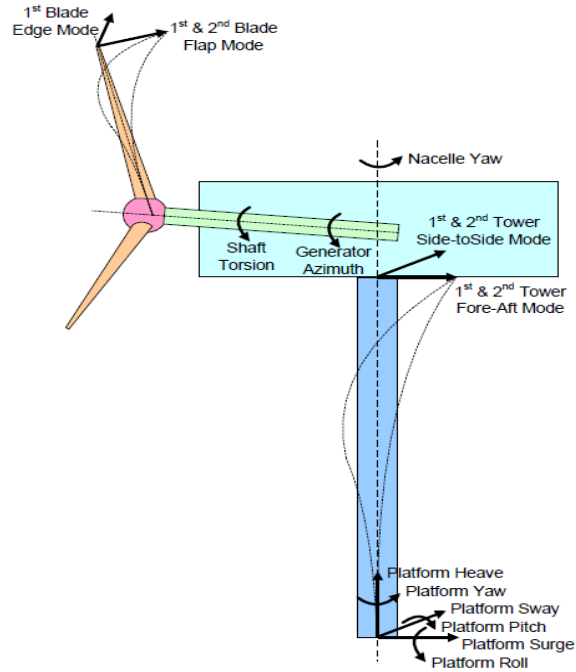


Figure 2.12 Annular plane used in blade element momentum theory in AeroDyn (Laino 2001)



*FAST DOFs for a 3-Bladed Turbine*

Figure 2.13 Layout of a conventional, upwind, three-bladed turbine (Jonkman 2005)

### **NREL's FAST**

The FAST (Fatigue, Aerodynamics, Structures, and Turbulence) code is a comprehensive aeroelastic simulator capable of predicting both the extreme and fatigue loads of two- and three-bladed horizontal-axis wind turbines (HAWTs). The FAST can model most common wind turbine configurations and control scenarios. The FAST code can model a three-bladed HAWT with 24 degrees of freedom (DOFs) under time variant wind conditions and allows for specified pitch and yaw maneuvers, as well as generator control, brake application, and a multitude of other possibilities. The DOFs and layout are shown in Figure 2.14. FAST models the blades and tower as individual flexible elements using a modal



representation. The flexibility characteristics of these members are determined by specifying distributed stiffness and mass properties along the span of the members and by prescribing their mode shapes through equivalent polynomial coefficients. (Jonkman 2005)

### **Sandia's NuMAD**

Sandia National Laboratories has created a software tool named NuMAD (Numerical Manufacturing and Design Tool). NuMAD is a stand-alone, user-friendly, windows based (GUI) pre-processor and post-processor for the ANSYS commercial finite element engine. It is designed to enable users to quickly and easily create a three-dimensional model of a turbine blade. This program allows the user to create a composite blade and extract section properties and modal curves to use as input into FAST. Additionally, it allowed us to create ANSYS input files for later stress analysis. (Laird 2009)

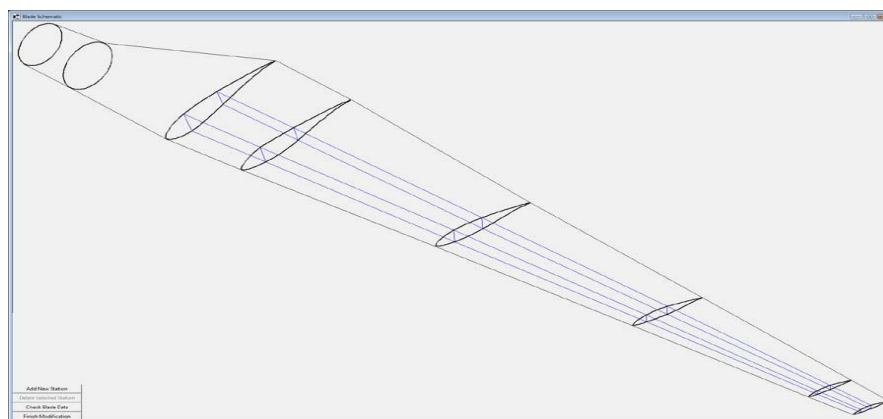


Figure 2.14 Blade schematic after all stations and shear webs have been defined (Laird 2009)

CHAPTER 3. MODELING AND NUMERICAL SIMULATION OF OCEAN  
CURRENT TURBINE BLADE

**3.1 Overall Design and Analysis Scheme**

In this dissertation, NREL's AirfoilPrep, PreComp, BModes, ModeShape, AeroDyn, FAST, NuMAD, and ANSYS were applied to model and analyze the SNMREC's composite OCT blade. Overall three types of modeling and analyses have been performed. These three modeling and analysis are as follows.

- i. Modeling and analysis OCT blade using NREL codes
- ii. Modeling and analysis OCT blade using NuMAD and NREL codes
- iii. Modeling and analysis OCT blade using NuMAD and ANSYS

The Modeling and analysis steps are depicted in the flowcharts of Figure 3.1.

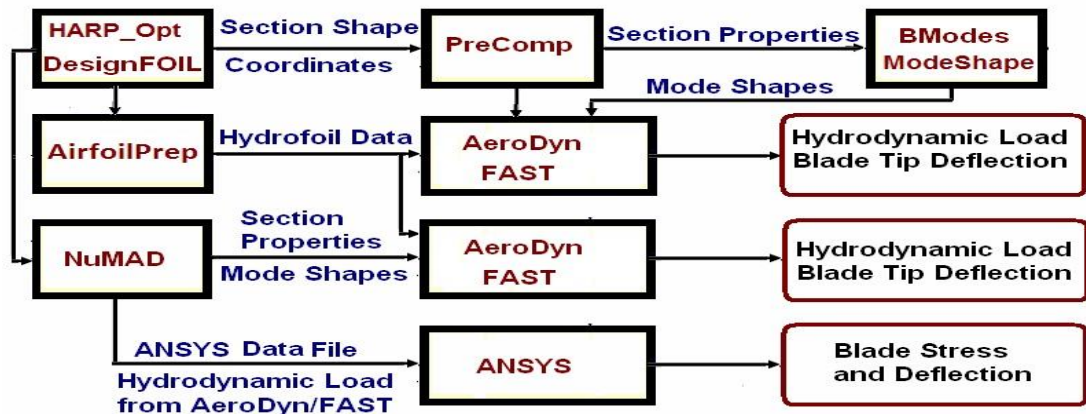


Figure 3.1 Flow diagram: Modeling and analysis OCT blade using NREL codes, NuMAD and ANSYS

### 3.2 OCT Blades Modeling and Analysis with NREL Codes

Since NREL codes were developed initially for wind turbine applications, it was quite challenging to adapt them to the hydrodynamic loading and proposed sandwich construction of an OCT blade. The OCT is operating under seawater conditions. The density of seawater is about 830 times the density of air. However, average ocean current velocity is an order of magnitude lower than nominal wind speed. The Reynolds numbers tend to be in the same range for both wind turbine and OCT blade, which allows the wind blade airfoil data to be used in the OCT blade design process. But unlike wind turbines, OCT must be designed to consider buoyancy forces and added mass effect. Figure 3.2 shows the flow diagram of OCT blade modeling using NREL codes.

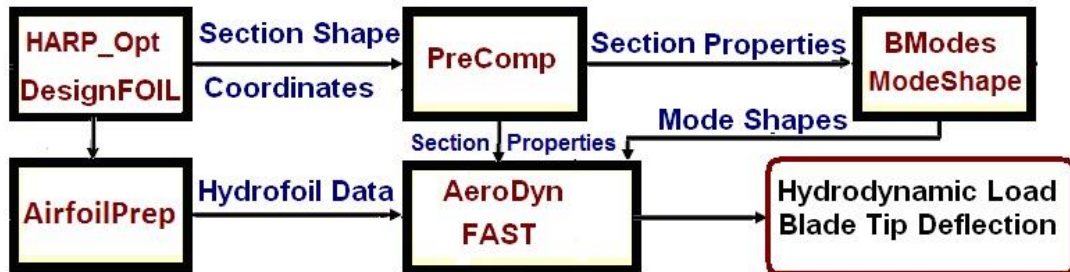


Figure 3.2 Flow diagram: Modeling and analysis OCT blade using NREL codes

#### 3.2.1 OCT Blade Design

The Southeast National Marine Renewable Energy Center (SNMREC) at Florida Atlantic University has collected more than 13 months of measurements near the core of the Florida Current off the coast of Ft. Lauderdale, Florida

(VanZwieten et al. 2011). These measurements show that the mean current speed at a depth of 25 m was 1.6 m/s, with a range between 0.5 and 2.5 m/s. A histogram of the measured current speed is shown in Figure 3.3

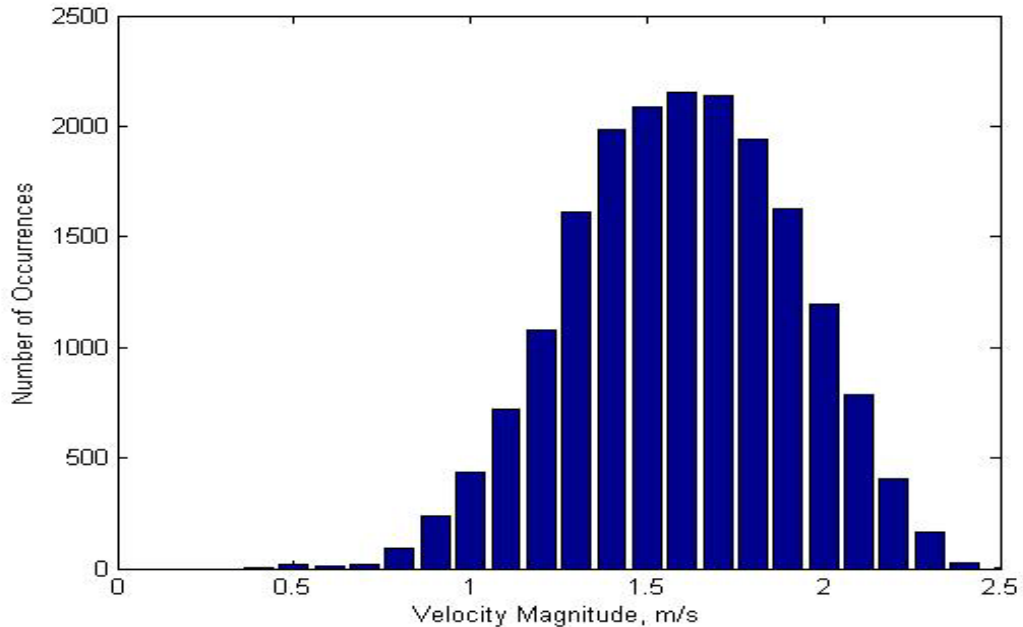


Figure 3.3 Histogram of the current speed at a depth of 25 m measured by the SNMREC at 30 minute intervals over a period of 13 months.

The design process for OCT blade involves many variables. Performing studies of all possible design is a time consuming and exhausting process. However, HARP\_Opt utilizes a multiple-objective genetic algorithm and blade-element momentum (BEM) theory flow model to design horizontal-axis wind and hydrokinetic turbine rotors. HARP\_Opt can function as a single or multiple objective optimization code. Harp\_Opt combines the blade element moment code WT\_Perf with a genetic algorithm to provide optimal blade twist angle

and chord distribution along the blade (Sale 2010). The primary optimization objective is to maximize the turbine's annual energy production (AEP). In this optimization method, an optimal stall-regulated rotor is one which produces an ideal power curve—i.e. the rotor should operate at high efficiencies from its cut-in to rated flow speed, and then begin to hydrodynamically stall and maintain a constant power output as the flow speed approaches and exceeds the rated speed of the turbine. The lowest fitness values are assigned to rotors which closely follow this ideal stall-regulated power curve. (Sale 2009)

The fitness function is defined by Equations (3.1), (3.2), and (3.3), where the values  $w_1$  and  $w_2$  are weight values specified by the user. WT\_Perf\_GA uses the default of  $w_1=w_2=1$ . Figure 3.4 further illustrates how the fitness function and its quantities of interest,  $Area_1$  and  $Area_2$ , are defined. (Sale 2009)

$$F = W_1 Area_1 + W_2 Area_2 \quad (3.1)$$

$$Area_1 = \int_{V_{cut-in}}^{V_{rated}} P_{Betz} - P_{turbine} dV_{\infty} \quad (3.2)$$

$$Area_2 = \int_{V_{rated}}^{V_{cut-out}} |P_{turbine} - P_{rated}| dV_{\infty} \quad (3.3)$$

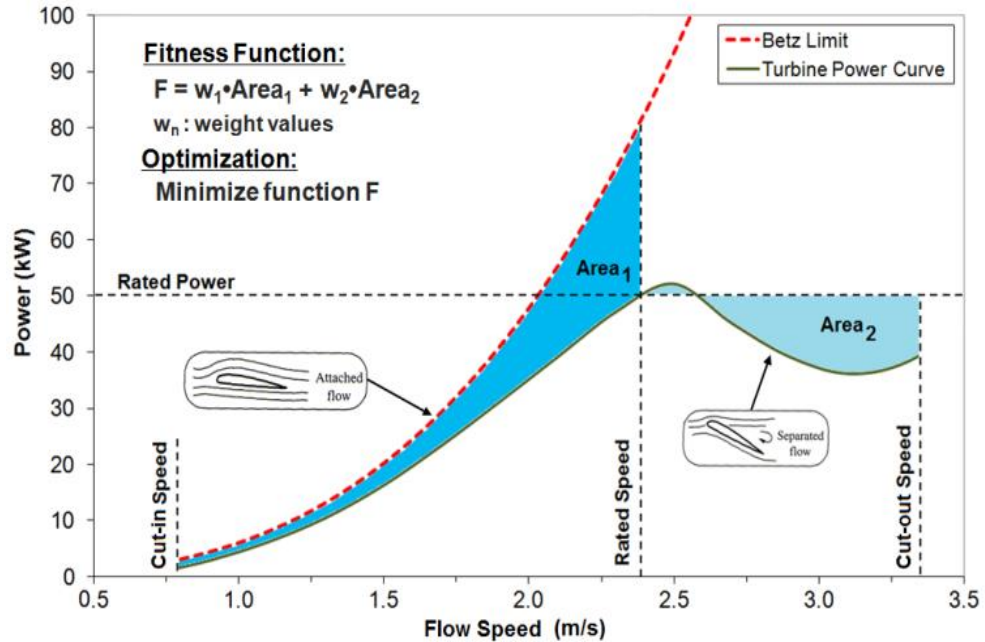


Figure 3.4 Example power curve for a stall-regulated turbine and definition of the fitness function and its quantities of interest (Sale 2009)

In order to help address various ocean current technological challenges and collect preliminary performance measurements, the SNMREC is fabricating an experimental research OCT to be deployed for short durations in the Florida Current. This system is designed to generate up to 20 kW of power in a horizontal axis orientation. It is fitted with a single 1.5 m radius rotor of 3 blades. The SNMREC's small-scale OCT rotor (Figure 3.5) design was optimized using HARP\_Opt. It predicts rotor performance, and the genetic algorithm maximizes the average power for measured environmental conditions. The optimization results predicted that the FX-77-W hydrofoil set outperformed other evaluated hydrofoil sets to produce more power (VanZwieten et al. 2011). Similar hydrofoil set (FX-77-W) was used in this dissertation. The rotor characteristics

are shown in Table 3.1. The OCT blade geometric properties and hydrofoils with blade twist angle are shown in Table 3.2. This experimental research OCT will undergo testing before integration with the electric generation sub system (Borghini et al. 2012).

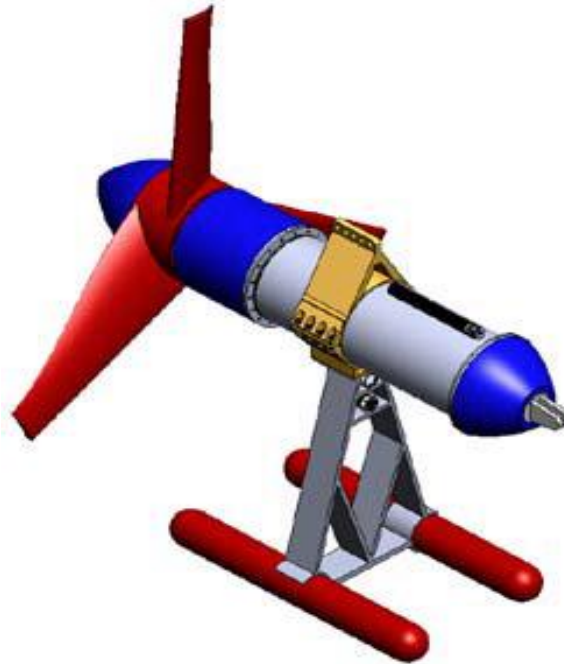


Figure 3.5 An characteristics of the SNMREC OCT

Table 3.1 Rotor design characteristics

Rating	20 KW
Rotor Orientation Configuration	Upwind, 3 Blades
Number of Blades	3
Rotor Diameter	3 m
Design Flow Speed	1.6 m/s
Min and Max Flow Speed	0.5 m/s--2.5 m/s
Hydrofoil Type	FX-77-W
Rated Rotor Speed	50 rpm

Table 3.2 OCT blade geometric properties and hydrofoils

Station Number	Radius (m)	Blade Fraction	Chord (m)	Twist (deg)	Hydrofoil
1	0.257	0	0.311	26.34	fx77_02349
2	0.277	0.016	0.311	26.34	fx77_02349
3	0.287	0.024	0.309	25.52	fx77_02336
4	0.306	0.04	0.305	24.07	fx77_02301
5	0.334	0.062	0.299	22.23	fx77_02273
6	0.371	0.092	0.29	20.22	fx77_02223
7	0.416	0.129	0.279	18.17	fx77_02162
8	0.469	0.171	0.267	16.13	fx77_02092
9	0.528	0.219	0.253	14.25	fx77_02012
10	0.593	0.271	0.239	12.47	fx77_01925
11	0.662	0.327	0.224	10.9	fx77_01832
12	0.735	0.386	0.21	9.5	fx77_01734
13	0.811	0.446	0.196	8.27	fx77_01633
14	0.888	0.508	0.182	7.22	fx77_01530
15	0.964	0.57	0.17	6.3	fx77_01486
16	1.04	0.631	0.159	5.49	fx77_01442
17	1.113	0.689	0.149	4.76	fx77_01400
18	1.182	0.745	0.14	4.1	fx77_01360
19	1.247	0.798	0.133	3.5	fx77_01323
20	1.306	0.845	0.127	2.95	fx77_01289
21	1.359	0.888	0.122	2.44	fx77_01258
22	1.404	0.924	0.118	1.99	fx77_01232
23	1.441	0.954	0.115	1.61	fx77_01211
24	1.469	0.977	0.114	1.3	fx77_01210
25	1.488	0.992	0.112	1.1	fx77_01210
26	1.498	1	0.112	0.99	fx77_01210

### 3.2.2 Blade Layup Definition

Table 3.3 lists the material property data for the laminates chosen for our OCT composite blade. These are glass fabrics and epoxy resin materials, which were selected from the DOE/MSU Composite Material Fatigue Database.



E-glass/epoxy laminate QQ1 ( $\pm 45/0_4/\pm 45$ , thickness 4.088 mm) was selected as the material for blade surfaces and the shear web. QQ1 laminate is based on  $0^\circ$  Saertex fabric (U14EU920-00940-T1300-100000) and  $\pm 45^\circ$  Saertex fabric (VU-90079-00830-01270-000000). (DOE/MSU 2010)

Table 3.3 Material properties for blade design

	U14EU920-	VU-90079-
$E_1$ (GPa)	38.4	13.8
$E_2$ (GPa)	12	11.8
$G_{12}$ (GPa)	6	6.00
$\nu_{12}$	0.27	0.25
Longitudinal Ultimate Tension Strength (MPa)	863	95.4
Longitudinal Ultimate Compressive Strength	-583	-166
Transverse Ultimate Tension Strength (MPa)	66.7	94.7
Longitudinal Ultimate Compressive Strength (MPa)	-197	-157
Density(kg/m <sup>3</sup> )	1690	1626
Laminate Lay-up	[0] <sub>2</sub>	[ $\pm 45$ ] <sub>4</sub>

For the OCT blade, the materials for blade surface buildup are composed of QQ1 ( $\pm 45/0_4/\pm 45$ ) laminate. A single shear web at 0.33 fraction of chord length is composed of 2 QQ1 ( $[\pm 45/0_4/\pm 45]_2$ ) laminates with a total thickness of 8.176 mm. The blade cross section is shown in Figure 3.6. At each station along the span of the blade, the layup design considered material choice and thickness of four regions of the station: (1) sector 1 (0% - 15% chord), (2) sector 2 spar cap (15% - 50% chord), (3) sector 3 (50% - 100% chord), and (4) shear web.

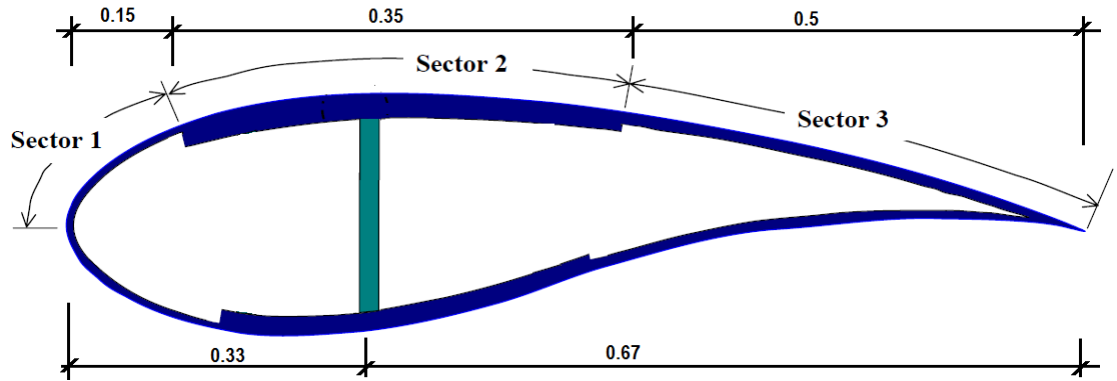


Figure 3.6 Layup of composites at the blade section

Table 3.4 lists composites layup at 26 stations along blade which correspond to the stations in Table 3.2. The entries in the second column of Table 3.4, labeled “Radius” are the spanwise locations along the blade-pitch axis relative to the rotor center (apex). “Blade Fraction” is the fractional distance along the blade-pitch axis from the root (0.0) to the tip (1.0). Along the pitch axis, the blade root was located at 0.257 m and the blade tip at 1.498 m from the rotor center separately.

Table 3.4 Composite layup of OCT blade

			Sector 1	Sector 2	Sector 3	Shear Web
Station Number	Radius	Blade Fraction	QQ1	QQ1	QQ1	QQ1 ([QQ1] <sub>2</sub> )
	(m)	(-)	(mm)	(mm)	(mm)	(mm)
1	0.257	0	12.266 ([QQ1] <sub>3</sub> )	12.266 ([QQ1] <sub>3</sub> )	12.266 ([QQ1] <sub>3</sub> )	8.176
2	0.277	0.016	12.266 ([QQ1] <sub>3</sub> )	12.266 ([QQ1] <sub>3</sub> )	12.266 ([QQ1] <sub>3</sub> )	8.176
3	0.287	0.024	12.266 ([QQ1] <sub>3</sub> )	12.266 ([QQ1] <sub>3</sub> )	12.266 ([QQ1] <sub>3</sub> )	8.176
4	0.306	0.04	12.266 ([QQ1] <sub>3</sub> )	12.266 ([QQ1] <sub>3</sub> )	12.266 ([QQ1] <sub>3</sub> )	8.176
5	0.334	0.062	12.266 ([QQ1] <sub>3</sub> )	12.266 ([QQ1] <sub>3</sub> )	12.266 ([QQ1] <sub>3</sub> )	8.176
6	0.371	0.092	8.176 ([QQ1] <sub>2</sub> )	12.266 ([QQ1] <sub>3</sub> )	8.176 ([QQ1] <sub>2</sub> )	8.176
7	0.416	0.129	8.176 ([QQ1] <sub>2</sub> )	12.266 ([QQ1] <sub>3</sub> )	8.176 ([QQ1] <sub>2</sub> )	8.176
8	0.469	0.171	8.176 ([QQ1] <sub>2</sub> )	12.266 ([QQ1] <sub>3</sub> )	8.176 ([QQ1] <sub>2</sub> )	8.176
9	0.528	0.219	8.176 ([QQ1] <sub>2</sub> )	12.266 ([QQ1] <sub>3</sub> )	8.176 ([QQ1] <sub>2</sub> )	8.176
10	0.593	0.271	8.176 ([QQ1] <sub>2</sub> )	12.266 ([QQ1] <sub>3</sub> )	8.176 ([QQ1] <sub>2</sub> )	8.176
11	0.662	0.327	8.176 ([QQ1] <sub>2</sub> )	12.266 ([QQ1] <sub>3</sub> )	8.176 ([QQ1] <sub>2</sub> )	8.176
12	0.735	0.386	8.176 ([QQ1] <sub>2</sub> )	12.266 ([QQ1] <sub>3</sub> )	8.176 ([QQ1] <sub>2</sub> )	8.176
13	0.811	0.446	8.176 ([QQ1] <sub>2</sub> )	12.266 ([QQ1] <sub>3</sub> )	8.176 ([QQ1] <sub>2</sub> )	8.176
14	0.888	0.508	8.176 ([QQ1] <sub>2</sub> )	8.176 ([QQ1] <sub>2</sub> )	8.176 ([QQ1] <sub>2</sub> )	8.176
15	0.964	0.57	8.176 ([QQ1] <sub>2</sub> )	8.176 ([QQ1] <sub>2</sub> )	8.176 ([QQ1] <sub>2</sub> )	8.176
16	1.04	0.631	8.176 ([QQ1] <sub>2</sub> )	8.176 ([QQ1] <sub>2</sub> )	8.176 ([QQ1] <sub>2</sub> )	8.176
17	1.113	0.689	8.176 ([QQ1] <sub>2</sub> )	8.176 ([QQ1] <sub>2</sub> )	8.176 ([QQ1] <sub>2</sub> )	8.176
18	1.182	0.745	8.176 ([QQ1] <sub>2</sub> )	8.176 ([QQ1] <sub>2</sub> )	8.176 ([QQ1] <sub>2</sub> )	8.176
19	1.247	0.798	4.088 (QQ1)	4.088 (QQ1)	4.088 (QQ1)	8.176
20	1.306	0.845	4.088 (QQ1)	4.088 (QQ1)	4.088 (QQ1)	8.176
21	1.359	0.888	4.088 (QQ1)	4.088 (QQ1)	4.088 (QQ1)	8.176
22	1.404	0.924	4.088 (QQ1)	4.088 (QQ1)	4.088 (QQ1)	8.176
23	1.441	0.954	4.088 (QQ1)	4.088 (QQ1)	4.088 (QQ1)	8.176
24	1.469	0.977	4.088 (QQ1)	4.088 (QQ1)	4.088 (QQ1)	8.176
25	1.488	0.992	4.088 (QQ1)	4.088 (QQ1)	4.088 (QQ1)	8.176
26	1.498	1	4.088 (QQ1)	4.088 (QQ1)	4.088 (QQ1)	8.176

### 3.2.3 Blade Structural Properties

PreComp was used for composite OCT blade to determine structural property. PreComp computed the stiffness and inertial properties of a hollow composite blade with FX-77-W set hydrofoil shapes. The coordinate

pairs of FX-77 series were exported to Excel where they were reordered in the way they needed to be in order to be used by PreComp: with the first node, (0, 0) being at the leading edge and the node numbering progressing clockwise from there onwards. The output file of PreComp included the calculated properties for different sections along the hollow composite blade. Table 3.5 lists the part of OCT blade properties.

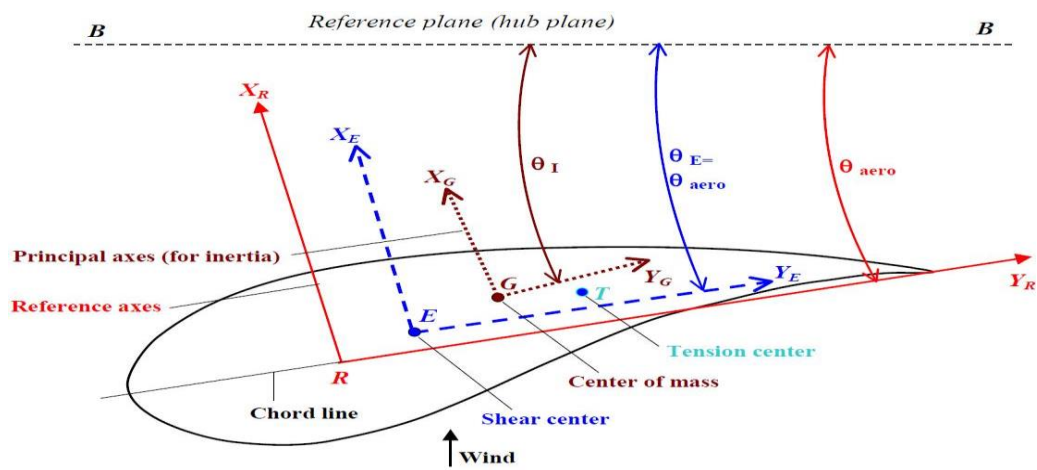


Figure 3.7 Reference axes for section properties in PreComp (Bir 2005)

The flapwise and edgewise section stiffness, “flp-stff” and “edg-stff” in Table 3.5, are given about the principal structural axes of each cross section as oriented by the structural-twist angle, “str\_tw”. “tor-stiff” represents the values of the blade torsion stiffness. PreComp computed the stiffness (flp-stff, edg-stff, and tor-stiff), principal axes, and coordinates of the shear-center and inertial properties of the composite blade’s cross-sections. Figure 3.7 shows reference axes for section properties in PreComp.

Section flapwise bending stiffness about the  $Y_E$  axis was calculated as:

$$\text{flp-stff} = \iint E(x, y)x^2 dx dy \quad (3.4)$$

Section edgewise bending stiffness about the  $X_E$  axis was calculated as:

$$\text{edg-stff} = \iint E(x, y)y^2 dx dy \quad (3.5)$$

Table 3.5 Blade structural properties computed by PreComp

span_loc	str_tw	tw_iner	mass_den	flp_iner	edge_iner	flp_stff	edge_stff	tor_stff
(-)	(deg)	(deg)	(kg/m)	(kg-m)	(kg-m)	(Nm^2)	(Nm^2)	(Nm^2)
0	23.696	23.717	1.44E+01	6.09E-03	1.13E-01	9.34E+04	1.73E+06	4.60E+04
0.016	23.695	23.716	1.44E+01	6.09E-03	1.13E-01	9.34E+04	1.73E+06	4.60E+04
0.024	23.093	23.113	1.42E+01	5.87E-03	1.11E-01	9.01E+04	1.70E+06	4.42E+04
0.04	21.473	21.494	1.40E+01	5.46E-03	1.06E-01	8.38E+04	1.63E+06	4.11E+04
0.062	19.716	19.736	1.37E+01	4.89E-03	9.97E-02	7.50E+04	1.53E+06	3.67E+04
0.092	17.776	17.795	1.05E+01	3.91E-03	6.47E-02	5.99E+04	9.95E+05	2.59E+04
0.129	15.64	15.658	1.01E+01	3.19E-03	5.74E-02	4.89E+04	8.82E+05	2.10E+04
0.171	13.668	13.685	9.61E+00	2.51E-03	5.01E-02	3.85E+04	7.69E+05	1.65E+04
0.219	11.837	11.852	9.06E+00	1.88E-03	4.24E-02	2.88E+04	6.51E+05	1.22E+04
0.271	10.106	10.12	8.51E+00	1.37E-03	3.55E-02	2.10E+04	5.46E+05	8.76E+03
0.327	8.472	8.484	7.93E+00	9.50E-04	2.91E-02	1.45E+04	4.47E+05	5.94E+03
0.386	7.096	7.107	7.39E+00	6.47E-04	2.39E-02	9.89E+03	3.66E+05	3.91E+03
0.446	5.855	5.865	6.85E+00	4.26E-04	1.93E-02	6.50E+03	2.96E+05	2.44E+03
0.508	4.796	4.804	5.45E+00	2.61E-04	1.45E-02	3.97E+03	2.22E+05	1.70E+03
0.57	3.911	3.919	5.08E+00	1.92E-04	1.17E-02	2.91E+03	1.80E+05	1.22E+03
0.631	3.139	3.147	4.74E+00	1.42E-04	9.56E-03	2.15E+03	1.47E+05	9.05E+02
0.689	2.449	2.456	4.42E+00	1.07E-04	7.83E-03	1.61E+03	1.20E+05	7.36E+02
0.745	1.729	1.736	4.15E+00	8.21E-05	6.47E-03	1.23E+03	9.94E+04	6.64E+02
0.798	1.322	1.341	2.08E+00	4.69E-05	2.83E-03	7.07E+02	4.36E+04	2.93E+02
0.845	0.796	0.815	1.98E+00	3.77E-05	2.46E-03	5.67E+02	3.79E+04	2.32E+02
0.888	0.305	0.323	1.90E+00	3.11E-05	2.18E-03	4.66E+02	3.35E+04	1.93E+02
0.924	-0.228	-0.21	1.83E+00	2.65E-05	1.97E-03	3.95E+02	3.03E+04	1.80E+02
0.954	-0.603	-0.586	1.78E+00	2.33E-05	1.82E-03	3.47E+02	2.80E+04	1.69E+02
0.977	-0.908	-0.891	1.77E+00	2.26E-05	1.77E-03	3.36E+02	2.73E+04	1.64E+02
0.992	-1.109	-1.091	1.73E+00	2.13E-05	1.68E-03	3.16E+02	2.59E+04	1.56E+02
1	-1.22	-1.202	1.73E+00	2.13E-05	1.68E-03	3.16E+02	2.59E+04	1.56E+02

Table 3.6 Buoyancy of Blade

Section Station	Buoyancy (kg/m)	Mass of Blade (Hollow) (kg/m)	Mass of Filler Core (HCP30) (kg/m)	Mass of Blade and Core (kg/m)	Net Gravity (kg/m)
1	14.5	14.35	1.54	15.89	1.39
2	14.5	14.35	1.54	15.89	1.39
3	14.19	14.24	1.49	15.73	1.54
4	13.67	14.04	1.40	15.44	1.77
5	12.94	13.73	1.29	15.02	2.08
6	11.93	10.53	1.39	11.92	-0.01
7	10.71	10.09	1.18	11.27	0.56
8	9.52	9.61	0.99	10.60	1.08
9	8.19	8.51	0.83	9.34	1.15
10	7.03	7.93	0.66	8.59	1.56
11	5.95	7.39	0.48	7.87	1.92
12	4.88	6.85	0.33	7.18	2.30
13	4.03	5.45	0.29	5.74	1.71
14	3.28	5.08	0.17	5.25	1.97
15	2.77	4.74	0.10	4.84	2.07
16	2.4	4.42	0.05	4.47	2.07
17	2.01	4.15	0.12	4.27	2.26
18	1.73	2.08	0.19	2.27	0.54
19	1.52	1.98	0.16	2.14	0.62
20	1.35	1.98	0.13	2.11	0.76
21	1.2	1.9	0.11	2.01	0.81
22	1.11	1.83	0.08	1.91	0.80
23	1.03	1.78	0.08	1.86	0.83
24	1.03	1.77	0.08	1.85	0.82
25	1	1.73	0.08	1.81	0.81
26	1	1.73	0.08	1.81	0.81

PreComp assumes that the each blade section is a thin-walled, closed, multi-cellular, hollow section. OCT blade experiences buoyancy forces when submerged in sea water. Because moments are caused by cyclical gravity force changes due to blade rotation, resulting fatigue damage of the blade can result.

To minimize these cyclic forces, unlike a wind turbine hollow blade section, OCT blades might use a filler material (core materials) to adjust the blades to achieve approximately neutral buoyancy (Bir 2011). The buoyancy of blade were calculated and shown in Table 3.6.

The entries in the section column of Table 3.6, labeled “Buoyancy”, are the displaced mass of water of OCT blade along the span. “Mass of Blade (Hollow)” is distributed blade hollow section mass per unit length. “Mass of Filler (HCP30)” is mass of filler per unit length if blade section is made of PVC HCP30 ( $200\text{kg/m}^3$ ) for blade interior. “Net Gravity” represents the net gravity of blade in water when blade section is filled with of PVC HCP30 (Mass of Blade + Mass of Filler HCP30 – Buoyancy).

The additional stiffness of section due to filling with HCP 30 core material of OCT blade was calculated. Additional stiffness and inertial properties were added to the quantities that were computed by PreComp. As a result, the flap and edge stiffness properties were increased by around 1%. In fact, for large scale commercial OCT blade, the “Buoyancy” of blade will be larger than “Gravity” of blade. OCT blades will be filled with core materials and water to adjust the blades to achieve approximately neutral buoyant as much as possible. The additional flap and edge stiffness of core materials may therefore be ignored in that case.

### **3.2.4 OCT Blade Mode shapes**

In the next step, BModes was used to compute natural frequencies and mode shapes of the OCT blade. FAST used an assumed-modes approach. It needed blade and tower modes as well as structural properties to compute modal integrals for its equations of motion. BModes was developed primarily to provide coupled mode shapes for FAST. BModes calculate natural frequencies and modes for both the blades in the turbine system. BModes required specification of rotor speed, blade geometry, and structural properties distribution along the blade as inputs. These properties were obtained from PreComp. The structural properties were specified in terms of the flap bending, edge bending, torsion, and axial stiffness; section moments of inertia; and mass. (Bir 2005)

Although BModes was primarily developed for wind turbine, it was successfully used for OCT. The structural model of FAST and BModes consider the blades to be flexible cantilevered beam with continuously distributed stiffness and mass. The biggest difference for an OCT blade was that it was vibrating in water instead of air. In fluid mechanics, added mass (or virtual mass) is the inertia added to a system because an accelerating or decelerating body must move some volume of surrounding fluid. For the case of unsteady motion of OCT blades in water, we must consider additional added mass force effects resulting from the water acting on the OCT blade when formulating the blade equation of motion. "Total mass" (blades mass and added mass) was accelerated and decelerated in both the flapwise and edgewise directions.



The added mass is proportional to the displaced mass of water and expressed as

$$A = \rho C_A A_R \quad (3.6)$$

where  $\rho$  is density of water;  $C_A$  is added mass coefficient;  $A_R$  is the reference area (blade section area).

Table 3.7 Added mass and all mass along the blade span

Section Station	Mass of Blade and Core (kg/m)	Displaced Mass of Water kg/m	Added Mass kg/m	Total Mass kg/m
1	15.89	14.5	7.25	23.14
2	15.89	14.5	7.25	23.14
3	15.73	14.19	7.1	22.83
4	15.44	13.67	6.84	22.28
5	15.02	12.94	6.47	21.49
6	11.92	11.93	5.97	17.89
7	11.27	10.71	5.36	16.63
8	10.60	9.52	4.76	15.36
9	9.34	8.19	4.1	13.44
10	8.59	7.03	3.52	12.11
11	7.87	5.9	2.95	10.82
12	7.18	4.88	2.44	9.62
13	5.74	4.03	2.02	7.76
14	5.25	3.28	1.64	6.89
15	4.84	2.77	1.38	6.22
16	4.47	2.4	1.2	5.67
17	4.27	2.01	1.01	5.28
18	2.27	1.73	0.87	3.14
19	2.14	1.52	0.76	2.90
20	2.11	1.35	0.68	2.79
21	2.01	1.2	0.6	2.61
22	1.91	1.11	0.55	2.46
23	1.86	1.03	0.52	2.38
24	1.85	1.03	0.51	2.36
25	1.81	1	0.5	2.31
26	1.81	1	0.5	2.31

The added mass coefficients are dependent upon the section shape and moving direction of the OCT blade (DNV 2011). It is difficult to find accurate added mass coefficients of OCT blade from current offshore standards. However, evaluation of the added-mass coefficients is beyond the scope of this dissertation. After comparing the added mass coefficients of different section shapes in DNV Offshore Standard, it was assumed that the added mass per unit length of the blade was 50% of the mass of water displaced by the blade. According to this assumption, the "added mass" and "total mass" along the blade span were calculated as Table 3.7.

BModes does not include the influence of added mass on the modal calculation. Blade mass was modified to account for the added mass and replaced the blade mass with "all mass" (blade mass + added mass) in BModes input file. Input data are provided to BModes via two files: a main input file and an auxiliary input file containing distributed properties (PreComp output file). For the blades, FAST use two flapwise modes and one edgewise mode. In FAST, each mode shape is assumed to be expressible as a polynomial. The mode shapes take the form of a sixth-order polynomial with the zeroth and first terms always being zero. This is because the mode shapes are cantilevered at the base so they must have zero deflection and slope there. At the tip of the blade, where the normalized height is 1, the deflection must have a normalized value of 1. This means the sum of the polynomial coefficients must add to 1. The BModes output file was exported to ModeShape. The polynomial coefficients were calculated in

ModeShape workbook.

Flapwise mode 1:

$$y = 0.3673x^2 - 0.8268x^3 + 3.1869x^4 - 1.6505x^5 - 0.0769x^6$$

Flapwise mode 2:

$$y = -3.5768x^2 + 49.7954x^3 - 153.8381x^4 + 169.5225x^5 - 60.9030x^6$$

Edgewise mode 1:

$$Y = 2.1978x^2 + 2.9477x^3 - 6.9603x^4 + 1.5391x^5 + 1.2757x^6$$

These coefficients were later copied and pasted into FAST input files. These input and output files given in Appendixes B. Figure 3.8 shows the OCT blade mode shapes.

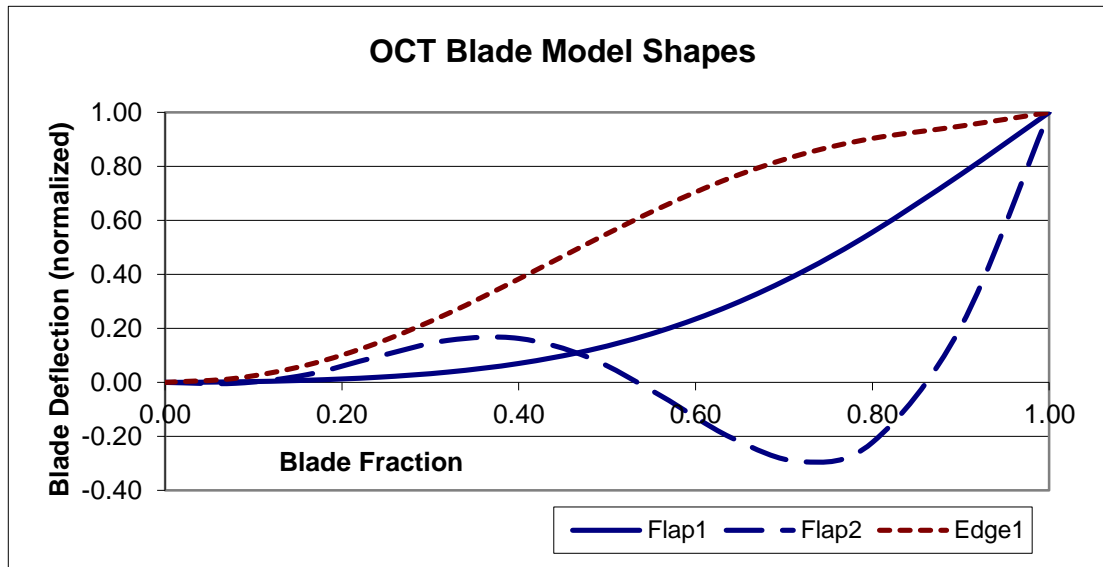


Figure 3.8 OCT blade flap and edge mode shapes

### 3.2.5 Blade Hydrodynamic Loading

In fluid dynamics, when fluid flows over an immersed body, forces will be

exerted on the body. Lift force is the component of this force that is perpendicular to the oncoming flow direction. Drag force is the component of the surface force parallel to the flow direction. The lift and drag coefficients are a dimensionless number. In general, the lift and drag coefficients are a function of the body shape, Reynolds number and angle of attack.

In this dissertation, using DesignFOIL (a commercial airfoil software), a preliminary hydrodynamic analysis was performed for each hydrofoil, which provided lift ( $C_L$ ) and drag ( $C_D$ ) coefficients for various angles of attack. DesignFOIL generated these lift and drag coefficients for angles of attack ranging from  $-20^\circ$  to  $+20^\circ$  based on a user-defined airfoil coordinate file and a user-specified Reynolds number. A Reynolds number of 1,000,000 was selected because it is near the midpoint of the expected Reynolds number range for a 1.5 meter blade operating at 50 RPM.

AirfoilPrep was used to prepare the OCT blade hydrofoil data input files for AeroDyn. The "3DStall" worksheet of AirfoilPrep was adjusted with  $C_L$  and  $C_D$  coefficients caused by delayed stall on a rotating blade. The "TableExtrap" worksheet extended the airfoil table from  $-20^\circ$  to  $+20^\circ$  angles of attack range to the entire  $\pm 180^\circ$  range required by AeroDyn. A resulting three-dimensionally corrected airfoil-data coefficients sample is illustrated graphically in Figure 3.9. The numerical values are documented in the AeroDyn airfoil-data input files that were shown in Appendixes.

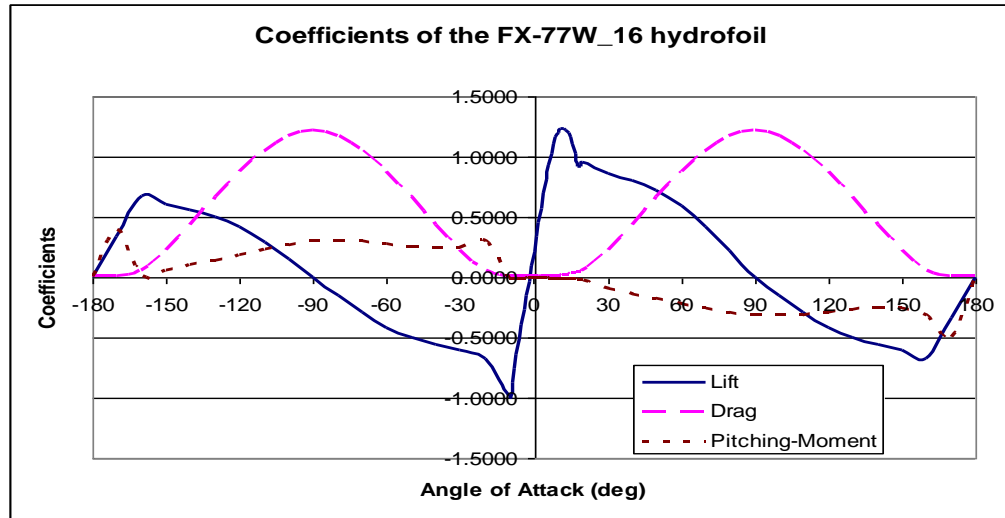


Figure 3.9 Corrected coefficients of the FX77\_W\_16 hydrofoil

### 3.2.6 FAST with AeroDyn Model

#### 3.2.6.1 FAST and AeroDyn Theory

FAST has been used to compute the structural-dynamic and control-system responses of wind turbines for many years. FAST with AeroDyn was evaluated by Germanischer Lloyd. The calculated loads from FAST were compared with those from analyses using GL Wind's own aeroelastic code DHAT V19. Comparison of results shows good agreement. The GL's Certificate attests that FAST "can be considered as suitable programs for the calculation of onshore wind turbine loads for design and certification." (GL WindEnergie 2005)

The structural model of FAST considers the blades to be flexible cantilevered beams with continuously distributed mass and stiffness. FAST models blades using the normal mode summation method and reduces the number of DOFs. Blades are modeled as a linear sum of known shapes of the dominant normal

vibration modes. For the blades, FAST use two flapwise modes and one edgewise mode (Jonkman 2003).

FAST uses Kane's method to set up equations of motion, which are then solved by numerical integration. By a direct result of Newton's laws ( $F=ma$ ) of motion, Kane's equations of motion for a simple holonomic system can be stated as:

$$F_r + F^* = 0$$

$F_r$  and  $F^*$  are called generalized active forces and generalized inertia forces, respectively. Generalized active forces ( $F_r$ ) include all external forces acting on the body, such as aerodynamic (hydrodynamic) forces, gravity, drive train forces, and forces due to the elastic bending of the blades. The generalized inertia forces ( $F^*$ ) include all effects of linearly and angularly accelerating mass. The equations prescribe the motion of the entire blade as a function of time. The numerical solution to the equations of motion is computed at each time step (Jonkman 2003).

AeroDyn gathers information about the turbine geometry, operating condition, blade-element velocity and location from input files and FAST program. It then uses this information to calculate the distributed forces on the turbine blades. These forces affect the blade deflections and vice versa. Typically, AeroDyn is called by FAST at each time step to calculate the changing aerodynamic (hydrodynamic) forces (Moriarty 2005).

Figure 3.10 shows an airfoil (hydrofoil) with the velocities and angles that

determine the forces on the element and also the induced velocities from the wake influence. Figure 3.11 shows the resultant aerodynamic (hydrodynamic) forces on the element and their components perpendicular and parallel to the rotor plane. These are the forces that dictate the thrust (perpendicular) and torque (parallel) of the rotor, which are the dominant forces for turbine design. In Figure 3.11, the angle relating the lift and drag of the airfoil element to the thrust and torque forces is the local inflow angle  $\phi$ . As shown in Figure 3.10, this inflow angle is the sum of the local pitch angle of the blade,  $\beta$ , and the angle of attack,  $\alpha$ . The local pitch angle is dependent on the static blade geometry, elastic deflections, and the active or passive blade pitch control system. The angle of attack is a function of the local velocity vector. Note in Figure 3.10 that the velocities of the element from blade deflections ( $v_{e-op}$  and  $v_{e-ip}$ ) affect the inflow angle and angle of attack (Moriarty 2005).

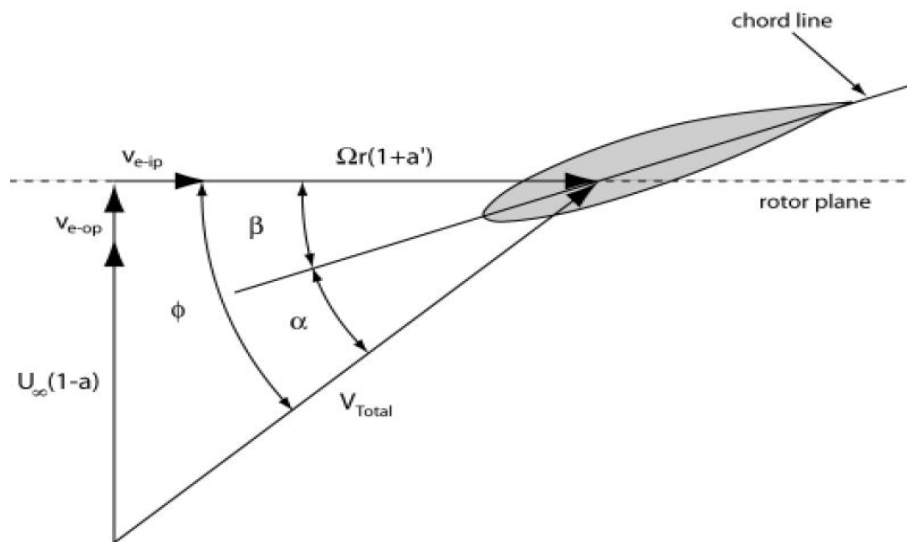


Figure 3.10 Local blade element velocities and flow angles (Moriarty 2005)

The inflow angle is determined based on the components of the local velocity vector. If the blade motion is significant, the local velocities must be included in the calculation of the inflow angle, as follows:

$$\tan \varphi = \frac{U_{\infty}(1 - a) + v_{e-op}}{\Omega r(1 + a') + v_{e-ip}} \quad (3.7)$$

Equation (3.7) holds for all elements of the blade along the span, although typically the inflow angle changes with element location. From blade element theory and Figure 3.11, the thrust (normal force  $F_N$ ) and torque (tangential force  $F_T$ ) on the blade element are (Moriarty 2005):

$$F_N = L \cos \phi + D \sin \phi \quad (3.8)$$

$$F_T = L \sin \phi - D \cos \phi \quad (3.9)$$

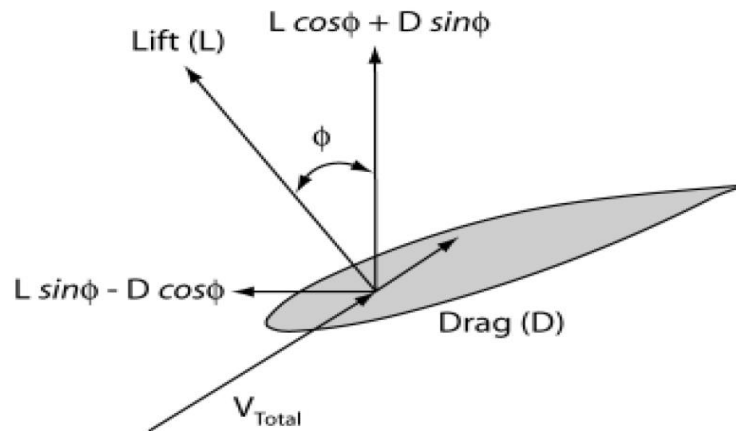


Figure 3.11 Local blade element forces (Moriarty 2005)

Using Equations (2.34) and (2.35), Equations (3.11) and (3.12) can be written as:



$$F_N = \rho B V_{\text{total}}^2 c (C_L \cos\phi + C_D \sin\phi) / 2 \quad (3.10)$$

$$F_T = \rho B V_{\text{total}}^2 c (C_L \sin\phi - C_D \cos\phi) / 2 \quad (3.11)$$

where  $\rho$  is the fluid density,  $B$  is the length of the blade element,  $V_{\text{Total}}$  is total induced flow velocity, and  $c$  is the chord length of the aerofoil.

An airfoil (hydrofoil) table for angles between  $-180^\circ$  and  $+180^\circ$  are shown in Table 3.8. The entries in the column of the table are angle of attack ( $\alpha$ ), lift coefficient ( $C_L$ ), drag coefficient ( $C_D$ ), and pitching moment coefficient ( $C_M$ ) separately. AeroDyn obtains all airfoil data by linear interpolation from the table. Normal force ( $F_N$ ) and tangential force ( $F_T$ ) are calculated and passed back to the dynamics routine (FAST). During a simulation, FAST numerically iterates to find the actual operating condition of each blade element at each time segment. A time step (DT) input for the constant-step-size numerical-integration scheme is used in FAST. Once the applied loads and motion of the entire system are characterized for a given time step, loads (forces and moments) at various critical points on the turbine are found by performing simple summations of these loads (Jonkman 2003).

Table 3.8 Airfoil( hydefoil)-date input file- fx77\_01486\_14

"fx77\_01486 Airfoil,DesignFoil data at Re=1.0 Million, Clean roughness"

Adjusted for Post Stall at r/R=0.204 by AirfoilPrep\_v2p2\_2. FAU.

1 Number of airfoil tables in this file

0 Table ID parameter

11 Stall angle (deg)\*\*

0 "No longer used, enter zero"

0 "No longer used, enter zero"

0 "No longer used, enter zero"

-2.0495 Zero Cn angle of attack (deg)

6.6090 Cn slope for zero lift (dimensionless)

1.5052 Cn extrapolated to value at positive stall angle of attack

-0.7232 Cn at stall value for negative angle of attack

5.00 Angle of attack for minimum CD (deg)

0.0078 Minimum CD value

-180.00 0.000 0.0100 0.0000

-170.00 0.370 0.0100 0.4000

-160.00 0.740 0.0822 0.0095

..... (Portion deleted for brevity)

-5.00 -0.389 0.0107 -0.0060

-4.00 -0.267 0.0101 -0.0050

-3.00 -0.145 0.0096 -0.0050

-2.00 -0.023 0.0092 -0.0050

-1.00 0.099 0.0088 -0.0040

0.00 0.221 0.0085 -0.0040

1.00 0.342 0.0089 -0.0040

2.00 0.464 0.0089 -0.0040

3.00 0.586 0.0085 -0.0050

4.00 0.707 0.0090 -0.0050

5.00 0.829 0.0078 -0.0050

6.00 0.942 0.0081 -0.0060

7.00 1.029 0.0091 -0.0070

8.00 1.097 0.0101 -0.0070

9.00 1.146 0.0137 -0.0080

10.00 1.179 0.0160 -0.0090

11.00 1.194 0.0189 -0.0100

12.00 1.192 0.0234 -0.0120

13.00 1.174 0.0284 -0.0130

14.00 1.139 0.0347 -0.0140

15.00 1.088 0.0424 -0.0160

16.00 1.013 0.0509 -0.0180

17.00 1.010 0.0591 -0.0190

18.00 0.996 0.0674 -0.0210

19.00 1.006 0.0753 -0.0230

20.00 1.057 0.0822 -0.0250

30.00 0.915 0.2497 -0.1010

40.00 0.837 0.4558 -0.1451

50.00 0.741 0.6763 -0.1835

60.00 0.604 0.8851 -0.2202

.....( Portion deleted for brevity)

160.00 -0.740 0.0822 -0.3521

170.00 -0.370 0.0100 -0.5000

180.00 0.000 0.0100 0.0000

### 3.2.6.2 OCT Blades Modeling with FAST and AeroDyn

AeroDyn and FAST were used to model an OCT blade. Sea water conditions such as viscosity and density of water, blade buoyancy, OCT blade added mass, etc. were considered in AeroDyn and FAST.

An added mass is created when the mass of water surrounding a body is accelerated or decelerated. The added mass is not accounted for wind turbine blade when formulating the blade equation of motion in relatively less dense air. The added mass needs to be considered when formulating the blade equation of motion for OCT blade in FAST since sea water is approximately 830 times denser than air. The OCT blades are also filled with PVC foam core materials (HCP 30). The added mass for the entire blade span with core material were calculated in Section 3.2.4 and are shown in Table 3.7. The blade mass is replaced by “All Mass” (blade mass + added mass) in FAST blade input file.

When OCT is submerged in sea water it experiences buoyancy force. FAST does not provide any procedure to represent the buoyancy effect. Buoyancies along the blade span were calculated as average as 21% of the blade section weight. Therefore, “Gravitational Acceleration” input was set to  $2.058 \text{ m/sec}^2$  (21% of  $9.8 \text{ m/sec}^2$ ) in FAST’s primary input file. Table 3.9 shows the ratio of net blade gravity to total mass along the blade span.

Table 3.9 Ratio of net blade gravity to total mass along the blade span

Section Station	Mass of Blade and Core (kg/m)	Added Mass (kg/m)	Total Mass (kg/m)	Buoyancy (kg/m)	Net Blade Gravity (kg/m)	Ratio of Net Blade Gravity to Total Mass
1	15.89	7.25	23.14	14.50	1.39	0.06
2	15.89	7.25	23.14	14.50	1.39	0.06
3	15.73	7.10	22.83	14.19	1.54	0.07
4	15.44	6.84	22.28	13.67	1.77	0.08
5	15.02	6.47	21.49	12.94	2.08	0.10
6	11.92	5.97	17.89	11.93	0.00	0.00
7	11.27	5.36	16.63	10.71	0.56	0.03
8	10.60	4.76	15.36	9.52	1.08	0.07
9	9.34	4.10	13.44	8.19	1.15	0.09
10	8.59	3.52	12.11	7.03	1.56	0.13
11	7.87	2.95	10.82	5.90	1.92	0.18
12	7.18	2.44	9.62	4.88	2.30	0.24
13	5.74	2.02	7.76	4.03	1.71	0.22
14	5.25	1.64	6.89	3.28	1.97	0.29
15	4.84	1.38	6.22	2.77	2.07	0.33
16	4.47	1.20	5.67	2.40	2.07	0.37
17	4.27	1.01	5.28	2.01	2.26	0.43
18	2.27	0.87	3.14	1.73	0.54	0.17
19	2.14	0.76	2.90	1.52	0.62	0.21
20	2.11	0.68	2.79	1.35	0.76	0.27
21	2.01	0.60	2.61	1.20	0.81	0.31
22	1.91	0.55	2.46	1.11	0.80	0.33
23	1.86	0.52	2.38	1.03	0.83	0.35
24	1.85	0.51	2.36	1.03	0.82	0.35
25	1.81	0.50	2.31	1.00	0.81	0.35
26	1.81	0.50	2.31	1.00	0.81	0.35
					Average	0.21

AeroDyn calculates the aerodynamic (hydrodynamic) loads on turbine blade elements based on velocities and positions provided by FAST. In AeroDyn, the input file allows the user to choose which "wind" file is to be used: the hub-height wind file or full-field turbulence wind files. If full-field turbulence "wind" files are

used, the input file needed for turbulent “wind” can be created using NREL’s TurbSim code (Jonkman & Buhl 2012).

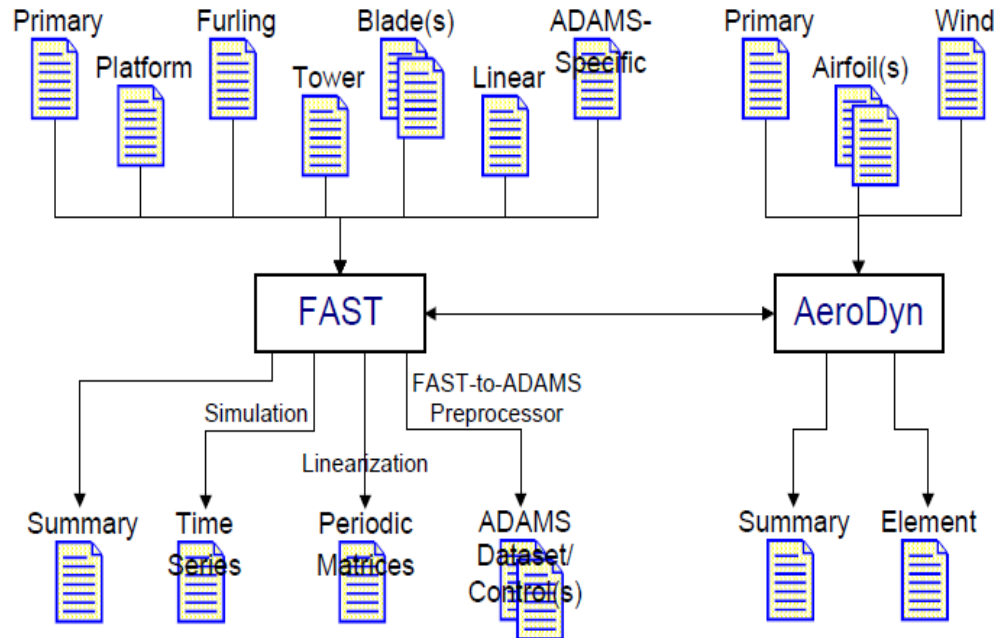


Figure 3.12 FAST and AeroDyn input and output files (Jonkman 2003)

FAST and AeroDyn generate one or more output files, with several options based on settings in the input file. Figure 3.12 shows FAST and AeroDyn input and output files. The primary output file (.out file) included time-series data, blade tip deflections, flapwise and edgewise shear force at blade root, flapwise and edgewise moment at blade root, local flapwise and edgewise moment at each blade section station and rotor power. Another main output file, the element file (.elm file), was generated by AeroDyn. This output element file is a tab-delimited time-series file containing "wind and aerodynamic" data for the blade elements

selected in the AeroDyn input file (.ipt file). The OCT blade element output file includes time-series data, Reynolds's numbers, lift coefficient, drag coefficient, pitching moment ( $M_P$ ), normal force ( $F_N$ ) and tangential force ( $F_T$ ) of each blade elements. The normal force is the component of the net force (lift and drag force) acting normal to the plane of rotation and tangential force is the component of the net force (lift and drag force) acting tangential to the plane of rotation. These characteristics are showed in Figure 3.13.

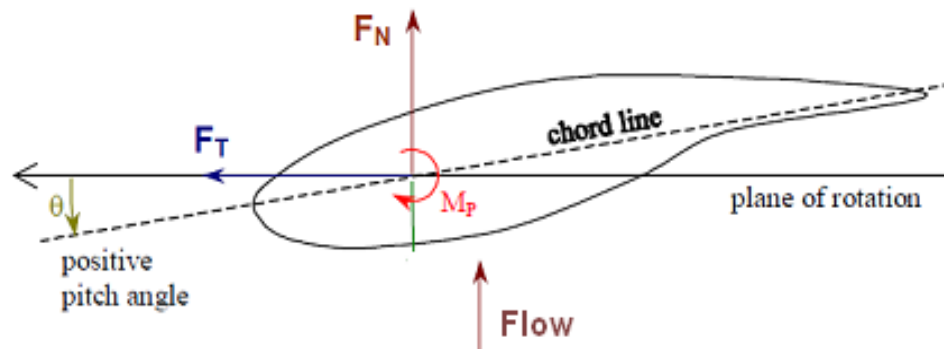


Figure 3.13 Cross-section view of a blade element indicating  $F_N$ ,  $F_T$ , and  $M_P$   
(Moriarty 2005)

For the OCT blade hydrodynamic simulation, the hub-height current input file was used. Each simulation examined the OCT blade subjected to a steady ocean current speed (0.5 m/s, 0.6 m/s ... 2.5 m/s), without velocity shear. Also, the viscosity and density values ( $1025 \text{ kg/m}^3$ ) were set for seawater in AeroDyn input files.

In FAST primary input file, a time-marching simulation selected for OCT analysis. The OCT simulations were run a time-marching analysis mode

without any pitch control and with a fixed rotation speed of 50RPM. The degrees of freedom (DOF)s of blades were enabled and all other DOFs such as tower, yaw, generator DOFs, etc., were disabled. Generator and gearbox parameters from Wind Turbine UAE VI Upwind/20KW (Jonkman 2005) were used for this OCT simulation. The Integration time step (DT) input was set to 0.0001 second.

### 3.2.6.3 OCT Blades Modeling Results and Discussion

The dynamic simulations for each mean current speed (0.5 m/s--2.5 m/s) were performed for the OCT blade using the FAST code. Some of the output results are shown as follows. The time histories of the blade root bending moments at 0.5 m/s, 1.5 m/s, and 2.5 m/s ocean current speed are shown in Figures 3.14, 3.15, and 3.16, respectively.

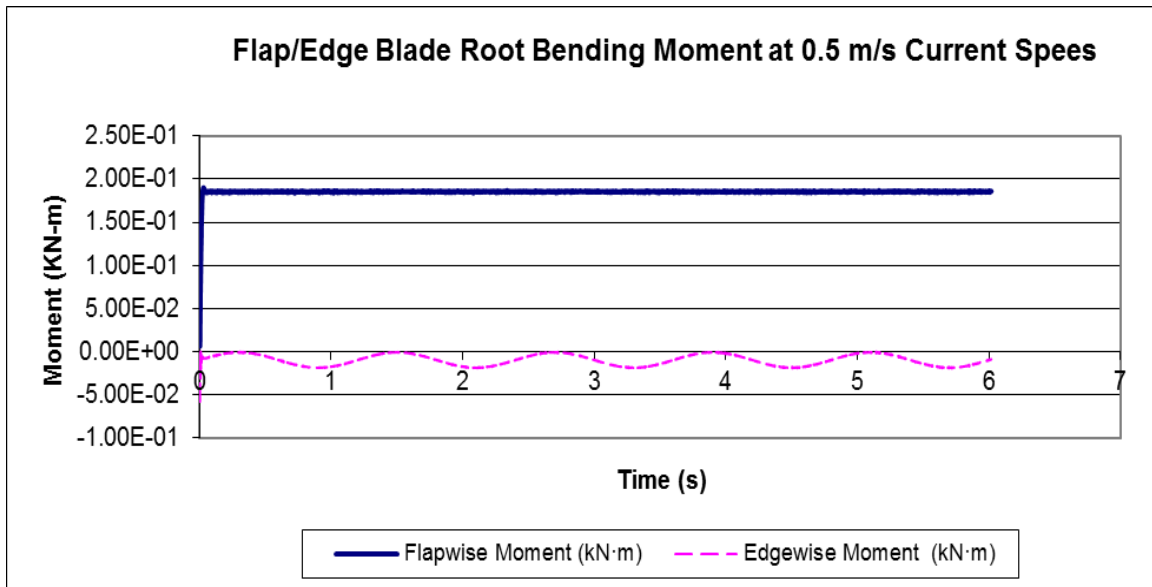


Figure 3.14 Flap/Edge bending moment of blade root at 0.5 m/s current speed

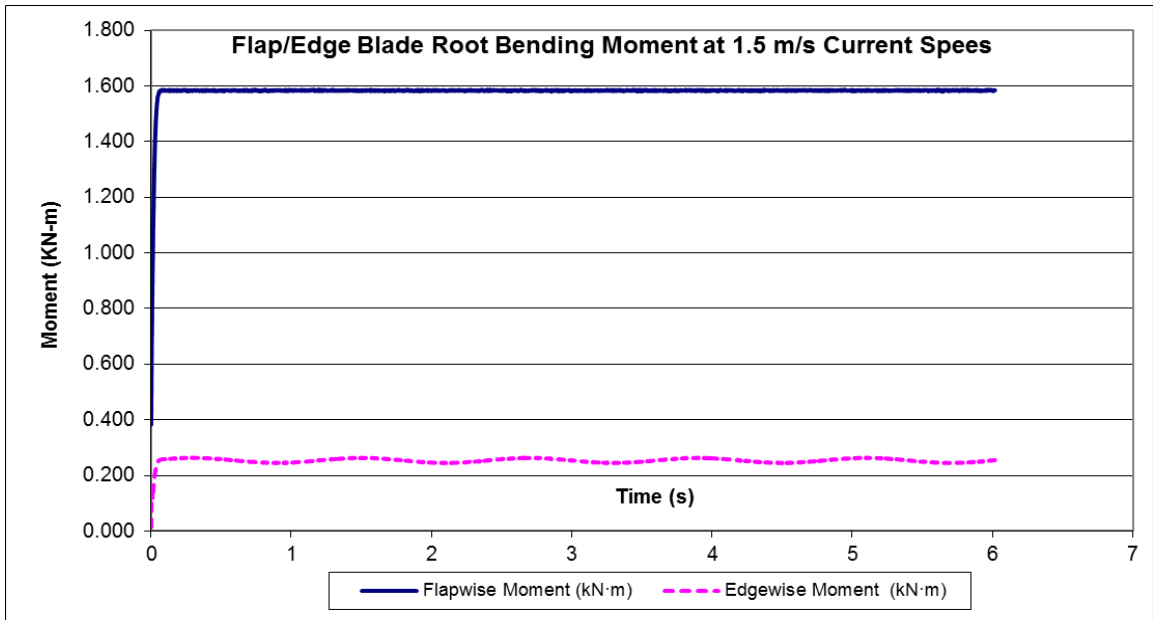


Figure 3.15 Flap/Edge bending moment of blade root at 1.5 m/s current speed

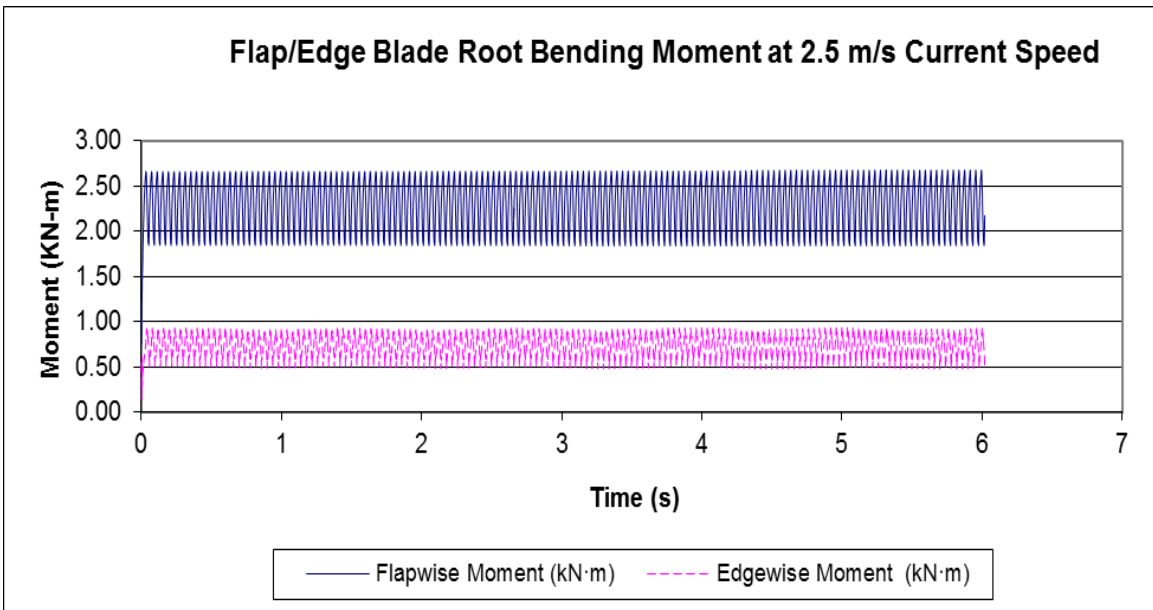


Figure 3.16 Flap/Edge bending moment of blade root at 2.5 m/s current speed



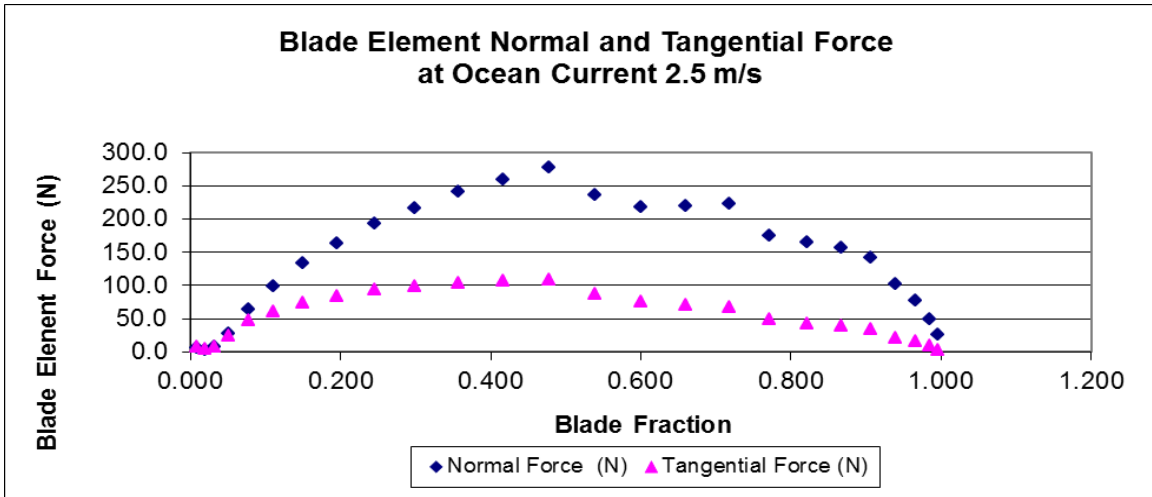


Figure 3.17 The normal and tangential force of each blade elements distributions calculated using FAST output at ocean current 2.5 m/s

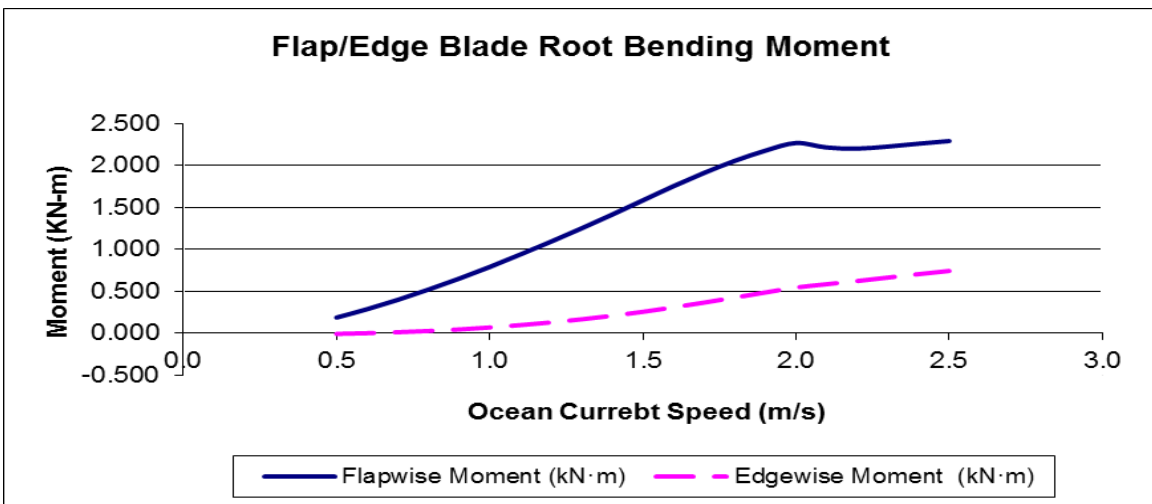


Figure 3.18 Variation of root flapwise and edgewise bending moment with ocean current speed

The normal force ( $F_N$ ) and tangential force ( $F_T$ ) of each blade elements along the blade span are shown in Figure 3.17. The normal forces (thrust) are noticeably larger than the tangential force, resulting in a larger flapwise bending moment than the edgewise moment (Figure 3.18). The variation of blade

root flapwise and edgewise bending moment with ocean current speed is shown in Figure. 3.18. The flapwise bending moment increases faster than the edgewise bending moment with the ocean current speed.

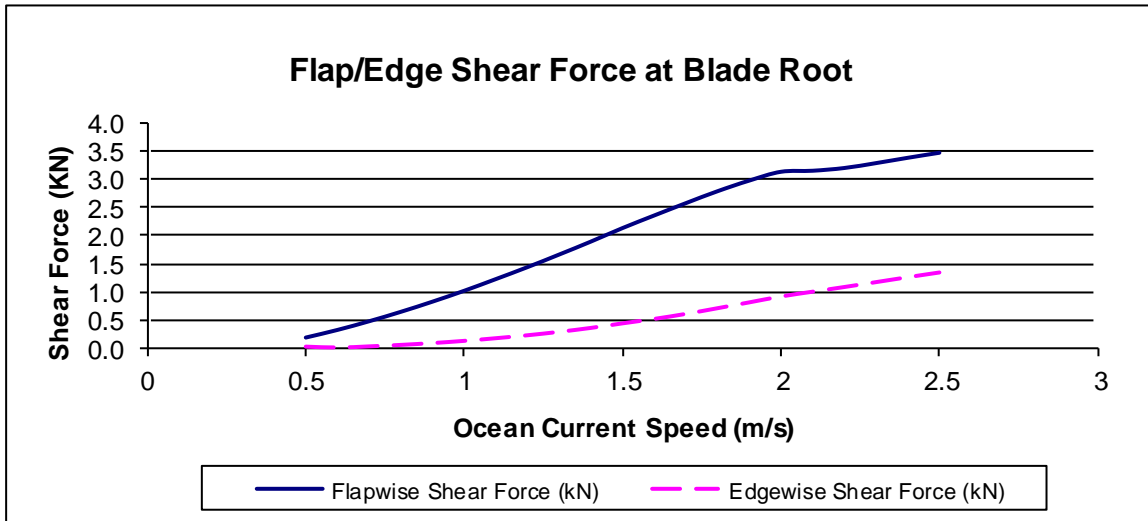


Figure 3.19 Variation of root flapwise and edgewise shear with ocean current speed

The variation of blade root flapwise and edgewise shear force with ocean current speed is shown in Figure 3.19. The flapwise and edgewise shear force at blade root are the sum total of normal force and tangential force of each blade element along the blade span. Again it is observed that the normal force increases faster than the tangential force.

The added mass effect for OCT blade was considered in BModes and FAST. The added mass coefficient was assumed as 0.5 in this dissertation. However, it is difficult to find accurate added mass coefficients of OCT blade from current offshore standards. The simulations for different the added mass coefficients (0.3, 0.5, and 0.7) at current speed 2.5 m/s were performed. Table 3.10 shows

the flapwise moment with different the added mass coefficients at blade root. It is obvious that the amplitude of the flapwise moment increases as the added mass coefficients increases. The amplitude of moment increment will affect the fatigue load on the blade, which decides the operational lifetime of the blade.

Table 3.10 Effect of added mass coefficients

Flap Moment (KN-m)	Without Added Mass	Added Mass Coefficient = 0.3	Added Mass Coefficient = 0.5	Added Mass Coefficient = 0.7
Min	1.880	1.860	1.846	1.835
Mean	2.294	2.292	2.291	2.290
Max	2.650	2.664	2.673	2.682
Amplitude	0.385	0.402	0.414	0.424

### 3.2.6.4 Comparison of FAST Results and CFD Results

A rotor with three-blades and having 1.6 meter radius was designed and analyzed during the first phase of testing (2011) by SNMREC with partner Embry-Riddle Aeronautical University (Borghetti et al. 2012). The predicted performance results from Computational Fluid Dynamics (CFD) and NREL's WT\_Perf (BEM code) are shown in Table 3.11 and Table 3.12. The flow conditions used were a 1.5 m/s current and 50 rpm rotor speed. The rotor hydrofoil and specifications (VanZwieten et al. 2011) were same as that in this dissertation. Normal force, edgewise moment and power results of 1.5 m radius rotor at 1.5 m/s current speed and 50 rpm rotor speed from FAST are shown in Table 3. 13. CFD and WT\_Perf results were compared with the FAST results.

Considering a 1.5 m radius rotor using in FAST, good agreement was observed between three sets of results.

Table 3.11 Drag (Normal force) and Moment (edgewise) results of 1.6 m radius rotor at 1.5 m/s current speed from CFD and NREL's WT\_Perf (Borghini 2012)

		Coefficient	Force/Torque
CFD	Drag	0.978	7781.95 N
	Moment	0.093	1111.40 N-m
BLADE ELEMENT METHOD	Drag	0.868	6900 N
	Moment	0.084	1100 N-m

Table 3.12 Power results of 1.6 m radius rotor at 1.5 m/s current speed from CFD and BEM (NREL's WT\_Perf) (Borghini 2012)

	Power (W)	Efficiency (%)
CFD	5819	48.8
BEM	5759	48.3
Freestream	11931	-

Table 3.13 Results of FAST, CFD, and WT\_Perf at 1.5 m/s current speed

	FAST (1.5 m radius)	CFD (1.6 m radius)	WT_Perf (1.6 m radius)
Total Normal force $F_N$ (N)	6405	7782	6900
Edgewise bending moment (N-m)	783	1111	1100
Rotor Power (W)	5730	5819	5759

### 3.3 OCT Blades Modeling with Sandia's NuMAD Codes

NuMAD is a stand-alone, GUI pre-processor for ANSYS finite element analysis software developed by Sandia National Laboratories. NuMAD is designed to enable users to quickly and easily create a three-dimensional model of a composite turbine blade for ANSYS analysis. This program also allows the user to extract blade section properties and modal curves to use as input into FAST. In order to have a comparison to the PreComp/BModes data and perform stress analysis, an ANSYS finite element blade model was created using NuMAD.

The required information of materials definition (materials, modulus, layer lay-up, and orientation) and geometric (hydrofoil, blade length, chord length, twist, and shear web) used by NuMAD are same as used by PreComp. E-glass/epoxy laminate QQ1 ( $\pm 45/0_4/\pm 45$ , thickness 4.088 mm) was selected as the material for blade surfaces and the shear web.

The first part of the NuMAD process is the definition of materials/material properties and hydrofoil shapes. Like PreComp, NuMAD stores a 'materials' file. Both isotropic and orthotropic materials can be defined. Once the materials are defined, they can be combined into composites. NuMAD allows the user to specify the thickness, material, and fiber orientation of each layer in a composite lamina. U14EU920 and VU-90079 was first defined as the orthotropic materials. QQ1\_1 (1 QQ1 laminate [ $\pm 45/0_4/\pm 45$ ]), QQ1\_2 (2 QQ1 laminates [ $\pm 45/0_4/\pm 45$ ]<sub>2</sub>), and QQ1\_3 (3 QQ1 laminates [ $\pm 45/0_4/\pm 45$ ]<sub>3</sub>) were then built layer - by - layer as shown in Figure 3.20.

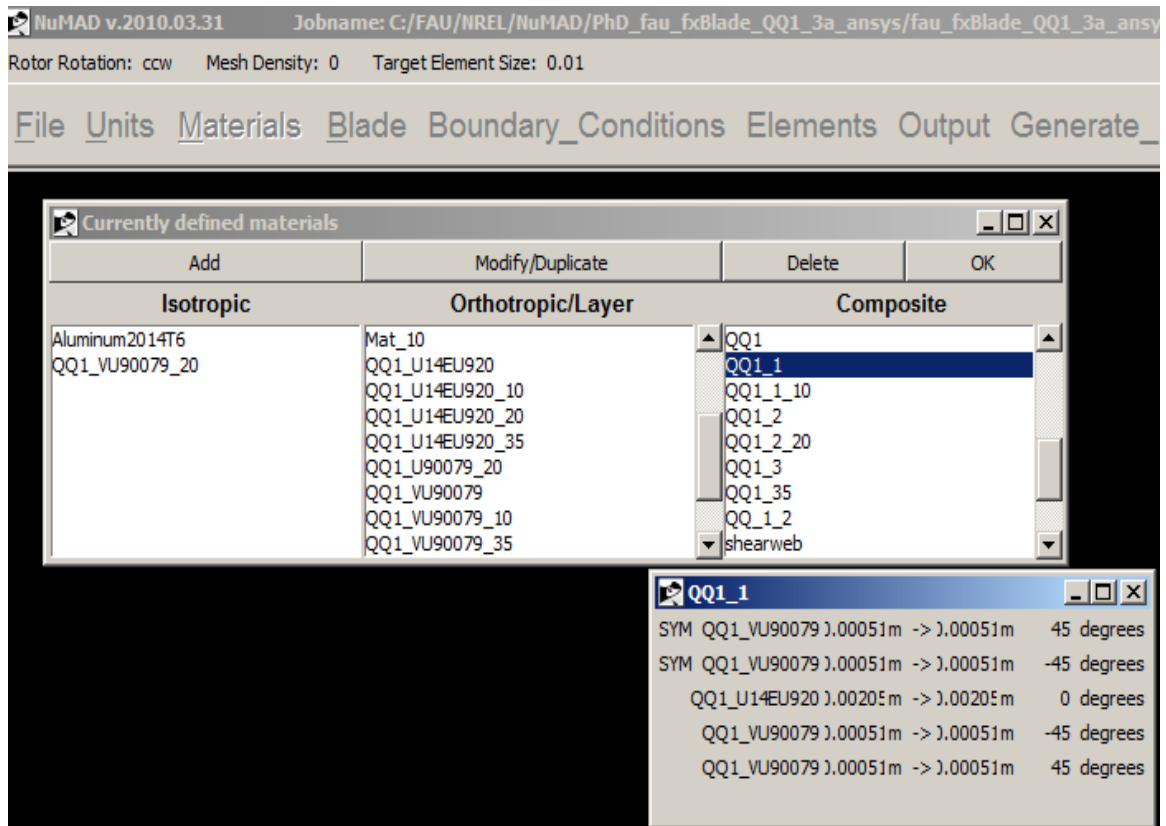


Figure 3.20 Materials and composites interface in NuMAD

Hydrofoil input files are required which are very similar to those used by PreComp. The difference is that the node numbering occurs in a different order (clockwise for PreComp vs. counterclockwise for NuMAD). Once the QQ1 composites and hydrofoils have been defined, the blade model was created through the graphical interface. The default blade is a 10m long and two stations with a circular cross section at each end. A total 26 blade stations were created at different locations along the blade. The section fractional distance, hydrofoil shape, blade twist, chord length, and aerodynamic center were be specified for each blade station (Table 3.2). Once all the stations have been added, each

station was specified with delineation point which corresponds to skin material divisions or shear web placements. Between these points, the skin material was selected from the list of defined composites. (Figure 3.21)

Table 3.2 Rotor design characteristics

Station Number	Radius (m)	Blade Fraction	Chord (m)	Twist (deg)	Hydrofoil
1	0.257	0	0.311	26.34	fx77_02349
2	0.277	0.016	0.311	26.34	fx77_02349
3	0.287	0.024	0.309	25.52	fx77_02336
4	0.306	0.04	0.305	24.07	fx77_02301
5	0.334	0.062	0.299	22.23	fx77_02273
6	0.371	0.092	0.29	20.22	fx77_02223
7	0.416	0.129	0.279	18.17	fx77_02162
8	0.469	0.171	0.267	16.13	fx77_02092
9	0.528	0.219	0.253	14.25	fx77_02012
10	0.593	0.271	0.239	12.47	fx77_01925
11	0.662	0.327	0.224	10.9	fx77_01832
12	0.735	0.386	0.21	9.5	fx77_01734
13	0.811	0.446	0.196	8.27	fx77_01633
14	0.888	0.508	0.182	7.22	fx77_01530
15	0.964	0.57	0.17	6.3	fx77_01486
16	1.04	0.631	0.159	5.49	fx77_01442
17	1.113	0.689	0.149	4.76	fx77_01400
18	1.182	0.745	0.14	4.1	fx77_01360
19	1.247	0.798	0.133	3.5	fx77_01323
20	1.306	0.845	0.127	2.95	fx77_01289
21	1.359	0.888	0.122	2.44	fx77_01258
22	1.404	0.924	0.118	1.99	fx77_01232
23	1.441	0.954	0.115	1.61	fx77_01211
24	1.469	0.977	0.114	1.3	fx77_01210
25	1.488	0.992	0.112	1.1	fx77_01210
26	1.498	1	0.112	0.99	fx77_01210

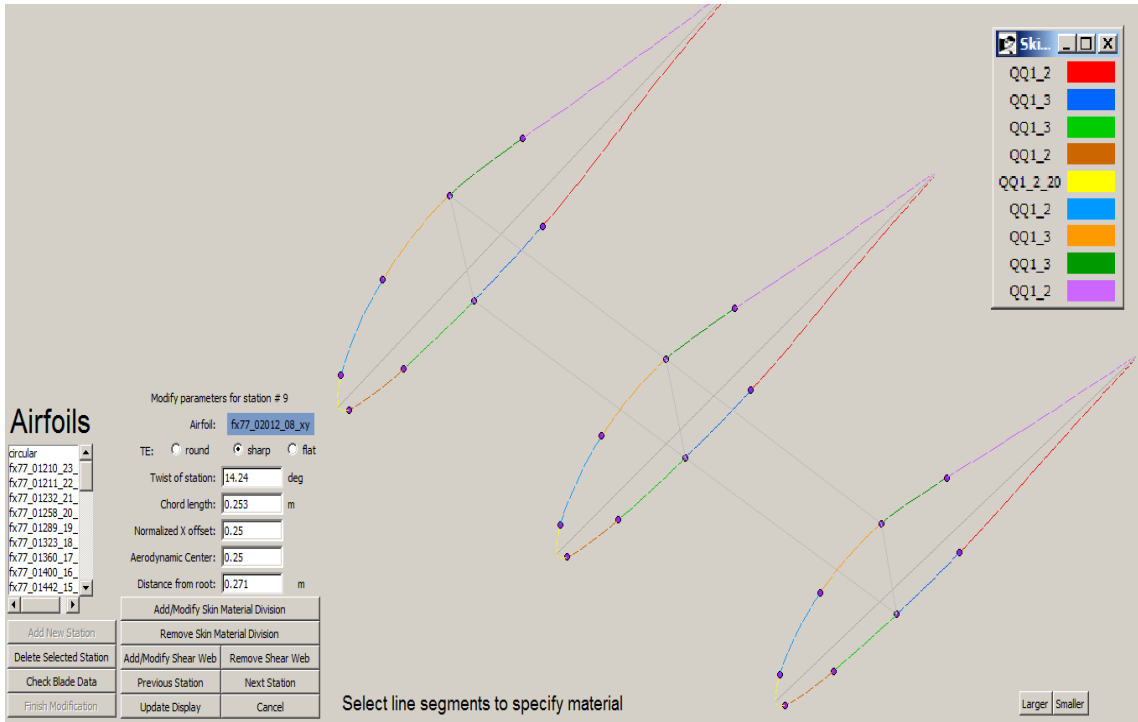


Figure 3.21 The delineation points at blade station

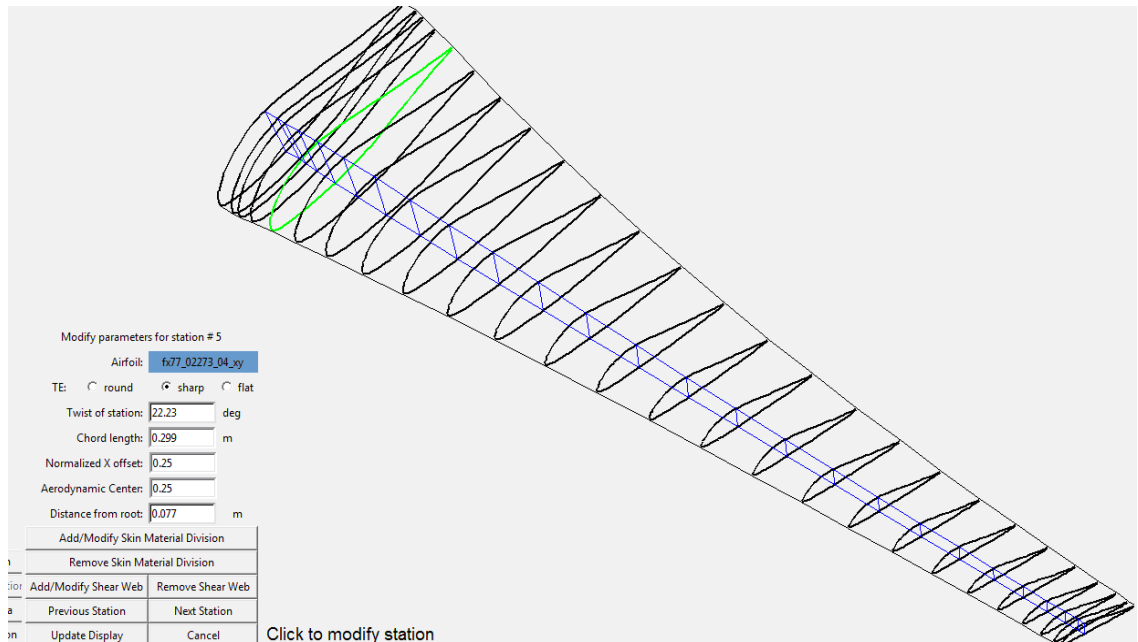


Figure 3.22 Final blade schematic representation after all stations and web have been added and modified



After all stations and web was defined, the resulting blade schematic looks like the one shown in Figure 3.22. Once the blade was designed, ANSYS model was generated for the blade structure. Some basic settings were used:

- Boundary\_Conditions ->Cantilevered
- Elements -> 8-node Structural Shells (Shell 281)
- Output -> ANSYS database (.db)
- Output -> FAST input->Set Blade Elements
- Generate\_Model -> Mesh Density -> Element Size ->  
Target Element Size 0.01m
- Generate\_Model-> Generate Now

NuMAD checks the geometry before generating the model in ANSYS. The program automatically interfaces with ANSYS and creates an ANSYS database for the blade. When using a NuMAD-generated OCT blade ANSYS model, the FX-77-W hydrofoil had a small radius of curvature problem at the leading edge. In ANSYS, the ratio of shell element thickness to radius of curvature of FX-77-W was unacceptable (the ratio is too high).

This problem was fixed by reducing the thickness of the shell elements in the leading edge region. Replace with the “new material” at the leading edge with an equivalent stiffness, but with smaller thickness and higher elastic constants. A “new material” was assigned to leading edge region (2% HP side - 2%chord LP side). This material had a density and stiffness of 10 times the original and a thickness of 1/10 scale the original (See NuMAD User's Manual, page 96 for

more details). Later, ANSYS stress results of leading edge region would be converted to real material stress by dividing by 10. Accordingly, QQ1\_1\_10, QQ1\_2\_20, and QQ1\_3\_35 were built layer - by - layer. Figure 3.23 shows the blade data check display for a successful blade design.

After the small radius of curvature problem was fixed, selection of "Generate\_Model" and "Generate Now" was initiated to create of an ANSYS file named "master.db". NuMAD generated all models using the ANSYS Shell element.

If "Output -> FAST input -> Set Blade Elements" was set, NuMAD also extracted the stiffness properties and modal shapes of the blade. NuMAD generated the sectional beam properties from a 3D ANSYS model through a functionality called the Blade Property Extractor (BPE). Basically, the BPE process is a technique to determine equivalent beam properties for a number of lengths along a three dimensional model of a structure. The section properties represent an effective, average value between NuMAD blade stations, except for the values at tip and root which are extrapolated. Tip and root values were determined using a linear extrapolation of the two midsection nodes at both the tip and the root of the blade (Figure 3.24). The results of these analyses were then stored in an output file which served as an input file for FAST. Table 3.14 shows the OCT blade properties extracted by NuMAD. Figure 3.25 shows OCT blade mode shapes extracted by NuMAD.

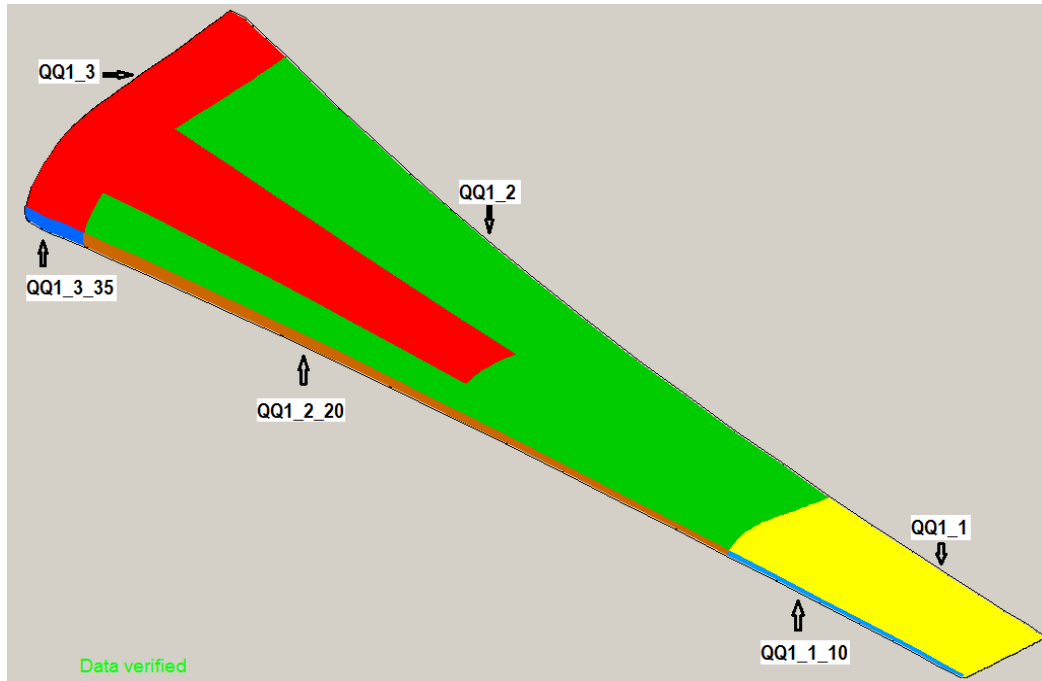


Figure 3.23 Blade data check display for a successful OCT blade design

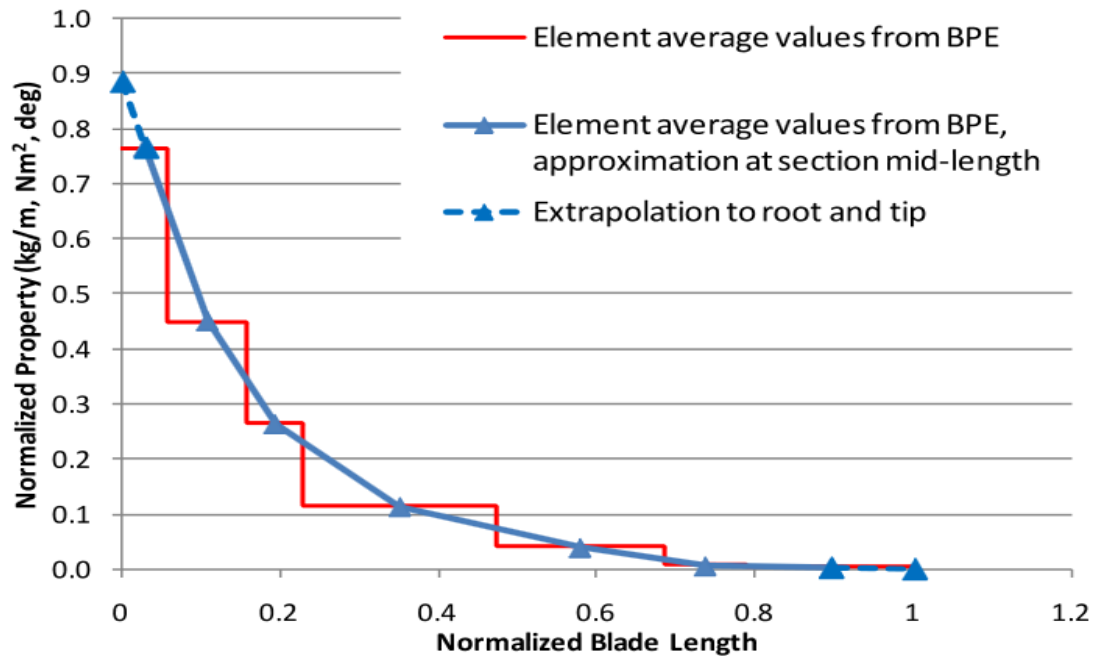


Figure 3.24 Blade property distributions (Laird 2009)

Table 3.14 Blade properties extracted by NuMAD

BIFract	AeroCent	StrcTwst	BMassDen	FlpStff	EdgStff
(-)	(-)	(deg)	(kg/m)	(Nm^2)	(Nm^2)
0.000	0.25	26.4	6.66667	342726	1.95E+06
0.008	0.25	27.0	3.50	42416	217463
0.020	0.25	27.9	5.00	373116	152664
0.032	0.25	24.3	4.21	21053	78495
0.051	0.25	21.0	3.93	18637	69400
0.077	0.25	18.1	4.05	20640	123234
0.110	0.25	16.0	3.78	20079	187062
0.149	0.25	14.8	3.58	19682	213986
0.195	0.25	13.1	3.39	14941	176080
0.245	0.25	11.1	3.23	12520	200975
0.299	0.25	9.4	3.04	8956	171688
0.356	0.25	8.0	2.88	6519	146208
0.416	0.25	6.7	2.76	4644	123811
0.477	0.25	5.6	2.47	3126	100605
0.539	0.25	4.6	2.24	2236	83122
0.600	0.25	3.7	2.11	1669	68646
0.660	0.25	3.0	1.92	1239	56014
0.718	0.25	2.2	1.74	906	50942
0.772	0.25	1.5	3.38	854	59918
0.822	0.25	0.9	3.22	767	66521
0.867	0.25	0.4	3.02	651	58524
0.906	0.25	-0.1	2.89	563	52786
0.939	0.25	-0.6	2.97	500	48458
0.965	0.25	-0.6	2.86	459	46958
0.984	0.25	-1.9	2.63	409	38431
0.996	0.25	-1.7	3.00	241	21398
1	0.25	-1.6	3.13	183	15525

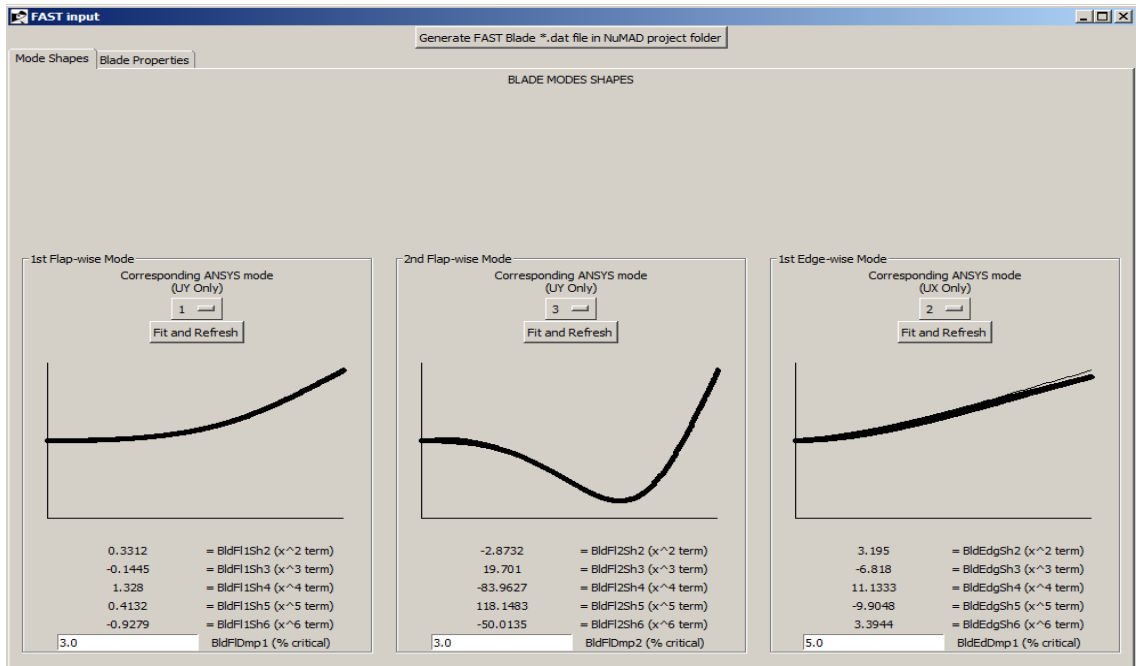


Figure 3.25 OCT blade mode shapes extracted by NuMAD

With the addition of the section properties/modal shapes file from NuMAD. There were two sets of data to input into FAST, and could compare the results.

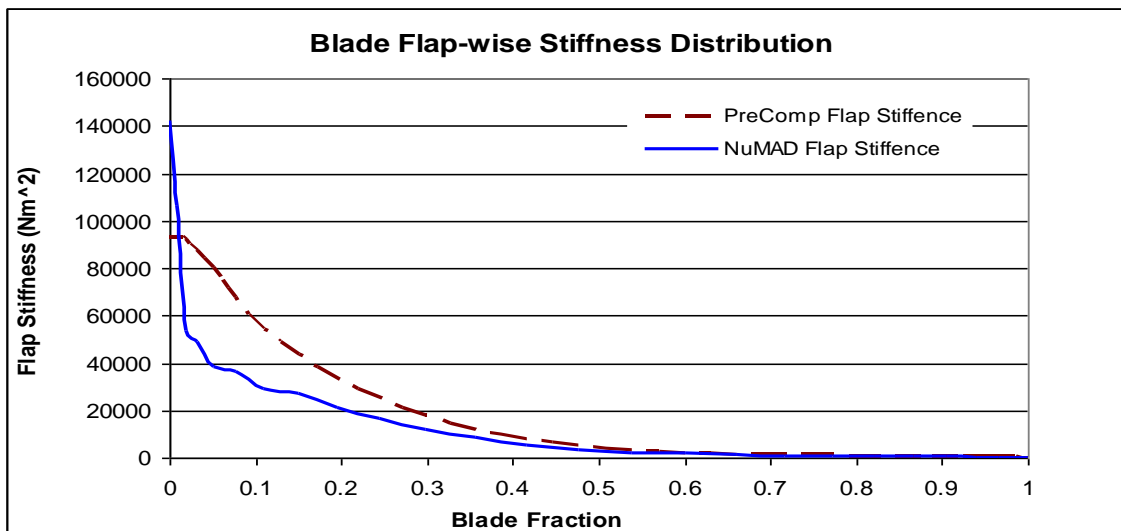


Figure 3.26 Distribution of flap stiffness generated by PreComp and NuMAD

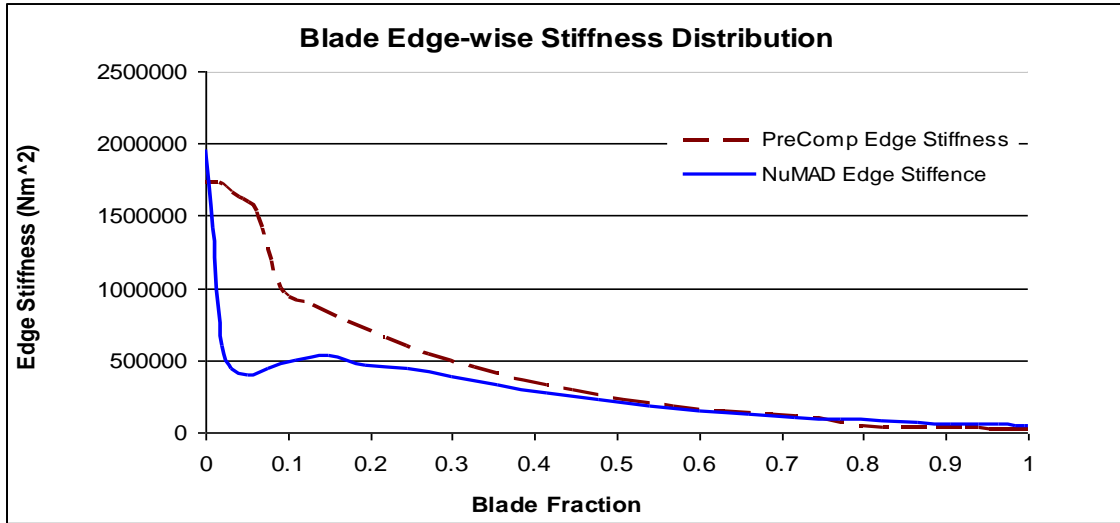


Figure 3.27 Distribution of edge stiffness generated by PreComp and NuMAD

Figure 3.26 and figure 3.27 show the comparison of the flap and edge stiffness generated by NuMAD and Precomp. It is seen that the flap stiffness of the blade calculated by NuMAD is significantly higher near the blade root. This discrepancy near the root is due to the properties at the tip and root are linearly extrapolated from the nearby sections and may be inaccurate. The actual values should be close to those generated by PreComp. The flap and edge stiffness calculated by PreComp are also larger than the values generated by NuMAD.

### 3.4 Modeling OCT Blade Using NREL Codes, NuMAD, and ANSYS

NuMAD is designed to enable users to quickly and easily create an ANSYS model. ANSYS model was generated by using the ANSYS SHELL281 element (size 0.01m) and selecting “cantilevered” boundary condition. SHELL281 (Figure 3.28) is suitable for analyzing thin to moderately-thick shell structures. It is

an 8-node element with six degrees of freedom at each node: translations in the x, y, and z axes, and rotations about the x, y, and z-axes. SHELL281 may be used for layered applications for modeling laminated composite shells that can take up to 250 layers. The final model consisted of 6624 elements and 19657 nodes. The finished ANSYS blade model is shown in Figure 3.29.

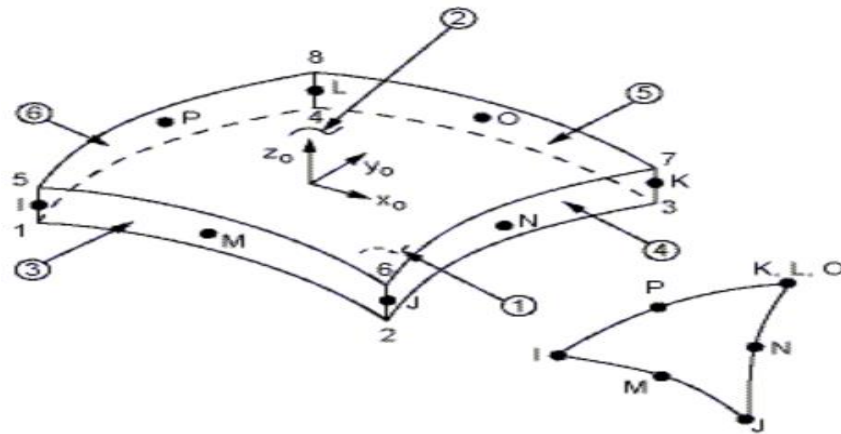


Figure 3.28 SHELL281 element geometry (ANSYS 2010)

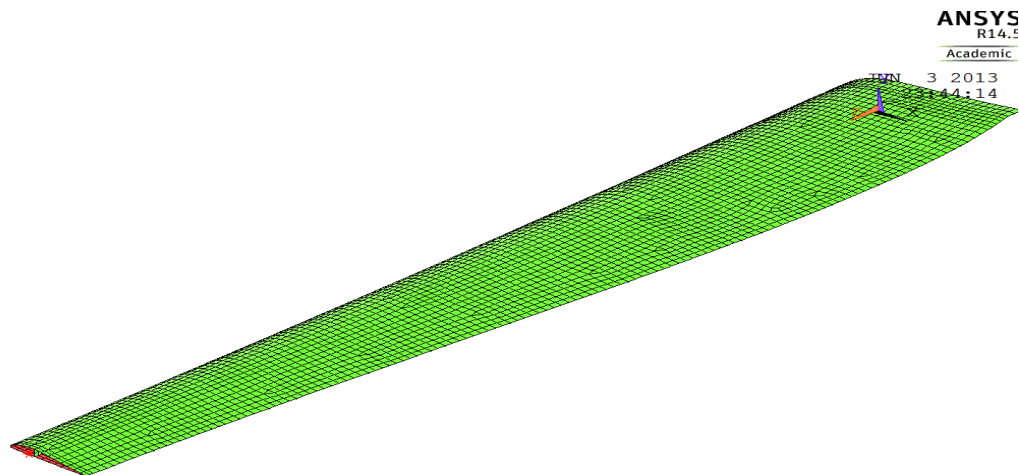


Figure 3.29 Finished ANSYS blade model

## CHAPTER 4. RESULTS AND DISCUSSION -- SIMULATION UNDER HYDRODYNAMICS LOADS

### **4.1 Load cases assumptions**

Ocean currents result from the wave, wind, Coriolis effect, temperature, salinity differences, tides and the earth's rotation. There are many factors that determine the strength of a current. Depth contours, shoreline configurations and interaction with other currents influence a current's direction and strength. OCT blades must be able to withstand the expected hydrodynamic loads due to varying ocean current and a set of ocean environmental conditions. It is often difficult to predict accurately loads on the OCT blade resulting from ocean current, wave, as well as turbine operation. No standards about OCT loading exist in U.S. now.

Germanischer Lloyd (GL) was founded in 1867 and is a technical supervisory organization based in the city of Hamburg, Germany. GL also is one of the leading certification organizations for wind turbines. GL developed its own rules and guidelines. Germanischer Lloyd (GL) has issued the draft " Guideline for Certification of Ocean Energy Converters Part 1: Ocean Current Turbines" (GL 2005) in 2005. Load assumptions are described in the draft GL Guideline of OCT (Chapter 4). Following are few related sections:



## Section 4.1 General

4.1(1) Loading of OCT results mainly from sea currents and wave interaction, as well as operational loads.

4.1(2) The load assumptions have to be prepared in relation to the intended service life of the structure under consideration. The design life time to be assumed for OCTs in this Guideline is 20 years.

4.1(3) Fatigue load analysis shall consider all conditions contributing to fatigue during transport, installation and operation during the intended lifetime.

4.1(4) Loads for fracture/ultimate strength and stability analysis include loading during extreme external conditions with a recurrence period of 50 years, during normal operation, maintenance, during or after activation of the safety system or/and occurrence of any single fault situation as well as during transport or installation of the ocean current turbine.

4.1(5) The general assumptions to be drawn for environmental conditions, load analysis, site assessment, safety level and documentation are described in Guideline for the Certification of Offshore Wind Turbines (GL WindEnergie, 2005) have to be applied in design and certification of an OCTs.

## Section 4.4.2 Design situations and load cases

### 4.4.2.1 Ultimate loading

(1) Ultimate loads may arise from the different design situations and environmental conditions in combination with the systems operation conditions (power production, start, stop and idling condition) or installation procedure. In

general a combined recurrence period of 50 years is considered for extreme environmental actions during operation. During installation, operation and fault occurrence normal environmental conditions with a recurrence period of up to 1-year shall be considered.

(2) The following table shows the basic combinations to be considered:

(3) For simplification, if joint probabilities of extreme situations are not exactly known, following load cases may be considered for ultimate load design (load group I). If no extra comments are given the OCT is either operating or parked. Where wind speed is given, the associated wind generated current and storm surge shall be considered.

- A. 50-year extreme regular current (tidal and circulation), combined with long term mean wave and wind speed. The wave direction can be assumed to be either in line or opposite to the current.
- B. 50-year extreme storm conditions (wind and wave), see [1], Chapter 4, combined with long term mean (absolute value) regular current. The direction of the storm may be arbitrary.
- C. 50-year extreme storm conditions (wind and wave) combined extreme water level tidal current. The direction of the storm may be arbitrary.
- D. 50-year extreme current (regular and wind induced), combined with storm surge and long term mean wave conditions. The mean wave direction may vary up to 30° from the mean current direction.
- E. Daily mean (long term) maximum current, combined with 1-year wave

conditions of any direction. The system is in operation.

F. Maximum regular cross-flow current, combined with 50-year extreme storm conditions (wind and wave) from any direction.

(4) The normal conditions to be considered during design for ultimate loading in combination with load group II and IV may be summarized in following list:

A. Variation of current between mean daily maximum and minimum, with associated water direction according to the tidal ellipsis. The direction of wind and waves may vary up to 30° from the direction in line or opposite to the regular current.

B. Long term mean (absolute value) regular current, combined with wind and wave conditions up to 1-year recurrence period. The misalignment between current and wind and waves shall be assumed to be arbitrary. Wind and waves shall be assumed to have a common direction.

C. Wind and wave conditions with 1-year recurrence period combined with 1-year recurrence water levels.

D. Current with a recurrence period of 1 year, combined with positive and negative storm surge. Direction arbitrary. Long term mean wave conditions.

Table 4.1 Load groups to be considered for design of ocean current turbines (GL 2005)

Load Group	Design condition	Environmental conditions	recurrence period
I	Normal operation, parked	Extreme	≤ 50 years
II	Operation, emergency stop, fault occurrence, parked after fault	Normal	≤ 1-year
III	Installation and Maintenance	To be defined by the designer	-
IV	Secured/Parked during installation	Normal	≤ 1-year

#### Section 4.4.2.2 Fatigue loading

(1) The fatigue load cases shall cover all variations of load having a considerable contribution during the system's lifetime. The lifetime shall be at least 20 years, see Chapter 1.

(2) The load cases to be used for fatigue analysis generally arise only from the combination of normal external and operating conditions. It is assumed in this context that other combinations will not have any significant effect on fatigue strength because they occur so rarely. The turbulence of the current quoted for normal external conditions are to be taken into account in the fatigue analysis.

(3) The combinations of load cases which are to be investigated in the fatigue analysis can be built by combining normal operation and occurrence of a fault if applicable with the environmental conditions shown in 4.4.2.1.

...

(8) All cases have to be weighted according to their probability of occurrence within the design life time of the system.

#### Section 4.4.2.4 Partial safety factors for loads

(1) The partial safety factors for the loads defined in [1], Chapter 4 shall be used for OCT too.

(2) In the case the current turbulence was not considered during fatigue analysis, an extra safety factor of 1.25 on the range of fatigue loads shall be used.

## 4.2 Safety Factors for OCT

According to Section 4.4.2.4 (1) of the draft GL Guideline for OCT, the partial safety factors for the loads defined in Guideline for the Certification of Offshore Wind Turbines (GL WindEnergie 2005) shall be used for OCT. The GL partial safety factors for wind blade loads and materials were used in this investigation for ultimate strength and fatigue life.

For each design load case, the appropriate type of analysis is stated by “F” and “U” in the Guideline of Offshore Wind Turbines. F refers to analysis of fatigue loads, to be used in the assessment of fatigue strength. U refers to the analysis of ultimate loads, such as analysis of exceeding the maximum material strength, analysis of tip deflection, and stability analysis. The design situations indicated with U are classified further as normal (N), extreme (E), abnormal (A), or transport and erection (T). The type of design situation (N, E, A, or T) determines the partial safety factor  $\gamma$  to be applied to the ultimate loads. These factors are given in Table 4.2.

### Hydrodynamic Loading

For an extreme design situation a normal turbine with extreme external conditions is considered. For hydrodynamic loading, the partial safety factor for ultimate loads in the analysis of the ultimate strength is:

$$\gamma_F (\text{ultimate loads}) = 1.35$$

For all design situations, the partial safety factor for the loads in the analysis of the fatigue strength is:

$$\gamma_F (\text{fatigue loads}) = 1.0$$

In the case the current turbulence was not considered during fatigue analysis, an extra safety factor is:

$$\gamma_F (\text{fatigue loads}) = 1.25$$

Table 4.2 Partial safety factors for loads  $\gamma_F$  (GL 2005)

Source of loading	Unfavourable loads				Favourable loads
	Type of design situation (see Table 4.3.1)				All design situations
	N Normal	E Extreme	A Abnormal	T Transport and erection	
Environmental	1.2	1.35	1.1	1.5	0.9
Operational	1.2	1.35	1.1	1.5	0.9
Gravity	1.1/1.35*	1.1/1.35*	1.1	1.25	0.9
Other inertial forces	1.2	1.25	1.1	1.3	0.9
Heat influence	–	1.35	–	–	0.9

\* in the event of the masses not being determined by weighing.

### Composite materials

According to Section 5.5.2.4 of draft GL Guideline of Offshore Wind, GL partial safety factors for composite materials are:

$$\gamma_{Mx} = \gamma_{M0} \prod_i C_{ix} \quad (3)$$

where the general factor  $\gamma_{M0} = 1.35$  for all analyses, and the reduction factors  $C_{ix}$  may be adjusted by the method of fabrication and material types.

To take account of influences on the material properties, the following

reduction factors shall be used in the short-term strength verification:

$$C_{1a} \text{ (influence of aging)} = 1.35$$

$$C_{2a} \text{ (temperature effect)} = 1.10$$

$$C_{3a} \text{ (hand lay-up laminate)} = 1.20$$

$$C_{4a} \text{ (non-post-cured laminate)} = 1.10$$

For strength analysis, which includes the effects of aging and temperature, automated layup, and a post-cured laminate, the GL partial safety factors for composite materials are:

$$\gamma_{Mx} = 1.35 [(1.35)(1.1)(1.2)(1.0)] = 2.406$$

The following reduction factors shall be used in the fatigue verification:

$$C_{1b} \text{ (curve of high-cycle fatigue for the load cycle number } N \text{ and slope parameter } m) = 1.35$$

$$C_{2b} \text{ (temperature effect)} = 1.10$$

$$C_{3b} \text{ (for unidirectional reinforcement products)} = 1.20$$

$$\text{(for non-woven fabrics and UD woven roving)} = 1.1$$

$$\text{(for woven fabrics and mats)} = 1.2$$

$$C_{4b} \text{ (for post-cured laminate)} = 1.20$$

$$\text{(for non post-cured laminate)} = 1.1$$

$$C_{4b} \text{ (for blade trailing edge)} = 1.0 \text{ to } 1.2$$

For fatigue analysis, the GL partial safety factors for composite materials are:

$$\gamma_{Mx} = 1.35 [(1.0)(1.1)(1.1)(1.0)(1.0)] = 1.634.$$

The following reduction factors shall be used in the stability analysis (against

buckling and wrinkling):

$C_{1c}$  (for massive laminates and the skin layers of sandwich structures, to account for the scattering of the moduli) = 1.1

(for core materials, to account for the scattering of the moduli) = 1.3

(for the core materials, if verified minimum characteristics are used)  
= 1.0

$C_{2c}$  (temperature effect) = 1.1

$\gamma_{FE}$  (linear FE computation) = 1.25

(nonlinear FE computation) = 1.1

For stability (buckling) analysis, the GL partial safety factors for materials are:

$$\gamma_{Mx} = 1.35 [(1.1)(1.1)(1.25)] = 2.042.$$

A total partial safety factors for loads and materials are computed and listed in Table 4.3. Depending on whether the current turbulence was considered, the load factor is 1.0 or 1.25 respectively for fatigue analysis.

Table 4.3 Partial safety factors for OCT blade

	Ultimate Strength	Fatigue	Buckling
Loads	1.35	1.0/1.25	1
Materials	2.406	1.634	2.042
Combined(Loads and Materials)	3.25	1.634/2.043	2.042



### 4.3 Ultimate loads on OCT blades

The main load cases to be considered are ultimate loading and fatigue loading. Load case "Maximum regular cross-flow current, combined with 50-year extreme storm conditions (wind and wave) from any direction", defined in Section 4.4.2.1 (3) (F) of draft GL Guideline was considered as ultimate load case for the OCT blade simulation.

#### 4.3.1 Maximum regular cross-flow current

The Florida Current measurements were collected by SNMREC over a period of more than 13 months. Ocean current measurements were taken off of Southeast Florida (Lat: 26° 04.3' N, Lon: 79° 50.5' W). These measurements show that the current speed at a depth of 25 m was between 0.5 and 2.5 m/s. Ocean current speed 2.5 m/s is considered as the maximum regular cross-flow current.

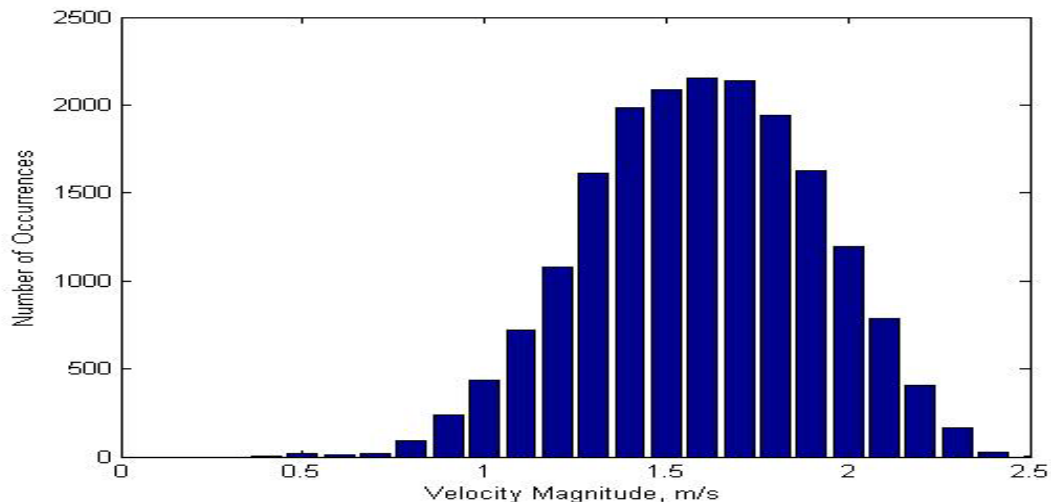


Figure 3.3 Histogram of the current speed at a depth of 25 m measured by the SNMREC at 30 minute intervals over a period of 13 months

### **4.3.2 Extreme storm conditions**

A hurricane is a type of tropical cyclone or severe tropical storm that forms in the southern Atlantic Ocean, Caribbean Sea, Gulf of Mexico, and in the eastern Pacific Ocean. All Atlantic and Gulf of Mexico coastal areas are subject to hurricanes. South Florida has quite a history with hurricanes. Hurricane Andrew hit South Florida in August 1992. Andrew brought very high winds. According to data from National Climatic Data Center (NOAA), maximum sustained surface wind speed, which is a 1-minute average, was estimated to have been 125 knots (about 145 mph).

Wind speed 145 mph (65 m/s) was considered as “50-year extreme storm condition” for OCT ultimate load case.

### **4.3.3 Ekman Solution for wind-driven current**

Ekman layer is a vertical region of the ocean affected by the movement of wind-driven surface waters. Ekman motion theory was investigated by Vagn Walfrid Ekman. At the surface of the ocean, the source of friction is the wind stress. Wind speeds are typically much bigger than ocean currents so that there is a frictional stress at the ocean surface. Within the oceanic Ekman layer, the wind stress is balanced by the Coriolis force and frictional forces. The surface water is directed at an angle of  $45^\circ$  to the wind, to the right in the Northern Hemisphere and to the left in the Southern Hemisphere. Ekman theory explains the theoretical state of circulation if water currents were driven only by the

transfer of momentum from the wind. After making a series of assumptions, Ekman obtained a mathematical solution to this problem in 1904. (Oceanworld 2004)

The assumptions made by Ekman were:

No boundaries;

Infinitely deep water;

Eddy viscosity,  $A_z$ , is constant (this is now known not to be totally true);

The wind forcing is steady and has been blowing for a long time;

Barotropic conditions with no geostrophic flow;

The Coriolis parameter,  $f$ , is kept constant.

Ekman assumed a steady, homogeneous, horizontal flow with friction on a rotating Earth. Thus horizontal and temporal derivatives are zero:

$$\frac{\partial}{\partial t} = \frac{\partial}{\partial x} = \frac{\partial}{\partial y} = 0 \quad (4.1)$$

Ekman further assumed vertical eddy viscosity  $A_z$  as a constant.

$$T_{xz} = \rho_w A_z \frac{\partial u}{\partial z}, \quad T_{yz} = \rho_w A_z \frac{\partial v}{\partial z} \quad (4.2)$$

where  $T_{xz}$ ,  $T_{yz}$  are the components of the wind stress in the x, y directions, u and v are the velocities in the x and y directions, and  $\rho_w$  is the density of sea water. (Oceanworld 2004)

The simplified equations for the Coriolis force in the x and y directions for a homogeneous, steady-state, turbulent boundary layer above or below a horizontal surface are:

$$\frac{1}{\rho} \frac{\partial T_{xz}}{\partial z} = -fv \quad (4.3)$$

$$\frac{1}{\rho} \frac{\partial T_{yz}}{\partial z} = fu \quad (4.4)$$

where  $f$  is the local Coriolis parameter,  $f = 2\Omega \sin\phi$ . The rotation rate of the Earth  $\Omega = 7.2921 \times 10^{-5}$  rad/s,  $\phi$  is the latitude of position.

Using Equations (4.2), Equations (4.3) and (4.4) can be rewritten in terms of the vertical eddy viscosity  $A_z$  term (Oceanworld 2004):

$$fv + A_z \frac{\partial^2 u}{\partial z^2} = 0 \quad (4.5)$$

$$-fu + A_z \frac{\partial^2 v}{\partial z^2} = 0 \quad (4.6)$$

In order to solve this system of two differential equations, two boundary conditions can be applied:

$$u \rightarrow 0, \text{ as } z \rightarrow \infty$$

$$v \rightarrow 0, \text{ as } z \rightarrow \infty$$

The Equations (4.5) and (4.6) have solutions:

$$u = V_0 \exp(az) \sin(\pi/4 - az) \quad (4.7)$$

$$v = V_0 \exp(az) \cos(\pi/4 - az) \quad (4.8)$$

The constants are (Oceanworld 2004):

$$V_0 = \frac{T}{\sqrt{\rho_w^2 f A_z}} \quad \text{and} \quad a = \sqrt{\frac{f}{2A_z}} \quad (4.10)$$

and  $V_0$  is the velocity of the current at the sea surface.

The wind stress  $T$  is well known, and Ekman used:

$$T_{yz} = T = \rho_{air} C_D U_{10}^2 \quad (4.11)$$

where  $\rho_{air}$  is the density of air,  $C_D$  is the drag coefficient, and  $U_{10}$  is the wind speed at 10m above the sea. Ekman turned to the literature to obtain values for  $V_0$  as a function of wind speed. He found (Oceanworld 2004)::

$$V_0 = \frac{0.0127}{\sqrt{\sin |\varphi|}} U_{10}, \quad |\varphi| \geq 10 \quad (4.12)$$

With this information, he then calculated the velocity as a function of depth knowing the wind speed  $U_{10}$  and wind direction.

Ekman proposed that the thickness of the depth  $D_E$  at which the current velocity is opposite to the velocity at the surface, is:

$$D_E = \sqrt{\frac{2\pi^2 A_z}{f}} \quad (4.13)$$

Using Equations (4.10), (4.11), (4.12), and (4.13), Ekman layer depth was written as (Oceanworld 2004):

$$D_E = \frac{7.6}{\sqrt{\sin |\varphi|}} U_{10} \quad (4.14)$$

The constant in Equation (4.14) is based on  $\rho_w = 1027 \text{ kg/m}^3$ ,  $\rho_{\text{air}} = 1.25 \text{ kg/m}^3$ , and Ekman's value of  $C_D = 2.6 \times 10^{-3}$  for the drag coefficient.

For northern hemisphere, the current velocity at a depth  $Z$  is:

$$u_Z = V_0 \sin\left(\frac{\pi}{4} + \frac{\pi}{D_E} Z\right) \exp\left(-\frac{\pi}{D_E} Z\right) \quad (4.15)$$

$$v_Z = V_0 \cos\left(\frac{\pi}{4} + \frac{\pi}{D_E} Z\right) \exp\left(-\frac{\pi}{D_E} Z\right) \quad (4.16)$$

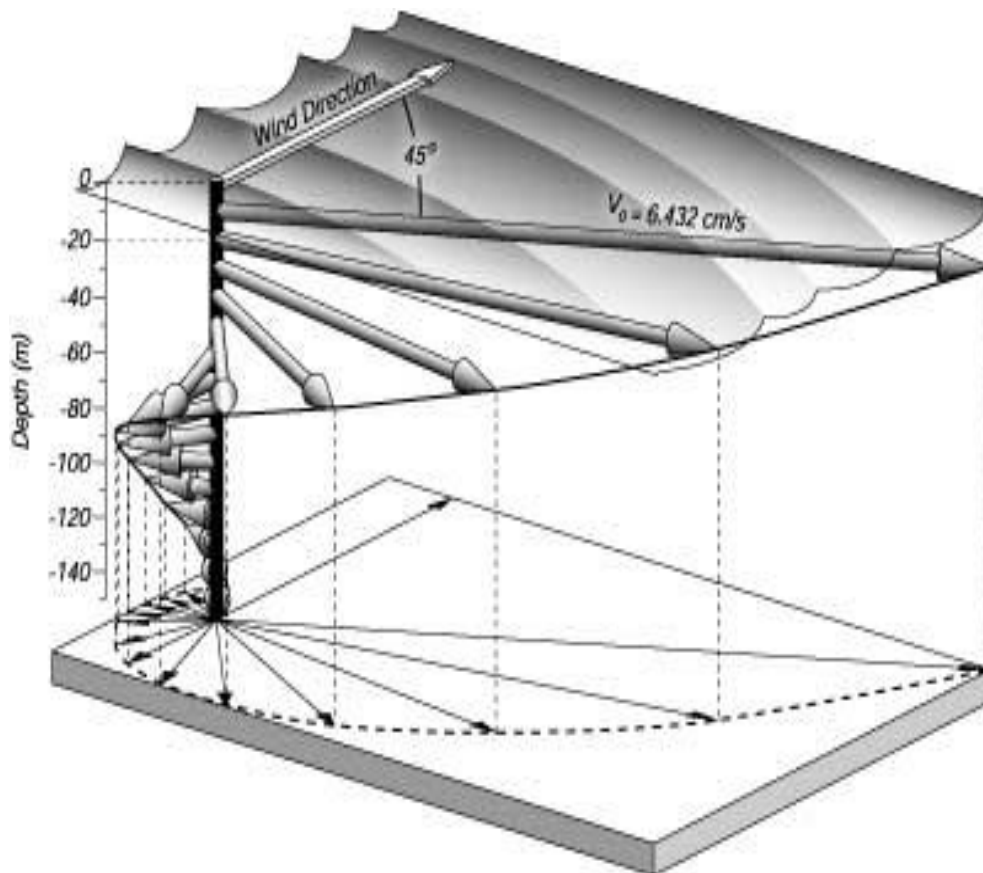


Figure 4.1 Ekman current generated by wind (Oceanworld 2004)

## Hurricane- Driven Current Velocity

Ekman Solution assumes wind forcing is steady and has been blowing for a long time. Although hurricanes do not satisfy these assumptions, Ekman Solution can still be used to predict the hurricane- driven current velocity. The results by using Ekman Solution are an extreme case.

Wind speed 145 mph (65 m/s) is considered as “50-year extreme storm condition” for OCT ultimate load case.

Using Equation (4.12), the velocity of the current at the sea surface was computed:

$$V_0 = \frac{0.0127}{\sqrt{|\sin|\varphi|}} U_{10} = \frac{0.0127}{\sqrt{|\sin|26|}} 65 = 1.24m / s$$

where

$U_{10}$  (wind speed at 10m above the sea) = 65 m/s,

$\varphi = 26^\circ$  (position at Lat:  $26^\circ 04.3'$ ).

From Equation (4.14), Ekman layer depth  $D_E$  was obtained:

$$D_E = \frac{7.6}{\sqrt{|\sin|\varphi|}} U_{10} = \frac{7.6}{\sqrt{|\sin|26|}} 65 = 895m$$

Using Equations (4.7) and (4.8), the current velocity at a depth 25 m was found:

$$V_{-25} = V_0 \exp\left(\frac{\pi}{D_E} Z\right) = 1.24 \exp\left(\frac{\pi}{895} (-25)\right) = 1.0m / s$$

Load case for "Maximum regular cross-flow current, combined with 50-year extreme storm conditions (wind and wave) from any direction" was considered as ultimate load case for our OCT blade simulation. Maximum regular cross-flow current velocity is 2.5 m/s and wind-driven current velocity at extreme storm condition (Hurricane Category 5) is 1.0 m/s. The combined maximum current velocity 3.5 m/s was considered as ultimate load case.

#### **4.3.4 Deterministic Ultimate load for OCT Blade**

The hydrodynamic normal force ( $F_N$ ) and tangential force ( $F_T$ ) were calculated by running FAST (combined with AeroDyn) at a current speed of 3.5 m/s for turbine normal operation (50RPM) and parked condition. Comparing two results, it was observed that  $F_N$  and  $F_T$  were larger at turbine normal operation. There are total 25  $F_N$  and  $F_T$  along the blade span, with each having a distance from the root corresponding to the center of the blade element in AeroDyn. These loads were multiplied by a safety factor of 3.25 as the ultimate load in Table 4.4.

#### **4.4 OCT Blade Static Analysis**

A linear static analysis was performed with the ultimate loads derived from a FAST analysis. The ultimate loads (25  $F_N$  and  $F_T$  along the blade span) in Table 4.4 were applied at nearby nodes along the blade's pitch axis as shown in the FE model of ANSYS (Figure 4.2).



Table 4.4 Normal force ( $F_N$ ), Tangential force ( $F_T$ ) and Ultimate loads

Node	Center of Blade Element to Root (m)	$F_N$ (N)	$F_T$ (N)	Safety Factor	Ultimate Load $F_N$ (N)	Ultimate Load $F_T$ (N)
1	0.267	16.2	15.7	3.25	52.8	50.9
2	0.282	8.1	7.8	3.25	26.3	25.3
3	0.297	18.7	15.5	3.25	60.6	50.4
4	0.320	44.5	37.7	3.25	144.6	122.4
5	0.353	81.1	62.3	3.25	263.4	202.4
6	0.394	125.0	85.7	3.25	406.2	278.5
7	0.443	167.1	106.3	3.25	543.2	345.5
8	0.499	196.3	116.0	3.25	638.1	377.0
9	0.561	224.2	124.2	3.25	728.5	403.6
10	0.628	246.4	129.3	3.25	800.8	420.2
11	0.699	271.4	135.9	3.25	882.0	441.6
12	0.773	292.0	139.4	3.25	949.0	453.2
13	0.849	312.6	141.4	3.25	1015.9	459.7
14	0.926	251.5	100.5	3.25	817.3	326.5
15	1.002	239.0	92.1	3.25	776.7	299.4
16	1.076	258.2	87.7	3.25	839.1	284.9
17	1.147	266.5	82.1	3.25	866.1	267.0
18	1.214	214.5	63.3	3.25	697.0	205.7
19	1.276	191.1	59.2	3.25	621.2	192.5
20	1.332	197.5	55.0	3.25	641.9	178.6
21	1.381	179.5	52.1	3.25	583.5	169.2
22	1.422	134.3	33.1	3.25	436.5	107.7
23	1.454	100.7	28.1	3.25	327.2	91.4
24	1.478	70.9	17.5	3.25	230.4	56.9
25	1.493	42.3	9.9	3.25	137.4	32.1

Maximum stress theory states that failure will occur in the multi-axial state of stress when the maximum stress induced in a material exceeds the ultimate tensile or compressive strength. The QQ1 ultimate tensile strength and compressive strength were selected from the DOE/MSU Composite Material Database.

Figure 4.3 shows the bending stress along the blade span. Figure 4.4 shows the maximum and minimum of stress at blade root. During NuMAD-generated OCT blade ANSYS model, the hydrofoil had a small radius of curvature problem at the leading edge. This problem was fixed by replacing a “new material” with stiffness of 35 times the original and a thickness of 1/35 scale the original in the leading edge region. In consideration of the material in blade root leading edge region had a stiffness of 35 times the original, ANSYS stress results of leading edge region would be converted to real material stress by dividing by 35. Table 4.5 shows the stresses at blade root completed by ANSYS at the ultimate loads. The maximum compressive stress of the blade is -291 MPa at 36% of span. The maximum tensile stress is 143 MPa at blade root. It was revealed that the highest concentrations of stress were at the root. In blade root, the maximum tensile and compressive stresses are 143 MPa and -281MPa, respectively. All of these stresses fell well within the allowable tensile and compressive strength of the QQ1 E-glass composite material. The QQ1 E-glass/epoxy composite lamina was adequate for this OCT turbine blade.

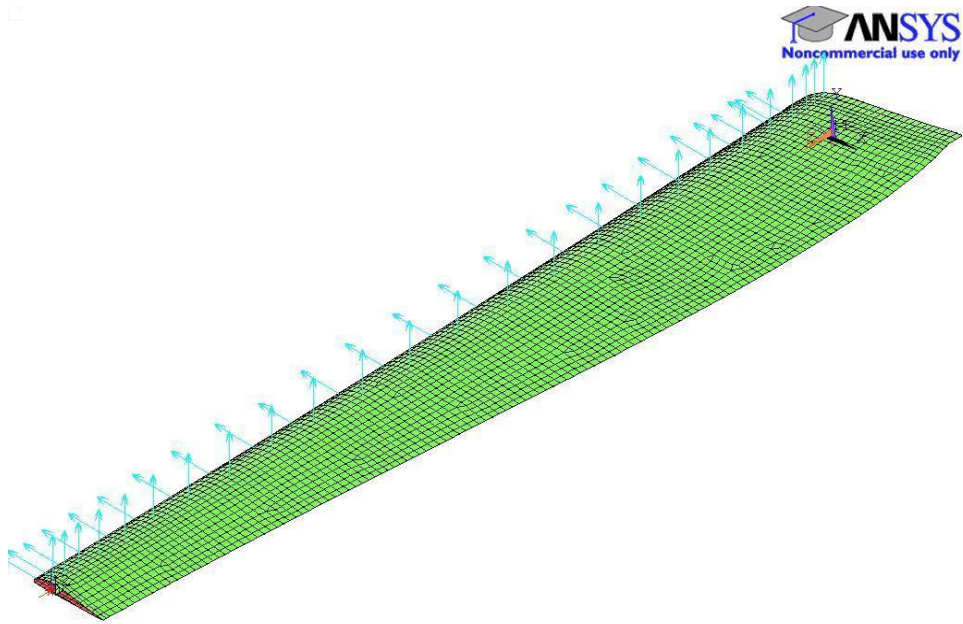


Figure 4.2 The ultimate loads applied at nearby nodes along the blade's pitch axis of blade FE model in ANSYS

Table 4.5 Stresses at blade root computed by ANSYS at the ultimate loads

Stresses Results	X-Axis (Edge-wise) (MPa)	Y-Axis (Flap-wise) (MPa)	Z-Axis (Along the blade ) (MPa)
Max	21	12	143
Min	-15	-10	-291
QQ1 ultimate tensile strength	150	-	827
QQ1 ultimate compressive strength	-261	-	-654

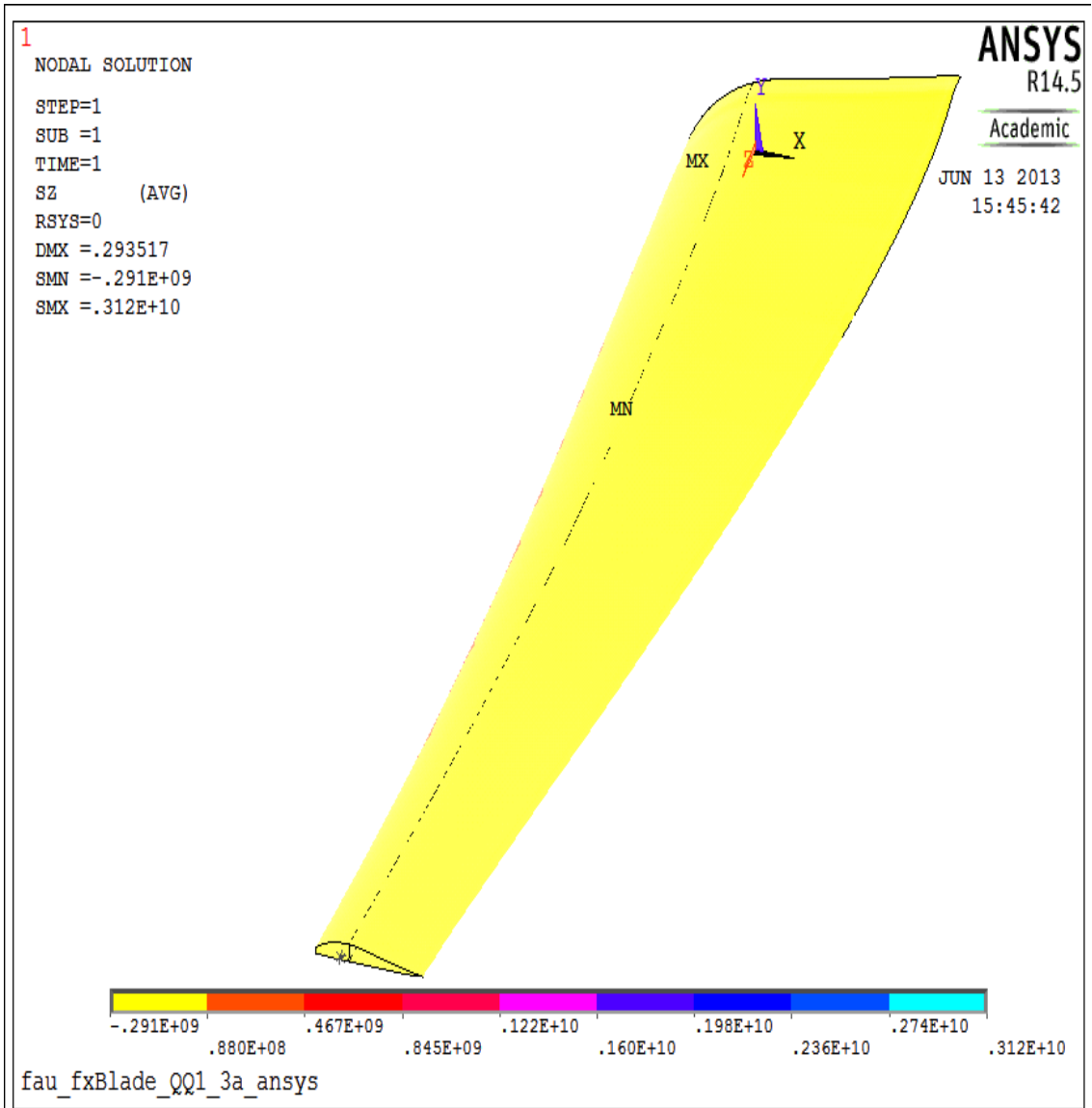


Figure 4.3 Bending stress along the blade span

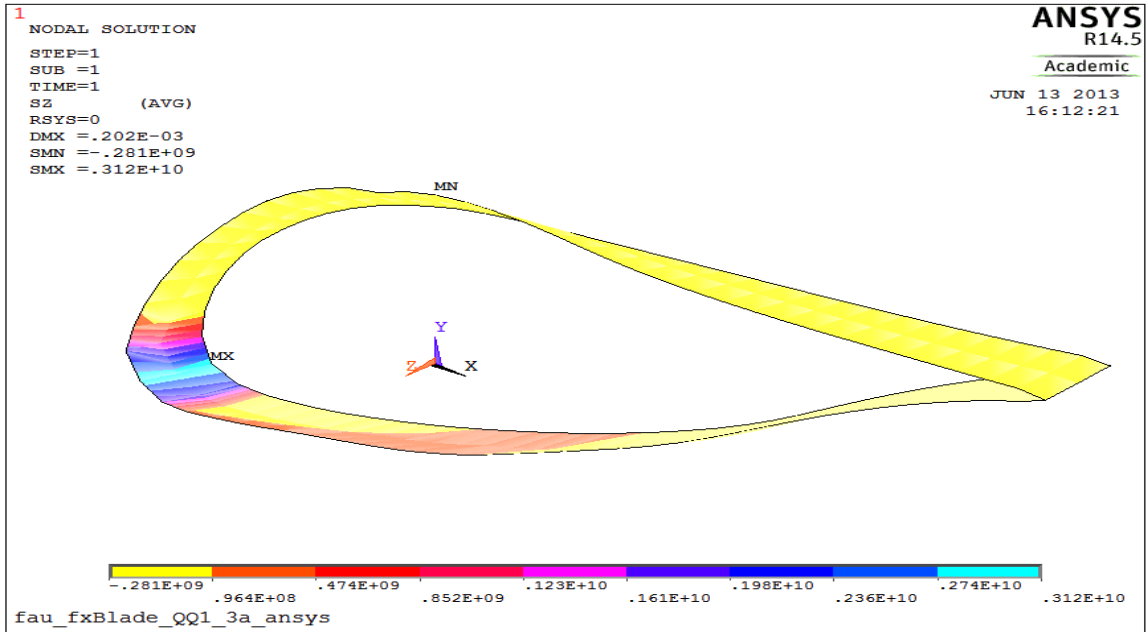


Figure 4.4 The maximum and minimum stresses at blade root

Table 4.6 Blade tip deflection results of FAST and ANSYS at speed 3.5 m/s

Blade Tip Deflection	Flapwise (m)	Edgewise(m)
FAST (PreComp)	0.060 (mean) 0.078 (max)	0.007 (mean) 0.009 (max)
FAST (NuMAD)	0.085 (mean) 0.104 (max)	0.009 (mean) 0.013 (max)
ANSYS	0.089	0.012

In order to make a direct comparison with FAST, ANSYS was run with applying  $F_N$  and  $F_T$  in Table 4.4 (without the load safety factor 3.25). Table 4.6 shows blade tip deflections as obtained from FAST and ANSYS at 3.5 m/s current speed. The first set was from FAST using section properties calculate by PrcComp. The second set was from FAST using section properties

extracted by NuMAD. The third set was from the ANSYS analysis. The correlation between three sets of results is very reasonable.

#### 4.5 Buckling Evaluation

Buckling is structure instability, leading to a failure mode. Instability failure is due to in-plane compressive forces. Buckling failure occurs before the ultimate failure. This mode of failure is also described as failure due to elastic instability.

Linear buckling analysis can be reduced to the solution of an eigenvalue problem. Eigenvalue buckling analysis predicts the theoretical buckling strength of an ideal elastic structure. Eigenvalue buckling problem is formulated as (Locke 2004):

$$([K] + \lambda_i [S]) \{u\}_i = \{0\} \quad (4.17)$$

Where:

[K] = the stiffness matrix,

[S] = the geometric stiffness matrix,

$\lambda_i$  = ith eigenvalue (the buckling load scale factor)

$\{u\}_i$  = eigenvector of displacements.

ANSYS uses an iterative method to find first few set of buckling eigenvalues and eigenvectors from Equation (4.16). It computes the structural eigenvalues for the given system loading and constraints. The geometric stiffness matrix includes initial stresses that are determined from a linear static analysis. The eigenvalue buckling analysis requires the static solution be solved first. A linear static

analysis with prestress effects was applied with 25  $F_N$  and  $F_T$  in Table 4.4 (without the ultimate strength load safety factor 3.25) along the blade span.

The “TIME/FREQ” values listed under “Results Summary” are -2.9098, -2.8818, 2.9455, 2.9804, and 3.2535 for 5 modes that were selected in the ANSYS analysis. For the harmonic response analyses, “TIME/FREQ” corresponds to the frequency. While for the buckling analysis, “TIME/FREQ” corresponds to the load factor. These lowest buckling modes have the load factors of -2.9098, -2.8818, 2.9455, 2.9804, and 3.2535. The negative factor means that loads are applied in opposite directions.

Because the full load was applied on the blade, buckling requirement is satisfied when buckling load factors are computed to be larger than the required buckling safety factor. These load factors are all above the required buckling safety factor of 2.042 in Table 4.3. OCT blade has satisfied buckling requirement.

Three lowest buckling modes are shown in Figures 4.5, 4.6, and 4.7. The buckling locations are described in Table 4.7. For these analyses, the buckling will occur in the spar cap to trailing edge panel (50-75% chord) at approximately 15% to 50% span. Although the buckling criterion was satisfied, adding foam core and reinforcement materials in these areas will improve buckling resistance (Figure 4.8). As a result, the blade will satisfy the buckling and ultimate strength requirements as well as minimize the amount of fiberglass materials.

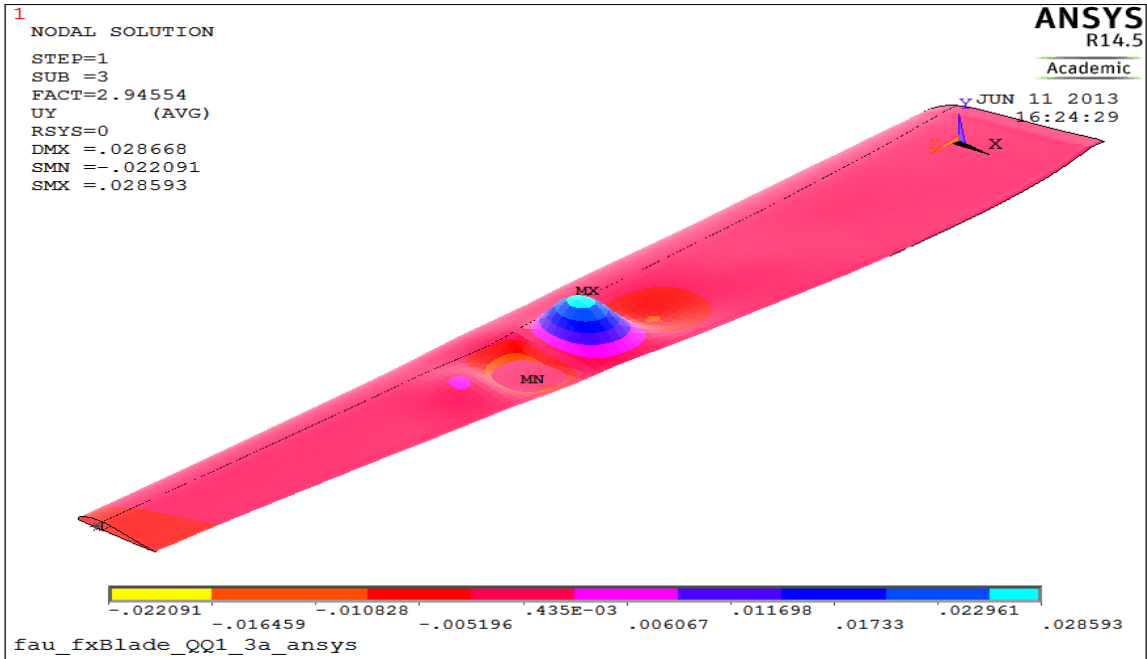


Figure 4.5 The lowest buckling mode at 50% span

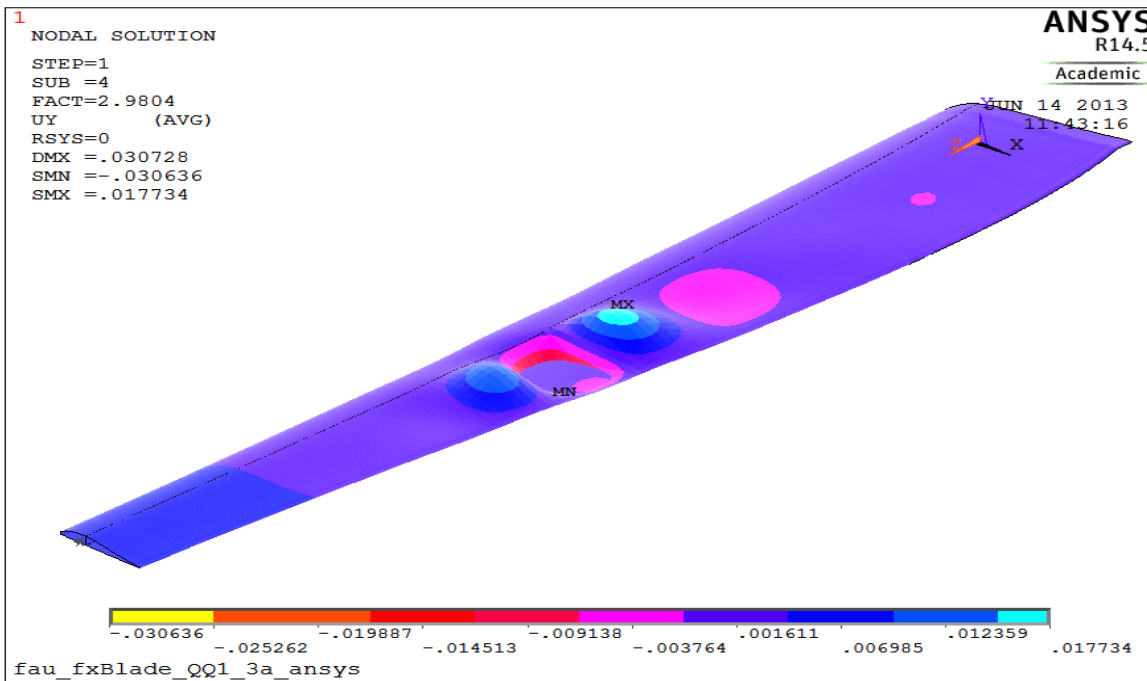


Figure 4.6 Second buckling mode at 46% span



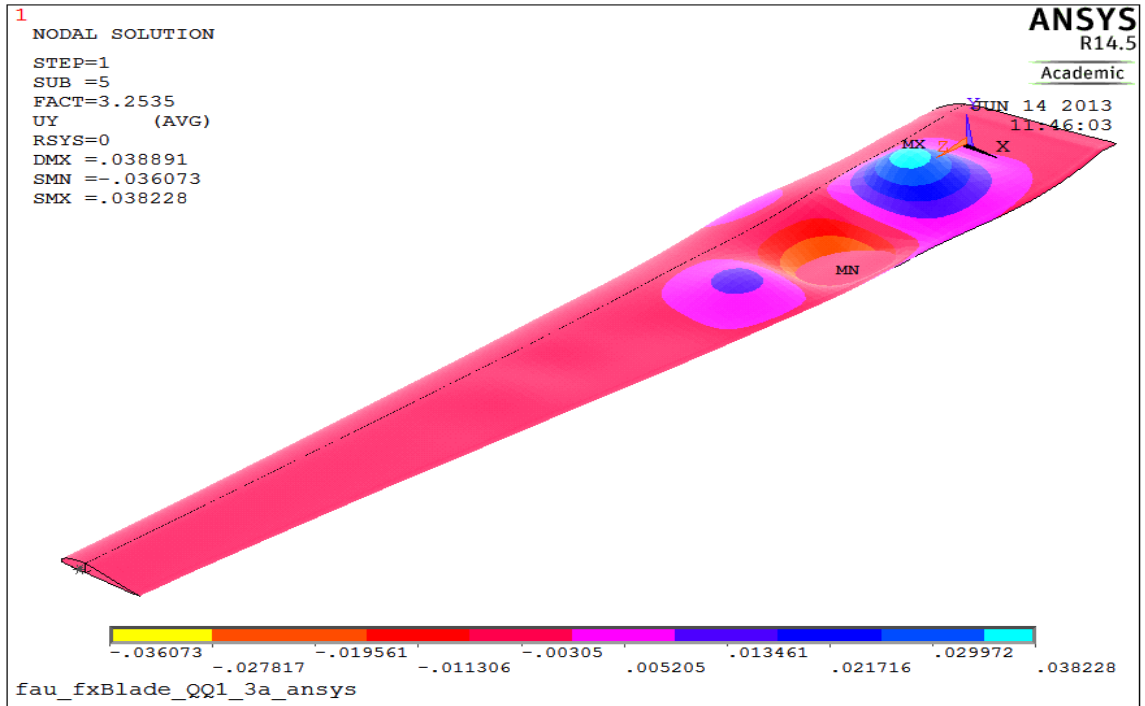


Figure 4.7 Third buckling mode at 15-33% span

Table 4.7 List of principal buckling modes

Load Factor	Span_wise Location	Chord-wise Location
2.9455	60% Span	40% Chord
2.9804	50%- 60% Span	50% Chord
3.2535	10%-30% Span	50% Chord

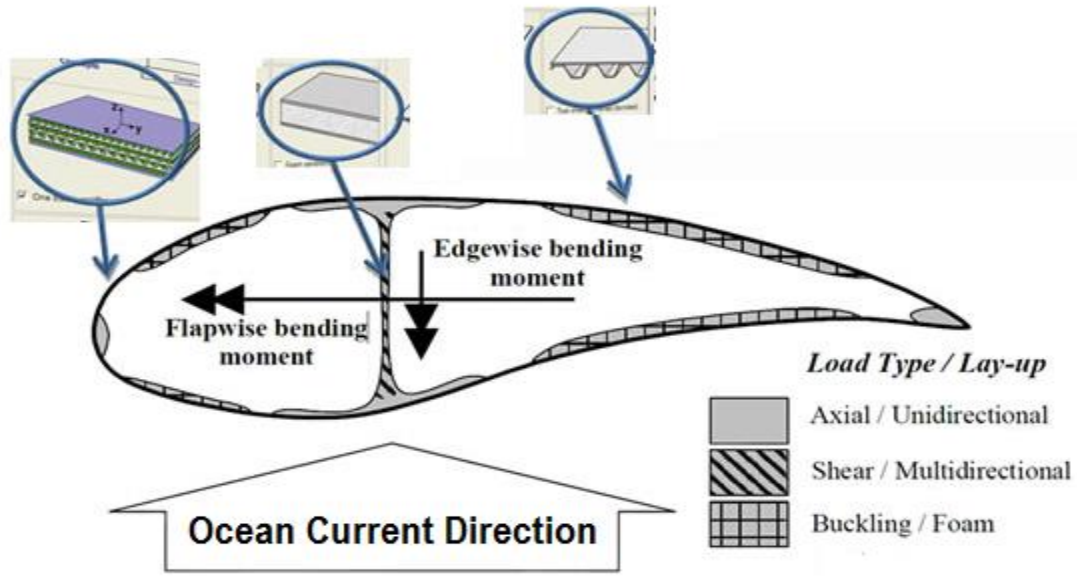


Figure 4.8 Adding foam core and reinforcement materials for all strength and stability criteria (HyperSizer 2010)

#### 4.6 Fatigue Analysis

OCT blades will be subjected to several fatigue loads during its operation. These alternating loads can originate from a variety of sources such as blade rotation, randomness of ocean current, and velocity shears i.e. variation of ocean current velocity with depth.

Section 4.4..2.2 of the draft GL Guideline OCT states that the load cases to be used for fatigue analysis generally arise only from the combination of normal external and operating conditions; the turbulence of the current quoted for normal external conditions are to be taken into account in the fatigue analysis; all cases have to be weighted according to their probability of occurrence within the design life time of the system. Due to lack of full-field turbulence current data, hub-

height current files were used in AeroDyn. The fatigue evaluation of our OCT blade did not include full-field turbulence current effects. Fatigue damages arising at each mean current speed were weighted according to the occurrence of the current speed measured by the SNMREC and added together. A Palmgren-Miner's linear rule (Miner 1945) was selected to predict the fatigue life of the OCT blade.

Among various sources of fatigue loading, blade rotation and random ocean currents were the most dominant. The hydrodynamic load, gravity and inertial load will result in alternating flapwise bending moments and edgewise bending moments.

The strain  $\varepsilon(x, y)$  in the cross-section of the blade is related to bending moments as:

$$\varepsilon(x, y) = \frac{Mc}{[EI]} = \frac{M_Y}{[EI]_{Flap}} X_E - \frac{M_X}{[EI]_{Edge}} Y_E \quad (4.18)$$

where

$E(x, y)$  = Young's Modulus of a specific material

$X_E$  = X-coordinate value of the blade skin with respect to  $X_E$ - $Y_E$  principal axes

$Y_E$  = Y-coordinate value of the blade skin with respect to  $X_E$ - $Y_E$  principal axes

$M_X$  = the bending moment about the principal axes  $X_E$

$M_Y$  = the bending moment about the principal axes  $Y_E$

The section stiffness,  $[EI]$ , includes effects of blade composite materials and the blade cross sectional shape. It is defined as follows

$[EI]_{\text{Flap}} = \iint E(x, y)x^2 dx dy$ , section flap bending stiffness about the  $Y_E$  axis

$[EI]_{\text{Edge}} = \iint E(x, y)y^2 dx dy$ , section edge bending stiffness about the  $X_E$  axis

Also from the relationship between the stress and strain, the stress  $\sigma(x, y)$  in the cross-section of the blade is proportional to strain

$$\sigma(x, y) = E(x, y)\varepsilon(x, y) \quad (4.19)$$

PreComp computed the stiffness ( $[EI]_{\text{Flap}}$  and  $[EI]_{\text{Edge}}$ ), principal axes, coordinates of the shear-center, and inertial properties of the composite blade's cross-sections. Reference axes for section properties in PreComp are shown in Figure 3.7.

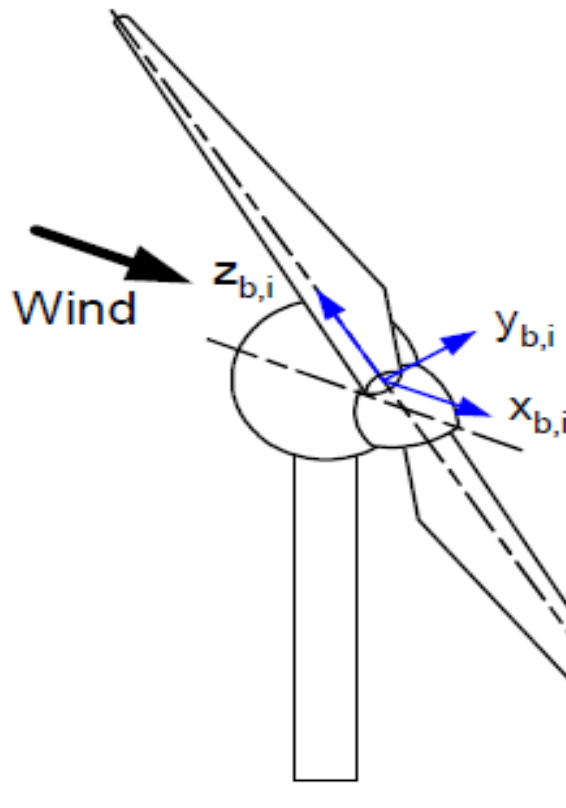


Figure 4.9 Blade coordinate system in FAST (Jonkman 2005)

In FAST, there is a blade coordinate system for each blade. Figure 4.9 shows the blade coordinate system. The origin is the intersection of the blade's pitch axis and the blade root. In Figure 4.9,  $x_b$  axis always points nominally downwind regardless of whether the rotor is upwind or downwind of the tower;  $y_b$  axis points towards the trailing edge of the blade and parallel with the chord line at the zero-twist blade station;  $z_b$  axis points along the pitch axis towards the tip of blade. The output of motions and loads for blade root are about these axes, such as edgewise moment ( $\text{RootM}_{x_b}$ ) is about  $x_b$  axis and flapwise moment ( $\text{RootM}_{y_b}$ ) is about  $y_b$  axis. The local coordinate systems are similar to the standard blade system. But the  $x$ -axis and  $y$ -axis are aligned with the local principal axes and the local coordinate systems orient themselves with the deflected blade. (Jonkman 2005, see FAST User's Guide for more details)

The dynamic simulations for each mean current speed (0.5m/s, 0.6m/s ... 2.5m/s) were performed for the OCT blade using the FAST code. FAST outputted the edgewise moment and flapwise moment at the blade root of OCT blade, as well as local edgewise and flapwise moment along the blade span. Output file contained columns of moment values with respect to time. These bending moment- time histories were converted to stress-time histories using Equations (4.18) and (4.19). Figure (4.10) and Figure (4.11) show stress-time history of X2 and X8 points in blade root section at ocean current speed of 2.5 m/s.

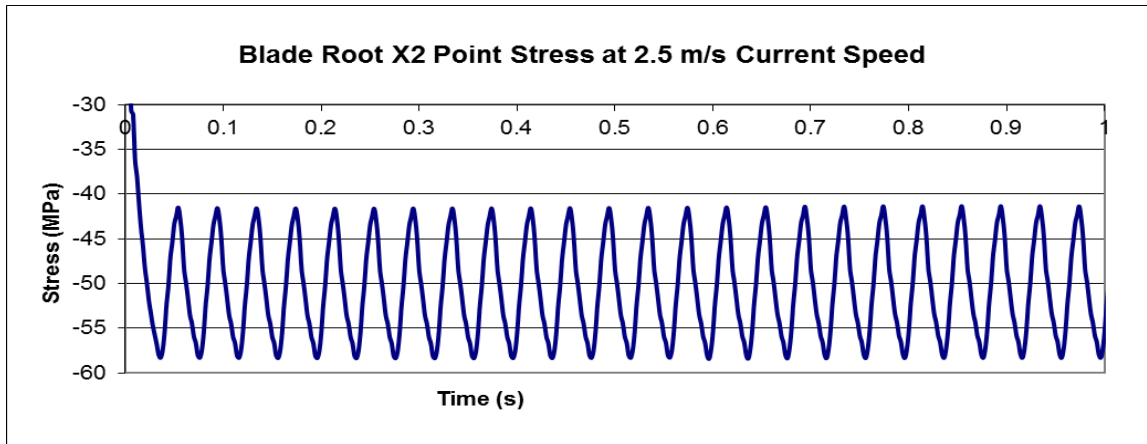


Figure 4.10 Stress-time history of X2 point in blade root section at ocean current 2.5 m/s

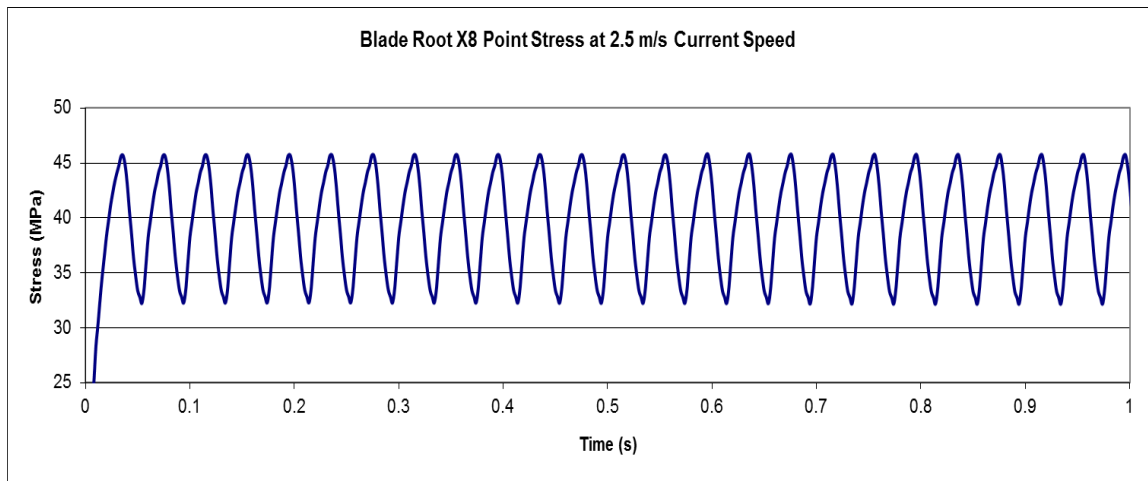


Figure 4.11 Stress-time history of X8 point in blade root section at ocean current 2.5 m/s

The ten points of each section at multiple span stations were evaluated in terms of stress. Maximum compressive stress occurred at x2 (33% chord) location and maximum tensile stress occurred at x8 (33% chord) of blade root section. Figure 4.12 shows stresses at 10 points for blade root section at 2.5 m/s ocean current speed.

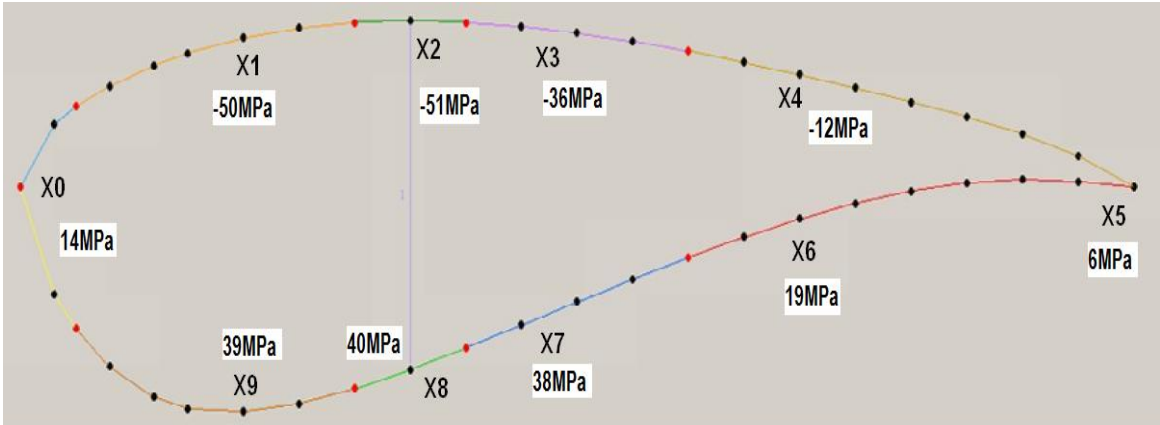


Figure 4.12 Stress evaluations of 10 points for blade root section at 2.5 m/s ocean current speed using Equations (4.18) and (4.19)

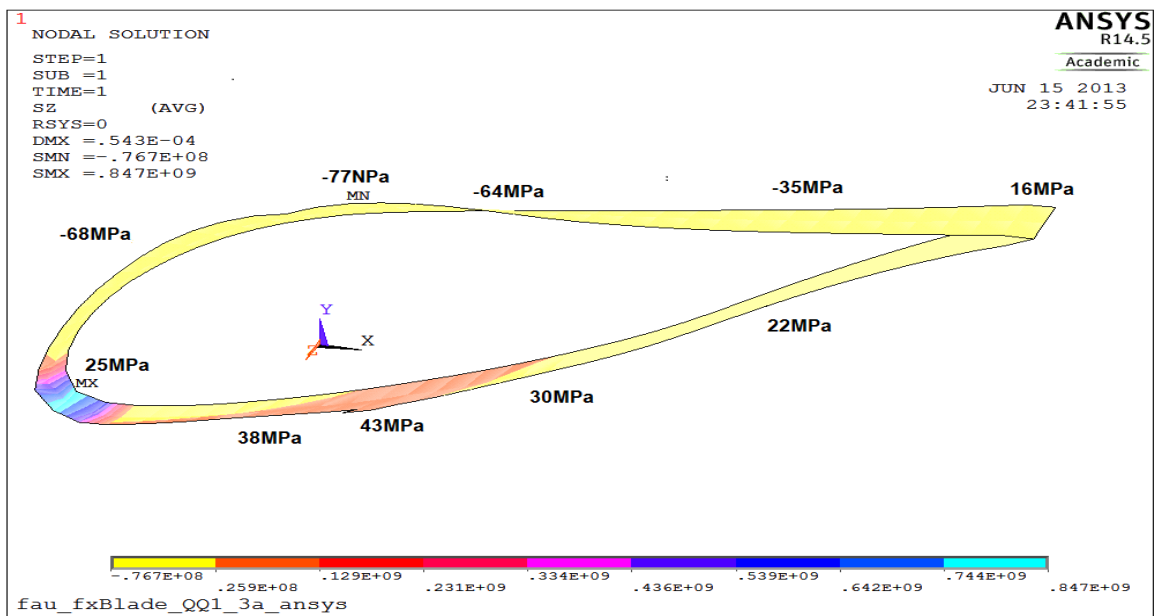


Figure 4.13 ANSYS stress results of blade root section at 2.5 m/s current speed

In order to make a comparison with ANSYS stress and deflection results, ANSYS was run with applying  $F_N$  and  $F_T$  loads at 2.5 m/s ocean current speed (without the load safety factor). Figure 4.13 shows ANSYS stress results

(nodal solution) of 10 points for blade root section. Table 4.8 shows blade tip deflections obtained from FAST and ANSYS at 2.5 m/s current speed. The first set was from FAST using section properties calculate by PrcComp. The second set was from FAST using section properties extracted by NuMAD. The third set was from the ANSYS analysis. Good agreement was observed between these analyses.

Table 4.8 Blade tip deflection results of FAST and ANSYS at speed 2.5 m/s

Blade Tip Deflection	Flapwise (m)	Edgewise(m)
FAST (PreComp)	0.058 (mean) 0.071 (max)	0.007 (mean) 0.009 (max)
FAST (NuMAD)	0.085 (mean) 0.099 (max)	0.010 (mean) 0.012 (max)
ANSYS	0.082	0.011

Fatigue life is usually expressed in terms of cycles of failure. A cumulated damage parameter (D) was calculated using Palmgren-Miner's linear rule, i.e.

$$D = \sum_{i=1}^k D_i = \sum_{i=1}^k \frac{n_i}{N_i (\gamma_F \gamma_M S_i)} \quad (4.20)$$

where:

D = damage factor or total damage

$n_i$  = number of cycles at a particular stress level  $S_i$

$\gamma_F, \gamma_M$  = partial factors of safety for loads and materials

$N_i$  = number of cycles to failure at stress level  $S_i$



The number of cycles to failure  $N_i$  depends on material properties derived from fatigue testing. The number of cycles  $n_i$  were found from the loading spectrum, while  $N_i$  were obtained from the Goodman diagram. If  $D$  exceeded unity, failure was declared. A safe operational life was calculated until  $D$  reached unity.

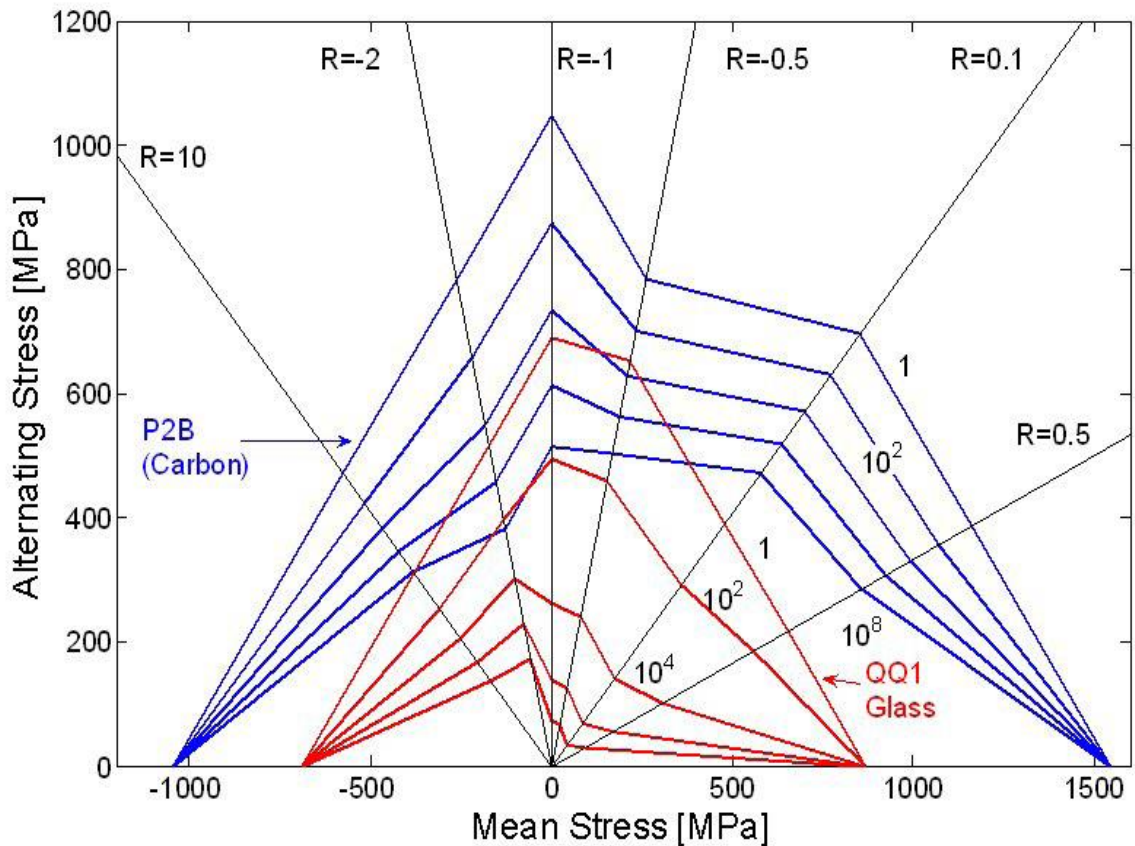


Figure 4.14 DOE/MSU Composite Material Fatigue Database: Constant life diagrams for materials QQ1 (DOE/MSU 2008)

The material fatigue properties of QQ1 material used in our OCT blade design were derived from a Goodman diagram in the DOE/MSU Composite

Material Fatigue Database. Material fatigue tests may be performed at a variety of mean levels and alternating stress (or stress ratio R). In the Goodman diagram (Figure 4.14), the resulting data of the cycles-to-failure are plotted as functions of mean stress  $\sigma_m$  and alternating stress  $\sigma_a$  along lines of constant R-values.

$$\text{The alternating stress, } \sigma_a = (\sigma_{\max} - \sigma_{\min})/2$$

$$\text{The stress ratio, } R = \sigma_{\min}/\sigma_{\max}$$

Miner's Rule calculation was used to predict the fatigue life of the blade. Fatigue damage,  $D_i = n_i/N_i$  for each mean current speed was calculated. The number of cycles to failure  $N_i = N_i(\gamma_F \gamma_M S_i)$  was calculated from Figure 4.14. Combined safety factors for OCT blade, was  $\gamma_F \gamma_M = 2.042$  since the current turbulence was not considered. It was seen that tension controlled the fatigue life of QQ1 material from Figure 4.15. The number of cycles to failure at stress level  $S_i$  (tension) was considered as follows:

$$N_1(S_1) = 5 \times 10^9 \quad (\sigma_a \leq 5 \text{ MPa})$$

$$N_2(S_2) = 1 \times 10^9 \quad (\sigma_a > 5 \text{ MPa})$$

For example, the fatigue damages ( $n_i/N_i$ ) arising at 1.5 m/s mean current speed at X8 point was calculated as follows. The mean tensile stress, alternating stress, and stress ratio were computed as 25.9 MPa, 0.12 MPa, and 0.99 MPa, respectively from Figure 4.15. The number of occurrence of 1.5 m/s current speed (30 minutes long) was obtained as 2069 over 13 months from Figure 3.3. The number of cycles at this stress level over one minute was found to be 50 from Figure 4.15. Accordingly, the number of cycles ( $n_i$ ) at this stress level over

one year was  $2.865 \times 10^6$  (2069x30x50x12/13). The number of cycles to failure at this stress level ( $N_i$ ) was found as  $5 \times 10^9$  from Figure 4.14. Finally fatigue damage  $D$  ( $D = n_i/N_i$ ) for one year at 1.5 m/s current speed at X8 point was calculated as  $2.865 \times 10^6 / 5 \times 10^9 = 5.73 \times 10^{-4}$ .

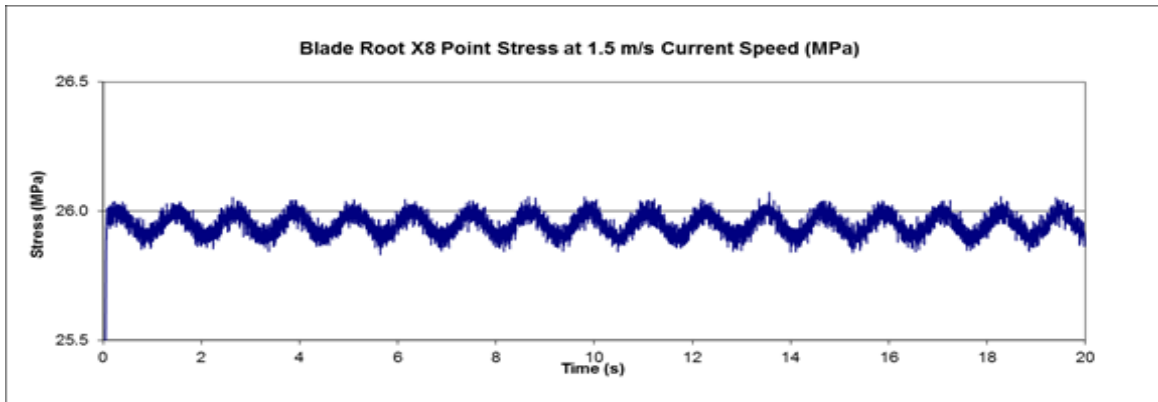


Figure 4.15 Stress-time history of X8 point in blade root section at ocean current 1.5 m/s

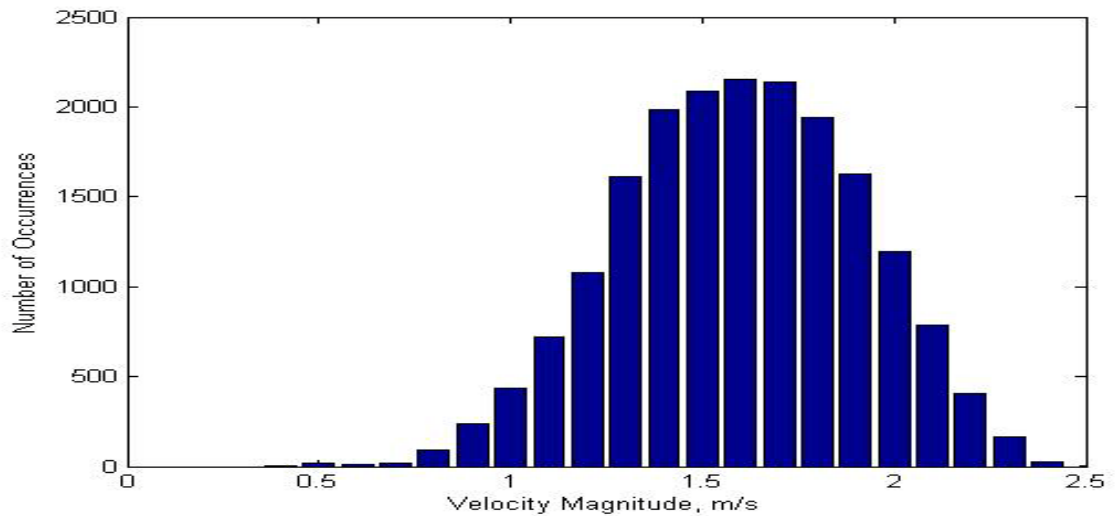


Figure 3.3 Histogram of the current speed at a depth of 25 m measured by the SNMREC at 30 minute intervals over a period of 13 months

According to Miner's rule, fatigue damages ( $D_i$ 's) were obtained together arising at each mean current speed, using the histogram of Figure 4.2. This provided the total fatigue damage during normal OCT operation. Maximum mean compressive stress and alternating stress were 50.6 MPa and 8.8 MPa at X2 point (Figure 4.10). On the other hand, maximum mean tensile stress and alternating stress were found to be 39.5 MPa and 7.5 MPa at X8 point (Figure 4.11). These stresses fell below the material fatigue test data in DOE/MSU Composite Material Fatigue Database. The largest total damage was found at X8 point in the blade root section. The total fatigue damage for one year at root section was 0.0481. The simple extrapolation shows QQ1 composite material at blade root surviving for  $1/0.0481 = 20.8$  years. The more detailed results can be found in Table 4.9.

Table 4.9 Miner' fatigue damage results at X8 (33% chord) point of root section for one year

Ocean Current Speed (m/s)	Stress Ratio	Mean Stress (Mpa)	Alternating Stress (MPa)	Stress Cycles in 1 Years ( $n_i$ )	Stress Cycles to Failure ( $N_i$ )	Miner's Fatigue Damage Values ( $n_i/N_i$ )
0.5	0.95	2.8	0.07	8.31E+03	5.E+09	1.66E-06
0.6	0.97	4.4	0.07	2.35E+04	5.E+09	4.71E-06
0.7	0.97	6.3	0.07	1.66E+04	5.E+09	3.32E-06
0.8	0.98	8.2	0.09	6.23E+04	5.E+09	1.25E-05
0.9	0.98	10.3	0.10	2.17E+05	5.E+09	4.35E-05
1.0	0.99	12.6	0.10	4.57E+05	5.E+09	9.14E-05
1.1	0.99	15.1	0.11	7.73E+05	5.E+09	1.55E-04
1.2	0.99	17.7	0.11	1.26E+06	5.E+09	2.51E-04
1.3	0.99	20.3	0.12	1.85E+06	5.E+09	3.70E-04
1.4	0.99	23.1	0.12	2.51E+06	5.E+09	5.03E-04
1.5	0.99	25.9	0.12	2.86E+06	5.E+09	5.73E-04
1.6	0.99	28.9	0.13	2.97E+06	5.E+09	5.94E-04
1.7	0.99	31.6	0.12	2.91E+06	5.E+09	5.82E-04
1.8	0.99	34.2	0.09	2.97E+06	5.E+09	5.94E-04
1.9	0.99	36.4	0.09	2.38E+06	5.E+09	4.77E-04
2.0	0.99	38.0	0.09	1.91E+06	5.E+09	3.82E-04
2.1	0.80	37.5	4.00	3.62E+07	1.E+09	7.24E-03
2.2	0.72	37.5	6.00	2.21E+07	1.E+09	2.21E-02
2.3	0.69	38.1	6.70	1.12E+07	1.E+09	1.12E-02
2.4	0.69	38.8	6.90	2.75E+06	1.E+09	2.75E-03
2.5	0.70	39.5	7.50	2.08E+05	1.E+09	2.08E-04
Total						4.81E-02

## CHAPTER 5. SUMMARY AND FUTURE WORK

### 5.1 Summary

- Several NREL codes, NuMAD, and ANSYS have been applied to design and analyze composite horizontal-axis OCT blades. The procedure shows that NREL's wind turbine codes can be adapted to model composite OCT blades and couple it with commercial codes to perform static and dynamic analysis. Especially, use of NuMAD and ANSYS allowed calculation of stresses on the blade.
- Simulations were performed using ocean current speeds collected by SNMREC. OCT blade buoyancy forces and added mass effect were considered. The same OCT model was developed for ANSYS finite element analysis using NuMAD.
- Hydrodynamic loads for OCT blades were calculated by modifying the inputs to AeroDyn and FAST. Load case assumptions and partial safety factors for loads and materials recommended by Germanischer Lloyd (GL) were used. Ekman Solution was used to determine the hurricane-driven ocean current speed.

- Normal forces were found to be major loading on OCT blade, with the resulting flapwise bending moment being 8 to 5 times larger than the edgewise moment.
- Static analysis was performed using ANSYS with the ultimate loads. It was observed that maximum compressive stress occurred at the top shell and maximum tensile stress occurred at the bottom shell near the 33% chord location for each span station. The maximum compressive stress of the blade occurred at about 40% of span. The maximum tensile stress of the blade occurred at root. All of these stresses fell well within the allowable tensile and compressive strengths of the QQ1 E-glass composite material.
- Linear buckling analysis was performed with full loads applied along the blade span using ANSYS. It is observed that the lowest buckling occurs in the spar cap to trailing edge panel at approximately between 60% and 20% span. The buckling safety factor was computed as 2.955. It is larger than the required safety factor 2.042.
- Fatigue life prediction was performed based on the stresses at the critical location. A cumulative damage parameter (D) was calculated using Palmgren-Miner's linear rule. Fatigue life was calculated to be 20.8 years according to the occurrences of current speed measured by the SNMREC and the DOE/MSU Composite Material Fatigue Database. It was noticed that fatigue life was dictated by the tensile stress. The ocean current

turbulence was not considered in the fatigue life evaluation. Accordingly, fatigue safety factor of 2.043 was used.

- Results from FAST were compared with those of ANSYS. The correlation between the blade tip displacements is very reasonable. ANSYS finite element model predicted slightly higher tip displacement. Blade stresses computed using the simple beam theory was also compared with ANSYS results. The correlation between the two results was also reasonable. Again ANSYS's estimates were slightly higher.

## **5.2 Future Work**

- In the present study, loads for OCT blades were calculated by modifying the input files to AeroDyn. The hydrodynamic data files (lift and drag coefficients) of OCT blade were generated by XFOIL and DesignFOIL programs which were designed for analysis of isolated airfoils. NREL's AirfoilPrep was used to adjust lift and drag coefficients caused by three-dimensionally delayed stall on a rotating OCT blade. It is also designed for wind turbine. Available experiment airfoil/hydrofoil database are all based on wind tunnel testing. Therefore lift and drag coefficients of hydrofoil and hydrodynamic loading on the OCT blades must be investigated further. CFD modules available in ANSYS can probably be used in the future.



- This dissertation includes descriptions of how to model the added mass effect for OCT blade in FAST. The added mass coefficients were used to account for added mass effect in BModes and AeroDyn/FAST in this dissertation. The added mass coefficients are dependent upon the section shape and moving direction of the OCT blade. It is difficult to find accurate added mass coefficients of OCT blade from current offshore standards. Added mass coefficients of OCT blade need to be studied. The influences of added mass effect and the effective methods for representing added mass effect in AeroDyn/FAST are required for more research.
- Due to lack of full-field turbulence current data, the fatigue evaluation of OCT blade did not include full-field turbulence current effects in the present investigation. In addition, fatigue load due to velocity shear has not been considered. Though the variation of loading owing to velocity shear is very low in present OCT (3 m diameter), this will rise with commercial scale OCT blade having larger radius. Turbulence and velocity shear effects will change fatigue loading and need to be investigated.
- Current fatigue analysis is based on maximum stress criteria. However, other failure modes such as buckling, shear, and delamination will need to be considered in future.

# APPENDIXES

## A. PreComp Files

### A.1. Main Input File - fau\_fxBlade\_QQ1\_glass\_3a.pci

\*\*\*\*\* main input file for PreComp \*\*\*\*\*

Sample Composite Blade Section Properties

General information -----

1.241 BL\_length : blade length (m)  
26 N\_sections : no of blade sections (-)  
10 N\_materials : no of materials listed in the materials table (material.inp)  
3 Out\_format : output file (1: general format, 2: BModes-format, 3: both)  
f TabDelim (true: tab-delimited table; false: space-delimited table)

Blade-sections-specific data -----

Sec span l.e. chord aerodynamic af\_shape int str layup  
location position length twist file file  
Span\_loc Le\_loc Chord Tw\_aero Af\_shape\_file Int\_str\_file  
(-) (-) (m) (degrees) (-) (-)

0.0000	0.25	0.311	26.34	'af-fx77_02349_01.inp'	'fau_int_3.inp'
0.0160	0.25	0.311	26.34	'af-fx77_02349_01.inp'	'fau_int_3.inp'
0.0240	0.25	0.309	25.52	'af-fx77_02336_02.inp'	'fau_int_3.inp'
0.0400	0.25	0.305	24.07	'af-fx77_02301_03.inp'	'fau_int_3.inp'
0.0620	0.25	0.299	22.23	'af-fx77_02273_04.inp'	'fau_int_3.inp'
0.0920	0.25	0.290	20.22	'af-fx77_02223_05.inp'	'fau_int_2a.inp'
0.1290	0.25	0.279	18.17	'af-fx77_02162_06.inp'	'fau_int_2a.inp'
0.1710	0.25	0.267	16.13	'af-fx77_02092_07.inp'	'fau_int_2a.inp'
0.2190	0.25	0.253	14.25	'af-fx77_02012_08.inp'	'fau_int_2a.inp'
0.2710	0.25	0.239	12.47	'af-fx77_01925_09.inp'	'fau_int_2a.inp'
0.3270	0.25	0.224	10.90	'af-fx77_01832_10.inp'	'fau_int_2a.inp'
0.3860	0.25	0.210	9.50	'af-fx77_01734_11.inp'	'fau_int_2a.inp'
0.4460	0.25	0.196	8.27	'af-fx77_01633_12.inp'	'fau_int_2a.inp'
0.5080	0.25	0.182	7.22	'af-fx77_01530_13.inp'	'fau_int_2.inp'
0.5700	0.25	0.170	6.30	'af-fx77_01486_14.inp'	'fau_int_2.inp'
0.6310	0.25	0.159	5.49	'af-fx77_01442_15.inp'	'fau_int_2.inp'
0.6890	0.25	0.149	4.76	'af-fx77_01400_16.inp'	'fau_int_2.inp'
0.7450	0.25	0.140	4.10	'af-fx77_01360_17.inp'	'fau_int_2.inp'
0.7980	0.25	0.133	3.50	'af-fx77_01323_18.inp'	'fau_int_1.inp'
0.8450	0.25	0.127	2.95	'af-fx77_01289_19.inp'	'fau_int_1.inp'
0.8880	0.25	0.122	2.44	'af-fx77_01258_20.inp'	'fau_int_1.inp'
0.9240	0.25	0.118	1.99	'af-fx77_01232_21.inp'	'fau_int_1.inp'
0.9540	0.25	0.115	1.61	'af-fx77_01211_22.inp'	'fau_int_1.inp'
0.9770	0.25	0.114	1.30	'af-fx77_01210_23.inp'	'fau_int_1.inp'
0.9920	0.25	0.112	1.10	'af-fx77_01210_23.inp'	'fau_int_1.inp'
1.0000	0.25	0.112	0.99	'af-fx77_01210_23.inp'	'fau_int_1.inp'

Webs (spars) data -----

1 Nweb : number of webs (-) ! enter 0 if the blade has no webs  
1 lb\_sp\_stn : blade station number where inner-most end of webs is located (-)  
26 Ob\_sp\_stn : blade station number where outer-most end of webs is located (-)

Web\_num Inb\_end\_ch\_loc Oub\_end\_ch\_loc (fraction of chord length)  
1 0.33 0.33

## A.2. Internal Structure Data File - fau\_int\_3.inp

Composite laminae lay-up inside the blade section

\*\*\*\*\* TOP SURFACE \*\*\*\*\*

3 N\_scts(1): no of sectors on top surface

normalized chord location of nodes defining airfoil sectors boundaries (xsec\_node)

0.0 0.15 0.50 1.00

.....

Sect\_num no of laminae (N\_laminas)  
1 15

lamina number	num of plies	thickness of ply (m)	fibers_direction (deg)	composite_material ID (-)
lam_num	N_plies	Tply	Tht_lam	Mat_id
1	1	0.000511	45	10 (QQ1/2-Glass)
2	1	0.000511	-45	10 (QQ1/2-Glass)
3	4	0.000511	0	9 (QQ1/1-Glass)
4	1	0.000511	-45	10 (QQ1/2-Glass)
5	1	0.000511	45	10 (QQ1/2-Glass)
6	1	0.000511	45	10 (QQ1/2-Glass)
7	1	0.000511	-45	10 (QQ1/2-Glass)
8	4	0.000511	0	9 (QQ1/1-Glass)
9	1	0.000511	-45	10 (QQ1/2-Glass)
10	1	0.000511	45	10 (QQ1/2-Glass)
11	1	0.000511	45	10 (QQ1/2-Glass)
12	1	0.000511	-45	10 (QQ1/2-Glass)
13	4	0.000511	0	9 (QQ1/1-Glass)
14	1	0.000511	-45	10 (QQ1/2-Glass)
15	1	0.000511	45	10 (QQ1/2-Glass)

.....

Sect\_num no of laminae  
2 15

lamina number	num of plies	thickness of ply (m)	fibers_direction (deg)	composite_material ID (-)
lam_num	N_plies	Tply	Tht_lam	Mat_id
1	1	0.000511	45	10 (QQ1/2-Glass)
2	1	0.000511	-45	10 (QQ1/2-Glass)
3	4	0.000511	0	9 (QQ1/1-Glass)
4	1	0.000511	-45	10 (QQ1/2-Glass)
5	1	0.000511	45	10 (QQ1/2-Glass)
6	1	0.000511	45	10 (QQ1/2-Glass)
7	1	0.000511	-45	10 (QQ1/2-Glass)
8	4	0.000511	0	9 (QQ1/1-Glass)
9	1	0.000511	-45	10 (QQ1/2-Glass)
10	1	0.000511	45	10 (QQ1/2-Glass)
11	1	0.000511	45	10 (QQ1/2-Glass)
12	1	0.000511	-45	10 (QQ1/2-Glass)
13	4	0.000511	0	9 (QQ1/1-Glass)
14	1	0.000511	-45	10 (QQ1/2-Glass)
15	1	0.000511	45	10 (QQ1/2-Glass)

.....

Sect\_num no of laminae  
3 15

lamina number	num of plies	thickness of ply (m)	fibers_direction (deg)	composite_material ID (-)
lam_num	N_plies	Tply	Tht_lam	Mat_id
1	1	0.000511	45	10 (QQ1/2-Glass)
2	1	0.000511	-45	10 (QQ1/2-Glass)
3	4	0.000511	0	9 (QQ1/1-Glass)
4	1	0.000511	-45	10 (QQ1/2-Glass)
5	1	0.000511	45	10 (QQ1/2-Glass)
6	1	0.000511	45	10 (QQ1/2-Glass)
7	1	0.000511	-45	10 (QQ1/2-Glass)

8	4	0.000511	0	9 (QQ1/1-Glass)
9	1	0.000511	-45	10 (QQ1/2-Glass)
10	1	0.000511	45	10 (QQ1/2-Glass)
11	1	0.000511	45	10 (QQ1/2-Glass)
12	1	0.000511	-45	10 (QQ1/2-Glass)
13	4	0.000511	0	9 (QQ1/1-Glass)
14	1	0.000511	-45	10 (QQ1/2-Glass)
15	1	0.000511	45	10 (QQ1/2-Glass)

\*\*\*\*\* BOTTOM SURFACE \*\*\*\*\*

3 N\_scts(2): no of sectors on bottom surfaces

normalized chord location of surface nodes defining sector boundaries (xsec\_node)  
 0.0 0.15 0.50 1.00

Sect\_num no of laminae  
 1 15

lamina number	num of plies	thickness of ply (m)	fibers_direction (deg)	composite_material ID (-)
lam_num	N_plies	Tply	Tht_lam	Mat_id
1	1	0.000511	45	10 (QQ1/2-Glass)
2	1	0.000511	-45	10 (QQ1/2-Glass)
3	4	0.000511	0	9 (QQ1/1-Glass)
4	1	0.000511	-45	10 (QQ1/2-Glass)
5	1	0.000511	45	10 (QQ1/2-Glass)
6	1	0.000511	45	10 (QQ1/2-Glass)
7	1	0.000511	-45	10 (QQ1/2-Glass)
8	4	0.000511	0	9 (QQ1/1-Glass)
9	1	0.000511	-45	10 (QQ1/2-Glass)
10	1	0.000511	45	10 (QQ1/2-Glass)
11	1	0.000511	45	10 (QQ1/2-Glass)
12	1	0.000511	-45	10 (QQ1/2-Glass)
13	4	0.000511	0	9 (QQ1/1-Glass)
14	1	0.000511	-45	10 (QQ1/2-Glass)
15	1	0.000511	45	10 (QQ1/2-Glass)

Sect\_num no of laminae  
 2 15

lamina number	num of plies	thickness of ply (m)	fibers_direction (deg)	composite_material ID (-)
lam_num	N_plies	Tply	Tht_Lam	Mat_Id
1	1	0.000511	45	10 (QQ1/2-Glass)
2	1	0.000511	-45	10 (QQ1/2-Glass)
3	4	0.000511	0	9 (QQ1/1-Glass)
4	1	0.000511	-45	10 (QQ1/2-Glass)
5	1	0.000511	45	10 (QQ1/2-Glass)
6	1	0.000511	45	10 (QQ1/2-Glass)
7	1	0.000511	-45	10 (QQ1/2-Glass)
8	4	0.000511	0	9 (QQ1/1-Glass)
9	1	0.000511	-45	10 (QQ1/2-Glass)
10	1	0.000511	45	10 (QQ1/2-Glass)
11	1	0.000511	45	10 (QQ1/2-Glass)
12	1	0.000511	-45	10 (QQ1/2-Glass)
13	4	0.000511	0	9 (QQ1/1-Glass)
14	1	0.000511	-45	10 (QQ1/2-Glass)
15	1	0.000511	45	10 (QQ1/2-Glass)

Sect\_num no of laminae  
 3 15

lamina number	num of plies	thickness of ply (m)	fibers_direction (deg)	composite_material ID (-)
lam_num	N_Plies	Tply	Tht_Lam	Mat_Id
1	1	0.000511	45	10 (QQ1/2-Glass)
2	1	0.000511	-45	10 (QQ1/2-Glass)

3	4	0.000511	0	9 (QQ1/1-Glass)
4	1	0.000511	-45	10 (QQ1/2-Glass)
5	1	0.000511	45	10 (QQ1/2-Glass)
6	1	0.000511	45	10 (QQ1/2-Glass)
7	1	0.000511	-45	10 (QQ1/2-Glass)
8	4	0.000511	0	9 (QQ1/1-Glass)
9	1	0.000511	-45	10 (QQ1/2-Glass)
10	1	0.000511	45	10 (QQ1/2-Glass)
11	1	0.000511	45	10 (QQ1/2-Glass)
12	1	0.000511	-45	10 (QQ1/2-Glass)
13	4	0.000511	0	9 (QQ1/1-Glass)
14	1	0.000511	-45	10 (QQ1/2-Glass)
15	1	0.000511	45	10 (QQ1/2-Glass)

\*\*\*\*\*  
Laminae schedule for webs (input required only if webs exist at this section):

web\_num no of laminae (N\_weblams)  
1 5

lamina number	num of plies	thickness of ply (m)	fibers_direction (deg)	composite_material ID (-)
wlam_num	N_Plies	w_tply	Tht_Wlam	Wmat_Id
1	2	0.000511	45	10 (QQ1/2-Glass)
2	2	0.000511	-45	10 (QQ1/2-Glass)
3	8	0.000511	0	9 (QQ1/1-Glass)
4	2	0.000511	-45	10 (QQ1/2-Glass)
5	2	0.000511	45	10 (QQ1/2-Glass)

### A.3. Internal Structure Data File - fau\_int\_2a.inp

Composite laminae lay-up inside the blade section

\*\*\*\*\* TOP SURFACE \*\*\*\*\*  
3 N\_scts(1): no of sectors on top surface

normalized chord location of nodes defining airfoil sectors boundaries (xsec\_node)  
0.0 0.15 0.50 1.00

.....  
Sect\_num no of laminae (N\_laminas)  
1 10

lamina number	num of plies	thickness of ply (m)	fibers_direction (deg)	composite_material ID (-)
lam_num	N_plies	Tply	Tht_lam	Mat_id
1	1	0.000511	45	10 (QQ1/2-Glass)
2	1	0.000511	-45	10 (QQ1/2-Glass)
3	4	0.000511	0	9 (QQ1/1-Glass)
4	1	0.000511	-45	10 (QQ1/2-Glass)
5	1	0.000511	45	10 (QQ1/2-Glass)
6	1	0.000511	45	10 (QQ1/2-Glass)
7	1	0.000511	-45	10 (QQ1/2-Glass)
8	4	0.000511	0	9 (QQ1/1-Glass)
9	1	0.000511	-45	10 (QQ1/2-Glass)
10	1	0.000511	45	10 (QQ1/2-Glass)

.....  
Sect\_num no of laminae  
2 15

lamina number	num of plies	thickness of ply (m)	fibers_direction (deg)	composite_material ID (-)
lam_num	N_plies	Tply	Tht_lam	Mat_id
1	1	0.000511	45	10 (QQ1/2-Glass)
2	1	0.000511	-45	10 (QQ1/2-Glass)
3	4	0.000511	0	9 (QQ1/1-Glass)

4	1	0.000511	-45	10 (QQ1/2-Glass)
5	1	0.000511	45	10 (QQ1/2-Glass)
6	1	0.000511	45	10 (QQ1/2-Glass)
7	1	0.000511	-45	10 (QQ1/2-Glass)
8	4	0.000511	0	9 (QQ1/1-Glass)
9	1	0.000511	-45	10 (QQ1/2-Glass)
10	1	0.000511	45	10 (QQ1/2-Glass)
11	1	0.000511	45	10 (QQ1/2-Glass)
12	1	0.000511	-45	10 (QQ1/2-Glass)
13	4	0.000511	0	9 (QQ1/1-Glass)
14	1	0.000511	-45	10 (QQ1/2-Glass)
15	1	0.000511	45	10 (QQ1/2-Glass)

.....  
Sect\_num no of laminae  
3 10

lamina number	num of plies	thickness of ply (m)	fibers_direction (deg)	composite_material (-)	ID
lam_num	N_plies	Tply	Tht_lam	Mat_id	
1	1	0.000511	45	10 (QQ1/2-Glass)	
2	1	0.000511	-45	10 (QQ1/2-Glass)	
3	4	0.000511	0	9 (QQ1/1-Glass)	
4	1	0.000511	-45	10 (QQ1/2-Glass)	
5	1	0.000511	45	10 (QQ1/2-Glass)	
6	1	0.000511	45	10 (QQ1/2-Glass)	
7	1	0.000511	-45	10 (QQ1/2-Glass)	
8	4	0.000511	0	9 (QQ1/1-Glass)	
9	1	0.000511	-45	10 (QQ1/2-Glass)	
10	1	0.000511	45	10 (QQ1/2-Glass)	

\*\*\*\*\* BOTTOM SURFACE \*\*\*\*\*  
3 N\_scts(2): no of sectors on bottom surfaces

normalized chord location of surface nodes defining sector boundaries (xsec\_node)  
0.0 0.15 0.50 1.00

.....  
Sect\_num no of laminae  
1 10

lamina number	num of plies	thickness of ply (m)	fibers_direction (deg)	composite_material (-)	ID
lam_num	N_plies	Tply	Tht_lam	Mat_id	
1	1	0.000511	45	10 (QQ1/2-Glass)	
2	1	0.000511	-45	10 (QQ1/2-Glass)	
3	4	0.000511	0	9 (QQ1/1-Glass)	
4	1	0.000511	-45	10 (QQ1/2-Glass)	
5	1	0.000511	45	10 (QQ1/2-Glass)	
6	1	0.000511	45	10 (QQ1/2-Glass)	
7	1	0.000511	-45	10 (QQ1/2-Glass)	
8	4	0.000511	0	9 (QQ1/1-Glass)	
9	1	0.000511	-45	10 (QQ1/2-Glass)	
10	1	0.000511	45	10 (QQ1/2-Glass)	

.....  
Sect\_num no of laminae  
2 15

lamina number	num of plies	thickness of ply (m)	fibers_direction (deg)	composite_material (-)	ID
lam_num	N_plies	Tply	Tht_Lam	Mat_Id	
1	1	0.000511	45	10 (QQ1/2-Glass)	
2	1	0.000511	-45	10 (QQ1/2-Glass)	
3	4	0.000511	0	9 (QQ1/1-Glass)	
4	1	0.000511	-45	10 (QQ1/2-Glass)	
5	1	0.000511	45	10 (QQ1/2-Glass)	
6	1	0.000511	45	10 (QQ1/2-Glass)	
7	1	0.000511	-45	10 (QQ1/2-Glass)	
8	4	0.000511	0	9 (QQ1/1-Glass)	

9	1	0.000511	-45	10 (QQ1/2-Glass)
10	1	0.000511	45	10 (QQ1/2-Glass)
11	1	0.000511	45	10 (QQ1/2-Glass)
12	1	0.000511	-45	10 (QQ1/2-Glass)
13	4	0.000511	0	9 (QQ1/1-Glass)
14	1	0.000511	-45	10 (QQ1/2-Glass)
15	1	0.000511	45	10 (QQ1/2-Glass)

.....  
Sect\_num no of laminae  
3 10

lamina number	num of plies	thickness of ply (m)	fibers_direction (deg)	composite_material ID (-)
lam_num	N_Plies	Tply	Tht_Lam	Mat_Id
1	1	0.000511	45	10 (QQ1/2-Glass)
2	1	0.000511	-45	10 (QQ1/2-Glass)
3	4	0.000511	0	9 (QQ1/1-Glass)
4	1	0.000511	-45	10 (QQ1/2-Glass)
5	1	0.000511	45	10 (QQ1/2-Glass)
6	1	0.000511	45	10 (QQ1/2-Glass)
7	1	0.000511	-45	10 (QQ1/2-Glass)
8	4	0.000511	0	9 (QQ1/1-Glass)
9	1	0.000511	-45	10 (QQ1/2-Glass)
10	1	0.000511	45	10 (QQ1/2-Glass)

\*\*\*\*\*  
Laminae schedule for webs (input required only if webs exist at this section):

web\_num no of laminae (N\_weblams)  
1 5

lamina number	num of plies	thickness of ply (m)	fibers_direction (deg)	composite_material ID (-)
wlam_num	N_Plies	w_tply	Tht_Wlam	Wmat_Id
1	2	0.000511	45	10 (QQ1/2-Glass)
2	2	0.000511	-45	10 (QQ1/2-Glass)
3	8	0.000511	0	9 (QQ1/1-Glass)
4	2	0.000511	-45	10 (QQ1/2-Glass)
5	2	0.000511	45	10 (QQ1/2-Glass)

#### A.4. Internal Structure Data File - fau\_int\_2.inp

Composite laminae lay-up inside the blade section

\*\*\*\*\* TOP SURFACE \*\*\*\*\*  
3 N\_scts(1): no of sectors on top surface

normalized chord location of nodes defining airfoil sectors boundaries (xsec\_node)  
0.0 0.15 0.50 1.00

.....  
Sect\_num no of laminae (N\_laminas)  
1 10

lamina number	num of plies	thickness of ply (m)	fibers_direction (deg)	composite_material ID (-)
lam_num	N_plies	Tply	Tht_lam	Mat_id
1	1	0.000511	45	10 (QQ1/2-Glass)
2	1	0.000511	-45	10 (QQ1/2-Glass)
3	4	0.000511	0	9 (QQ1/1-Glass)
4	1	0.000511	-45	10 (QQ1/2-Glass)
5	1	0.000511	45	10 (QQ1/2-Glass)
6	1	0.000511	45	10 (QQ1/2-Glass)
7	1	0.000511	-45	10 (QQ1/2-Glass)
8	4	0.000511	0	9 (QQ1/1-Glass)
9	1	0.000511	-45	10 (QQ1/2-Glass)
10	1	0.000511	45	10 (QQ1/2-Glass)

Sect\_num no of laminae  
2 10

lamina number	num of plies	thickness of ply (m)	fibers_direction (deg)	composite_material ID (-)
lam_num	N_plies	Tply	Tht_lam	Mat_id
1	1	0.000511	45	10 (QQ1/2-Glass)
2	1	0.000511	-45	10 (QQ1/2-Glass)
3	4	0.000511	0	9 (QQ1/1-Glass)
4	1	0.000511	-45	10 (QQ1/2-Glass)
5	1	0.000511	45	10 (QQ1/2-Glass)
6	1	0.000511	45	10 (QQ1/2-Glass)
7	1	0.000511	-45	10 (QQ1/2-Glass)
8	4	0.000511	0	9 (QQ1/1-Glass)
9	1	0.000511	-45	10 (QQ1/2-Glass)
10	1	0.000511	45	10 (QQ1/2-Glass)

.....  
Sect\_num no of laminae  
3 10

lamina number	num of plies	thickness of ply (m)	fibers_direction (deg)	composite_material ID (-)
lam_num	N_plies	Tply	Tht_lam	Mat_id
1	1	0.000511	45	10 (QQ1/2-Glass)
2	1	0.000511	-45	10 (QQ1/2-Glass)
3	4	0.000511	0	9 (QQ1/1-Glass)
4	1	0.000511	-45	10 (QQ1/2-Glass)
5	1	0.000511	45	10 (QQ1/2-Glass)
6	1	0.000511	45	10 (QQ1/2-Glass)
7	1	0.000511	-45	10 (QQ1/2-Glass)
8	4	0.000511	0	9 (QQ1/1-Glass)
9	1	0.000511	-45	10 (QQ1/2-Glass)
10	1	0.000511	45	10 (QQ1/2-Glass)

\*\*\*\*\* BOTTOM SURFACE \*\*\*\*\*

3 N\_scts(2): no of sectors on bottom surfaces

normalized chord location of surface nodes defining sector boundaries (xsec\_node)  
0.0 0.15 0.50 1.00

.....  
Sect\_num no of laminae  
1 10

lamina number	num of plies	thickness of ply (m)	fibers_direction (deg)	composite_material ID (-)
lam_num	N_plies	Tply	Tht_lam	Mat_id
1	1	0.000511	45	10 (QQ1/2-Glass)
2	1	0.000511	-45	10 (QQ1/2-Glass)
3	4	0.000511	0	9 (QQ1/1-Glass)
4	1	0.000511	-45	10 (QQ1/2-Glass)
5	1	0.000511	45	10 (QQ1/2-Glass)
6	1	0.000511	45	10 (QQ1/2-Glass)
7	1	0.000511	-45	10 (QQ1/2-Glass)
8	4	0.000511	0	9 (QQ1/1-Glass)
9	1	0.000511	-45	10 (QQ1/2-Glass)
10	1	0.000511	45	10 (QQ1/2-Glass)

.....  
Sect\_num no of laminae  
2 10

lamina number	num of plies	thickness of ply (m)	fibers_direction (deg)	composite_material ID (-)
lam_num	N_plies	Tply	Tht_Lam	Mat_Id
1	1	0.000511	45	10 (QQ1/2-Glass)
2	1	0.000511	-45	10 (QQ1/2-Glass)
3	4	0.000511	0	9 (QQ1/1-Glass)
4	1	0.000511	-45	10 (QQ1/2-Glass)



5	1	0.000511	45	10 (QQ1/2-Glass)
6	1	0.000511	45	10 (QQ1/2-Glass)
7	1	0.000511	-45	10 (QQ1/2-Glass)
8	4	0.000511	0	9 (QQ1/1-Glass)
9	1	0.000511	-45	10 (QQ1/2-Glass)
10	1	0.000511	45	10 (QQ1/2-Glass)

.....  
Sect\_num no of laminae  
3 10

lamina number	num of plies	thickness of ply (m)	fibers_direction (deg)	composite_material ID (-)
lam_num	N_Plies	Tply	Tht_Lam	Mat_Id
1	1	0.000511	45	10 (QQ1/2-Glass)
2	1	0.000511	-45	10 (QQ1/2-Glass)
3	4	0.000511	0	9 (QQ1/1-Glass)
4	1	0.000511	-45	10 (QQ1/2-Glass)
5	1	0.000511	45	10 (QQ1/2-Glass)
6	1	0.000511	45	10 (QQ1/2-Glass)
7	1	0.000511	-45	10 (QQ1/2-Glass)
8	4	0.000511	0	9 (QQ1/1-Glass)
9	1	0.000511	-45	10 (QQ1/2-Glass)
10	1	0.000511	45	10 (QQ1/2-Glass)

\*\*\*\*\*  
Laminae schedule for webs (input required only if webs exist at this section):

web\_num no of laminae (N\_weblams)  
1 5

lamina number	num of plies	thickness of ply (m)	fibers_direction (deg)	composite_material ID (-)
wlam_num	N_Plies	w_tply	Tht_Wlam	Wmat_Id
1	2	0.000511	45	10 (QQ1/2-Glass)
2	2	0.000511	-45	10 (QQ1/2-Glass)
3	8	0.000511	0	9 (QQ1/1-Glass)
4	2	0.000511	-45	10 (QQ1/2-Glass)
5	2	0.000511	45	10 (QQ1/2-Glass)

### A.5. Internal Structure Data File - fau\_int\_1a.inp

Composite laminae lay-up inside the blade section

\*\*\*\*\* TOP SURFACE \*\*\*\*\*

3 N\_scts(1): no of sectors on top surface

normalized chord location of nodes defining airfoil sectors boundaries (xsec\_node)  
0.0 0.15 0.50 1.00

.....  
Sect\_num no of laminae (N\_laminas)  
1 5

lamina number	num of plies	thickness of ply (m)	fibers_direction (deg)	composite_material ID (-)
lam_num	N_plies	Tply	Tht_lam	Mat_id
1	1	0.000511	45	10 (QQ1/2-Glass)
2	1	0.000511	-45	10 (QQ1/2-Glass)
3	4	0.000511	0	9 (QQ1/1-Glass)
4	1	0.000511	-45	10 (QQ1/2-Glass)
5	1	0.000511	45	10 (QQ1/2-Glass)

.....  
Sect\_num no of laminae  
2 10

lamina num of thickness fibers\_direction composite\_material ID

number	plies	of ply (m)	(deg)	(-)
lam_num	N_plies	Tply	Tht_lam	Mat_id
1	1	0.000511	45	10 (QQ1/2-Glass)
2	1	0.000511	-45	10 (QQ1/2-Glass)
3	4	0.000511	0	9 (QQ1/1-Glass)
4	1	0.000511	-45	10 (QQ1/2-Glass)
5	1	0.000511	45	10 (QQ1/2-Glass)
6	1	0.000511	45	10 (QQ1/2-Glass)
7	1	0.000511	-45	10 (QQ1/2-Glass)
8	4	0.000511	0	9 (QQ1/1-Glass)
9	1	0.000511	-45	10 (QQ1/2-Glass)
10	1	0.000511	45	10 (QQ1/2-Glass)

.....  
Sect\_num no of laminae  
3 5

lamina number	num of plies	thickness of ply (m)	fibers_direction (deg)	composite_material ID (-)
lam_num	N_plies	Tply	Tht_lam	Mat_id
1	1	0.000511	45	10 (QQ1/2-Glass)
2	1	0.000511	-45	10 (QQ1/2-Glass)
3	4	0.000511	0	9 (QQ1/1-Glass)
4	1	0.000511	-45	10 (QQ1/2-Glass)
5	1	0.000511	45	10 (QQ1/2-Glass)

\*\*\*\*\* BOTTOM SURFACE \*\*\*\*\*

3 N\_scts(2): no of sectors on bottom surfaces

normalized chord location of surface nodes defining sector boundaries (xsec\_node)  
0.0 0.15 0.50 1.00

.....  
Sect\_num no of laminae  
1 5

lamina number	num of plies	thickness of ply (m)	fibers_direction (deg)	composite_material ID (-)
lam_num	N_plies	Tply	Tht_lam	Mat_id
1	1	0.000511	45	10 (QQ1/2-Glass)
2	1	0.000511	-45	10 (QQ1/2-Glass)
3	4	0.000511	0	9 (QQ1/1-Glass)
4	1	0.000511	-45	10 (QQ1/2-Glass)
5	1	0.000511	45	10 (QQ1/2-Glass)

.....  
Sect\_num no of laminae  
2 10

lamina number	num of plies	thickness of ply (m)	fibers_direction (deg)	composite_material ID (-)
lam_num	N_plies	Tply	Tht_Lam	Mat_Id
1	1	0.000511	45	10 (QQ1/2-Glass)
2	1	0.000511	-45	10 (QQ1/2-Glass)
3	4	0.000511	0	9 (QQ1/1-Glass)
4	1	0.000511	-45	10 (QQ1/2-Glass)
5	1	0.000511	45	10 (QQ1/2-Glass)
6	1	0.000511	45	10 (QQ1/2-Glass)
7	1	0.000511	-45	10 (QQ1/2-Glass)
8	4	0.000511	0	9 (QQ1/1-Glass)
9	1	0.000511	-45	10 (QQ1/2-Glass)
10	1	0.000511	45	10 (QQ1/2-Glass)

.....  
Sect\_num no of laminae  
3 5

lamina number	num of plies	thickness of ply (m)	fibers_direction (deg)	composite_material ID (-)
lam_num	N_Plies	Tply	Tht_Lam	Mat_Id
1	1	0.000511	45	10 (QQ1/2-Glass)

2	1	0.000511	-45	10 (QQ1/2-Glass)
3	4	0.000511	0	9 (QQ1/1-Glass)
4	1	0.000511	-45	10 (QQ1/2-Glass)
5	1	0.000511	45	10 (QQ1/2-Glass)

\*\*\*\*\*  
 Laminae schedule for webs (input required only if webs exist at this section):

web\_num no of laminae (N\_weblams)  
 1 5

lamina number	num of plies	thickness of ply (m)	fibers_direction (deg)	composite_material ID (-)
wlam_num	N_Plies	w_tply	Tht_Wlam	Wmat_Id
1	2	0.000511	45	10 (QQ1/2-Glass)
2	2	0.000511	-45	10 (QQ1/2-Glass)
3	8	0.000511	0	9 (QQ1/1-Glass)
4	2	0.000511	-45	10 (QQ1/2-Glass)
5	2	0.000511	45	10 (QQ1/2-Glass)

## A.6. Internal Structure Data File - fau\_int\_1.inp

Composite laminae lay-up inside the blade section

\*\*\*\*\* TOP SURFACE \*\*\*\*\*

3 N\_scts(1): no of sectors on top surface

normalized chord location of nodes defining airfoil sectors boundaries (xsec\_node)  
 0.0 0.15 0.50 1.00

.....  
 Sect\_num no of laminae (N\_laminas)  
 1 5

lamina number	num of plies	thickness of ply (m)	fibers_direction (deg)	composite_material ID (-)
lam_num	N_plies	Tply	Tht_lam	Mat_id
1	1	0.000511	45	10 (QQ1/2-Glass)
2	1	0.000511	-45	10 (QQ1/2-Glass)
3	4	0.000511	0	9 (QQ1/1-Glass)
4	1	0.000511	-45	10 (QQ1/2-Glass)
5	1	0.000511	45	10 (QQ1/2-Glass)

.....  
 Sect\_num no of laminae  
 2 5

lamina number	num of plies	thickness of ply (m)	fibers_direction (deg)	composite_material ID (-)
lam_num	N_plies	Tply	Tht_lam	Mat_id
1	1	0.000511	45	10 (QQ1/2-Glass)
2	1	0.000511	-45	10 (QQ1/2-Glass)
3	4	0.000511	0	9 (QQ1/1-Glass)
4	1	0.000511	-45	10 (QQ1/2-Glass)
5	1	0.000511	45	10 (QQ1/2-Glass)

.....  
 Sect\_num no of laminae  
 3 5

lamina number	num of plies	thickness of ply (m)	fibers_direction (deg)	composite_material ID (-)
lam_num	N_plies	Tply	Tht_lam	Mat_id
1	1	0.000511	45	10 (QQ1/2-Glass)
2	1	0.000511	-45	10 (QQ1/2-Glass)
3	4	0.000511	0	9 (QQ1/1-Glass)
4	1	0.000511	-45	10 (QQ1/2-Glass)
5	1	0.000511	45	10 (QQ1/2-Glass)

\*\*\*\*\* BOTTOM SURFACE \*\*\*\*\*

3 N\_scts(2): no of sectors on bottom surfaces

normalized chord location of surface nodes defining sector boundaries (xsec\_node)

0.0 0.15 0.50 1.00

.....  
Sect\_num no of laminae

1 5

lamina number	num of plies	thickness of ply (m)	fibers_direction (deg)	composite_material ID (-)
lam_num	N_plies	Tply	Tht_Lam	Mat_id
1	1	0.000511	45	10 (QQ1/2-Glass)
2	1	0.000511	-45	10 (QQ1/2-Glass)
3	4	0.000511	0	9 (QQ1/1-Glass)
4	1	0.000511	-45	10 (QQ1/2-Glass)
5	1	0.000511	45	10 (QQ1/2-Glass)

.....  
Sect\_num no of laminae

2 5

lamina number	num of plies	thickness of ply (m)	fibers_direction (deg)	composite_material ID (-)
lam_num	N_plies	Tply	Tht_Lam	Mat_id
1	1	0.000511	45	10 (QQ1/2-Glass)
2	1	0.000511	-45	10 (QQ1/2-Glass)
3	4	0.000511	0	9 (QQ1/1-Glass)
4	1	0.000511	-45	10 (QQ1/2-Glass)
5	1	0.000511	45	10 (QQ1/2-Glass)

.....  
Sect\_num no of laminae

3 5

lamina number	num of plies	thickness of ply (m)	fibers_direction (deg)	composite_material ID (-)
lam_num	N_Plies	Tply	Tht_Lam	Mat_id
1	1	0.000511	45	10 (QQ1/2-Glass)
2	1	0.000511	-45	10 (QQ1/2-Glass)
3	4	0.000511	0	9 (QQ1/1-Glass)
4	1	0.000511	-45	10 (QQ1/2-Glass)
5	1	0.000511	45	10 (QQ1/2-Glass)

\*\*\*\*\*

Laminae schedule for webs (input required only if webs exist at this section):

web\_num no of laminae (N\_weblams)

1 5

lamina number	num of plies	thickness of ply (m)	fibers_direction (deg)	composite_material ID (-)
wlam_num	N_Plies	w_tply	Tht_Wlam	Wmat_id
1	2	0.000511	45	10 (QQ1/2-Glass)
2	2	0.000511	-45	10 (QQ1/2-Glass)
3	8	0.000511	0	9 (QQ1/1-Glass)
4	2	0.000511	-45	10 (QQ1/2-Glass)
5	2	0.000511	45	10 (QQ1/2-Glass)

## A.7. Hydrifoil Input File - af-fx77\_02349\_01.inp

71 N\_af\_nodes :no of airfoil nodes, counted clockwise starting with leading edge (see users' manual, fig xx)

Xnode Ynode !! chord-normalized coordinated of the 124airfoil nodes

0.00E+00 0.00E+00 !! the first node, a leading-edge node, must be (0,0)

0.00201	0.02083
0.00804	0.03597
0.01802	0.05130
0.03188	0.06754
0.04952	0.08355
0.07078	0.09952
0.09549	0.11520
0.12346	0.12936
0.15447	0.14161
0.18826	0.15210
0.22455	0.16003
0.26307	0.16468
0.30349	0.16590
0.34549	0.16316
0.38874	0.15603
0.43288	0.14592
0.47757	0.13481
0.52243	0.12309
0.56712	0.11111
0.61126	0.09958
0.65451	0.08817
0.69651	0.07699
0.73693	0.06642
0.77545	0.05658
0.81174	0.04750
0.84553	0.03930
0.87654	0.03207
0.90451	0.02565
0.92922	0.02014
0.95048	0.01551
0.96812	0.01180
0.98198	0.00889
0.99196	0.00682
0.99799	0.00545
1.00000	0.00496
1.00000	-0.00496
0.99799	-0.00490
0.99196	-0.00479
0.98198	-0.00482
0.96812	-0.00520
0.95048	-0.00602
0.92922	-0.00735
0.90451	-0.00934
0.87654	-0.01205
0.84553	-0.01557
0.81174	-0.02006
0.77545	-0.02549
0.73693	-0.03187
0.69651	-0.03928
0.65451	-0.04760
0.61126	-0.05614
0.56712	-0.06305
0.52243	-0.06801
0.47757	-0.07095
0.43288	-0.07260
0.38874	-0.07321
0.34549	-0.07270
0.30349	-0.07120
0.26307	-0.06900
0.22455	-0.06614
0.18826	-0.06238
0.15447	-0.05806
0.12346	-0.05344
0.09549	-0.04799
0.07078	-0.04200
0.04952	-0.03607
0.03188	-0.02956

0.01802 -0.02248  
0.00804 -0.01530  
0.00201 -0.00693

## A.8. Hydrifoil Input File - af-fx77\_01442\_15.inp

71 N\_af\_nodes :no of airfoil nodes, counted clockwise starting  
with leading edge (see users' manual, fig xx)

Xnode Ynode !! chord-normalized coordinated of the airfoil nodes  
0.00E+00 0.00E+00 !! the first node, a leading-edge node, must be (0,0)  
0.00201 0.00711  
0.00804 0.01720  
0.01802 0.02905  
0.03188 0.04170  
0.04952 0.05466  
0.07078 0.06762  
0.09549 0.07970  
0.12346 0.09076  
0.15447 0.10027  
0.18826 0.10765  
0.22455 0.11287  
0.26307 0.11598  
0.30349 0.11642  
0.34549 0.11292  
0.38874 0.10714  
0.43288 0.09980  
0.47757 0.09167  
0.52243 0.08322  
0.56712 0.07469  
0.61126 0.06625  
0.65451 0.05807  
0.69651 0.05039  
0.73693 0.04310  
0.77545 0.03637  
0.81174 0.03025  
0.84553 0.02465  
0.87654 0.01961  
0.90451 0.01502  
0.92922 0.01077  
0.95048 0.00718  
0.96812 0.00434  
0.98198 0.00245  
0.99196 0.00139  
0.99799 0.00083  
1.00000 0.00066  
1.00000 -0.00066  
0.99799 -0.00105  
0.99196 -0.00205  
0.98198 -0.00341  
0.96812 -0.00527  
0.95048 -0.00739  
0.92922 -0.00944  
0.90451 -0.01126  
0.87654 -0.01294  
0.84553 -0.01452  
0.81174 -0.01602  
0.77545 -0.01738  
0.73693 -0.01873  
0.69651 -0.01999  
0.65451 -0.02110  
0.61126 -0.02217  
0.56712 -0.02321  
0.52243 -0.02411  
0.47757 -0.02499  
0.43288 -0.02585  
0.38874 -0.02646

0.34549 -0.02692  
 0.30349 -0.02747  
 0.26307 -0.02762  
 0.22455 -0.02757  
 0.18826 -0.02748  
 0.15447 -0.02700  
 0.12346 -0.02619  
 0.09549 -0.02515  
 0.07078 -0.02380  
 0.04952 -0.02186  
 0.03188 -0.01952  
 0.01802 -0.01696  
 0.00804 -0.01289  
 0.00201 -0.00668

## A.9. Materials Data File

Mat_Id	E1	E2	G12	Nu12	Density	Mat_Name
(-)	(Pa)	(Pa)	(Pa)	(-)	(Kg/m^3)	(-)
1	37.0e+9	9.0e+9	4.0e+9	0.28	1860.0	(uni-directional FRP)
2	10.3e+9	10.3e+9	8.0e+9	0.30	1830.0	(double-bias FRP)
3	0.1e+2	0.1e+2	0.1e+1	0.30	1830.0	(gelcoat)
4	10.3e+9	10.3e+9	8.0e+9	0.30	1664.0	(nexus)
5	1.0e+7	1.0e+7	0.2e+6	0.30	0128.0	(balsa)
6	143e+9	10e+9	6.0e+9	0.3	1580.0	(Carbon/Epoxy AS4/3501-6)
7	51e+9	17e+9	7.0e+9	0.25	1980.0	(S2-Glass/XP125S)
8	0.24e+9	0.24e+9	0.085e+9	0.45	200.0	(HCP30)
9	38.4e+9	12.0e+9	5.0e+9	0.27	1690.0	(QQ1/1-Glass)
10	13.8e+9	11.8e+9	5.0e+9	0.25	1626.0	(QQ1/2-Glass)

## A.10. Output File - fau\_fxBlade\_QQ1\_glass\_3a.OUT\_BMD

Results generated by PreComp (v1.00.03, 11-Jun-2012, compiled using double precision) on 10-Jun-2013 at 16:52:30.  
 Sample Composite Blade Section Properties

blade length (meters) = 1.24

span_loc	str_tw	tw_iner	mass_den	flp_iner	edge_iner	flp_stff	edge_stff	tor_stff	axial_stff	cg_offst	sc_offst	tc_offst			
(-)	(deg)	(deg)	(kg/m)	(kg-m)	(kg-m)	(Nm^2)	(Nm^2)	(Nm^2)	(N)	(m)	(m)	(m)			
0.0000	24.097	24.104	0.1435E+02	0.6089E-02	0.1128E+00	0.9338E+05	0.1733E+07	0.4599E+05	0.2202E+09	0.069	0.072	0.069			
0.0160	24.097	24.103	0.1435E+02	0.6090E-02	0.1128E+00	0.9338E+05	0.1734E+07	0.4599E+05	0.2202E+09	0.069	0.072	0.069			
0.0240	23.485	23.491	0.1424E+02	0.5874E-02	0.1105E+00	0.9007E+05	0.1699E+07	0.4424E+05	0.2186E+09	0.069	0.072	0.069			
0.0400	21.867	21.874	0.1404E+02	0.5463E-02	0.1061E+00	0.8376E+05	0.1630E+07	0.4114E+05	0.2154E+09	0.068	0.071	0.068			
0.0620	20.102	20.108	0.1373E+02	0.4892E-02	0.9967E-01	0.7500E+05	0.1532E+07	0.3670E+05	0.2107E+09	0.067	0.070	0.067			
0.0920	17.970	17.978	0.1053E+02	0.3906E-02	0.6471E-01	0.5988E+05	0.9945E+06	0.2586E+05	0.1616E+09	0.058	0.061	0.058			
0.1290	15.831	15.838	0.1009E+02	0.3188E-02	0.5739E-01	0.4887E+05	0.8820E+06	0.2104E+05	0.1549E+09	0.056	0.059	0.056			
0.1710	13.851	13.858	0.9611E+01	0.2514E-02	0.5007E-01	0.3852E+05	0.7694E+06	0.1649E+05	0.1475E+09	0.054	0.057	0.054			
0.2190	12.011	12.018	0.9060E+01	0.1883E-02	0.4238E-01	0.2884E+05	0.6512E+06	0.1223E+05	0.1390E+09	0.051	0.054	0.051			
0.2710	10.272	10.278	0.8511E+01	0.1370E-02	0.3554E-01	0.2097E+05	0.5461E+06	0.8764E+04	0.1306E+09	0.049	0.051	0.049			
0.3270	8.631	8.636	0.7929E+01	0.9502E-03	0.2910E-01	0.1453E+05	0.4471E+06	0.5943E+04	0.1217E+09	0.046	0.048	0.046			
0.3860	7.247	7.252	0.7388E+01	0.6473E-03	0.2386E-01	0.9886E+04	0.3664E+06	0.3911E+04	0.1134E+09	0.043	0.045	0.043			
0.4460	5.998	6.002	0.6853E+01	0.4263E-03	0.1930E-01	0.6496E+04	0.2964E+06	0.2443E+04	0.1052E+09	0.041	0.042	0.041			
0.5080	5.058	5.064	0.5454E+01	0.2610E-03	0.1448E-01	0.3970E+04	0.2224E+06	0.1697E+04	0.8370E+08	0.042	0.044	0.042			
0.5700	4.167	4.173	0.5078E+01	0.1916E-03	0.1174E-01	0.2907E+04	0.1803E+06	0.1216E+04	0.7793E+08	0.039	0.041	0.039			
0.6310	3.389	3.395	0.4735E+01	0.1419E-03	0.9557E-02	0.2146E+04	0.1468E+06	0.9049E+03	0.7267E+08	0.037	0.038	0.037			
0.6890	2.693	2.698	0.4424E+01	0.1067E-03	0.7830E-02	0.1608E+04	0.1203E+06	0.7356E+03	0.6790E+08	0.035	0.036	0.035			
0.7450	1.968	1.973	0.4146E+01	0.8214E-04	0.6469E-02	0.1232E+04	0.9936E+05	0.6644E+03	0.6363E+08	0.033	0.034	0.033			
0.7980	1.322	1.341	0.2081E+01	0.4686E-04	0.2834E-02	0.7070E+03	0.4363E+05	0.2933E+03	0.3194E+08	0.030	0.032	0.030			
0.8450	0.796	0.815	0.1981E+01	0.3769E-04	0.2462E-02	0.5666E+03	0.3789E+05	0.2324E+03	0.3040E+08	0.029	0.031	0.029			
0.8880	0.305	0.323	0.1897E+01	0.3112E-04	0.2178E-02	0.4660E+03	0.3352E+05	0.1934E+03	0.2912E+08	0.028	0.030	0.028			
0.9240	-0.228	-0.210	0.1830E+01	0.2649E-04	0.1968E-02	0.3953E+03	0.3028E+05	0.1803E+03	0.2809E+08	0.027	0.029	0.027			
0.9540	-0.603	-0.586	0.1780E+01	0.2334E-04	0.1819E-02	0.3471E+03	0.2800E+05	0.1685E+03	0.2732E+08	0.026	0.028	0.026			
0.9770	-0.908	-0.891	0.1765E+01	0.2261E-04	0.1773E-02	0.3361E+03	0.2729E+05	0.1638E+03	0.2708E+08	0.026	0.028	0.026			
0.9920	-1.109	-1.091	0.1734E+01	0.2128E-04	0.1681E-02	0.3158E+03	0.2588E+05	0.1559E+03	0.2661E+08	0.026	0.027	0.026			
1.0000	-1.220	-1.202	0.1734E+01	0.2128E-04	0.1682E-02	0.3158E+03	0.2589E+05	0.1559E+03	0.2661E+08	0.026	0.027	0.026			

## B. BModes Files

### B.1. Main Input File - fau\_fxBlade\_QQ1\_glass\_3a.bmi

```
===== BModes v3.00 Main Input File =====
Sample non-uniform blade

----- General parameters -----
true Echo Echo input file contents to *.echo file if true.
1 beam_type 1: blade, 2: tower (-)
50.0 rot_rpm: rotor speed, automatically set to zero for tower modal analysis (rpm)
1.0 rpm_mult: rotor speed multiplicative factor (-)
1.498 radius: rotor tip radius measured along coned blade axis OR tower height (m)
0.257 hub_rad: hub radius measured along coned blade axis OR tower rigid-base height (m)
0. precone: built-in precone angle, automatically set to zero for a tower (deg)
0. bl_thp: blade pitch setting, automatically set to zero for a tower (deg)
1 hub_conn: hub-to-blade or tower-base boundary condition [1: cantilevered; 2: free-free; 3: only axial and torsion
constraints] (-)
20 modepr: number of modes to be printed (-)
t TabDelim (true: tab-delimited output tables; false: space-delimited tables)
f mid_node_tw (true: output twist at mid-node of elements; false: no mid-node outputs)

----- Blade-tip or tower-top mass properties -----
0. tip_mass blade-tip or tower-top mass (kg)
0. cm_loc tip-mass c.m. offset from the blade axis measured along the tip section y reference axis (m)
0. cm_axial tip-mass c.m. offset tower tip measures axially along the z axis (m)
0. ixx_tip blade lag mass moment of inertia about the tip-section x reference axis (kg-m^2)
0. iyy_tip blade flap mass moment of inertia about the tip-section y reference axis (kg-m^2)
0. izz_tip torsion mass moment of inertia about the tip-section z reference axis (kg-m^2)
0. ixy_tip cross product of inertia about x and y reference axes(kg-m^2)
0. izx_tip cross product of inertia about z and x reference axes(kg-m^2)
0. iyz_tip cross product of inertia about y and z reference axes(kg-m^2)

----- Distributed-property identifiers -----
1 id_mat: material_type [1: isotropic; non-isotropic composites option not yet available]
'fau_fxBlade_QQ1_glass_3a_props.dat' sec_props_file name of beam section properties file (-)

Property scaling factors.....
1.0 sec_mass_mult: mass density multiplier (-)
1.0 flp_iner_mult: blade flap or tower f-a inertia multiplier (-)
1.0 lag_iner_mult: blade lag or tower s-s inertia multiplier (-)
1.0 flp_stff_mult: blade flap or tower f-a bending stiffness multiplier (-)
1.0 edge_stff_mult: blade lag or tower s-s bending stiffness multiplier (-)
1.0 tor_stff_mult: torsion stiffness multiplier (-)
1.0 axial_stff_mult: axial stiffness multiplier (-)
1.0 cg_offst_mult: cg offset multiplier (-)
1.0 sc_offst_mult: shear center multiplier (-)
1.0 tc_offst_mult: tension center multiplier (-)

----- Finite element discretization -----
12 nselt: no of blade or tower elements (-)
Distance of element boundary nodes from blade or flexible-tower root (normalized wrt blade or tower length), el_loc()
0. 0.08 0.16 0.24 0.32 0.40 0.48 0.56 0.64 0.72 0.80 0.90 1.0

END of Main Input File Data *****
*****
```

### B.2. Output File - fau\_fxBlade\_QQ1\_glass\_3a.OUT

Results generated by BModes (v1.03.01, 25-Sept-2007, compiled using double precision) on 10-Jun-2013 at 22:06:39.

Sample non-uniform blade



rotating blade frequencies & mode shapes  
 --- only first 20 modes printed

----- Mode No. 1 (freq = 0.299618E+02 Hz)

span_loc	flap disp	flap slope	lag disp	lag slope	twist
0.0000	0.000000	0.000000	0.000000	0.000000	0.000000
0.0800	0.000274	0.008198	0.000112	0.003189	-0.000771
0.1600	0.001232	0.020495	0.000448	0.006723	-0.002192
0.2400	0.003171	0.037622	0.001028	0.010555	-0.004431
0.3200	0.006482	0.061591	0.001878	0.014787	-0.008078
0.4000	0.011697	0.094635	0.003021	0.019378	-0.014094
0.4800	0.019549	0.140367	0.004485	0.024380	-0.024458
0.5600	0.031035	0.202973	0.006297	0.029829	-0.039468
0.6400	0.046800	0.268488	0.008438	0.034273	-0.058801
0.7200	0.066852	0.331367	0.010829	0.037459	-0.079968
0.8000	0.090848	0.386753	0.013385	0.039310	-0.100027
0.9000	0.125691	0.442901	0.016694	0.040236	-0.136755
1.0000	0.163206	0.456227	0.020026	0.040204	-0.154041

----- Mode No. 2 (freq = 0.867890E+02 Hz)

span_loc	flap disp	flap slope	lag disp	lag slope	twist
0.0000	0.000000	0.000000	0.000000	0.000000	0.000000
0.0800	0.000549	0.015974	0.000246	0.006856	-0.003493
0.1600	0.002300	0.035846	0.000940	0.013513	-0.009830
0.2400	0.005448	0.057589	0.002050	0.019411	-0.019410
0.3200	0.010035	0.078511	0.003516	0.024238	-0.033806
0.4000	0.015794	0.092071	0.005244	0.027338	-0.054503
0.4800	0.021846	0.086462	0.007093	0.027996	-0.082917
0.5600	0.026219	0.041195	0.008873	0.025418	-0.110898
0.6400	0.025960	-0.050859	0.010390	0.020438	-0.127059
0.7200	0.017987	-0.186431	0.011537	0.014651	-0.119265
0.8000	-0.000063	-0.347213	0.012336	0.010197	-0.084901
0.9000	-0.038536	-0.546423	0.013050	0.007983	0.026216
1.0000	-0.087159	-0.601084	0.013730	0.008327	0.094884

----- Mode No. 3 (freq = 0.159823E+03 Hz)

span_loc	flap disp	flap slope	lag disp	lag slope	twist
0.0000	0.000000	0.000000	0.000000	0.000000	0.000000
0.0800	-0.000580	-0.015805	-0.000401	-0.010967	0.000220
0.1600	-0.002047	-0.026492	-0.001494	-0.021103	0.000282
0.2400	-0.003942	-0.028782	-0.003184	-0.029221	-0.000952
0.3200	-0.005562	-0.018382	-0.005347	-0.035528	-0.006474
0.4000	-0.005897	0.008847	-0.007867	-0.040234	-0.022674
0.4800	-0.003799	0.052355	-0.010659	-0.044013	-0.062334
0.5600	0.001381	0.097054	-0.013728	-0.048840	-0.130588
0.6400	0.008263	0.100526	-0.017206	-0.056223	-0.217340
0.7200	0.012963	0.032888	-0.021258	-0.065708	-0.288526
0.8000	0.010462	-0.106946	-0.025960	-0.075184	-0.310007
0.9000	-0.009033	-0.331588	-0.032661	-0.084218	-0.237763
1.0000	-0.040861	-0.403113	-0.039695	-0.085076	-0.159168

## C. AeroDyn Files

### C.1. Primary Input File - fau\_fxBlade\_AD1\_5.ipt

fx77 aerodynamic parameters for FAST Certification fau\_fxBlade.

```

SI                      SysUnits - System of units for used for input and output [must be SI for FAST] (unquoted string)
STEADY                  StallMod - Dynamic stall included [BEDDOES or STEADY] (unquoted string)
USE_CM                  UseCm   - Use aerodynamic pitching moment model? [USE_CM or NO_CM] (unquoted
string)
EQUIL                  InfModel - Inflow model [DYNIN or EQUIL] (unquoted string)
SWIRL                  IndModel - Induction-factor model [NONE or WAKE or SWIRL] (unquoted string)
0.005                  AToler  - Induction-factor tolerance (convergence criteria) (-)
PRANDtl                TLModel - Tip-loss model (EQUIL only) [PRANDtl, GTECH, or NONE] (unquoted string)
NONE                   HLMModel - Hub-loss model (EQUIL only) [PRANDtl or NONE] (unquoted string)
"Wind\fx\fauxBlade_1_5.wnd" WindFile - Name of file containing wind data (quoted string)
10.0                   HH      - Wind reference (hub) height [TowerHt+Twr2Shft+OverHang*SIN(ShftTilt)] (m)
0.0                    TwrShad - Tower-shadow velocity deficit (-)
0.1                    ShadHWid - Tower-shadow half width (m)
0.0                    T_Shad_Refpt - Tower-shadow reference point (m)
1025                   SeaWaterDens - Sea water density (kg/m^3)
1.05e-6                KinVisc - Kinematic sea water viscosity (m^2/sec)
0.0001                 DTAero  - Time interval for aerodynamic calculations (sec)
23                     NumFoil - Number of airfoil files (-)
"AeroData\fx\fx77_02349_01.DAT " FoilNm  - Names of the airfoil files [NumFoil lines] (quoted strings)
"AeroData\fx\fx77_02336_02.DAT "
"AeroData\fx\fx77_02301_03.DAT "
"AeroData\fx\fx77_02273_04.DAT "
"AeroData\fx\fx77_02223_05.DAT "
"AeroData\fx\fx77_02162_06.DAT "
"AeroData\fx\fx77_02092_07.DAT "
"AeroData\fx\fx77_02012_08.DAT "
"AeroData\fx\fx77_01925_09.DAT "
"AeroData\fx\fx77_01832_10.DAT "
"AeroData\fx\fx77_01734_11.DAT "
"AeroData\fx\fx77_01633_12.DAT "
"AeroData\fx\fx77_01530_13.DAT "
"AeroData\fx\fx77_01486_14.DAT "
"AeroData\fx\fx77_01442_15.DAT "
"AeroData\fx\fx77_01400_16.DAT "
"AeroData\fx\fx77_01360_17.DAT "
"AeroData\fx\fx77_01323_18.DAT "
"AeroData\fx\fx77_01289_19.DAT "
"AeroData\fx\fx77_01258_20.DAT "
"AeroData\fx\fx77_01232_21.DAT "
"AeroData\fx\fx77_01211_22.DAT "
"AeroData\fx\fx77_01210_23.DAT "
25                     BldNodes - Number of blade nodes used for analysis (-)
RNodes AeroTwst DRNodes Chord NFoil PrnElm
0.2670 26.340 0.020 0.311 1 PRINT
0.2820 25.929 0.010 0.310 1 PRINT
0.2965 24.794 0.019 0.307 2 PRINT
0.3200 23.150 0.028 0.302 3 PRINT
0.3525 21.227 0.037 0.294 4 PRINT
0.3935 19.195 0.045 0.285 5 PRINT
0.4425 17.147 0.053 0.273 6 PRINT
0.4985 15.182 0.059 0.260 7 PRINT
0.5605 13.353 0.065 0.246 8 PRINT
0.6275 11.684 0.069 0.232 9 PRINT
0.6985 10.202 0.073 0.217 10 PRINT
0.7725 8.889 0.075 0.203 11 PRINT
0.8485 7.748 0.077 0.189 12 PRINT
0.9255 6.762 0.077 0.176 13 PRINT
1.0015 5.893 0.075 0.164 14 PRINT
1.0755 5.124 0.073 0.154 15 PRINT
1.1465 4.432 0.069 0.144 16 PRINT

```

1.2135	3.803	0.065	0.137	17	PRINT
1.2755	3.224	0.059	0.130	18	PRINT
1.3315	2.695	0.053	0.124	19	PRINT
1.3805	2.218	0.045	0.120	20	PRINT
1.4215	1.800	0.037	0.117	21	PRINT
1.4540	1.456	0.028	0.114	22	PRINT
1.4775	1.200	0.019	0.113	23	PRINT
1.4925	1.044	0.011	0.112	23	PRINT

## C.2. Primary Input File - fau\_fxBlade\_AD2\_5.ipt

```

fx77 aerodynamic parameters for FAST Certification fau_fxBlade.
SI                               SysUnits - System of units for used for input and output [must be SI for FAST] (unquoted string)
STEADY                           StallMod - Dynamic stall included [BEDDOES or STEADY] (unquoted string)
USE_CM                           UseCm - Use aerodynamic pitching moment model? [USE_CM or NO_CM] (unquoted
string)
EQUIL                            InfModel - Inflow model [DYNIN or EQUIL] (unquoted string)
SWIRL                            IndModel - Induction-factor model [NONE or WAKE or SWIRL] (unquoted string)
  0.005                          AToler - Induction-factor tolerance (convergence criteria) (-)
PRANDtl                          TLModel - Tip-loss model (EQUIL only) [PRANDtl, GTECH, or NONE] (unquoted string)
NONE                             HLMModel - Hub-loss model (EQUIL only) [PRANDtl or NONE] (unquoted string)
"Wind\xfau_fxBlade_2_5.wnd"      WindFile - Name of file containing wind data (quoted string)
  10.0                           HH - Wind reference (hub) height [TowerHt+Twr2Shft+OverHang*SIN(ShftTilt)] (m)
  0.0                            TwrShad - Tower-shadow velocity deficit (-)
  0.1                            ShadHWid - Tower-shadow half width (m)
  0.0                            T_Shad_Refpt - Tower-shadow reference point (m)
  1025                          SeaWaterDens - Sea water density (kg/m^3)
  1.05e-6                       KinVisc - Kinematic sea water viscosity (m^2/sec)
  0.0001                        DTAero - Time interval for aerodynamic calculations (sec)
  23                             NumFoil - Number of airfoil files (-)
"AeroData\xfa77_02349_01.DAT "   FoilNm - Names of the airfoil files [NumFoil lines] (quoted strings)
"AeroData\xfa77_02336_02.DAT "
"AeroData\xfa77_02301_03.DAT "
"AeroData\xfa77_02273_04.DAT "
"AeroData\xfa77_02223_05.DAT "
"AeroData\xfa77_02162_06.DAT "
"AeroData\xfa77_02092_07.DAT "
"AeroData\xfa77_02012_08.DAT "
"AeroData\xfa77_01925_09.DAT "
"AeroData\xfa77_01832_10.DAT "
"AeroData\xfa77_01734_11.DAT "
"AeroData\xfa77_01633_12.DAT "
"AeroData\xfa77_01530_13.DAT "
"AeroData\xfa77_01486_14.DAT "
"AeroData\xfa77_01442_15.DAT "
"AeroData\xfa77_01400_16.DAT "
"AeroData\xfa77_01360_17.DAT "
"AeroData\xfa77_01323_18.DAT "
"AeroData\xfa77_01289_19.DAT "
"AeroData\xfa77_01258_20.DAT "
"AeroData\xfa77_01232_21.DAT "
"AeroData\xfa77_01211_22.DAT "
"AeroData\xfa77_01210_23.DAT "
  25                             BldNodes - Number of blade nodes used for analysis (-)
RNodes AeroTwst DRNodes Chord NFoil PrnElm
0.2670 26.340 0.020 0.311 1 PRINT
0.2820 25.929 0.010 0.310 1 PRINT
0.2965 24.794 0.019 0.307 2 PRINT
0.3200 23.150 0.028 0.302 3 PRINT
0.3525 21.227 0.037 0.294 4 PRINT
0.3935 19.195 0.045 0.285 5 PRINT
0.4425 17.147 0.053 0.273 6 PRINT
0.4985 15.182 0.059 0.260 7 PRINT
0.5605 13.353 0.065 0.246 8 PRINT
0.6275 11.684 0.069 0.232 9 PRINT
0.6985 10.202 0.073 0.217 10 PRINT

```

0.7725	8.889	0.075	0.203	11	PRINT
0.8485	7.748	0.077	0.189	12	PRINT
0.9255	6.762	0.077	0.176	13	PRINT
1.0015	5.893	0.075	0.164	14	PRINT
1.0755	5.124	0.073	0.154	15	PRINT
1.1465	4.432	0.069	0.144	16	PRINT
1.2135	3.803	0.065	0.137	17	PRINT
1.2755	3.224	0.059	0.130	18	PRINT
1.3315	2.695	0.053	0.124	19	PRINT
1.3805	2.218	0.045	0.120	20	PRINT
1.4215	1.800	0.037	0.117	21	PRINT
1.4540	1.456	0.028	0.114	22	PRINT
1.4775	1.200	0.019	0.113	23	PRINT
1.4925	1.044	0.011	0.112	23	PRINT

### C.3. Hydrofoil Input File - fx77\_02349\_01.dat

"fx77\_02349 Airfoil,DesignFoil data at Re=1.0 Million, Clean roughness"  
Adjusted for Post Stall at r/R=.185 by AirfoilPrep\_v2p2\_2. FAU.

```

1      Number of airfoil tables in this file
0      Table ID parameter
7      Stall angle (deg)**
0      "No longer used, enter zero"
0      "No longer used, enter zero"
0      "No longer used, enter zero"
-15.4760 Zero Cn angle of attack (deg)
2.6517 Cn slope for zero lift (dimensionless)
1.0402 Cn extrapolated to value at positive stall angle of attack
-1.3915 Cn at stall value for negative angle of attack
10.00 Angle of attack for minimum CD (deg)
0.0047 Minimum CD value
-180.00 0.000 0.0100 0.0000
-170.00 0.038 0.0100 0.4000
-160.00 0.075 0.0100 0.0944
-150.00 0.255 0.0100 0.2567
-140.00 0.351 0.2198 0.3683
-130.00 0.380 0.4782 0.4341
-120.00 0.348 0.7311 0.4525
-110.00 0.266 0.9527 0.4256
-100.00 0.144 1.1217 0.3548
-90.00 0.000 1.2234 0.2452
-80.00 -0.144 1.1217 0.0888
-70.00 -0.266 0.9527 -0.0537
-60.00 -0.348 0.7311 -0.1700
-50.00 -0.380 0.4782 -0.2500
-40.00 -0.351 0.2198 -0.2844
-30.00 -0.255 0.0100 -0.2651
-20.00 -0.075 0.0100 -0.1784
-10.00 -1.375 0.2131 -0.0510
-9.00 -1.189 0.1836 -0.0520
-8.00 -1.002 0.1563 -0.0530
-7.00 -0.813 0.1313 -0.0540
-6.00 -0.624 0.1084 -0.0550
-5.00 -0.435 0.0880 -0.0570
-4.00 -0.246 0.0697 -0.0590
-3.00 -0.057 0.0535 -0.0600
-2.00 0.132 0.0398 -0.0620
-1.00 0.321 0.0283 -0.0640
0.00 0.510 0.0189 -0.0660
1.00 0.699 0.0116 -0.0680
2.00 0.823 0.0089 -0.0700
3.00 0.892 0.0100 -0.0730
4.00 0.942 0.0113 -0.0750
5.00 0.977 0.0133 -0.0780
6.00 0.994 0.0147 -0.0800
7.00 0.998 0.0151 -0.0830
8.00 0.987 0.0144 -0.0860

```

9.00	0.963	0.0107	-0.0880
10.00	0.925	0.0047	-0.0910
11.00	0.875	0.0100	-0.0940
12.00	0.814	0.0100	-0.0970
13.00	0.742	0.0100	-0.1000
14.00	0.659	0.0100	-0.1040
15.00	0.565	0.0100	-0.1070
16.00	0.484	0.0100	-0.1100
17.00	0.396	0.0100	-0.1130
18.00	0.304	0.0100	-0.1170
19.00	0.208	0.0100	-0.1200
20.00	0.108	0.0100	-0.1240
30.00	0.364	0.0100	-0.5109
40.00	0.502	0.2198	-0.6101
50.00	0.543	0.4782	-0.6401
60.00	0.498	0.7311	-0.6211
70.00	0.379	0.9527	-0.5660
80.00	0.206	1.1217	-0.4800
90.00	0.000	1.2234	-0.3665
100.00	-0.144	1.1217	-0.2100
110.00	-0.266	0.9527	-0.0675
120.00	-0.348	0.7311	0.0488
130.00	-0.380	0.4782	0.1288
140.00	-0.351	0.2198	0.1632
150.00	-0.255	0.0100	0.1439
160.00	-0.075	0.0100	0.0572
170.00	-0.038	0.0100	-0.5000
180.00	0.000	0.0100	0.0000

#### C.4. Hydrofoil Input File - fx77\_02336\_02.dat

"fx77\_02336 Airfoil, DesignFoil data at Re=1.0 Million, Clean roughness"  
Adjusted for Post Stall at r/R=.185 by AirfoilPrep\_v2p2\_2. FAU.

1	Number of airfoil tables in this file		
0	Table ID parameter		
7	Stall angle (deg)**		
0	"No longer used, enter zero"		
0	"No longer used, enter zero"		
0	"No longer used, enter zero"		
-16.2642	Zero Cn angle of attack (deg)		
2.3293	Cn slope for zero lift (dimensionless)		
0.9458	Cn extrapolated to value at positive stall angle of attack		
-1.5486	Cn at stall value for negative angle of attack		
11.00	Angle of attack for minimum CD (deg)		
0.0045	Minimum CD value		
-180.00	0.000	0.0100	0.0000
-170.00	0.082	0.0100	0.4000
-160.00	0.163	0.0100	-0.0054
-150.00	0.306	0.0458	0.0298
-140.00	0.382	0.2755	0.0775
-130.00	0.398	0.5249	0.1243
-120.00	0.358	0.7674	0.1684
-110.00	0.270	0.9776	0.2060
-100.00	0.145	1.1344	0.2330
-90.00	0.000	1.2234	0.2462
-80.00	-0.145	1.1344	0.2189
-70.00	-0.270	0.9776	0.1802
-60.00	-0.358	0.7674	0.1342
-50.00	-0.398	0.5249	0.0855
-40.00	-0.382	0.2755	0.0382
-30.00	-0.306	0.0458	-0.0052
-20.00	-0.163	0.0100	-0.0356
-10.00	-1.528	0.2493	-0.0490
-9.00	-1.330	0.2138	-0.0500
-8.00	-1.131	0.1812	-0.0510
-7.00	-0.930	0.1516	-0.0530
-6.00	-0.729	0.1244	-0.0540
-5.00	-0.528	0.1000	-0.0550

-4.00	-0.327	0.0786	-0.0570
-3.00	-0.126	0.0597	-0.0590
-2.00	0.074	0.0434	-0.0600
-1.00	0.275	0.0297	-0.0620
0.00	0.476	0.0188	-0.0640
1.00	0.665	0.0115	-0.0660
2.00	0.745	0.0095	-0.0680
3.00	0.806	0.0099	-0.0710
4.00	0.853	0.0108	-0.0730
5.00	0.888	0.0126	-0.0750
6.00	0.908	0.0141	-0.0780
7.00	0.916	0.0141	-0.0800
8.00	0.912	0.0152	-0.0830
9.00	0.897	0.0131	-0.0860
10.00	0.872	0.0094	-0.0880
11.00	0.837	0.0045	-0.0910
12.00	0.792	0.0100	-0.0940
13.00	0.738	0.0100	-0.0970
14.00	0.675	0.0100	-0.1000
15.00	0.603	0.0100	-0.1030
16.00	0.537	0.0100	-0.1060
17.00	0.468	0.0100	-0.1090
18.00	0.392	0.0100	-0.1120
19.00	0.314	0.0100	-0.1150
20.00	0.233	0.0100	-0.1190
30.00	0.437	0.0458	-0.1843
40.00	0.546	0.2755	-0.2333
50.00	0.569	0.5249	-0.2742
60.00	0.512	0.7674	-0.3084
70.00	0.385	0.9776	-0.3357
80.00	0.207	1.1344	-0.3551
90.00	0.000	1.2234	-0.3655
100.00	-0.145	1.1344	-0.3381
110.00	-0.270	0.9776	-0.2994
120.00	-0.358	0.7674	-0.2535
130.00	-0.398	0.5249	-0.2048
140.00	-0.382	0.2755	-0.1574
150.00	-0.306	0.0458	-0.1140
160.00	-0.163	0.0100	-0.0837
170.00	-0.082	0.0100	-0.5000
180.00	0.000	0.0100	0.0000

### C.5. Hydrofoil Input File -fx77\_02301\_03.dat

"fx77\_02301 Airfoil,DesignFoil data at Re=1.0 Million, Clean roughness"  
Adjusted for Post Stall at r/R=0.204 by AirfoilPrep\_v2p2\_2. FAU.

1	Number of airfoil tables in this file
0	Table ID parameter
12	Stall angle (deg)**
0	"No longer used, enter zero"
0	"No longer used, enter zero"
0	"No longer used, enter zero"
-9.8797	Zero Cn angle of attack (deg)
3.8184	Cn slope for zero lift (dimensionless)
1.4581	Cn extrapolated to value at positive stall angle of attack
-0.8200	Cn at stall value for negative angle of attack
19.00	Angle of attack for minimum CD (deg)
0.0016	Minimum CD value
-180.00	0.000 0.0100 0.0000
-170.00	0.357 0.0100 0.4000
-160.00	0.715 0.0100 -0.0108
-150.00	0.626 0.1723 0.0290
-140.00	0.577 0.3873 0.0624
-130.00	0.514 0.6188 0.1007
-120.00	0.420 0.8404 0.1430
-110.00	0.296 1.0275 0.1856
-100.00	0.152 1.1597 0.2232
-90.00	0.000 1.2234 0.2508

-80.00	-0.152	1.1597	0.2509
-70.00	-0.296	1.0275	0.2377
-60.00	-0.420	0.8404	0.2157
-50.00	-0.514	0.6188	0.1912
-40.00	-0.577	0.3873	0.1730
-30.00	-0.626	0.1723	0.1751
-20.00	-0.715	0.0100	0.2382
-10.00	-0.827	0.0401	-0.0480
-9.00	-0.691	0.0354	-0.0490
-8.00	-0.554	0.0312	-0.0500
-7.00	-0.417	0.0277	-0.0510
-6.00	-0.279	0.0243	-0.0520
-5.00	-0.143	0.0212	-0.0540
-4.00	-0.005	0.0186	-0.0550
-3.00	0.132	0.0164	-0.0570
-2.00	0.270	0.0144	-0.0590
-1.00	0.408	0.0127	-0.0600
0.00	0.545	0.0115	-0.0620
1.00	0.682	0.0106	-0.0640
2.00	0.804	0.0097	-0.0660
3.00	0.883	0.0102	-0.0690
4.00	0.951	0.0107	-0.0710
5.00	1.011	0.0113	-0.0730
6.00	1.059	0.0136	-0.0760
7.00	1.101	0.0149	-0.0780
8.00	1.133	0.0165	-0.0810
9.00	1.158	0.0167	-0.0840
10.00	1.175	0.0168	-0.0870
11.00	1.185	0.0171	-0.0900
12.00	1.188	0.0164	-0.0920
13.00	1.185	0.0153	-0.0950
14.00	1.176	0.0137	-0.0990
15.00	1.159	0.0116	-0.1020
16.00	1.142	0.0093	-0.1050
17.00	1.119	0.0069	-0.1080
18.00	1.091	0.0046	-0.1110
19.00	1.059	0.0016	-0.1150
20.00	1.021	0.0100	-0.1180
30.00	0.895	0.1723	-0.1702
40.00	0.825	0.3873	-0.2048
50.00	0.734	0.6188	-0.2382
60.00	0.600	0.8404	-0.2722
70.00	0.423	1.0275	-0.3056
80.00	0.217	1.1597	-0.3360
90.00	0.000	1.2234	-0.3609
100.00	-0.152	1.1597	-0.3610
110.00	-0.296	1.0275	-0.3479
120.00	-0.420	0.8404	-0.3259
130.00	-0.514	0.6188	-0.3014
140.00	-0.577	0.3873	-0.2831
150.00	-0.626	0.1723	-0.2853
160.00	-0.715	0.0100	-0.3484
170.00	-0.357	0.0100	-0.5000
180.00	0.000	0.0100	0.0000

## C.6. Hydrofoil Input File -fx77\_02273\_04.dat

"fx77\_02273 Airfoil, DesignFoil data at Re=1.0 Million, Clean roughness"  
 Adjusted for Post Stall at r/R=0.204 by AirfoilPrep\_v2p2\_2. FAU.

1        Number of airfoil tables in this file  
 0        Table ID parameter  
 12       Stall angle (deg)\*\*  
 0        "No longer used, enter zero"  
 0        "No longer used, enter zero"  
 0        "No longer used, enter zero"  
 -7.5747 Zero Cn angle of attack (deg)  
 4.5814 Cn slope for zero lift (dimensionless)  
 2.2049 Cn extrapolated to value at positive stall angle of 135° attack

-1.0784 Cn at stall value for negative angle of attack  
-3.00 Angle of attack for minimum CD (deg)  
0.0015 Minimum CD value

-180.00	0.000	0.0100	0.0000
-170.00	0.551	0.0250	0.4000
-160.00	1.101	0.1275	-0.0085
-150.00	0.842	0.2846	0.0510
-140.00	0.701	0.4773	0.0826
-130.00	0.580	0.6826	0.1150
-120.00	0.450	0.8758	0.1510
-110.00	0.305	1.0338	0.1875
-100.00	0.151	1.1375	0.2197
-90.00	0.000	1.1748	0.2423
-80.00	-0.151	1.1375	0.2507
-70.00	-0.305	1.0338	0.2474
-60.00	-0.450	0.8758	0.2379
-50.00	-0.580	0.6826	0.2300
-40.00	-0.701	0.4773	0.2364
-30.00	-0.842	0.2846	0.2820
-20.00	-1.101	0.1275	0.4449
-10.00	-0.635	0.0100	-0.0460
-9.00	-0.518	0.0100	-0.0460
-8.00	-0.401	0.0100	-0.0470
-7.00	-0.283	0.0100	-0.0480
-6.00	-0.166	0.0100	-0.0490
-5.00	-0.048	0.0100	-0.0510
-4.00	0.069	0.0100	-0.0520
-3.00	0.187	0.0015	-0.0540
-2.00	0.305	0.0041	-0.0550
-1.00	0.423	0.0063	-0.0570
0.00	0.541	0.0082	-0.0590
1.00	0.658	0.0081	-0.0610
2.00	0.774	0.0093	-0.0630
3.00	0.861	0.0095	-0.0650
4.00	0.943	0.0100	-0.0670
5.00	1.018	0.0102	-0.0690
6.00	1.088	0.0109	-0.0720
7.00	1.153	0.0120	-0.0740
8.00	1.214	0.0146	-0.0770
9.00	1.270	0.0209	-0.0790
10.00	1.321	0.0246	-0.0820
11.00	1.368	0.0294	-0.0850
12.00	1.411	0.0354	-0.0880
13.00	1.451	0.0428	-0.0900
14.00	1.486	0.0514	-0.0930
15.00	1.518	0.0628	-0.0960
16.00	1.540	0.0736	-0.1000
17.00	1.556	0.0855	-0.1030
18.00	1.567	0.0984	-0.1060
19.00	1.573	0.1124	-0.1090
20.00	1.573	0.1275	-0.1120
30.00	1.203	0.2846	-0.1906
40.00	1.001	0.4773	-0.2220
50.00	0.828	0.6826	-0.2475
60.00	0.642	0.8758	-0.2736
70.00	0.435	1.0338	-0.3003
80.00	0.215	1.1375	-0.3252
90.00	0.000	1.1748	-0.3451
100.00	-0.151	1.1375	-0.3535
110.00	-0.305	1.0338	-0.3503
120.00	-0.450	0.8758	-0.3407
130.00	-0.580	0.6826	-0.3328
140.00	-0.701	0.4773	-0.3393
150.00	-0.842	0.2846	-0.3849
160.00	-1.101	0.1275	-0.5477
170.00	-0.551	0.0250	-0.5000
180.00	0.000	0.0100	0.0000



## C.7. Hydrofoil Input File - fx77\_02223\_05.dat

"fx77\_02223 Airfoil, DesignFoil data at Re=1.0 Million, Clean roughness"  
Adjusted for Post Stall at r/R=0.204 by AirfoilPrep\_v2p2\_2. FAU.

```
1      Number of airfoil tables in this file
0      Table ID parameter
20     Stall angle (deg)**
0      "No longer used, enter zero"
0      "No longer used, enter zero"
0      "No longer used, enter zero"
-6.2749 Zero Cn angle of attack (deg)
5.0642  Cn slope for zero lift (dimensionless)
2.3224  Cn extrapolated to value at positive stall angle of attack
-1.3410 Cn at stall value for negative angle of attack
-1.00   Angle of attack for minimum CD (deg)
0.0030  Minimum CD value
-180.00 0.000 0.0756 0.0000
-170.00 0.670 0.1114 0.4000
-160.00 1.341 0.2142 -0.0060
-150.00 0.990 0.3713 0.0695
-140.00 0.799 0.5634 0.1037
-130.00 0.644 0.7665 0.1361
-120.00 0.490 0.9554 0.1715
-110.00 0.327 1.1062 0.2072
-100.00 0.159 1.1996 0.2381
-90.00  0.000 1.2234 0.2587
-80.00 -0.159 1.1996 0.2721
-70.00 -0.327 1.1062 0.2740
-60.00 -0.490 0.9554 0.2703
-50.00 -0.644 0.7665 0.2702
-40.00 -0.799 0.5634 0.2889
-30.00 -0.990 0.3713 0.3577
-20.00 -1.341 0.2142 0.5783
-10.00 -0.557 0.0100 -0.0420
-9.00  -0.450 0.0100 -0.0430
-8.00  -0.342 0.0100 -0.0440
-7.00  -0.235 0.0100 -0.0440
-6.00  -0.127 0.0100 -0.0450
-5.00  -0.019 0.0100 -0.0470
-4.00  0.089 0.0100 -0.0480
-3.00  0.197 0.0100 -0.0490
-2.00  0.304 0.0100 -0.0510
-1.00  0.412 0.0030 -0.0520
0.00   0.520 0.0064 -0.0540
1.00   0.628 0.0077 -0.0560
2.00   0.735 0.0099 -0.0580
3.00   0.829 0.0095 -0.0600
4.00   0.919 0.0098 -0.0620
5.00   1.005 0.0096 -0.0640
6.00   1.089 0.0102 -0.0660
7.00   1.170 0.0117 -0.0680
8.00   1.248 0.0153 -0.0710
9.00   1.324 0.0234 -0.0730
10.00  1.398 0.0298 -0.0760
11.00  1.469 0.0382 -0.0780
12.00  1.538 0.0489 -0.0810
13.00  1.606 0.0619 -0.0840
14.00  1.671 0.0773 -0.0870
15.00  1.735 0.0965 -0.0900
16.00  1.782 0.1165 -0.0930
17.00  1.824 0.1379 -0.0960
18.00  1.860 0.1614 -0.0990
19.00  1.891 0.1868 -0.1020
20.00  1.916 0.2142 -0.1050
30.00  1.414 0.3713 -0.2049
40.00  1.141 0.5634 -0.2387
50.00  0.920 0.7665 -0.2630
```

60.00	0.700	0.9554	-0.2873
70.00	0.467	1.1062	-0.3121
80.00	0.227	1.1996	-0.3352
90.00	0.000	1.2234	-0.3530
100.00	-0.159	1.1996	-0.3664
110.00	-0.327	1.1062	-0.3684
120.00	-0.490	0.9554	-0.3646
130.00	-0.644	0.7665	-0.3645
140.00	-0.799	0.5634	-0.3832
150.00	-0.990	0.3713	-0.4520
160.00	-1.341	0.2142	-0.6727
170.00	-0.670	0.1114	-0.5000
180.00	0.000	0.0756	0.0000

## C.8. Hydrofoil Input File -fx77\_02162\_06.dat

"fx77\_02162 Airfoil,DesignFoil data at Re=1.0 Million, Clean roughness"  
Adjusted for Post Stall at r/R=0.204 by AirfoilPrep\_v2p2\_2. FAU.

```

1      Number of airfoil tables in this file
0      Table ID parameter
20     Stall angle (deg)**
0      "No longer used, enter zero"
0      "No longer used, enter zero"
0      "No longer used, enter zero"
-5.2678 Zero Cn angle of attack (deg)
5.6739 Cn slope for zero lift (dimensionless)
2.5022 Cn extrapolated to value at positive stall angle of attack
-1.4644 Cn at stall value for negative angle of attack
-2.00  Angle of attack for minimum CD (deg)
0.0019 Minimum CD value
-180.00 0.000 0.1070 0.0000
-170.00 0.732 0.1423 0.4000
-160.00 1.464 0.2437 -0.0032
-150.00 1.062 0.3985 0.0798
-140.00 0.842 0.5875 0.1141
-130.00 0.670 0.7867 0.1453
-120.00 0.504 0.9711 0.1794
-110.00 0.333 1.1169 0.2138
-100.00 0.161 1.2051 0.2436
-90.00 0.000 1.2234 0.2632
-80.00 -0.161 1.2051 0.2784
-70.00 -0.333 1.1169 0.2825
-60.00 -0.504 0.9711 0.2818
-50.00 -0.670 0.7867 0.2861
-40.00 -0.842 0.5875 0.3120
-30.00 -1.062 0.3985 0.3943
-20.00 -1.464 0.2437 0.6477
-10.00 -0.638 0.0100 -0.0380
-9.00 -0.525 0.0100 -0.0390
-8.00 -0.412 0.0100 -0.0390
-7.00 -0.299 0.0100 -0.0400
-6.00 -0.186 0.0100 -0.0410
-5.00 -0.072 0.0100 -0.0420
-4.00 0.041 0.0100 -0.0430
-3.00 0.154 0.0100 -0.0440
-2.00 0.268 0.0019 -0.0460
-1.00 0.381 0.0049 -0.0470
0.00 0.495 0.0073 -0.0490
1.00 0.608 0.0076 -0.0500
2.00 0.721 0.0093 -0.0520
3.00 0.828 0.0102 -0.0540
4.00 0.928 0.0095 -0.0560
5.00 1.026 0.0092 -0.0580
6.00 1.120 0.0098 -0.0600
7.00 1.212 0.0114 -0.0620
8.00 1.302 0.0156 -0.0650
9.00 1.389 0.0240 -0.0670

```

10.00	1.474	0.0313	-0.0700
11.00	1.557	0.0407	-0.0720
12.00	1.638	0.0530	-0.0750
13.00	1.717	0.0678	-0.0780
14.00	1.794	0.0856	-0.0800
15.00	1.870	0.1075	-0.0830
16.00	1.926	0.1295	-0.0860
17.00	1.977	0.1551	-0.0890
18.00	2.022	0.1822	-0.0920
19.00	2.060	0.2116	-0.0950
20.00	2.092	0.2437	-0.0980
30.00	1.517	0.3985	-0.2082
40.00	1.203	0.5875	-0.2418
50.00	0.957	0.7867	-0.2642
60.00	0.720	0.9711	-0.2866
70.00	0.475	1.1169	-0.3098
80.00	0.229	1.2051	-0.3317
90.00	0.000	1.2234	-0.3485
100.00	-0.161	1.2051	-0.3637
110.00	-0.333	1.1169	-0.3678
120.00	-0.504	0.9711	-0.3671
130.00	-0.670	0.7867	-0.3714
140.00	-0.842	0.5875	-0.3973
150.00	-1.062	0.3985	-0.4796
160.00	-1.464	0.2437	-0.7329
170.00	-0.732	0.1423	-0.5000
180.00	0.000	0.1070	0.0000

### C.9. Hydrofoil Input File -fx77\_02092\_07.dat

"fx77\_02092 Airfoil,DesignFoil data at Re=1.0 Million, Clean roughness"  
Adjusted for Post Stall at r/R=0.204 by AirfoilPrep\_v2p2\_2. FAU.

1	Number of airfoil tables in this file		
0	Table ID parameter		
20	Stall angle (deg)**		
0	"No longer used, enter zero"		
0	"No longer used, enter zero"		
0	"No longer used, enter zero"		
-4.4992	Zero Cn angle of attack (deg)		
5.9994	Cn slope for zero lift (dimensionless)		
2.5653	Cn extrapolated to value at positive stall angle of attack		
-1.4437	Cn at stall value for negative angle of attack		
-4.00	Angle of attack for minimum CD (deg)		
0.0013	Minimum CD value		
-180.00	0.000	0.1003	0.0000
-170.00	0.725	0.1357	0.4000
-160.00	1.450	0.2374	-0.0012
-150.00	1.053	0.3927	0.0826
-140.00	0.837	0.5823	0.1175
-130.00	0.667	0.7824	0.1491
-120.00	0.502	0.9677	0.1835
-110.00	0.332	1.1146	0.2183
-100.00	0.160	1.2039	0.2486
-90.00	0.000	1.2234	0.2686
-80.00	-0.160	1.2039	0.2836
-70.00	-0.332	1.1146	0.2875
-60.00	-0.502	0.9677	0.2865
-50.00	-0.667	0.7824	0.2904
-40.00	-0.837	0.5823	0.3157
-30.00	-1.053	0.3927	0.3971
-20.00	-1.450	0.2374	0.6485
-10.00	-0.748	0.0100	-0.0330
-9.00	-0.630	0.0100	-0.0340
-8.00	-0.511	0.0100	-0.0340
-7.00	-0.392	0.0100	-0.0350
-6.00	-0.273	0.0100	-0.0350
-5.00	-0.154	0.0100	-0.0360
-4.00	-0.034	0.0013	-0.0370

-3.00	0.085	0.0034	-0.0380
-2.00	0.204	0.0053	-0.0390
-1.00	0.323	0.0067	-0.0410
0.00	0.442	0.0080	-0.0420
1.00	0.561	0.0076	-0.0430
2.00	0.680	0.0085	-0.0450
3.00	0.797	0.0094	-0.0470
4.00	0.903	0.0092	-0.0490
5.00	1.005	0.0090	-0.0500
6.00	1.103	0.0095	-0.0520
7.00	1.199	0.0119	-0.0540
8.00	1.291	0.0159	-0.0570
9.00	1.380	0.0207	-0.0590
10.00	1.466	0.0302	-0.0610
11.00	1.550	0.0395	-0.0640
12.00	1.631	0.0514	-0.0660
13.00	1.710	0.0658	-0.0690
14.00	1.786	0.0832	-0.0710
15.00	1.860	0.1046	-0.0740
16.00	1.916	0.1263	-0.0770
17.00	1.964	0.1501	-0.0800
18.00	2.007	0.1776	-0.0820
19.00	2.043	0.2064	-0.0850
20.00	2.071	0.2374	-0.0880
30.00	1.505	0.3927	-0.1995
40.00	1.196	0.5823	-0.2340
50.00	0.953	0.7824	-0.2570
60.00	0.717	0.9677	-0.2799
70.00	0.474	1.1146	-0.3036
80.00	0.229	1.2039	-0.3260
90.00	0.000	1.2234	-0.3431
100.00	-0.160	1.2039	-0.3582
110.00	-0.332	1.1146	-0.3621
120.00	-0.502	0.9677	-0.3611
130.00	-0.667	0.7824	-0.3650
140.00	-0.837	0.5823	-0.3903
150.00	-1.053	0.3927	-0.4717
160.00	-1.450	0.2374	-0.7230
170.00	-0.725	0.1357	-0.5000
180.00	0.000	0.1003	0.0000

## C.10. Hydrofoil Input File - fx77\_02012\_08.dat

"fx77\_02012 Airfoil, DesignFoil data at Re=1.0 Million, Clean roughness"  
 Adjusted for Post Stall at  $r/R=0.204$  by AirfoilPrep\_v2p2\_2. FAU.

1	Number of airfoil tables in this file
0	Table ID parameter
20	Stall angle (deg)**
0	"No longer used, enter zero"
0	"No longer used, enter zero"
0	"No longer used, enter zero"
-3.9660	Zero Cn angle of attack (deg)
6.1399	Cn slope for zero lift (dimensionless)
2.5682	Cn extrapolated to value at positive stall angle of attack
-1.3653	Cn at stall value for negative angle of attack
-8.00	Angle of attack for minimum CD (deg)
0.0009	Minimum CD value
-180.00	0.000 0.0754 0.0000
-170.00	0.688 0.1111 0.4000
-160.00	1.375 0.2139 0.0011
-150.00	1.010 0.3711 0.0823
-140.00	0.811 0.5632 0.1176
-130.00	0.651 0.7664 0.1503
-120.00	0.494 0.9552 0.1858
-110.00	0.328 1.1061 0.2217
-100.00	0.159 1.1996 0.2529

-90.00	0.000	1.2234	0.2741
-80.00	-0.159	1.1996	0.2880
-70.00	-0.328	1.1061	0.2906
-60.00	-0.494	0.9552	0.2877
-50.00	-0.651	0.7664	0.2891
-40.00	-0.811	0.5632	0.3103
-30.00	-1.010	0.3711	0.3842
-20.00	-1.375	0.2139	0.6180
-10.00	-0.830	0.0100	-0.0280
-9.00	-0.708	0.0100	-0.0280
-8.00	-0.585	0.0009	-0.0290
-7.00	-0.464	0.0020	-0.0290
-6.00	-0.341	0.0032	-0.0300
-5.00	-0.219	0.0044	-0.0300
-4.00	-0.097	0.0054	-0.0310
-3.00	0.026	0.0063	-0.0320
-2.00	0.148	0.0071	-0.0330
-1.00	0.270	0.0080	-0.0340
0.00	0.393	0.0087	-0.0350
1.00	0.515	0.0077	-0.0360
2.00	0.637	0.0089	-0.0380
3.00	0.760	0.0094	-0.0390
4.00	0.870	0.0091	-0.0410
5.00	0.973	0.0088	-0.0420
6.00	1.072	0.0101	-0.0440
7.00	1.166	0.0115	-0.0460
8.00	1.256	0.0141	-0.0480
9.00	1.343	0.0191	-0.0500
10.00	1.426	0.0275	-0.0520
11.00	1.505	0.0361	-0.0540
12.00	1.581	0.0468	-0.0570
13.00	1.654	0.0596	-0.0590
14.00	1.723	0.0752	-0.0610
15.00	1.789	0.0935	-0.0640
16.00	1.838	0.1139	-0.0670
17.00	1.880	0.1352	-0.0690
18.00	1.916	0.1591	-0.0720
19.00	1.944	0.1845	-0.0750
20.00	1.964	0.2139	-0.0780
30.00	1.443	0.3711	-0.1861
40.00	1.158	0.5632	-0.2217
50.00	0.931	0.7664	-0.2463
60.00	0.705	0.9552	-0.2708
70.00	0.469	1.1061	-0.2958
80.00	0.228	1.1996	-0.3193
90.00	0.000	1.2234	-0.3376
100.00	-0.159	1.1996	-0.3516
110.00	-0.328	1.1061	-0.3542
120.00	-0.494	0.9552	-0.3513
130.00	-0.651	0.7664	-0.3526
140.00	-0.811	0.5632	-0.3739
150.00	-1.010	0.3711	-0.4478
160.00	-1.375	0.2139	-0.6816
170.00	-0.688	0.1111	-0.5000
180.00	0.000	0.0754	0.0000

### C.11. Hydrofoil Input File - fx77\_01925\_09.dat

"fx77\_02012 Airfoil, DesignFoil data at Re=1.0 Million, Clean roughness"  
Adjusted for Post Stall at r/R=0.204 by AirfoilPrep\_v2p2\_2. FAU.

```

1      Number of airfoil tables in this file
0      Table ID parameter
20     Stall angle (deg)**
0      "No longer used, enter zero"
0      "No longer used, enter zero"
0      "No longer used, enter zero"
-3.4069 Zero Cn angle of attack (deg)
6.3216  Cn slope for zero lift (dimensionless)

```

2.5826 Cn extrapolated to value at positive stall angle of attack  
 -1.2734 Cn at stall value for negative angle of attack  
 1.00 Angle of attack for minimum CD (deg)  
 0.0076 Minimum CD value

-180.00	0.000	0.0423	0.0000
-170.00	0.644	0.0786	0.4000
-160.00	1.289	0.1829	0.0037
-150.00	0.960	0.3425	0.0817
-140.00	0.780	0.5379	0.1176
-130.00	0.633	0.7451	0.1514
-120.00	0.484	0.9387	0.1881
-110.00	0.324	1.0948	0.2254
-100.00	0.158	1.1939	0.2580
-90.00	0.000	1.2234	0.2806
-80.00	-0.158	1.1939	0.2931
-70.00	-0.324	1.0948	0.2940
-60.00	-0.484	0.9387	0.2889
-50.00	-0.633	0.7451	0.2871
-40.00	-0.780	0.5379	0.3036
-30.00	-0.960	0.3425	0.3689
-20.00	-1.289	0.1829	0.5825
-10.00	-0.900	0.0092	-0.0230
-9.00	-0.776	0.0091	-0.0230
-8.00	-0.652	0.0087	-0.0230
-7.00	-0.527	0.0087	-0.0240
-6.00	-0.403	0.0087	-0.0240
-5.00	-0.278	0.0087	-0.0240
-4.00	-0.154	0.0088	-0.0250
-3.00	-0.030	0.0088	-0.0250
-2.00	0.095	0.0089	-0.0260
-1.00	0.220	0.0090	-0.0270
0.00	0.345	0.0089	-0.0280
1.00	0.469	0.0076	-0.0290
2.00	0.593	0.0078	-0.0300
3.00	0.718	0.0088	-0.0310
4.00	0.837	0.0090	-0.0330
5.00	0.942	0.0095	-0.0340
6.00	1.042	0.0098	-0.0360
7.00	1.136	0.0109	-0.0370
8.00	1.225	0.0140	-0.0390
9.00	1.308	0.0173	-0.0410
10.00	1.387	0.0222	-0.0430
11.00	1.461	0.0318	-0.0450
12.00	1.531	0.0405	-0.0470
13.00	1.596	0.0514	-0.0490
14.00	1.657	0.0644	-0.0510
15.00	1.713	0.0799	-0.0540
16.00	1.753	0.0975	-0.0560
17.00	1.786	0.1157	-0.0580
18.00	1.813	0.1362	-0.0610
19.00	1.831	0.1587	-0.0640
20.00	1.841	0.1829	-0.0660
30.00	1.371	0.3425	-0.1702
40.00	1.114	0.5379	-0.2069
50.00	0.905	0.7451	-0.2334
60.00	0.692	0.9387	-0.2596
70.00	0.463	1.0948	-0.2863
80.00	0.226	1.1939	-0.3113
90.00	0.000	1.2234	-0.3311
100.00	-0.158	1.1939	-0.3436
110.00	-0.324	1.0948	-0.3444
120.00	-0.484	0.9387	-0.3394
130.00	-0.633	0.7451	-0.3376
140.00	-0.780	0.5379	-0.3540
150.00	-0.960	0.3425	-0.4194
160.00	-1.289	0.1829	-0.6330
170.00	-0.644	0.0786	-0.5000
180.00	0.000	0.0423	0.0000

## C.12. Hydrofoil Input File - fx77\_01832\_10.dat

"fx77\_01832 Airfoil,DesignFoil data at Re=1.0 Million, Clean roughness"  
Adjusted for Post Stall at r/R=0.204 by AirfoilPrep\_v2p2\_2. FAU.

```

1      Number of airfoil tables in this file
0      Table ID parameter
20     Stall angle (deg)**
0      "No longer used, enter zero"
0      "No longer used, enter zero"
0      "No longer used, enter zero"
-3.0311 Zero Cn angle of attack (deg)
6.4763 Cn slope for zero lift (dimensionless)
2.6033 Cn extrapolated to value at positive stall angle of attack
-1.1937 Cn at stall value for negative angle of attack
1.00   Angle of attack for minimum CD (deg)
0.0075 Minimum CD value
-180.00 0.000 0.0094 0.0000
-170.00 0.607 0.0461 0.4000
-160.00 1.215 0.1519 0.0064
-150.00 0.917 0.3140 0.0814
-140.00 0.754 0.5127 0.1175
-130.00 0.618 0.7240 0.1521
-120.00 0.476 0.9222 0.1899
-110.00 0.321 1.0835 0.2284
-100.00 0.158 1.1881 0.2623
-90.00 0.000 1.2234 0.2864
-80.00 -0.158 1.1881 0.2974
-70.00 -0.321 1.0835 0.2966
-60.00 -0.476 0.9222 0.2894
-50.00 -0.618 0.7240 0.2848
-40.00 -0.754 0.5127 0.2971
-30.00 -0.917 0.3140 0.3551
-20.00 -1.215 0.1519 0.5515
-10.00 -0.934 0.0143 -0.0190
-9.00 -0.809 0.0133 -0.0190
-8.00 -0.685 0.0122 -0.0190
-7.00 -0.560 0.0116 -0.0180
-6.00 -0.435 0.0110 -0.0190
-5.00 -0.311 0.0105 -0.0190
-4.00 -0.186 0.0101 -0.0190
-3.00 -0.060 0.0097 -0.0190
-2.00 0.065 0.0095 -0.0200
-1.00 0.190 0.0094 -0.0200
0.00 0.315 0.0083 -0.0210
1.00 0.440 0.0075 -0.0220
2.00 0.565 0.0082 -0.0230
3.00 0.690 0.0086 -0.0240
4.00 0.814 0.0087 -0.0250
5.00 0.924 0.0093 -0.0260
6.00 1.026 0.0096 -0.0280
7.00 1.121 0.0113 -0.0290
8.00 1.209 0.0129 -0.0310
9.00 1.290 0.0155 -0.0320
10.00 1.365 0.0192 -0.0340
11.00 1.434 0.0269 -0.0360
12.00 1.498 0.0343 -0.0380
13.00 1.556 0.0429 -0.0400
14.00 1.608 0.0540 -0.0420
15.00 1.655 0.0669 -0.0440
16.00 1.687 0.0806 -0.0470
17.00 1.711 0.0958 -0.0490
18.00 1.728 0.1129 -0.0510
19.00 1.736 0.1317 -0.0540
20.00 1.736 0.1519 -0.0560
30.00 1.310 0.3140 -0.1565
40.00 1.077 0.5127 -0.1938
50.00 0.883 0.7240 -0.2218

```

60.00	0.680	0.9222	-0.2495
70.00	0.458	1.0835	-0.2776
80.00	0.225	1.1881	-0.3041
90.00	0.000	1.2234	-0.3253
100.00	-0.158	1.1881	-0.3364
110.00	-0.321	1.0835	-0.3355
120.00	-0.476	0.9222	-0.3284
130.00	-0.618	0.7240	-0.3238
140.00	-0.754	0.5127	-0.3361
150.00	-0.917	0.3140	-0.3941
160.00	-1.215	0.1519	-0.5904
170.00	-0.607	0.0461	-0.5000
180.00	0.000	0.0094	0.0000

### C.13. Hydrofoil Input File - fx77\_01734\_11.dat

"fx77\_01734 Airfoil, DesignFoil data at Re=1.0 Million, Clean roughness"

Adjusted for Post Stall at r/R=0.204 by AirfoilPrep\_v2p2\_2. FAU.

```

1      Number of airfoil tables in this file
0      Table ID parameter
18     Stall angle (deg)**
0      "No longer used, enter zero"
0      "No longer used, enter zero"
0      "No longer used, enter zero"
-2.5663 Zero Cn angle of attack (deg)
6.6502 Cn slope for zero lift (dimensionless)
2.3871 Cn extrapolated to value at positive stall angle of attack
-1.1210 Cn at stall value for negative angle of attack
2.00   Angle of attack for minimum CD (deg)
0.0079 Minimum CD value
-180.00 0.000 0.0100 0.0000
-170.00 0.574 0.0165 0.4000
-160.00 1.148 0.1236 0.0079
-150.00 0.878 0.2879 0.0807
-140.00 0.730 0.4896 0.1172
-130.00 0.604 0.7046 0.1527
-120.00 0.468 0.9072 0.1916
-110.00 0.317 1.0732 0.2312
-100.00 0.157 1.1829 0.2664
-90.00 0.000 1.2234 0.2919
-80.00 -0.157 1.1829 0.3017
-70.00 -0.317 1.0732 0.2993
-60.00 -0.468 0.9072 0.2903
-50.00 -0.604 0.7046 0.2833
-40.00 -0.730 0.4896 0.2919
-30.00 -0.878 0.2879 0.3434
-20.00 -1.148 0.1236 0.5246
-10.00 -0.962 0.0147 -0.0150
-9.00 -0.838 0.0136 -0.0150
-8.00 -0.715 0.0127 -0.0140
-7.00 -0.591 0.0118 -0.0140
-6.00 -0.467 0.0112 -0.0140
-5.00 -0.343 0.0106 -0.0130
-4.00 -0.218 0.0102 -0.0130
-3.00 -0.094 0.0098 -0.0140
-2.00 0.030 0.0094 -0.0140
-1.00 0.154 0.0092 -0.0140
0.00 0.278 0.0090 -0.0150
1.00 0.403 0.0085 -0.0150
2.00 0.527 0.0079 -0.0160
3.00 0.651 0.0081 -0.0170
4.00 0.775 0.0090 -0.0170
5.00 0.893 0.0092 -0.0180
6.00 1.001 0.0094 -0.0200
7.00 1.100 0.0109 -0.0210
8.00 1.190 0.0119 -0.0220
9.00 1.272 0.0137 -0.0240
10.00 1.346 0.0164 -0.0250

```



11.00	1.413	0.0213	-0.0270
12.00	1.472	0.0272	-0.0280
13.00	1.524	0.0353	-0.0300
14.00	1.569	0.0438	-0.0320
15.00	1.607	0.0542	-0.0340
16.00	1.632	0.0650	-0.0360
17.00	1.648	0.0774	-0.0380
18.00	1.655	0.0915	-0.0410
19.00	1.653	0.1068	-0.0430
20.00	1.640	0.1236	-0.0450
30.00	1.254	0.2879	-0.1428
40.00	1.043	0.4896	-0.1811
50.00	0.863	0.7046	-0.2106
60.00	0.669	0.9072	-0.2398
70.00	0.453	1.0732	-0.2694
80.00	0.224	1.1829	-0.2972
90.00	0.000	1.2234	-0.3199
100.00	-0.157	1.1829	-0.3297
110.00	-0.317	1.0732	-0.3273
120.00	-0.468	0.9072	-0.3183
130.00	-0.604	0.7046	-0.3113
140.00	-0.730	0.4896	-0.3199
150.00	-0.878	0.2879	-0.3714
160.00	-1.148	0.1236	-0.5526
170.00	-0.574	0.0165	-0.5000
180.00	0.000	0.0100	0.0000

#### C.14. Hydrofoil Input File - fx77\_01633\_12.dat

"fx77\_01633 Airfoil, DesignFoil data at Re=1.0 Million, Clean roughness"  
Adjusted for Post Stall at r/R=0.204 by AirfoilPrep\_v2p2\_2. FAU.

1	Number of airfoil tables in this file		
0	Table ID parameter		
17	Stall angle (deg)**		
0	"No longer used, enter zero"		
0	"No longer used, enter zero"		
0	"No longer used, enter zero"		
-2.2412	Zero Cn angle of attack (deg)		
6.7326	Cn slope for zero lift (dimensionless)		
2.2610	Cn extrapolated to value at positive stall angle of attack		
-1.0537	Cn at stall value for negative angle of attack		
3.00	Angle of attack for minimum CD (deg)		
0.0079	Minimum CD value		
-180.00	0.000	0.0100	0.0000
-170.00	0.542	0.0100	0.4000
-160.00	1.085	0.1006	0.0111
-150.00	0.841	0.2667	0.0815
-140.00	0.708	0.4709	0.1182
-130.00	0.591	0.6889	0.1546
-120.00	0.461	0.8950	0.1944
-110.00	0.314	1.0648	0.2350
-100.00	0.156	1.1787	0.2713
-90.00	0.000	1.2234	0.2979
-80.00	-0.156	1.1787	0.3066
-70.00	-0.314	1.0648	0.3031
-60.00	-0.461	0.8950	0.2924
-50.00	-0.591	0.6889	0.2831
-40.00	-0.708	0.4709	0.2882
-30.00	-0.841	0.2667	0.3334
-20.00	-1.085	0.1006	0.4997
-10.00	-0.982	0.0148	-0.0120
-9.00	-0.859	0.0138	-0.0110
-8.00	-0.736	0.0127	-0.0100
-7.00	-0.613	0.0119	-0.0100
-6.00	-0.490	0.0111	-0.0090
-5.00	-0.367	0.0107	-0.0090
-4.00	-0.244	0.0101	-0.0090

-3.00	-0.121	0.0097	-0.0080
-2.00	0.002	0.0093	-0.0080
-1.00	0.126	0.0090	-0.0080
0.00	0.249	0.0088	-0.0090
1.00	0.373	0.0092	-0.0090
2.00	0.496	0.0084	-0.0090
3.00	0.619	0.0079	-0.0100
4.00	0.742	0.0087	-0.0110
5.00	0.864	0.0089	-0.0110
6.00	0.977	0.0090	-0.0120
7.00	1.078	0.0101	-0.0130
8.00	1.170	0.0106	-0.0140
9.00	1.252	0.0119	-0.0150
10.00	1.326	0.0139	-0.0170
11.00	1.390	0.0200	-0.0180
12.00	1.446	0.0243	-0.0200
13.00	1.492	0.0296	-0.0210
14.00	1.531	0.0364	-0.0230
15.00	1.563	0.0444	-0.0250
16.00	1.580	0.0531	-0.0260
17.00	1.587	0.0634	-0.0280
18.00	1.585	0.0746	-0.0300
19.00	1.572	0.0871	-0.0330
20.00	1.549	0.1006	-0.0350
30.00	1.202	0.2667	-0.1299
40.00	1.011	0.4709	-0.1690
50.00	0.844	0.6889	-0.1998
60.00	0.659	0.8950	-0.2303
70.00	0.449	1.0648	-0.2611
80.00	0.223	1.1787	-0.2900
90.00	0.000	1.2234	-0.3139
100.00	-0.156	1.1787	-0.3226
110.00	-0.314	1.0648	-0.3191
120.00	-0.461	0.8950	-0.3084
130.00	-0.591	0.6889	-0.2991
140.00	-0.708	0.4709	-0.3042
150.00	-0.841	0.2667	-0.3494
160.00	-1.085	0.1006	-0.5157
170.00	-0.542	0.0100	-0.5000
<b>180.00</b>	<b>0.000</b>	<b>0.0100</b>	<b>0.0000</b>

### C.15. Hydrofoil Input File - fx77\_01530\_13.dat

"fx77\_01530 Airfoil, DesignFoil data at Re=1.0 Million, Clean roughness"  
Adjusted for Post Stall at r/R=0.204 by AirfoilPrep\_v2p2\_2. FAU.

1	Number of airfoil tables in this file		
0	Table ID parameter		
13	Stall angle (deg)**		
0	"No longer used, enter zero"		
0	"No longer used, enter zero"		
0	"No longer used, enter zero"		
-2.0160	Zero Cn angle of attack (deg)		
6.7236	Cn slope for zero lift (dimensionless)		
1.7621	Cn extrapolated to value at positive stall angle of attack		
-0.7900	Cn at stall value for negative angle of attack		
5.00	Angle of attack for minimum CD (deg)		
0.0078	Minimum CD value		
-180.00	0.000	0.0100	0.0000
-170.00	0.403	0.0100	0.4000
-160.00	0.807	0.0966	0.0116
-150.00	0.679	0.2630	0.0715
-140.00	0.610	0.4676	0.1112
-130.00	0.533	0.6861	0.1520
-120.00	0.430	0.8928	0.1953
-110.00	0.301	1.0634	0.2379
-100.00	0.153	1.1779	0.2751
-90.00	0.000	1.2234	0.3019
-80.00	-0.153	1.1779	0.3102

-70.00	-0.301	1.0634	0.3052
-60.00	-0.430	0.8928	0.2909
-50.00	-0.533	0.6861	0.2740
-40.00	-0.610	0.4676	0.2645
-30.00	-0.679	0.2630	0.2805
-20.00	-0.807	0.0966	0.3759
-10.00	-0.995	0.0152	-0.0090
-9.00	-0.874	0.0136	-0.0080
-8.00	-0.753	0.0125	-0.0070
-7.00	-0.631	0.0120	-0.0060
-6.00	-0.509	0.0112	-0.0060
-5.00	-0.387	0.0105	-0.0050
-4.00	-0.265	0.0100	-0.0050
-3.00	-0.143	0.0094	-0.0040
-2.00	-0.020	0.0093	-0.0040
-1.00	0.102	0.0089	-0.0040
0.00	0.224	0.0087	-0.0040
1.00	0.347	0.0090	-0.0040
2.00	0.469	0.0090	-0.0040
3.00	0.591	0.0085	-0.0040
4.00	0.713	0.0090	-0.0050
5.00	0.835	0.0078	-0.0050
6.00	0.953	0.0083	-0.0060
7.00	1.049	0.0091	-0.0070
8.00	1.129	0.0101	-0.0080
9.00	1.194	0.0139	-0.0090
10.00	1.244	0.0161	-0.0100
11.00	1.280	0.0195	-0.0110
12.00	1.302	0.0237	-0.0120
13.00	1.310	0.0298	-0.0130
14.00	1.304	0.0367	-0.0150
15.00	1.285	0.0453	-0.0170
16.00	1.245	0.0547	-0.0180
17.00	1.191	0.0655	-0.0200
18.00	1.119	0.0778	-0.0220
19.00	1.155	0.0862	-0.0240
20.00	1.152	0.0966	-0.0260
30.00	0.971	0.2630	-0.1059
40.00	0.871	0.4676	-0.1492
50.00	0.761	0.6861	-0.1863
60.00	0.615	0.8928	-0.2218
70.00	0.430	1.0634	-0.2556
80.00	0.218	1.1779	-0.2858
90.00	0.000	1.2234	-0.3099
100.00	-0.153	1.1779	-0.3182
110.00	-0.301	1.0634	-0.3132
120.00	-0.430	0.8928	-0.2989
130.00	-0.533	0.6861	-0.2820
140.00	-0.610	0.4676	-0.2725
150.00	-0.679	0.2630	-0.2885
160.00	-0.807	0.0966	-0.3839
170.00	-0.403	0.0100	-0.5000
180.00	0.000	0.0100	0.0000

## C.16. Hydrofoil Input File - fx77\_01486\_14.dat

"fx77\_01486 Airfoil,DesignFoil data at Re=1.0 Million, Clean roughness"

Adjusted for Post Stall at  $r/R=0.204$  by AirfoilPrep\_v2p2\_2. FAU.

1	Number of airfoil tables in this file
0	Table ID parameter
11	Stall angle (deg)**
0	"No longer used, enter zero"
0	"No longer used, enter zero"
0	"No longer used, enter zero"
-2.0495	Zero Cn angle of attack (deg)

6.6090	Cn slope for zero lift (dimensionless)		
1.5052	Cn extrapolated to value at positive stall angle of attack		
-0.7232	Cn at stall value for negative angle of attack		
5.00	Angle of attack for minimum CD (deg)		
0.0078	Minimum CD value		
-180.00	0.000	0.0100	0.0000
-170.00	0.370	0.0100	0.4000
-160.00	0.740	0.0822	0.0095
-150.00	0.641	0.2497	0.0665
-140.00	0.586	0.4558	0.1066
-130.00	0.519	0.6763	0.1482
-120.00	0.423	0.8851	0.1924
-110.00	0.298	1.0581	0.2358
-100.00	0.152	1.1753	0.2736
-90.00	0.000	1.2234	0.3010
-80.00	-0.152	1.1753	0.3086
-70.00	-0.298	1.0581	0.3026
-60.00	-0.423	0.8851	0.2870
-50.00	-0.519	0.6763	0.2679
-40.00	-0.586	0.4558	0.2547
-30.00	-0.641	0.2497	0.2638
-20.00	-0.740	0.0822	0.3425
-10.00	-0.994	0.0149	-0.0100
-9.00	-0.873	0.0133	-0.0090
-8.00	-0.753	0.0131	-0.0080
-7.00	-0.631	0.0122	-0.0070
-6.00	-0.510	0.0114	-0.0060
-5.00	-0.389	0.0107	-0.0060
-4.00	-0.267	0.0101	-0.0050
-3.00	-0.145	0.0096	-0.0050
-2.00	-0.023	0.0092	-0.0050
-1.00	0.099	0.0088	-0.0040
0.00	0.221	0.0085	-0.0040
1.00	0.342	0.0089	-0.0040
2.00	0.464	0.0089	-0.0040
3.00	0.586	0.0085	-0.0050
4.00	0.707	0.0090	-0.0050
5.00	0.829	0.0078	-0.0050
6.00	0.942	0.0081	-0.0060
7.00	1.029	0.0091	-0.0070
8.00	1.097	0.0101	-0.0070
9.00	1.146	0.0137	-0.0080
10.00	1.179	0.0160	-0.0090
11.00	1.194	0.0189	-0.0100
12.00	1.192	0.0234	-0.0120
13.00	1.174	0.0284	-0.0130
14.00	1.139	0.0347	-0.0140
15.00	1.088	0.0424	-0.0160
16.00	1.013	0.0509	-0.0180
17.00	1.010	0.0591	-0.0190
18.00	0.996	0.0674	-0.0210
19.00	1.006	0.0753	-0.0230
20.00	1.057	0.0822	-0.0250
30.00	0.915	0.2497	-0.1010
40.00	0.837	0.4558	-0.1451
50.00	0.741	0.6763	-0.1835
60.00	0.604	0.8851	-0.2202
70.00	0.425	1.0581	-0.2550
80.00	0.217	1.1753	-0.2859
90.00	0.000	1.2234	-0.3107
100.00	-0.152	1.1753	-0.3182
110.00	-0.298	1.0581	-0.3123
120.00	-0.423	0.8851	-0.2966
130.00	-0.519	0.6763	-0.2775
140.00	-0.586	0.4558	-0.2644
150.00	-0.641	0.2497	-0.2734
160.00	-0.740	0.0822	-0.3521
170.00	-0.370	0.0100	-0.5000

180.00 0.000 0.0100 0.0000

### C.17. Hydrofoil Input File - fx77\_01442\_15.dat

"fx77\_01442 Airfoil, DesignFoil data at Re=1.0 Million, Clean roughness"  
Adjusted for Post Stall at r/R=0.204 by AirfoilPrep\_v2p2\_2. FAU.

1 Number of airfoil tables in this file  
0 Table ID parameter  
11 Stall angle (deg)\*\*  
0 "No longer used, enter zero"  
0 "No longer used, enter zero"  
0 "No longer used, enter zero"  
-2.0585 Zero Cn angle of attack (deg)  
6.5962 Cn slope for zero lift (dimensionless)  
1.5034 Cn extrapolated to value at positive stall angle of attack  
-0.6801 Cn at stall value for negative angle of attack  
5.00 Angle of attack for minimum CD (deg)  
0.0078 Minimum CD value  
-180.00 0.000 0.0100 0.0000  
-170.00 0.349 0.0100 0.4000  
-160.00 0.699 0.0686 0.0095  
-150.00 0.617 0.2371 0.0641  
-140.00 0.571 0.4447 0.1042  
-130.00 0.510 0.6669 0.1462  
-120.00 0.418 0.8779 0.1909  
-110.00 0.296 1.0532 0.2348  
-100.00 0.151 1.1727 0.2731  
-90.00 0.000 1.2234 0.3010  
-80.00 -0.151 1.1727 0.3079  
-70.00 -0.296 1.0532 0.3010  
-60.00 -0.418 0.8779 0.2842  
-50.00 -0.510 0.6669 0.2636  
-40.00 -0.571 0.4447 0.2480  
-30.00 -0.617 0.2371 0.2526  
-20.00 -0.699 0.0686 0.3209  
-10.00 -0.994 0.0149 -0.0100  
-9.00 -0.873 0.0133 -0.0090  
-8.00 -0.753 0.0131 -0.0080  
-7.00 -0.631 0.0122 -0.0070  
-6.00 -0.510 0.0114 -0.0060  
-5.00 -0.389 0.0107 -0.0060  
-4.00 -0.267 0.0101 -0.0050  
-3.00 -0.145 0.0096 -0.0050  
-2.00 -0.023 0.0092 -0.0050  
-1.00 0.099 0.0088 -0.0040  
0.00 0.221 0.0085 -0.0040  
1.00 0.342 0.0089 -0.0040  
2.00 0.464 0.0089 -0.0040  
3.00 0.586 0.0085 -0.0050  
4.00 0.707 0.0090 -0.0050  
5.00 0.829 0.0078 -0.0050  
6.00 0.942 0.0081 -0.0060  
7.00 1.027 0.0091 -0.0070  
8.00 1.092 0.0100 -0.0070  
9.00 1.139 0.0135 -0.0080  
10.00 1.167 0.0154 -0.0090  
11.00 1.178 0.0177 -0.0100  
12.00 1.171 0.0215 -0.0120  
13.00 1.147 0.0255 -0.0130  
14.00 1.105 0.0305 -0.0140  
15.00 1.047 0.0365 -0.0160  
16.00 0.965 0.0432 -0.0180  
17.00 0.958 0.0499 -0.0190  
18.00 0.940 0.0566 -0.0210  
19.00 0.948 0.0629 -0.0230  
20.00 0.998 0.0686 -0.0250  
30.00 0.881 0.2371 -0.0980  
40.00 0.816 0.4447 -0.1421

50.00	0.729	0.6669	-0.1812
60.00	0.597	0.8779	-0.2186
70.00	0.422	1.0532	-0.2539
80.00	0.216	1.1727	-0.2854
90.00	0.000	1.2234	-0.3107
100.00	-0.151	1.1727	-0.3175
110.00	-0.296	1.0532	-0.3106
120.00	-0.418	0.8779	-0.2938
130.00	-0.510	0.6669	-0.2732
140.00	-0.571	0.4447	-0.2576
150.00	-0.617	0.2371	-0.2623
160.00	-0.699	0.0686	-0.3306
170.00	-0.349	0.0100	-0.5000
180.00	0.000	0.0100	0.0000

### C.18. Hydrofoil Input File - fx77\_01400\_16.dat

"fx77\_01400 Airfoil,DesignFoil data at Re=1.0 Million, Clean roughness"  
Adjusted for Post Stall at  $r/R=0.204$  by AirfoilPrep\_v2p2\_2. FAU.

```

1      Number of airfoil tables in this file
0      Table ID parameter
12     Stall angle (deg)**
0      "No longer used, enter zero"
0      "No longer used, enter zero"
0      "No longer used, enter zero"
-1.9105 Zero Cn angle of attack (deg)
6.6675  Cn slope for zero lift (dimensionless)
1.6188  Cn extrapolated to value at positive stall angle of attack
-0.6484 Cn at stall value for negative angle of attack
4.00    Angle of attack for minimum CD (deg)
0.0069  Minimum CD value
-180.00 0.000 0.0100 0.0000
-170.00 0.335 0.0100 0.4000
-160.00 0.670 0.0560 0.0077
-150.00 0.600 0.2255 0.0612
-140.00 0.561 0.4344 0.1014
-130.00 0.504 0.6583 0.1438
-120.00 0.415 0.8712 0.1889
-110.00 0.294 1.0486 0.2333
-100.00 0.151 1.1704 0.2723
-90.00  0.000 1.2234 0.3009
-80.00 -0.151 1.1704 0.3071
-70.00 -0.294 1.0486 0.2996
-60.00 -0.415 0.8712 0.2821
-50.00 -0.504 0.6583 0.2604
-40.00 -0.561 0.4344 0.2431
-30.00 -0.600 0.2255 0.2449
-20.00 -0.670 0.0560 0.3065
-10.00 -0.994 0.0152 -0.0110
-9.00  -0.875 0.0143 -0.0100
-8.00  -0.755 0.0132 -0.0090
-7.00  -0.635 0.0122 -0.0080
-6.00  -0.514 0.0114 -0.0070
-5.00  -0.393 0.0107 -0.0070
-4.00  -0.273 0.0101 -0.0060
-3.00  -0.152 0.0097 -0.0060
-2.00  -0.031 0.0093 -0.0050
-1.00  0.090 0.0089 -0.0050
0.00   0.211 0.0087 -0.0050
1.00   0.332 0.0085 -0.0050
2.00   0.453 0.0083 -0.0050
3.00   0.574 0.0083 -0.0050
4.00   0.694 0.0069 -0.0050
5.00   0.815 0.0078 -0.0050
6.00   0.934 0.0081 -0.0060
7.00   1.027 0.0090 -0.0060
8.00   1.104 0.0098 -0.0070
9.00   1.161 0.0130 -0.0080

```

10.00	1.203	0.0145	-0.0090
11.00	1.227	0.0165	-0.0100
12.00	1.236	0.0192	-0.0110
13.00	1.227	0.0222	-0.0120
14.00	1.202	0.0258	-0.0130
15.00	1.160	0.0302	-0.0140
16.00	1.100	0.0349	-0.0160
17.00	1.021	0.0403	-0.0170
18.00	0.923	0.0464	-0.0190
19.00	0.917	0.0515	-0.0210
20.00	0.957	0.0560	-0.0230
30.00	0.857	0.2255	-0.0946
40.00	0.802	0.4344	-0.1391
50.00	0.720	0.6583	-0.1787
60.00	0.593	0.8712	-0.2168
70.00	0.420	1.0486	-0.2528
80.00	0.216	1.1704	-0.2849
90.00	0.000	1.2234	-0.3109
100.00	-0.151	1.1704	-0.3171
110.00	-0.294	1.0486	-0.3096
120.00	-0.415	0.8712	-0.2921
130.00	-0.504	0.6583	-0.2704
140.00	-0.561	0.4344	-0.2531
150.00	-0.600	0.2255	-0.2549
160.00	-0.670	0.0560	-0.3165
170.00	-0.335	0.0100	-0.5000
180.00	0.000	0.0100	0.0000

### C.19. Hydrofoil Input File - fx77\_01360\_17.dat

"fx77\_01360 Airfoil, DesignFoil data at Re=1.0 Million, Clean roughness"  
Adjusted for Post Stall at r/R=0.204 by AirfoilPrep\_v2p2\_2. FAU.

1	Number of airfoil tables in this file		
0	Table ID parameter		
8	Stall angle (deg)**		
0	"No longer used, enter zero"		
0	"No longer used, enter zero"		
0	"No longer used, enter zero"		
-2.2294	Zero Cn angle of attack (deg)		
6.2992	Cn slope for zero lift (dimensionless)		
1.1246	Cn extrapolated to value at positive stall angle of attack		
-0.8000	Cn at stall value for negative angle of attack		
4.00	Angle of attack for minimum CD (deg)		
0.0069	Minimum CD value		
-180.00	0.000	0.0100	0.0000
-170.00	0.273	0.0100	0.4000
-160.00	0.545	0.0508	0.0077
-150.00	0.528	0.2208	0.0560
-140.00	0.517	0.4303	0.0972
-130.00	0.478	0.6548	0.1414
-120.00	0.401	0.8685	0.1879
-110.00	0.288	1.0467	0.2331
-100.00	0.150	1.1695	0.2723
-90.00	0.000	1.2234	0.3009
-80.00	-0.150	1.1695	0.3065
-70.00	-0.288	1.0467	0.2979
-60.00	-0.401	0.8685	0.2784
-50.00	-0.478	0.6548	0.2531
-40.00	-0.517	0.4303	0.2291
-30.00	-0.528	0.2208	0.2177
-20.00	-0.545	0.0508	0.2472
-10.00	-0.983	0.0156	-0.0120
-9.00	-0.864	0.0142	-0.0110
-8.00	-0.744	0.0131	-0.0100
-7.00	-0.625	0.0122	-0.0090
-6.00	-0.505	0.0114	-0.0080
-5.00	-0.384	0.0107	-0.0070

-4.00	-0.264	0.0101	-0.0060
-3.00	-0.144	0.0095	-0.0060
-2.00	-0.023	0.0091	-0.0050
-1.00	0.098	0.0089	-0.0050
0.00	0.218	0.0087	-0.0050
1.00	0.339	0.0085	-0.0050
2.00	0.459	0.0079	-0.0050
3.00	0.580	0.0083	-0.0050
4.00	0.700	0.0069	-0.0050
5.00	0.820	0.0078	-0.0050
6.00	0.929	0.0081	-0.0060
7.00	0.982	0.0091	-0.0060
8.00	1.004	0.0099	-0.0070
9.00	0.996	0.0132	-0.0080
10.00	0.959	0.0150	-0.0090
11.00	0.892	0.0174	-0.0100
12.00	0.795	0.0201	-0.0110
13.00	0.798	0.0229	-0.0120
14.00	0.797	0.0259	-0.0130
15.00	0.763	0.0295	-0.0150
16.00	0.823	0.0324	-0.0160
17.00	0.818	0.0374	-0.0180
18.00	0.744	0.0422	-0.0190
19.00	0.832	0.0458	-0.0210
20.00	0.779	0.0508	-0.0230
30.00	0.754	0.2208	-0.0871
40.00	0.739	0.4303	-0.1330
50.00	0.683	0.6548	-0.1752
60.00	0.573	0.8685	-0.2153
70.00	0.412	1.0467	-0.2524
80.00	0.214	1.1695	-0.2850
90.00	0.000	1.2234	-0.3109
100.00	-0.150	1.1695	-0.3165
110.00	-0.288	1.0467	-0.3079
120.00	-0.401	0.8685	-0.2884
130.00	-0.478	0.6548	-0.2631
140.00	-0.517	0.4303	-0.2391
150.00	-0.528	0.2208	-0.2277
160.00	-0.545	0.0508	-0.2572
170.00	-0.273	0.0100	-0.5000
180.00	0.000	0.0100	0.0000

## C.20. Hydrofoil Input File - fx77\_01323\_18.dat

"fx77\_01323 Airfoil, DesignFoil data at Re=1.0 Million, Clean roughness"  
Adjusted for Post Stall at r/R=0.204 by AirfoilPrep\_v2p2\_2. FAU.

1	Number of airfoil tables in this file
0	Table ID parameter
8	Stall angle (deg)**
0	"No longer used, enter zero"
0	"No longer used, enter zero"
0	"No longer used, enter zero"
-2.1473	Zero Cn angle of attack (deg)
6.3416	Cn slope for zero lift (dimensionless)
1.1231	Cn extrapolated to value at positive stall angle of attack
-0.8000	Cn at stall value for negative angle of attack
3.00	Angle of attack for minimum CD (deg)
0.0063	Minimum CD value
-180.00	0.000 0.0100 0.0000
-170.00	0.273 0.0100 0.4000
-160.00	0.546 0.0428 0.0057
-150.00	0.528 0.2134 0.0541
-140.00	0.518 0.4237 0.0952
-130.00	0.478 0.6493 0.1393
-120.00	0.401 0.8642 0.1859
-110.00	0.288 1.0438 0.2314
-100.00	0.150 1.1680 0.2710
-90.00	0.000 1.2234 0.3001



-80.00	-0.150	1.1680	0.3055
-70.00	-0.288	1.0438	0.2967
-60.00	-0.401	0.8642	0.2770
-50.00	-0.478	0.6493	0.2516
-40.00	-0.518	0.4237	0.2277
-30.00	-0.528	0.2134	0.2165
-20.00	-0.546	0.0428	0.2468
-10.00	-0.984	0.0158	-0.0120
-9.00	-0.865	0.0145	-0.0110
-8.00	-0.746	0.0134	-0.0100
-7.00	-0.626	0.0123	-0.0090
-6.00	-0.507	0.0114	-0.0080
-5.00	-0.387	0.0107	-0.0070
-4.00	-0.267	0.0101	-0.0070
-3.00	-0.147	0.0096	-0.0060
-2.00	-0.027	0.0092	-0.0060
-1.00	0.093	0.0088	-0.0050
0.00	0.214	0.0085	-0.0050
1.00	0.334	0.0085	-0.0050
2.00	0.454	0.0078	-0.0050
3.00	0.574	0.0063	-0.0050
4.00	0.694	0.0069	-0.0050
5.00	0.813	0.0076	-0.0050
6.00	0.925	0.0081	-0.0060
7.00	0.983	0.0090	-0.0060
8.00	1.011	0.0097	-0.0070
9.00	1.009	0.0128	-0.0070
10.00	0.978	0.0145	-0.0080
11.00	0.918	0.0162	-0.0090
12.00	0.829	0.0182	-0.0100
13.00	0.711	0.0206	-0.0110
14.00	0.757	0.0236	-0.0130
15.00	0.784	0.0262	-0.0140
16.00	0.717	0.0294	-0.0150
17.00	0.771	0.0324	-0.0170
18.00	0.762	0.0357	-0.0180
19.00	0.747	0.0393	-0.0200
20.00	0.781	0.0428	-0.0220
30.00	0.755	0.2134	-0.0864
40.00	0.739	0.4237	-0.1324
50.00	0.683	0.6493	-0.1746
60.00	0.573	0.8642	-0.2149
70.00	0.412	1.0438	-0.2523
80.00	0.214	1.1680	-0.2852
90.00	0.000	1.2234	-0.3116
100.00	-0.150	1.1680	-0.3171
110.00	-0.288	1.0438	-0.3083
120.00	-0.401	0.8642	-0.2886

## C.21. Hydrofoil Input File - fx77\_01289\_19.dat

"fx77\_01289 Airfoil, DesignFoil data at Re=1.0 Million, Clean roughness"  
Adjusted for Post Stall at  $r/R=0.204$  by AirfoilPrep\_v2p2\_2. FAU.

1	Number of airfoil tables in this file
0	Table ID parameter
9	Stall angle (deg)**
0	"No longer used, enter zero"
0	"No longer used, enter zero"
0	"No longer used, enter zero"
-1.9358	Zero Cn angle of attack (deg)
6.5731	Cn slope for zero lift (dimensionless)
1.2546	Cn extrapolated to value at positive stall angle of attack
-0.8000	Cn at stall value for negative angle of attack
3.00	Angle of attack for minimum CD (deg)
0.0063	Minimum CD value
-180.00	0.000 0.0100 0.0000
-170.00	0.278 0.0100 0.4000
-160.00	0.555 0.0362 0.0050

-150.00	0.534	0.2073	0.0537
-140.00	0.521	0.4183	0.0946
-130.00	0.480	0.6448	0.1386
-120.00	0.402	0.8607	0.1851
-110.00	0.289	1.0414	0.2308
-100.00	0.150	1.1668	0.2707
-90.00	0.000	1.2234	0.3001
-80.00	-0.150	1.1668	0.3053
-70.00	-0.289	1.0414	0.2964
-60.00	-0.402	0.8607	0.2766
-50.00	-0.480	0.6448	0.2513
-40.00	-0.521	0.4183	0.2278
-30.00	-0.534	0.2073	0.2177
-20.00	-0.555	0.0362	0.2507
-10.00	-0.984	0.0163	-0.0120
-9.00	-0.866	0.0146	-0.0110
-8.00	-0.747	0.0135	-0.0100
-7.00	-0.628	0.0124	-0.0090
-6.00	-0.509	0.0115	-0.0080
-5.00	-0.389	0.0107	-0.0070
-4.00	-0.270	0.0100	-0.0070
-3.00	-0.150	0.0095	-0.0060
-2.00	-0.030	0.0092	-0.0060
-1.00	0.090	0.0088	-0.0050
0.00	0.210	0.0086	-0.0050
1.00	0.329	0.0084	-0.0050
2.00	0.449	0.0078	-0.0050
3.00	0.569	0.0063	-0.0050
4.00	0.688	0.0068	-0.0050
5.00	0.808	0.0072	-0.0050
6.00	0.927	0.0081	-0.0050
7.00	1.011	0.0090	-0.0060
8.00	1.057	0.0094	-0.0060
9.00	1.074	0.0125	-0.0070
10.00	1.064	0.0139	-0.0080
11.00	1.026	0.0151	-0.0090
12.00	0.960	0.0171	-0.0100
13.00	0.867	0.0189	-0.0110
14.00	0.743	0.0211	-0.0120
15.00	0.794	0.0232	-0.0130
16.00	0.758	0.0255	-0.0140
17.00	0.760	0.0281	-0.0160
18.00	0.816	0.0305	-0.0170
19.00	0.817	0.0333	-0.0190
20.00	0.793	0.0362	-0.0210
30.00	0.762	0.2073	-0.0860
40.00	0.744	0.4183	-0.1318
50.00	0.686	0.6448	-0.1738
60.00	0.575	0.8607	-0.2140
70.00	0.412	1.0414	-0.2516
80.00	0.214	1.1668	-0.2848
90.00	0.000	1.2234	-0.3116
100.00	-0.150	1.1668	-0.3168
110.00	-0.289	1.0414	-0.3079
120.00	-0.402	0.8607	-0.2881
130.00	-0.480	0.6448	-0.2628
140.00	-0.521	0.4183	-0.2393
150.00	-0.534	0.2073	-0.2292
160.00	-0.555	0.0362	-0.2622
170.00	-0.278	0.0100	-0.5000
180.00	0.000	0.0100	0.0000

## C.22. Hydrofoil Input File - fx77\_01258\_20.dat

"fx77\_01289 Airfoil, DesignFoil data at Re=1.0 Million, Clean roughness"  
Adjusted for Post Stall at r/R=0.204 by AirfoilPrep\_v2p2\_2. FAU.

1        Number of airfoil tables in this file  
0        Table ID parameter

```

10    Stall angle (deg)**
0     "No longer used, enter zero"
0     "No longer used, enter zero"
0     "No longer used, enter zero"
-1.7760 Zero Cn angle of attack (deg)
6.7595 Cn slope for zero lift (dimensionless)
1.3893 Cn extrapolated to value at positive stall angle of attack
-0.9719 Cn at stall value for negative angle of attack
3.00 Angle of attack for minimum CD (deg)
0.0062 Minimum CD value
-180.00 0.000 0.0100 0.0000
-170.00 0.306 0.0100 0.4000
-160.00 0.611 0.0337 0.0043
-150.00 0.566 0.2051 0.0554
-140.00 0.540 0.4163 0.0958
-130.00 0.492 0.6431 0.1390
-120.00 0.408 0.8594 0.1850
-110.00 0.291 1.0405 0.2304
-100.00 0.150 1.1663 0.2704
-90.00 0.000 1.2234 0.3001
-80.00 -0.150 1.1663 0.3055
-70.00 -0.291 1.0405 0.2969
-60.00 -0.408 0.8594 0.2778
-50.00 -0.492 0.6431 0.2540
-40.00 -0.540 0.4163 0.2335
-30.00 -0.566 0.2051 0.2294
-20.00 -0.611 0.0337 0.2771
-10.00 -0.984 0.0165 -0.0130
-9.00 -0.866 0.0150 -0.0110
-8.00 -0.748 0.0135 -0.0100
-7.00 -0.629 0.0124 -0.0090
-6.00 -0.510 0.0115 -0.0080
-5.00 -0.391 0.0108 -0.0080
-4.00 -0.272 0.0100 -0.0070
-3.00 -0.152 0.0095 -0.0060
-2.00 -0.033 0.0091 -0.0060
-1.00 0.087 0.0088 -0.0050
0.00 0.206 0.0085 -0.0050
1.00 0.326 0.0084 -0.0050
2.00 0.445 0.0062 -0.0050
3.00 0.565 0.0062 -0.0050
4.00 0.684 0.0064 -0.0050
5.00 0.803 0.0071 -0.0050
6.00 0.922 0.0079 -0.0050
7.00 1.040 0.0088 -0.0060
8.00 1.113 0.0094 -0.0060
9.00 1.151 0.0126 -0.0070
10.00 1.160 0.0135 -0.0080
11.00 1.143 0.0150 -0.0080
12.00 1.098 0.0163 -0.0090
13.00 1.024 0.0176 -0.0100
14.00 0.922 0.0192 -0.0110
15.00 0.791 0.0209 -0.0130
16.00 0.872 0.0227 -0.0140
17.00 0.865 0.0246 -0.0150
18.00 0.797 0.0266 -0.0170
19.00 0.844 0.0308 -0.0180
20.00 0.873 0.0337 -0.0200
30.00 0.808 0.2051 -0.0886
40.00 0.772 0.4163 -0.1337
50.00 0.703 0.6431 -0.1746
60.00 0.583 0.8594 -0.2140
70.00 0.416 1.0405 -0.2512
80.00 0.215 1.1663 -0.2845
90.00 0.000 1.2234 -0.3116
100.00 -0.150 1.1663 -0.3170
110.00 -0.291 1.0405 -0.3083
120.00 -0.408 0.8594 -0.2892

```

130.00	-0.492	0.6431	-0.2654
140.00	-0.540	0.4163	-0.2450
150.00	-0.566	0.2051	-0.2409
160.00	-0.611	0.0337	-0.2885
170.00	-0.306	0.0100	-0.5000
180.00	0.000	0.0100	0.0000

### C.23. Hydrofoil Input File - fx77\_01232\_21.dat

"fx77\_01232 Airfoil, DesignFoil data at Re=1.0 Million, Clean roughness"  
Adjusted for Post Stall at r/R=0.204 by AirfoilPrep\_v2p2\_2. FAU.

```

1      Number of airfoil tables in this file
0      Table ID parameter
8      Stall angle (deg)**
0      "No longer used, enter zero"
0      "No longer used, enter zero"
0      "No longer used, enter zero"
-2.0291 Zero Cn angle of attack (deg)
6.4984  Cn slope for zero lift (dimensionless)
1.1375  Cn extrapolated to value at positive stall angle of attack
-0.9611 Cn at stall value for negative angle of attack
2.00    Angle of attack for minimum CD (deg)
0.0061  Minimum CD value
-180.00 0.000 0.0100 0.0000
-170.00 0.238 0.0100 0.4000
-160.00 0.475 0.0306 0.0042
-150.00 0.487 0.2022 0.0497
-140.00 0.492 0.4138 0.0913
-130.00 0.463 0.6410 0.1365
-120.00 0.393 0.8577 0.1840
-110.00 0.285 1.0393 0.2303
-100.00 0.149 1.1657 0.2705
-90.00  0.000 1.2234 0.3000
-80.00  -0.149 1.1657 0.3048
-70.00  -0.285 1.0393 0.2952
-60.00  -0.393 0.8577 0.2741
-50.00  -0.463 0.6410 0.2464
-40.00  -0.492 0.4138 0.2186
-30.00  -0.487 0.2022 0.2001
-20.00  -0.475 0.0306 0.2127
-10.00  -0.973 0.0165 -0.0130
-9.00   -0.855 0.0150 -0.0120
-8.00   -0.737 0.0136 -0.0100
-7.00   -0.619 0.0124 -0.0090
-6.00   -0.500 0.0114 -0.0080
-5.00   -0.381 0.0106 -0.0080
-4.00   -0.262 0.0100 -0.0070
-3.00   -0.143 0.0094 -0.0060
-2.00   -0.023 0.0090 -0.0060
-1.00   0.096 0.0087 -0.0050
0.00    0.215 0.0084 -0.0050
1.00    0.335 0.0084 -0.0050
2.00    0.454 0.0061 -0.0050
3.00    0.573 0.0062 -0.0050
4.00    0.692 0.0065 -0.0050
5.00    0.811 0.0071 -0.0050
6.00    0.929 0.0079 -0.0050
7.00    1.008 0.0089 -0.0060
8.00    1.024 0.0095 -0.0060
9.00    1.001 0.0125 -0.0070
10.00   0.941 0.0132 -0.0080
11.00   0.843 0.0145 -0.0080
12.00   0.705 0.0154 -0.0090
13.00   0.697 0.0166 -0.0100
14.00   0.725 0.0179 -0.0120
15.00   0.682 0.0192 -0.0130
16.00   0.771 0.0207 -0.0140
17.00   0.737 0.0233 -0.0160

```

18.00	0.670	0.0257	-0.0170
19.00	0.727	0.0281	-0.0190
20.00	0.679	0.0306	-0.0200
30.00	0.696	0.2022	-0.0805
40.00	0.703	0.4138	-0.1274
50.00	0.662	0.6410	-0.1711
60.00	0.562	0.8577	-0.2126
70.00	0.407	1.0393	-0.2511
80.00	0.213	1.1657	-0.2847
90.00	0.000	1.2234	-0.3117
100.00	-0.149	1.1657	-0.3165
110.00	-0.285	1.0393	-0.3068
120.00	-0.393	0.8577	-0.2857
130.00	-0.463	0.6410	-0.2580
140.00	-0.492	0.4138	-0.2302
150.00	-0.487	0.2022	-0.2117
160.00	-0.475	0.0306	-0.2243
170.00	-0.238	0.0100	-0.5000
180.00	0.000	0.0100	0.0000

## C.24. Hydrofoil Input File - fx77\_01211\_22.dat

"fx77\_01211 Airfoil, DesignFoil data at Re=1.0 Million, Clean roughness"  
 Adjusted for Post Stall at  $r/R=0.204$  by AirfoilPrep\_v2p2\_2. FAU.

```

1      Number of airfoil tables in this file
0      Table ID parameter
8      Stall angle (deg)**
0      "No longer used, enter zero"
0      "No longer used, enter zero"
0      "No longer used, enter zero"
-1.9779 Zero Cn angle of attack (deg)
6.5442 Cn slope for zero lift (dimensionless)
1.1397 Cn extrapolated to value at positive stall angle of attack
-0.9600 Cn at stall value for negative angle of attack
2.00   Angle of attack for minimum CD (deg)
0.0060 Minimum CD value
-180.00 0.000 0.0100 0.0000
-170.00 0.265 0.0100 0.4000
-160.00 0.530 0.0284 0.0042
-150.00 0.519 0.2001 0.0518
-140.00 0.512 0.4120 0.0928
-130.00 0.475 0.6395 0.1371
-120.00 0.399 0.8565 0.1840
-110.00 0.288 1.0385 0.2300
-100.00 0.149 1.1653 0.2702
-90.00 0.000 1.2234 0.3001
-80.00 -0.149 1.1653 0.3049
-70.00 -0.288 1.0385 0.2955
-60.00 -0.399 0.8565 0.2751
-50.00 -0.475 0.6395 0.2489
-40.00 -0.512 0.4120 0.2241
-30.00 -0.519 0.2001 0.2114
-20.00 -0.530 0.0284 0.2383
-10.00 -0.972 0.0166 -0.0130
-9.00 -0.854 0.0151 -0.0120
-8.00 -0.737 0.0137 -0.0110
-7.00 -0.618 0.0126 -0.0090
-6.00 -0.500 0.0114 -0.0090
-5.00 -0.381 0.0106 -0.0080
-4.00 -0.262 0.0100 -0.0070
-3.00 -0.143 0.0093 -0.0060
-2.00 -0.024 0.0089 -0.0060
-1.00 0.095 0.0086 -0.0050
0.00 0.214 0.0084 -0.0050
1.00 0.333 0.0083 -0.0050
2.00 0.452 0.0060 -0.0050
3.00 0.571 0.0062 -0.0050
4.00 0.690 0.0064 -0.0050

```

5.00	0.808	0.0071	-0.0050
6.00	0.927	0.0078	-0.0050
7.00	1.013	0.0088	-0.0060
8.00	1.029	0.0096	-0.0060
9.00	1.005	0.0123	-0.0070
10.00	0.942	0.0131	-0.0070
11.00	0.839	0.0142	-0.0080
12.00	0.695	0.0148	-0.0090
13.00	0.680	0.0158	-0.0100
14.00	0.749	0.0169	-0.0110
15.00	0.695	0.0178	-0.0120
16.00	0.669	0.0189	-0.0140
17.00	0.694	0.0219	-0.0150
18.00	0.701	0.0240	-0.0170
19.00	0.693	0.0260	-0.0180
20.00	0.758	0.0284	-0.0200
30.00	0.742	0.2001	-0.0836
40.00	0.731	0.4120	-0.1296
50.00	0.679	0.6395	-0.1722
60.00	0.571	0.8565	-0.2128
70.00	0.411	1.0385	-0.2508
80.00	0.214	1.1653	-0.2845
90.00	0.000	1.2234	-0.3116
100.00	-0.149	1.1653	-0.3165
110.00	-0.288	1.0385	-0.3071
120.00	-0.399	0.8565	-0.2867
130.00	-0.475	0.6395	-0.2605
140.00	-0.512	0.4120	-0.2357
150.00	-0.519	0.2001	-0.2230
160.00	-0.530	0.0284	-0.2499
170.00	-0.265	0.0100	-0.5000
180.00	0.000	0.0100	0.0000

## C.25. Hydrofoil Input File - fx77\_01210\_23.dat

"fx77\_01210 Airfoil,DesignFoil data at Re=1.0 Million, Clean roughness"  
Adjusted for Post Stall at  $r/R=0.204$  by AirfoilPrep\_v2p2\_2. FAU.

```

1      Number of airfoil tables in this file
0      Table ID parameter
8      Stall angle (deg)**
0      "No longer used, enter zero"
0      "No longer used, enter zero"
0      "No longer used, enter zero"
-1.9828 Zero Cn angle of attack (deg)
6.5621  Cn slope for zero lift (dimensionless)
1.1433  Cn extrapolated to value at positive stall angle of attack
-0.9581 Cn at stall value for negative angle of attack
2.00   Angle of attack for minimum CD (deg)
0.0062 Minimum CD value
-180.00 0.000 0.0100 0.0000
-170.00 0.245 0.0100 0.4000
-160.00 0.490 0.0268 0.0039
-150.00 0.496 0.1987 0.0498
-140.00 0.498 0.4107 0.0912
-130.00 0.467 0.6384 0.1361
-120.00 0.395 0.8557 0.1835
-110.00 0.286 1.0380 0.2297
-100.00 0.149 1.1650 0.2701
-90.00 0.000 1.2234 0.2999
-80.00 -0.149 1.1650 0.3045
-70.00 -0.286 1.0380 0.2948
-60.00 -0.395 0.8557 0.2738
-50.00 -0.467 0.6384 0.2464
-40.00 -0.498 0.4107 0.2194
-30.00 -0.496 0.1987 0.2025
-20.00 -0.490 0.0268 0.2191
-10.00 -0.970 0.0169 -0.0140
-9.00  -0.852 0.0153 -0.0120

```

```

-8.00 -0.735 0.0139 -0.0110
-7.00 -0.616 0.0127 -0.0100
-6.00 -0.498 0.0116 -0.0090
-5.00 -0.379 0.0107 -0.0080
-4.00 -0.260 0.0100 -0.0080
-3.00 -0.141 0.0094 -0.0070
-2.00 -0.022 0.0090 -0.0060
-1.00 0.097 0.0086 -0.0060
0.00 0.216 0.0085 -0.0060
1.00 0.335 0.0084 -0.0050
2.00 0.454 0.0062 -0.0050
3.00 0.573 0.0063 -0.0050
4.00 0.692 0.0065 -0.0050
5.00 0.810 0.0072 -0.0050
6.00 0.929 0.0080 -0.0060
7.00 1.018 0.0089 -0.0060
8.00 1.034 0.0095 -0.0070
9.00 1.010 0.0124 -0.0070
10.00 0.945 0.0132 -0.0080
11.00 0.840 0.0141 -0.0090
12.00 0.693 0.0146 -0.0100
13.00 0.769 0.0157 -0.0110
14.00 0.707 0.0163 -0.0120
15.00 0.693 0.0183 -0.0130
16.00 0.680 0.0196 -0.0140
17.00 0.678 0.0212 -0.0160
18.00 0.727 0.0230 -0.0170
19.00 0.702 0.0248 -0.0190
20.00 0.700 0.0268 -0.0200
30.00 0.708 0.1987 -0.0813
40.00 0.711 0.4107 -0.1278
50.00 0.667 0.6384 -0.1712
60.00 0.564 0.8557 -0.2125
70.00 0.408 1.0380 -0.2509
80.00 0.213 1.1650 -0.2847
90.00 0.000 1.2234 -0.3119
100.00 -0.149 1.1650 -0.3165
110.00 -0.286 1.0380 -0.3068
120.00 -0.395 0.8557 -0.2858
130.00 -0.467 0.6384 -0.2584
140.00 -0.498 0.4107 -0.2314
150.00 -0.496 0.1987 -0.2145
160.00 -0.490 0.0268 -0.2311
170.00 -0.245 0.0100 -0.5000
180.00 0.000 0.0100 0.0000

```

### C.26. Ocean current speed Input File - fau\_fxBlade\_0\_5.WND

```

! current file for sheared 0.0m/s wind with 0 degree direction.
! Time    current  current  Vert.  Horiz.  Vert.  LinV  Gust
!         Speed   Dir     Speed  Shear   Shear  Shear  Speed
0.0      0.5     0.0     0.0    0.0     0.0    0.0    0.0
0.1      0.5     0.0     0.0    0.0     0.0    0.0    0.0
999.9    0.5     0.0     0.0    0.0     0.0    0.0    0.0

```

### C.27. Ocean current speed Input File - fau\_fxBlade\_1\_5.WND

```

! current file for sheared 0.0m/s wind with 0 degree direction.
! Time    current  current  Vert.  Horiz.  Vert.  LinV  Gust
!         Speed   Dir     Speed  Shear   Shear  Shear  Speed
0.0      1.5     0.0     0.0    0.0     0.0    0.0    0.0
0.1      1.5     0.0     0.0    0.0     0.0    0.0    0.0
999.9    1.5     0.0     0.0    0.0     0.0    0.0    0.0

```

## C.28. Ocean current speed Input File - fau\_fxBlade\_2\_5.WND

```
! current file for sheared 0.0m/s wind with 0 degree direction.
! Time    current    current    Vert.    Horiz.    Vert.    LinV    Gust
!        Speed     Dir       Speed   Shear    Shear    Shear   Speed
  0.0    2.5     0.0     0.0     0.0     0.0     0.0     0.0
  0.1    2.5     0.0     0.0     0.0     0.0     0.0     0.0
 999.9   2.5     0.0     0.0     0.0     0.0     0.0     0.0
```

## C.29. Ocean current speed Input File - fau\_fxBlade\_3\_5.WND

```
! current file for sheared 0.0m/s wind with 0 degree direction.
! Time    current    current    Vert.    Horiz.    Vert.    LinV    Gust
!        Speed     Dir       Speed   Shear    Shear    Shear   Speed
  0.0    3.5     0.0     0.0     0.0     0.0     0.0     0.0
  0.1    3.5     0.0     0.0     0.0     0.0     0.0     0.0
 999.9   3.5     0.0     0.0     0.0     0.0     0.0     0.0
```

## D. FAST Files

### D.1. Primary Input File - fau\_fxBlade\_QQ1\_3a\_1\_5.fst

```
----- FAST INPUT FILE -----
FAST certification fau_fxBlade: fx77 with many DOFs with fixed yaw error and steady wind.
Many parameters are pure fiction. Compatible with FAST v7.00.00.
----- SIMULATION CONTROL -----
True   Echo   - Echo input data to "echo.out" (flag)
  1   ADAMSPrep - ADAMS preprocessor mode {1: Run FAST, 2: use FAST as a preprocessor to create an ADAMS
model, 3: do both} (switch)
  1   AnalMode - Analysis mode {1: Run a time-marching simulation, 2: create a periodic linearized model} (switch)
  3   NumBl   - Number of blades (-)
 20.0  TMax   - Total run time (s)
 0.0001 DT   - Integration time step (s)
----- TURBINE CONTROL -----
  0   YCMode - Yaw control mode {0: none, 1: user-defined from routine UserYawCont, 2: user-defined from
Simulink} (switch)
9999.9 TYCON - Time to enable active yaw control (s) [unused when YCMode=0]
  0   PCMode - Pitch control mode {0: none, 1: user-defined from routine PitchCntrl, 2: user-defined from Simulink}
(switch)
9999.9 TPCOn - Time to enable active pitch control (s) [unused when PCMode=0]
  0   VSContrl - Variable-speed control mode {0: none, 1: simple VS, 2: user-defined from routine UserVSCont, 3:
user-defined from Simulink} (switch)
9999.9 VS_RtGnSp - Rated generator speed for simple variable-speed generator control (HSS side) (rpm) [used only
when VSContrl=1]
9999.9 VS_RtTq - Rated generator torque/constant generator torque in Region 3 for simple variable-speed
generator control (HSS side) (N-m) [used only when VSContrl=1]
9999.9 VS_Rgn2K - Generator torque constant in Region 2 for simple variable-speed generator control (HSS side)
(N-m/rpm^2) [used only when VSContrl=1]
9999.9 VS_SlPc - Rated generator slip percentage in Region 2 1/2 for simple variable-speed generator control (%)
[used only when VSContrl=1]
  2   GenModel - Generator model {1: simple, 2: Thevenin, 3: user-defined from routine UserGen} (switch) [used only
when VSContrl=0]
True   GenTiStr - Method to start the generator {T: timed using TimGenOn, F: generator speed using SpdGenOn}
(flag)
True   GenTiStp - Method to stop the generator {T: timed using TimGenOf, F: when generator power = 0} (flag)
9999.9 SpdGenOn - Generator speed to turn on the generator for a startup (HSS speed) (rpm) [used only when
GenTiStr=False]
  0.0  TimGenOn - Time to turn on the generator for a startup (s) [used only when GenTiStr=True]
9999.9 TimGenOf - Time to turn off the generator (s) [used only when GenTiStp=True]
  1   HSSBrMode - HSS brake model {1: simple, 2: 160 user-defined from routine UserHSSBr} (switch)
```



9999.9 THSSBrDp - Time to initiate deployment of the HSS brake (s)  
 9999.9 TiDynBrk - Time to initiate deployment of the dynamic generator brake [CURRENTLY IGNORED] (s)  
 9999.9 TTpBrDp(1) - Time to initiate deployment of tip brake 1 (s)  
 9999.9 TTpBrDp(2) - Time to initiate deployment of tip brake 2 (s)  
 9999.9 TTpBrDp(3) - Time to initiate deployment of tip brake 3 (s) [unused for 2 blades]  
 9999.9 TBDepISp(1) - Deployment-initiation speed for the tip brake on blade 1 (rpm)  
 9999.9 TBDepISp(2) - Deployment-initiation speed for the tip brake on blade 2 (rpm)  
 9999.9 TBDepISp(3) - Deployment-initiation speed for the tip brake on blade 3 (rpm) [unused for 2 blades]  
 9999.9 TYawManS - Time to start override yaw maneuver and end standard yaw control (s)  
 9999.9 TYawManE - Time at which override yaw maneuver reaches final yaw angle (s)  
 0.0 NacYawF - Final yaw angle for yaw maneuvers (degrees)  
 9999.9 TPitManS(1) - Time to start override pitch maneuver for blade 1 and end standard pitch control (s)  
 9999.9 TPitManS(2) - Time to start override pitch maneuver for blade 2 and end standard pitch control (s)  
 9999.9 TPitManS(3) - Time to start override pitch maneuver for blade 3 and end standard pitch control (s) [unused for 2 blades]  
 9999.9 TPitManE(1) - Time at which override pitch maneuver for blade 1 reaches final pitch (s)  
 9999.9 TPitManE(2) - Time at which override pitch maneuver for blade 2 reaches final pitch (s)  
 9999.9 TPitManE(3) - Time at which override pitch maneuver for blade 3 reaches final pitch (s) [unused for 2 blades]  
 0.0 BIPitch(1) - Blade 1 initial pitch (degrees)  
 0.0 BIPitch(2) - Blade 2 initial pitch (degrees)  
 0.0 BIPitch(3) - Blade 3 initial pitch (degrees) [unused for 2 blades]  
 0.0 BIPitchF(1) - Blade 1 final pitch for pitch maneuvers (degrees)  
 0.0 BIPitchF(2) - Blade 2 final pitch for pitch maneuvers (degrees)  
 0.0 BIPitchF(3) - Blade 3 final pitch for pitch maneuvers (degrees) [unused for 2 blades]

----- ENVIRONMENTAL CONDITIONS -----

2.058 Gravity - Gravitational acceleration (m/s^2)

----- FEATURE FLAGS -----

True FlapDOF1 - First flapwise blade mode DOF (flag)  
 True FlapDOF2 - Second flapwise blade mode DOF (flag)  
 True EdgeDOF - First edgewise blade mode DOF (flag)  
 False TeetDOF - Rotor-teeter DOF (flag) [unused for 3 blades]  
 False DrTrDOF - Drivetrain rotational-flexibility DOF (flag)  
 False GenDOF - Generator DOF (flag)  
 False YawDOF - Yaw DOF (flag)  
 False TwFADOF1 - First fore-aft tower bending-mode DOF (flag)  
 False TwFADOF2 - Second fore-aft tower bending-mode DOF (flag)  
 False TwSSDOF1 - First side-to-side tower bending-mode DOF (flag)  
 False TwSSDOF2 - Second side-to-side tower bending-mode DOF (flag)  
 True CompAero - Compute aerodynamic forces (flag)  
 False CompNoise - Compute aerodynamic noise (flag)

----- INITIAL CONDITIONS -----

0.0 OoPDefl - Initial out-of-plane blade-tip displacement (meters)  
 0.0 IPDefl - Initial in-plane blade-tip deflection (meters)  
 0.0 TeetDefl - Initial or fixed teeter angle (degrees) [unused for 3 blades]  
 0.0 Azimuth - Initial azimuth angle for blade 1 (degrees)  
 50.0 RotSpeed - Initial or fixed rotor speed (rpm)  
 0.0 NacYaw - Initial or fixed nacelle-yaw angle (degrees)  
 0.0 TTDspFA - Initial fore-aft tower-top displacement (meters)  
 0.0 TTDspSS - Initial side-to-side tower-top displacement (meters)

----- TURBINE CONFIGURATION -----

1.498 TipRad - The distance from the rotor apex to the blade tip (meters)  
 0.257 HubRad - The distance from the rotor apex to the blade root (meters)  
 1 PSpnEIN - Number of the innermost blade element which is still part of the pitchable portion of the blade for partial-span pitch control [1 to BldNodes] [CURRENTLY IGNORED] (-)  
 0.0 UndSling - Undersling length [distance from teeter pin to the rotor apex] (meters) [unused for 3 blades]  
 0.0 HubCM - Distance from rotor apex to hub mass [positive downwind] (meters)  
 -0.5 OverHang - Distance from yaw axis to rotor apex [3 blades] or teeter pin [2 blades] (meters)  
 0.0 NacCMxn - Downwind distance from the tower-top to the nacelle CM (meters)  
 0.0 NacCMyn - Lateral distance from the tower-top to the nacelle CM (meters)  
 0.6 NacCMzn - Vertical distance from the tower-top to the nacelle CM (meters)  
 9.4 TowerHt - Height of tower above ground level [onshore] or MSL [offshore] (meters)  
 0.6 Twr2Shft - Vertical distance from the tower-top to the rotor shaft (meters)  
 0.0 TwrRBHt - Tower rigid base height (meters)  
 0.0 ShftTilt - Rotor shaft tilt angle (degrees)  
 0.0 Delta3 - Delta-3 angle for teetering rotors (degrees) [unused for 3 blades]  
 0.0 PreCone(1) - Blade 1 cone angle (degrees)  
 0.0 PreCone(2) - Blade 2 cone angle (degrees)  
 0.0 PreCone(3) - Blade 3 cone angle (degrees) [unused for 2 blades]

```

0.0 AzimB1Up - Azimuth value to use for I/O when blade 1 points up (degrees)
----- MASS AND INERTIA -----
0.0 YawBrMass - Yaw bearing mass (kg)
1747.0 NacMass - Nacelle mass (kg)
247.3 HubMass - Hub mass (kg)
0.0 TipMass(1) - Tip-brake mass, blade 1 (kg)
0.0 TipMass(2) - Tip-brake mass, blade 2 (kg)
0.0 TipMass(3) - Tip-brake mass, blade 3 (kg) [unused for 2 blades]
976.3 NacYIner - Nacelle inertia about yaw axis (kg m^2)
10.0 GenIner - Generator inertia about HSS (kg m^2)
9.0 HubIner - Hub inertia about rotor axis [3 blades] or teeter axis [2 blades] (kg m^2)
----- DRIVETRAIN -----
100.0 GBoxEff - Gearbox efficiency (%)
89.4 GenEff - Generator efficiency [ignored by the Thevenin and user-defined generator models] (%)
28.25 GBRatio - Gearbox ratio (-)
False GBRevers - Gearbox reversal (T: if rotor and generator rotate in opposite directions) (flag)
9999.9 HSSBrTqF - Fully deployed HSS-brake torque (N-m)
9999.9 HSSBrDt - Time for HSS-brake to reach full deployment once initiated (sec) [used only when HSSBrMode=1]
"" DynBrkFi - File containing a mech-gen-torque vs HSS-speed curve for a dynamic brake [CURRENTLY
IGNORED] (quoted string)
6.0E5 DTTorSpr - Drivetrain torsional spring (N-m/rad)
1.0E5 DTTorDmp - Drivetrain torsional damper (N-m/(rad/s))
----- SIMPLE INDUCTION GENERATOR ----- Crude approximation of torque/speed
curve.
2.222 SIG_SIPc - Rated generator slip percentage (%) [used only when VSContrl=0 and GenModel=1]
1800.0 SIG_SySp - Synchronous (zero-torque) generator speed (rpm) [used only when VSContrl=0 and
GenModel=1]
314.3 SIG_RtTq - Rated torque (N-m) [used only when VSContrl=0 and GenModel=1]
1.75 SIG_PORt - Pull-out ratio (Tpullout/Trated) (-) [used only when VSContrl=0 and GenModel=1]
----- THEVENIN-EQUIVALENT INDUCTION GENERATOR -----
60.0 TEC_Freq - Line frequency [50 or 60] (Hz) [used only when VSContrl=0 and GenModel=2]
4 TEC_NPol - Number of poles [even integer > 0] (-) [used only when VSContrl=0 and GenModel=2]
4.92E-02 TEC_SRes - Stator resistance (ohms) [used only when VSContrl=0 and GenModel=2]
5.34E-04 TEC_RRes - Rotor resistance (ohms) [used only when VSContrl=0 and GenModel=2]
480.0 TEC_VLL - Line-to-line RMS voltage (volts) [used only when VSContrl=0 and GenModel=2]
1.00E-04 TEC_SLR - Stator leakage reactance (ohms) [used only when VSContrl=0 and GenModel=2]
1.00E-04 TEC_RLR - Rotor leakage reactance (ohms) [used only when VSContrl=0 and GenModel=2]
4.49E-03 TEC_MR - Magnetizing reactance (ohms) [used only when VSContrl=0 and GenModel=2]
----- PLATFORM -----
0 PtfmModel - Platform model {0: none, 1: onshore, 2: fixed bottom offshore, 3: floating offshore} (switch)
"" PtfmFile - Name of file containing platform properties (quoted string) [unused when PtfmModel=0]
----- TOWER -----
11 TwrNodes - Number of tower nodes used for analysis (-)
"AOC_Tower.dat" TwrFile - Name of file containing tower properties (quoted string)
----- NACELLE-YAW -----
0.0 YawSpr - Nacelle-yaw spring constant (N-m/rad)
0.0 YawDamp - Nacelle-yaw damping constant (N-m/(rad/s))
0.0 YawNeut - Neutral yaw position--yaw spring force is zero at this yaw (degrees)
----- FURLING -----
False Furling - Read in additional model properties for furling turbine (flag)
"" FurlFile - Name of file containing furling properties (quoted string) [unused when Furling=False]
----- ROTOR-TEETER -----
0 TeetMod - Rotor-teeter spring/damper model {0: none, 1: standard, 2: user-defined from routine UserTeet}
[switch] [unused for 3 blades]
0.0 TeetDmpP - Rotor-teeter damper position (degrees) [used only for 2 blades and when TeetMod=1]
0.0 TeetDmp - Rotor-teeter damping constant (N-m/(rad/s)) [used only for 2 blades and when TeetMod=1]
0.0 TeetCDmp - Rotor-teeter rate-independent Coulomb-damping moment (N-m) [used only for 2 blades and when
TeetMod=1]
0.0 TeetSStP - Rotor-teeter soft-stop position (degrees) [used only for 2 blades and when TeetMod=1]
0.0 TeetHStP - Rotor-teeter hard-stop position (degrees) [used only for 2 blades and when TeetMod=1]
0.0 TeetSSSp - Rotor-teeter soft-stop linear-spring constant (N-m/rad) [used only for 2 blades and when
TeetMod=1]
0.0 TeetHSSp - Rotor-teeter hard-stop linear-spring constant (N-m/rad) [used only for 2 blades and when
TeetMod=1]
----- TIP-BRAKE -----
0.0 TBDrConN - Tip-brake drag constant during normal operation, Cd*Area (m^2)
0.0 TBDrConD - Tip-brake drag constant during fully-deployed operation, Cd*Area (m^2)
0.0 TpBrDT - Time for tip-brake to reach full deployment once released (sec)

```

```

----- BLADE -----
"fau_fxBlade_QQ1_3a_section.dat"  BldFile(1) - Name of file containing properties for blade 1 (quoted string)
"fau_fxBlade_QQ1_3a_section.dat"  BldFile(2) - Name of file containing properties for blade 2 (quoted string)
"fau_fxBlade_QQ1_3a_section.dat"  BldFile(3) - Name of file containing properties for blade 3 (quoted string) [unused
for 2 blades]
----- AERODYN -----
"fau_fxBlade_AD1_5.ipt"  ADFile  - Name of file containing AeroDyn input parameters (quoted string)
----- NOISE -----
""      NoiseFile  - Name of file containing aerodynamic noise input parameters (quoted string) [used only when
CompNoise=True]
----- ADAMS -----
"AOC_ADAMS.dat"  ADAMSFile  - Name of file containing ADAMS-specific input parameters (quoted string) [unused
when ADAMSPrep=1]
----- LINEARIZATION CONTROL -----
"AOC_Linear.dat"  LinFile  - Name of file containing FAST linearization parameters (quoted string) [unused when
AnalMode=1]
----- OUTPUT -----
True      SumPrint  - Print summary data to "<RootName>.fsm" (flag)
True      TabDelim  - Generate a tab-delimited tabular output file. (flag)
"ES10.3E2" OutFmt    - Format used for tabular output except time. Resulting field should be 10 characters. (quoted
string) [not checked for validity!]
0.0      TStart    - Time to begin tabular output (s)
20       DecFact   - Decimation factor for tabular output {1: output every time step} (-)
1.0      SttsTime  - Amount of time between screen status messages (sec)
0.0      NclIMUxn  - Downwind distance from the tower-top to the nacelle IMU (meters)
0.0      NclMUyn   - Lateral distance from the tower-top to the nacelle IMU (meters)
0.0      NclMUzn   - Vertical distance from the tower-top to the nacelle IMU (meters)
0.5      ShftGagL  - Distance from rotor apex [3 blades] or teeter pin [2 blades] to shaft strain gages [positive for upwind
rotors] (meters)
0        NTwGages  - Number of tower nodes that have strain gages for output [0 to 9] (-)
0        TwrGagNd  - List of tower nodes that have strain gages [1 to TwrNodes] (-) [unused if NTwGages=0]
9        NBlGages  - Number of blade nodes that have strain gages for output [0 to 9] (-)
1,3,5,7,9,11,14,17,20 BldGagNd - List of blade nodes that have strain gages [1 to BldNodes] (-) [unused if
NBlGages=0]
OutList  - The next line(s) contains a list of output parameters. See OutList.txt for a listing of available output
channels, (-)
"LSSGagPxa"  - LSS gage azimuth
"Azimuth"    - Rotor blade 1 azimuth angle
"RotSpeed , GenSpeed" - Low-speed shaft and high-speed shaft speeds
"TipDxb1,TipDxb2,TipDxb3" - Blade flapwise tip deflections (relative to the pitch axis) along xb axis
"TipDyb1,TipDyb2,TipDyb3" - Blade edgewise tip deflections (relative to the pitch axis) along yb axis
"TipDxc1,TipDxc2,TipDxc3" - Blade out-of-plane tip deflection (relative to the pitch axis) along xc axis
"TipDyc1,TipDyc2,TipDyc3" - Blade in-plane tip deflection (relative to the pitch axis) along yc axis
"TipDzb1,TipDzb2,TipDzb3" - Blade axial tip deflections along zb/zc axis
"TipALxb1,TipALxb2,TipALxb3" - Blade local flapwise tip acceleration (absolute) along the local xb axis
"TipALyb1,TipALyb2,TipALyb3" - Blade local edgewise tip acceleration (absolute) along the local yb axis
"TipALzb1,TipALzb2,TipALzb3" - Blade local axial tip acceleration (absolute) along the local zb axis
"RollDefl1,RollDefl2,RollDefl3" - Blade roll tip deflections
"PtchDefl1,PtchDefl2,PtchDefl3" - Blade pitch tip deflections
"Spn1ALxb1,Spn1ALyb1" - Blade 1 Gage #1 local flapwise and edgewise accelerations
"RootFxb1,RootFyb1" - Blade 1 root flapwise and edgewise shear forces
"RootMxc1,RootMyc1,RootMzc1" - Blade 1 root in-plane moment,out-of-plane moment,pitching moment
"RootMxb1,RootMyb1" - Blade 1 root edgewise moment,flapwise moment
"Spn1MLxb1, Spn1MLyb1" - Blade 1 local edgewise and flapwise bending moments at span station 1
"Spn2MLxb1, Spn2MLyb1" - Blade 1 local edgewise and flapwise bending moments at span station 2
"Spn3MLxb1, Spn3MLyb1" - Blade 1 local edgewise and flapwise bending moments at span station 3
"Spn4MLxb1, Spn4MLyb1" - Blade 1 local edgewise and flapwise bending moments at span station 4
"Spn5MLxb1, Spn5MLyb1" - Blade 1 local edgewise and flapwise bending moments at span station 5
"Spn6MLxb1, Spn6MLyb1" - Blade 1 local edgewise and flapwise bending moments at span station 6 (approx. 50%
span)
"Spn7MLxb1, Spn7MLyb1" - Blade 1 local edgewise and flapwise bending moments at span station 7
"Spn8MLxb1, Spn8MLyb1" - Blade 1 local edgewise and flapwise bending moments at span station 8
"Spn9MLxb1, Spn9MLyb1" - Blade 1 local edgewise and flapwise bending moments at span station 9
"HSShftV" - HSS speed
"TTDspRoll,TTDspPtch" - Tower top tilt angles.
"YawBrRVxp,YawBrRVyp" - Tower top tilt rates.
"YawBrRAXp,YawBrRAYp" - Tower top tilt accelerations.
"LSShftFya,LSShftFza" - Rotating LSS shear forces

```

"YawBrFxn,YawBrFyn" - Yaw-bearing shear forces in the yawed nacelle coordinates  
 "RotPwr" - Rotat power  
 END of FAST input file (the word "END" must appear in the first 3 columns of this last line).

## D.2. Primary Input File - fau\_fxBlade\_QQ1\_3a\_2\_5.fst

```

----- FAST INPUT FILE -----
FAST certification fau_fxBlade: fx77 with many DOFs with fixed yaw error and steady wind.
Many parameters are pure fiction. Compatible with FAST v7.00.00.
----- SIMULATION CONTROL -----
True Echo - Echo input data to "echo.out" (flag)
1 ADAMSPrep - ADAMS preprocessor mode {1: Run FAST, 2: use FAST as a preprocessor to create an ADAMS
model, 3: do both} (switch)
1 AnalMode - Analysis mode {1: Run a time-marching simulation, 2: create a periodic linearized model} (switch)
3 NumBl - Number of blades (-)
30.0 TMax - Total run time (s)
0.0001 DT - Integration time step (s)
----- TURBINE CONTROL -----
0 YCMode - Yaw control mode {0: none, 1: user-defined from routine UserYawCont, 2: user-defined from
Simulink} (switch)
9999.9 TYCon - Time to enable active yaw control (s) [unused when YCMode=0]
0 PCMode - Pitch control mode {0: none, 1: user-defined from routine PitchCntrl, 2: user-defined from Simulink}
(switch)
9999.9 TPCOn - Time to enable active pitch control (s) [unused when PCMode=0]
0 VSContrl - Variable-speed control mode {0: none, 1: simple VS, 2: user-defined from routine UserVSCont, 3:
user-defined from Simulink} (switch)
9999.9 VS_RtGnSp - Rated generator speed for simple variable-speed generator control (HSS side) (rpm) [used only
when VSContrl=1]
9999.9 VS_RtTq - Rated generator torque/constant generator torque in Region 3 for simple variable-speed
generator control (HSS side) (N-m) [used only when VSContrl=1]
9999.9 VS_Rgn2K - Generator torque constant in Region 2 for simple variable-speed generator control (HSS side)
(N-m/rpm^2) [used only when VSContrl=1]
9999.9 VS_SIPc - Rated generator slip percentage in Region 2 1/2 for simple variable-speed generator control (%)
[used only when VSContrl=1]
2 GenModel - Generator model {1: simple, 2: Thevenin, 3: user-defined from routine UserGen} (switch) [used only
when VSContrl=0]
True GenTiStr - Method to start the generator {T: timed using TimGenOn, F: generator speed using SpdGenOn}
(flag)
True GenTiStp - Method to stop the generator {T: timed using TimGenOf, F: when generator power = 0} (flag)
9999.9 SpdGenOn - Generator speed to turn on the generator for a startup (HSS speed) (rpm) [used only when
GenTiStr=False]
0.0 TimGenOn - Time to turn on the generator for a startup (s) [used only when GenTiStr=True]
9999.9 TimGenOf - Time to turn off the generator (s) [used only when GenTiStp=True]
1 HSSBrMode - HSS brake model {1: simple, 2: user-defined from routine UserHSSBr} (switch)
9999.9 THSSBrDp - Time to initiate deployment of the HSS brake (s)
9999.9 TiDynBrk - Time to initiate deployment of the dynamic generator brake [CURRENTLY IGNORED] (s)
9999.9 TTpBrDp(1) - Time to initiate deployment of tip brake 1 (s)
9999.9 TTpBrDp(2) - Time to initiate deployment of tip brake 2 (s)
9999.9 TTpBrDp(3) - Time to initiate deployment of tip brake 3 (s) [unused for 2 blades]
9999.9 TBDepISp(1) - Deployment-initiation speed for the tip brake on blade 1 (rpm)
9999.9 TBDepISp(2) - Deployment-initiation speed for the tip brake on blade 2 (rpm)
9999.9 TBDepISp(3) - Deployment-initiation speed for the tip brake on blade 3 (rpm) [unused for 2 blades]
9999.9 TYawManS - Time to start override yaw maneuver and end standard yaw control (s)
9999.9 TYawManE - Time at which override yaw maneuver reaches final yaw angle (s)
0.0 NacYawF - Final yaw angle for yaw maneuvers (degrees)
9999.9 TPitManS(1) - Time to start override pitch maneuver for blade 1 and end standard pitch control (s)
9999.9 TPitManS(2) - Time to start override pitch maneuver for blade 2 and end standard pitch control (s)
9999.9 TPitManS(3) - Time to start override pitch maneuver for blade 3 and end standard pitch control (s) [unused for
2 blades]
9999.9 TPitManE(1) - Time at which override pitch maneuver for blade 1 reaches final pitch (s)
9999.9 TPitManE(2) - Time at which override pitch maneuver for blade 2 reaches final pitch (s)
9999.9 TPitManE(3) - Time at which override pitch maneuver for blade 3 reaches final pitch (s) [unused for 2 blades]
0.0 BIPitch(1) - Blade 1 initial pitch (degrees)
0.0 BIPitch(2) - Blade 2 initial pitch (degrees)

```

0.0 BIPitch(3) - Blade 3 initial pitch (degrees) [unused for 2 blades]  
0.0 BIPitchF(1) - Blade 1 final pitch for pitch maneuvers (degrees)  
0.0 BIPitchF(2) - Blade 2 final pitch for pitch maneuvers (degrees)  
0.0 BIPitchF(3) - Blade 3 final pitch for pitch maneuvers (degrees) [unused for 2 blades]

----- ENVIRONMENTAL CONDITIONS -----  
2.058 Gravity - Gravitational acceleration (m/s^2)

----- FEATURE FLAGS -----  
True FlapDOF1 - First flapwise blade mode DOF (flag)  
True FlapDOF2 - Second flapwise blade mode DOF (flag)  
True EdgeDOF - First edgewise blade mode DOF (flag)  
False TeetDOF - Rotor-teeter DOF (flag) [unused for 3 blades]  
False DrTrDOF - Drivetrain rotational-flexibility DOF (flag)  
False GenDOF - Generator DOF (flag)  
False YawDOF - Yaw DOF (flag)  
False TwFADOF1 - First fore-aft tower bending-mode DOF (flag)  
False TwFADOF2 - Second fore-aft tower bending-mode DOF (flag)  
False TwSSDOF1 - First side-to-side tower bending-mode DOF (flag)  
False TwSSDOF2 - Second side-to-side tower bending-mode DOF (flag)  
True CompAero - Compute aerodynamic forces (flag)  
False CompNoise - Compute aerodynamic noise (flag)

----- INITIAL CONDITIONS -----  
0.0 OpPDefl - Initial out-of-plane blade-tip displacement (meters)  
0.0 IPDefl - Initial in-plane blade-tip deflection (meters)  
0.0 TeetDefl - Initial or fixed teeter angle (degrees) [unused for 3 blades]  
0.0 Azimuth - Initial azimuth angle for blade 1 (degrees)  
50.0 RotSpeed - Initial or fixed rotor speed (rpm)  
0.0 NacYaw - Initial or fixed nacelle-yaw angle (degrees)  
0.0 TTDspFA - Initial fore-aft tower-top displacement (meters)  
0.0 TTDspSS - Initial side-to-side tower-top displacement (meters)

----- TURBINE CONFIGURATION -----  
1.498 TipRad - The distance from the rotor apex to the blade tip (meters)  
0.257 HubRad - The distance from the rotor apex to the blade root (meters)  
1 PSpnEIN - Number of the innermost blade element which is still part of the pitchable portion of the blade for partial-span pitch control [1 to BldNodes] [CURRENTLY IGNORED] (-)  
0.0 UndSling - Undersling length [distance from teeter pin to the rotor apex] (meters) [unused for 3 blades]  
0.0 HubCM - Distance from rotor apex to hub mass [positive downwind] (meters)  
-0.5 OverHang - Distance from yaw axis to rotor apex [3 blades] or teeter pin [2 blades] (meters)  
0.0 NacCMxn - Downwind distance from the tower-top to the nacelle CM (meters)  
0.0 NacCMyn - Lateral distance from the tower-top to the nacelle CM (meters)  
0.6 NacCMzn - Vertical distance from the tower-top to the nacelle CM (meters)  
9.4 TowerHt - Height of tower above ground level [onshore] or MSL [offshore] (meters)  
0.6 Twr2Shft - Vertical distance from the tower-top to the rotor shaft (meters)  
0.0 TwrRBHt - Tower rigid base height (meters)  
0.0 ShftTilt - Rotor shaft tilt angle (degrees)  
0.0 Delta3 - Delta-3 angle for teetering rotors (degrees) [unused for 3 blades]  
0.0 PreCone(1) - Blade 1 cone angle (degrees)  
0.0 PreCone(2) - Blade 2 cone angle (degrees)  
0.0 PreCone(3) - Blade 3 cone angle (degrees) [unused for 2 blades]  
0.0 AzimB1Up - Azimuth value to use for I/O when blade 1 points up (degrees)

----- MASS AND INERTIA -----  
0.0 YawBrMass - Yaw bearing mass (kg)  
1747.0 NacMass - Nacelle mass (kg)  
247.3 HubMass - Hub mass (kg)  
0.0 TipMass(1) - Tip-brake mass, blade 1 (kg)  
0.0 TipMass(2) - Tip-brake mass, blade 2 (kg)  
0.0 TipMass(3) - Tip-brake mass, blade 3 (kg) [unused for 2 blades]  
976.3 NacYIner - Nacelle inertia about yaw axis (kg m^2)  
10.0 GenIner - Generator inertia about HSS (kg m^2)  
9.0 HubIner - Hub inertia about rotor axis [3 blades] or teeter axis [2 blades] (kg m^2)

----- DRIVETRAIN -----  
100.0 GBoxEff - Gearbox efficiency (%)  
89.4 GenEff - Generator efficiency [ignored by the Thevenin and user-defined generator models] (%)  
28.25 GBRatio - Gearbox ratio (-)  
False GBRevers - Gearbox reversal {T: if rotor and generator rotate in opposite directions} (flag)  
9999.9 HSSBrTqF - Fully deployed HSS-brake torque (N-m)  
9999.9 HSSBrDt - Time for HSS-brake to reach full deployment once initiated (sec) [used only when HSSBrMode=1]  
"" DynBrkFi - File containing a mech-gen-torque vs HSS-speed curve for a dynamic brake [CURRENTLY IGNORED] (quoted string)

6.0E5 DTTorSpr - Drivetrain torsional spring (N-m/rad)  
1.0E5 DTTorDmp - Drivetrain torsional damper (N-m/(rad/s))  
----- SIMPLE INDUCTION GENERATOR ----- Crude approximation of torque/speed  
curve.  
2.222 SIG\_SIPc - Rated generator slip percentage (%) [used only when VSContrl=0 and GenModel=1]  
1800.0 SIG\_SySp - Synchronous (zero-torque) generator speed (rpm) [used only when VSContrl=0 and  
GenModel=1]  
314.3 SIG\_RtTq - Rated torque (N-m) [used only when VSContrl=0 and GenModel=1]  
1.75 SIG\_PORt - Pull-out ratio (Tpullout/Trated) (-) [used only when VSContrl=0 and GenModel=1]  
----- THEVENIN-EQUIVALENT INDUCTION GENERATOR -----  
60.0 TEC\_Freq - Line frequency [50 or 60] (Hz) [used only when VSContrl=0 and GenModel=2]  
4 TEC\_NPol - Number of poles [even integer > 0] (-) [used only when VSContrl=0 and GenModel=2]  
4.92E-02 TEC\_SRes - Stator resistance (ohms) [used only when VSContrl=0 and GenModel=2]  
5.34E-04 TEC\_RRes - Rotor resistance (ohms) [used only when VSContrl=0 and GenModel=2]  
480.0 TEC\_VLL - Line-to-line RMS voltage (volts) [used only when VSContrl=0 and GenModel=2]  
1.00E-04 TEC\_SLR - Stator leakage reactance (ohms) [used only when VSContrl=0 and GenModel=2]  
1.00E-04 TEC\_RLR - Rotor leakage reactance (ohms) [used only when VSContrl=0 and GenModel=2]  
4.49E-03 TEC\_MR - Magnetizing reactance (ohms) [used only when VSContrl=0 and GenModel=2]  
----- PLATFORM -----  
0 PtfmModel - Platform model {0: none, 1: onshore, 2: fixed bottom offshore, 3: floating offshore} (switch)  
"" PtfmFile - Name of file containing platform properties (quoted string) [unused when PtfmModel=0]  
----- TOWER -----  
11 TwrNodes - Number of tower nodes used for analysis (-)  
"AOC\_Tower.dat" TwrFile - Name of file containing tower properties (quoted string)  
----- NACELLE-YAW -----  
0.0 YawSpr - Nacelle-yaw spring constant (N-m/rad)  
0.0 YawDamp - Nacelle-yaw damping constant (N-m/(rad/s))  
0.0 YawNeut - Neutral yaw position--yaw spring force is zero at this yaw (degrees)  
----- FURLING -----  
False Furling - Read in additional model properties for furling turbine (flag)  
"" FurlFile - Name of file containing furling properties (quoted string) [unused when Furling=False]  
----- ROTOR-TEETER -----  
0 TeetMod - Rotor-teeter spring/damper model {0: none, 1: standard, 2: user-defined from routine UserTeet}  
[unused for 3 blades]  
0.0 TeetDmpP - Rotor-teeter damper position (degrees) [used only for 2 blades and when TeetMod=1]  
0.0 TeetDmp - Rotor-teeter damping constant (N-m/(rad/s)) [used only for 2 blades and when TeetMod=1]  
0.0 TeetCDmp - Rotor-teeter rate-independent Coulomb-damping moment (N-m) [used only for 2 blades and when  
TeetMod=1]  
0.0 TeetSStP - Rotor-teeter soft-stop position (degrees) [used only for 2 blades and when TeetMod=1]  
0.0 TeetHStP - Rotor-teeter hard-stop position (degrees) [used only for 2 blades and when TeetMod=1]  
0.0 TeetSSSp - Rotor-teeter soft-stop linear-spring constant (N-m/rad) [used only for 2 blades and when  
TeetMod=1]  
0.0 TeetHSSp - Rotor-teeter hard-stop linear-spring constant (N-m/rad) [used only for 2 blades and when  
TeetMod=1]  
----- TIP-BRAKE -----  
0.0 TBDrConN - Tip-brake drag constant during normal operation, Cd\*Area (m^2)  
0.0 TBDrConD - Tip-brake drag constant during fully-deployed operation, Cd\*Area (m^2)  
0.0 TpBrDT - Time for tip-brake to reach full deployment once released (sec)  
----- BLADE -----  
"fau\_fxBlade\_QQ1\_3a\_section.dat" BldFile(1) - Name of file containing properties for blade 1 (quoted string)  
"fau\_fxBlade\_QQ1\_3a\_section.dat" BldFile(2) - Name of file containing properties for blade 2 (quoted string)  
"fau\_fxBlade\_QQ1\_3a\_section.dat" BldFile(3) - Name of file containing properties for blade 3 (quoted string) [unused  
for 2 blades]  
----- AERODYN -----  
"fau\_fxBlade\_AD2\_5.ipt" ADFile - Name of file containing AeroDyn input parameters (quoted string)  
----- NOISE -----  
"" NoiseFile - Name of file containing aerodynamic noise input parameters (quoted string) [used only when  
CompNoise=True]  
----- ADAMS -----  
"AOC\_ADAMS.dat" ADAMSFile - Name of file containing ADAMS-specific input parameters (quoted string) [unused  
when ADAMSPrep=1]  
----- LINEARIZATION CONTROL -----  
"AOC\_Linear.dat" LinFile - Name of file containing FAST linearization parameters (quoted string) [unused when  
AnalMode=1]  
----- OUTPUT -----  
True SumPrint - Print summary data to "<RootName>.fsm" (flag)  
True TabDelim - Generate a tab-delimited tabular output file. (flag)

"ES10.3E2" OutFmt - Format used for tabular output except time. Resulting field should be 10 characters. (quoted string) [not checked for validity!]

0.0 TStart - Time to begin tabular output (s)

20 DecFact - Decimation factor for tabular output {1: output every time step} (-)

1.0 SttsTime - Amount of time between screen status messages (sec)

0.0 NclMUxn - Downwind distance from the tower-top to the nacelle IMU (meters)

0.0 NclMUyn - Lateral distance from the tower-top to the nacelle IMU (meters)

0.0 NclMUzn - Vertical distance from the tower-top to the nacelle IMU (meters)

0.5 ShftGagL - Distance from rotor apex [3 blades] or teeter pin [2 blades] to shaft strain gages [positive for upwind rotors] (meters)

0 NTwGages - Number of tower nodes that have strain gages for output [0 to 9] (-)

0 TwrGagNd - List of tower nodes that have strain gages [1 to TwrNodes] (-) [unused if NTwGages=0]

9 NBIGages - Number of blade nodes that have strain gages for output [0 to 9] (-)

1,3,5,7,9,11,14,17,20 BldGagNd - List of blade nodes that have strain gages [1 to BldNodes] (-) [unused if NBIGages=0]

OutList - The next line(s) contains a list of output parameters. See OutList.txt for a listing of available output channels, (-)

"LSSGagPxa" - LSS gage azimuth

"Azimuth" - Rotor blade 1 azimuth angle

"RotSpeed , GenSpeed" - Low-speed shaft and high-speed shaft speeds

"TipDxb1,TipDxb2,TipDxb3" - Blade flapwise tip deflections (relative to the pitch axis) along xb axis

"TipDyb1,TipDyb2,TipDyb3" - Blade edgewise tip deflections (relative to the pitch axis) along yb axis

"TipDxc1,TipDxc2,TipDxc3" - Blade out-of-plane tip deflection (relative to the pitch axis) along xc axis

"TipDyc1,TipDyc2,TipDyc3" - Blade in-plane tip deflection (relative to the pitch axis) along yc axis

"TipDzb1,TipDzb2,TipDzb3" - Blade axial tip deflections along zb/zc axis

"TipALxb1,TipALxb2,TipALxb3" - Blade local flapwise tip acceleration (absolute) along the local xb axis

"TipALyb1,TipALyb2,TipALyb3" - Blade local edgewise tip acceleration (absolute) along the local yb axis

"TipALzb1,TipALzb2,TipALzb3" - Blade local axial tip acceleration (absolute) along the local zb axis

"RollDefl1,RollDefl2,RollDefl3" - Blade roll tip deflections

"PtchDefl1,PtchDefl2,PtchDefl3" - Blade pitch tip deflections

"Spn1ALxb1,Spn1ALyb1" - Blade 1 Gage #1 local flapwise and edgewise accelerations

"RootFxb1,RootFyb1" - Blade 1 root flapwise and edgewise shear forces

"RootMxc1,RootMyc1,RootMzc1" - Blade 1 root in-plane moment,out-of-plane moment,pitching moment

"RootMxb1,RootMyb1" - Blade 1 root edgewise moment,flapwise moment

"Spn1MLxb1, Spn1MLyb1" - Blade 1 local edgewise and flapwise bending moments at span station 1

"Spn2MLxb1, Spn2MLyb1" - Blade 1 local edgewise and flapwise bending moments at span station 2

"Spn3MLxb1, Spn3MLyb1" - Blade 1 local edgewise and flapwise bending moments at span station 3

"Spn4MLxb1, Spn4MLyb1" - Blade 1 local edgewise and flapwise bending moments at span station 4

"Spn5MLxb1, Spn5MLyb1" - Blade 1 local edgewise and flapwise bending moments at span station 5

"Spn6MLxb1, Spn6MLyb1" - Blade 1 local edgewise and flapwise bending moments at span station 6 (approx. 50% span)

"Spn7MLxb1, Spn7MLyb1" - Blade 1 local edgewise and flapwise bending moments at span station 7

"Spn8MLxb1, Spn8MLyb1" - Blade 1 local edgewise and flapwise bending moments at span station 8

"Spn9MLxb1, Spn9MLyb1" - Blade 1 local edgewise and flapwise bending moments at span station 9

"HSShftV" - HSS speed

"TTDspRoll,TTDspPtch" - Tower top tilt angles.

"YawBrRVxp,YawBrRVyp" - Tower top tilt rates.

"YawBrRAxp,YawBrRAYp" - Tower top tilt accelerations.

"LSShftFya,LSShftFza" - Rotating LSS shear forces

"YawBrFxn,YawBrFyn" - Yaw-bearing shear forces in the yawed nacelle coordinates

"RotPwr" - Rotat power

END OF FAST input file (the word "END" must appear in the first 3 columns of this last line).

-----

### D.3. Blade Input File - fau\_fxBlade\_QQ1\_3a\_section.dat

fau\_fx77 blade file. GJStiff -> EdgEAof are mostly lies.

----- BLADE PARAMETERS -----

26 NBlInpSt - Number of blade input stations (-)

False CalcBMode - Calculate blade mode shapes internally {T: ignore mode shapes from below, F: use mode shapes from below} [CURRENTLY IGNORED] (flag)

5.0 BldFIDmp(1) - Blade flap mode #1 structural damping in percent of critical (%)

5.0 BldFIDmp(2) - Blade flap mode #2 structural damping in percent of critical (%)

5.0 BldEdDmp(1) - Blade edge mode #1 structural damping in percent of critical (%)

----- BLADE ADJUSTMENT FACTORS -----

1.0 FIStTunr(1) - Blade flapwise modal stiffness tuner, 1st mode

- 1.0 FISTunr(2) - Blade flapwise modal stiffness tuner, 2nd mode (-)
- 1.0 AdjBIMs - Factor to adjust blade mass density (-)
- 1.0 AdjFISt - Factor to adjust blade flap stiffness (-)
- 1.0 AdjEdSt - Factor to adjust blade edge stiffness (-)

----- DISTRIBUTED BLADE PROPERTIES -----

BlFract	AeroCent	StrcTwst	BMassDen	FlpStff	EdgStff	GJStff	EASStff	Alpha	Flplnr	Edglnr	PrcrvRef		
(-)	(-)	(deg)	(kg/m)	(Nm^2)	(Nm^2)	(N)	(-)	(kg-m)	(kg-m)	(m)			
0	0.25	24.097	23.14	93380	1733000	45990	2202000000	0.00609	0.11280	0			
0.016	0.25	24.097	23.14	93380	1734000	45990	2202000000	0.00609	0.11280	0			
0.024	0.25	23.485	22.83	90070	1699000	44240	2186000000	0.00587	0.11050	0			
0.04	0.25	21.867	22.28	83760	1630000	41140	2154000000	0.00546	0.10610	0			
0.062	0.25	20.102	21.49	75000	1532000	36700	2107000000	0.00489	0.09967	0			
0.092	0.25	17.97	17.89	59880	994500	25860	1616000000	0.00391	0.06471	0			
0.129	0.25	15.831	16.63	48870	882000	21040	1549000000	0.00319	0.05739	0			
0.171	0.25	13.851	15.36	38520	769400	16490	1475000000	0.00251	0.05007	0			
0.219	0.25	12.011	13.44	28840	651200	12230	1390000000	0.00188	0.04238	0			
0.271	0.25	10.272	12.11	20970	546100	8764	1306000000	0.00137	0.03554	0			
0.327	0.25	8.631	10.82	14530	447100	5943	1217000000	0.00095	0.02910	0			
0.386	0.25	7.247	9.62	9886	366400	3911	1134000000	0.00065	0.02386	0			
0.446	0.25	5.998	7.76	6496	296400	2443	1052000000	0.00043	0.01930	0			
0.508	0.25	5.058	6.89	3970	222400	1697	837000000	0.00026	0.01448	0			
0.57	0.25	4.167	6.22	2907	180300	1216	779300000	0.00019	0.01174	0			
0.631	0.25	3.389	5.67	2146	146800	905	726700000	0.00014	0.00956	0			
0.745	0.25	1.968	3.14	1232	99360	664	636300000	0.00008	0.00647	0			
0.798	0.25	1.322	2.9	707	43630	293	319400000	0.00005	0.00283	0			
0.845	0.25	0.796	2.79	567	37890	232	304000000	0.00004	0.00246	0			
0.888	0.25	0.305	2.61	466	33520	193	291200000	0.00003	0.00218	0			
0.924	0.25	-0.228	2.46	395	30280	180	280900000	0.00003	0.00197	0			
0.954	0.25	-0.603	2.38	347	28000	169	273200000	0.00002	0.00182	0			
0.977	0.25	-0.908	2.36	336	27290	164	270800000	0.00002	0.00177	0			
0.992	0.25	-1.109	2.31	316	25880	156	266100000	0.00002	0.00168	0			
1	0.25	-1.22	2.31	316	25890	156	266100000	0.00002	0.00168	0			

----- BLADE MODE SHAPES -----

0.3673	BldFl1Sh(2)	- Flap mode 1, coeff of x^2
-0.8268	BldFl1Sh(3)	, coeff of x^3
3.1869	BldFl1Sh(4)	, coeff of x^4
-1.6505	BldFl1Sh(5)	, coeff of x^5
-0.0769	BldFl1Sh(6)	, coeff of x^6
-3.5768	BldFl2Sh(2)	- Flap mode 2, coeff of x^2
49.7954	BldFl2Sh(3)	, coeff of x^3
-153.8381	BldFl2Sh(4)	, coeff of x^4
169.5225	BldFl2Sh(5)	, coeff of x^5
-60.9030	BldFl2Sh(6)	, coeff of x^6
2.1978	BldEdgSh(2)	- Edge mode 1, coeff of x^2
2.9477	BldEdgSh(3)	, coeff of x^3
-6.9603	BldEdgSh(4)	, coeff of x^4
1.5391	BldEdgSh(5)	, coeff of x^5
1.2757	BldEdgSh(6)	, coeff of x^6

## D.4. FAST Output File - fau\_fxBlade\_QQ1\_3a\_1\_5.out (speed=1.5 m/)

(Portions deleted for brevity)

FAST certification fau\_fxBlade: fx77 with many DOFs with fixed yaw error and steady speed.

Time (s)	Azimuth (deg)	TipDxb1 (m)	TipDyb1 (m)	RootFxb1 (kN)	RootFyb1 (kN)	RootMxb1 (kN·m)	RootMyb1 (kN·m)	Spn1MLxb1 (kN·m)	Spn1MLyb1 (kN·m)
0.002	6.00E-01	1.99E-03	-2.24E-04	8.81E-01	-1.52E-01	1.36E-02	3.83E-01	-1.42E-01	3.46E-01
0.004	1.20E+00	5.63E-03	-6.73E-04	1.07E+00	-2.68E-01	1.04E-01	5.30E-01	-1.20E-01	1.16E-01
0.006	1.80E+00	9.50E-03	-1.13E-03	1.21E+00	-2.76E-01	1.09E-01	6.50E-01	-1.64E-01	1.26E-01
0.008	2.40E+00	1.31E-02	-1.56E-03	1.31E+00	-2.68E-01	1.05E-01	7.52E-01	-2.08E-01	1.16E-01
0.01	3.00E+00	1.65E-02	-1.97E-03	1.40E+00	-3.07E-01	1.33E-01	8.41E-01	-2.19E-01	1.08E-01
0.012	3.60E+00	1.96E-02	-2.34E-03	1.48E+00	-2.84E-01	1.19E-01	9.26E-01	-2.66E-01	1.79E-01
0.014	4.20E+00	2.25E-02	-2.68E-03	1.55E+00	-3.22E-01	1.47E-01	9.98E-01	-2.70E-01	1.56E-01
0.016	4.80E+00	2.51E-02	-2.99E-03	1.62E+00	-3.11E-01	1.41E-01	1.07E+00	-3.05E-01	1.02E+00
0.018	5.40E+00	2.75E-02	-3.28E-03	1.68E+00	-3.36E-01	1.62E-01	1.13E+00	-3.11E-01	1.08E+00
0.02	6.00E+00	2.96E-02	-3.53E-03	1.74E+00	-3.37E-01	1.64E-01	1.19E+00	-3.33E-01	1.14E+00
0.022	6.60E+00	3.16E-02	-3.77E-03	1.79E+00	-3.54E-01	1.78E-01	1.24E+00	-3.41E-01	1.19E+00
0.024	7.20E+00	3.33E-02	-3.98E-03	1.84E+00	-3.60E-01	1.85E-01	1.29E+00	-3.54E-01	1.24E+00
0.026	7.80E+00	3.49E-02	-4.16E-03	1.89E+00	-3.72E-01	1.95E-01	1.34E+00	-3.63E-01	1.28E+00
0.028	8.40E+00	3.63E-02	-4.33E-03	1.92E+00	-3.80E-01	2.03E-01	1.37E+00	-3.71E-01	1.32E+00
0.03	9.00E+00	3.75E-02	-4.48E-03	1.96E+00	-3.87E-01	2.10E-01	1.41E+00	-3.78E-01	1.35E+00



0.032	9.60E+00	3.86E-02	-4.61E-03	1.98E+00	-3.94E-01	2.16E-01	1.43E+00	-3.83E-01	1.38E+00	
0.034	1.02E+01	3.95E-02	-4.72E-03	2.01E+00	-4.01E-01	2.23E-01	1.46E+00	-3.88E-01	1.40E+00	
0.036	1.08E+01	4.03E-02	-4.82E-03	2.03E+00	-4.05E-01	2.27E-01	1.48E+00	-3.92E-01	1.42E+00	
0.038	1.14E+01	4.10E-02	-4.90E-03	2.05E+00	-4.13E-01	2.33E-01	1.50E+00	-3.95E-01	1.45E+00	
0.04	1.20E+01	4.16E-02	-4.97E-03	2.07E+00	-4.15E-01	2.36E-01	1.52E+00	-3.99E-01	1.46E+00	
0.042	1.26E+01	4.21E-02	-5.03E-03	2.08E+00	-4.20E-01	2.41E-01	1.53E+00	-4.00E-01	1.47E+00	
0.044	1.32E+01	4.25E-02	-5.08E-03	2.10E+00	-4.24E-01	2.43E-01	1.54E+00	-4.02E-01	1.49E+00	
0.046	1.38E+01	4.28E-02	-5.12E-03	2.10E+00	-4.27E-01	2.46E-01	1.55E+00	-4.03E-01	1.49E+00	
0.048	1.44E+01	4.31E-02	-5.15E-03	2.12E+00	-4.31E-01	2.49E-01	1.56E+00	-4.05E-01	1.51E+00	
0.05	1.50E+01	4.33E-02	-5.18E-03	2.12E+00	-4.31E-01	2.50E-01	1.56E+00	-4.05E-01	1.51E+00	
0.052	1.56E+01	4.35E-02	-5.20E-03	2.12E+00	-4.32E-01	2.51E-01	1.57E+00	-4.05E-01	1.51E+00	
0.054	1.62E+01	4.36E-02	-5.21E-03	2.12E+00	-4.31E-01	2.52E-01	1.57E+00	-4.06E-01	1.51E+00	
0.056	1.68E+01	4.37E-02	-5.23E-03	2.13E+00	-4.37E-01	2.54E-01	1.57E+00	-4.06E-01	1.52E+00	
0.058	1.74E+01	4.38E-02	-5.24E-03	2.13E+00	-4.37E-01	2.54E-01	1.58E+00	-4.07E-01	1.52E+00	
0.06	1.80E+01	4.39E-02	-5.25E-03	2.13E+00	-4.39E-01	2.56E-01	1.58E+00	-4.06E-01	1.53E+00	
0.062	1.86E+01	4.39E-02	-5.25E-03	2.14E+00	-4.40E-01	2.56E-01	1.58E+00	-4.07E-01	1.53E+00	
0.064	1.92E+01	4.40E-02	-5.26E-03	2.13E+00	-4.38E-01	2.56E-01	1.58E+00	-4.07E-01	1.53E+00	
0.066	1.98E+01	4.40E-02	-5.26E-03	2.13E+00	-4.37E-01	2.56E-01	1.58E+00	-4.06E-01	1.53E+00	
0.068	2.04E+01	4.41E-02	-5.27E-03	2.13E+00	-4.40E-01	2.57E-01	1.58E+00	-4.07E-01	1.53E+00	
0.07	2.10E+01	4.41E-02	-5.27E-03	2.14E+00	-4.40E-01	2.57E-01	1.58E+00	-4.07E-01	1.53E+00	
0.072	2.16E+01	4.41E-02	-5.27E-03	2.14E+00	-4.41E-01	2.58E-01	1.58E+00	-4.07E-01	1.53E+00	
0.074	2.22E+01	4.41E-02	-5.27E-03	2.14E+00	-4.41E-01	2.57E-01	1.59E+00	-4.07E-01	1.53E+00	
0.076	2.28E+01	4.41E-02	-5.28E-03	2.13E+00	-4.40E-01	2.58E-01	1.58E+00	-4.07E-01	1.53E+00	
0.078	2.34E+01	4.41E-02	-5.28E-03	2.14E+00	-4.42E-01	2.58E-01	1.59E+00	-4.07E-01	1.53E+00	
0.08	2.40E+01	4.41E-02	-5.28E-03	2.14E+00	-4.41E-01	2.58E-01	1.58E+00	-4.07E-01	1.53E+00	
0.082	2.46E+01	4.41E-02	-5.28E-03	2.14E+00	-4.42E-01	2.58E-01	1.59E+00	-4.07E-01	1.53E+00	
0.084	2.52E+01	4.41E-02	-5.28E-03	2.14E+00	-4.43E-01	2.59E-01	1.59E+00	-4.07E-01	1.53E+00	
0.086	2.58E+01	4.41E-02	-5.28E-03	2.14E+00	-4.42E-01	2.58E-01	1.59E+00	-4.07E-01	1.53E+00	
0.088	2.64E+01	4.41E-02	-5.28E-03	2.13E+00	-4.42E-01	2.58E-01	1.58E+00	-4.06E-01	1.53E+00	
0.09	2.70E+01	4.41E-02	-5.28E-03	2.14E+00	-4.43E-01	2.59E-01	1.59E+00	-4.07E-01	1.53E+00	
0.092	2.76E+01	4.41E-02	-5.28E-03	2.14E+00	-4.44E-01	2.59E-01	1.59E+00	-4.07E-01	1.53E+00	
0.094	2.82E+01	4.41E-02	-5.27E-03	2.14E+00	-4.45E-01	2.59E-01	1.59E+00	-4.06E-01	1.53E+00	
0.096	2.88E+01	4.41E-02	-5.27E-03	2.14E+00	-4.43E-01	2.59E-01	1.58E+00	-4.06E-01	1.53E+00	
0.098	2.94E+01	4.41E-02	-5.27E-03	2.14E+00	-4.43E-01	2.59E-01	1.58E+00	-4.06E-01	1.53E+00	
0.1	3.00E+01	4.41E-02	-5.27E-03	2.14E+00	-4.44E-01	2.59E-01	1.59E+00	-4.06E-01	1.53E+00	
0.102	3.06E+01	4.41E-02	-5.27E-03	2.13E+00	-4.43E-01	2.59E-01	1.58E+00	-4.05E-01	1.53E+00	
0.104	3.12E+01	4.41E-02	-5.27E-03	2.14E+00	-4.43E-01	2.58E-01	1.58E+00	-4.06E-01	1.53E+00	
0.106	3.18E+01	4.41E-02	-5.27E-03	2.14E+00	-4.46E-01	2.60E-01	1.58E+00	-4.05E-01	1.53E+00	
0.108	3.24E+01	4.41E-02	-5.27E-03	2.14E+00	-4.44E-01	2.58E-01	1.58E+00	-4.06E-01	1.53E+00	
0.11	3.30E+01	4.41E-02	-5.27E-03	2.14E+00	-4.46E-01	2.60E-01	1.58E+00	-4.05E-01	1.53E+00	
0.112	3.36E+01	4.41E-02	-5.27E-03	2.14E+00	-4.44E-01	2.59E-01	1.58E+00	-4.06E-01	1.53E+00	
0.114	3.42E+01	4.41E-02	-5.27E-03	2.13E+00	-4.44E-01	2.59E-01	1.58E+00	-4.05E-01	1.53E+00	
0.116	3.48E+01	4.41E-02	-5.27E-03	2.14E+00	-4.45E-01	2.59E-01	1.58E+00	-4.05E-01	1.53E+00	
0.118	3.54E+01	4.41E-02	-5.27E-03	2.14E+00	-4.46E-01	2.60E-01	1.58E+00	-4.05E-01	1.53E+00	
0.12	3.60E+01	4.41E-02	-5.27E-03	2.14E+00	-4.44E-01	2.59E-01	1.58E+00	-4.06E-01	1.53E+00	
0.122	3.66E+01	4.41E-02	-5.27E-03	2.14E+00	-4.48E-01	2.61E-01	1.59E+00	-4.04E-01	1.53E+00	
0.124	3.72E+01	4.41E-02	-5.27E-03	2.13E+00	-4.44E-01	2.58E-01	1.58E+00	-4.06E-01	1.53E+00	
0.126	3.78E+01	4.41E-02	-5.27E-03	2.14E+00	-4.47E-01	2.61E-01	1.58E+00	-4.04E-01	1.53E+00	
0.128	3.84E+01	4.41E-02	-5.27E-03	2.14E+00	-4.47E-01	2.59E-01	1.59E+00	-4.06E-01	1.53E+00	
0.13	3.90E+01	4.41E-02	-5.27E-03	2.14E+00	-4.47E-01	2.60E-01	1.58E+00	-4.04E-01	1.53E+00	
0.132	3.96E+01	4.41E-02	-5.27E-03	2.13E+00	-4.43E-01	2.59E-01	1.58E+00	-4.05E-01	1.53E+00	
0.134	4.02E+01	4.41E-02	-5.27E-03	2.14E+00	-4.47E-01	2.60E-01	1.59E+00	-4.05E-01	1.53E+00	
0.136	4.08E+01	4.41E-02	-5.27E-03	2.14E+00	-4.48E-01	2.60E-01	1.58E+00	-4.04E-01	1.53E+00	
0.138	4.14E+01	4.41E-02	-5.28E-03	2.13E+00	-4.46E-01	2.59E-01	1.58E+00	-4.05E-01	1.53E+00	
0.14	4.20E+01	4.41E-02	-5.28E-03	2.13E+00	-4.46E-01	2.60E-01	1.58E+00	-4.05E-01	1.53E+00	
0.142	4.26E+01	4.41E-02	-5.28E-03	2.14E+00	-4.48E-01	2.61E-01	1.59E+00	-4.05E-01	1.53E+00	
0.144	4.32E+01	4.41E-02	-5.28E-03	2.13E+00	-4.45E-01	2.60E-01	1.58E+00	-4.05E-01	1.53E+00	
0.146	4.38E+01	4.41E-02	-5.28E-03	2.14E+00	-4.48E-01	2.60E-01	1.58E+00	-4.04E-01	1.53E+00	
0.148	4.44E+01	4.41E-02	-5.28E-03	2.13E+00	-4.48E-01	2.60E-01	1.58E+00	-4.04E-01	1.53E+00	
0.15	4.50E+01	4.41E-02	-5.27E-03	2.14E+00	-4.49E-01	2.61E-01	1.59E+00	-4.04E-01	1.53E+00	
0.152	4.56E+01	4.41E-02	-5.27E-03	2.14E+00	-4.48E-01	2.61E-01	1.58E+00	-4.04E-01	1.53E+00	
0.154	4.62E+01	4.41E-02	-5.27E-03	2.13E+00	-4.46E-01	2.60E-01	1.58E+00	-4.04E-01	1.53E+00	
0.156	4.68E+01	4.41E-02	-5.27E-03	2.14E+00	-4.49E-01	2.61E-01	1.58E+00	-4.03E-01	1.53E+00	
0.158	4.74E+01	4.41E-02	-5.27E-03	2.14E+00	-4.48E-01	2.60E-01	1.58E+00	-4.05E-01	1.53E+00	
0.16	4.80E+01	4.41E-02	-5.27E-03	2.13E+00	-4.49E-01	2.61E-01	1.58E+00	-4.03E-01	1.53E+00	
0.162	4.86E+01	4.41E-02	-5.27E-03	2.14E+00	-4.49E-01	2.60E-01	1.59E+00	-4.05E-01	1.53E+00	
0.164	4.92E+01	4.41E-02	-5.27E-03	2.14E+00	-4.51E-01	2.62E-01	1.59E+00	-4.03E-01	1.53E+00	
0.166	4.98E+01	4.41E-02	-5.27E-03	2.14E+00	-4.49E-01		2.61E-01	1.58E+00	-4.04E-01	1.53E+00



0.304	9.12E+01	4.41E-02	-5.27E-03	2.14E+00	-4.55E-01	2.63E-01	1.59E+00	-4.03E-01	1.53E+00
0.306	9.18E+01	4.41E-02	-5.27E-03	2.14E+00	-4.57E-01	2.64E-01	1.59E+00	-4.02E-01	1.53E+00
0.308	9.24E+01	4.41E-02	-5.27E-03	2.14E+00	-4.55E-01	2.63E-01	1.59E+00	-4.03E-01	1.53E+00
0.31	9.30E+01	4.41E-02	-5.27E-03	2.14E+00	-4.56E-01	2.63E-01	1.58E+00	-4.01E-01	1.53E+00
0.312	9.36E+01	4.41E-02	-5.27E-03	2.13E+00	-4.53E-01	2.63E-01	1.58E+00	-4.02E-01	1.53E+00
0.314	9.42E+01	4.41E-02	-5.27E-03	2.14E+00	-4.55E-01	2.63E-01	1.58E+00	-4.02E-01	1.53E+00
0.316	9.48E+01	4.41E-02	-5.28E-03	2.14E+00	-4.55E-01	2.63E-01	1.59E+00	-4.02E-01	1.53E+00
0.318	9.54E+01	4.41E-02	-5.28E-03	2.14E+00	-4.56E-01	2.64E-01	1.59E+00	-4.02E-01	1.53E+00
0.32	9.60E+01	4.41E-02	-5.28E-03	2.13E+00	-4.53E-01	2.62E-01	1.58E+00	-4.02E-01	1.53E+00
0.322	9.66E+01	4.41E-02	-5.28E-03	2.14E+00	-4.54E-01	2.63E-01	1.58E+00	-4.02E-01	1.53E+00
0.324	9.72E+01	4.41E-02	-5.28E-03	2.14E+00	-4.56E-01	2.64E-01	1.59E+00	-4.02E-01	1.53E+00
0.326	9.78E+01	4.41E-02	-5.28E-03	2.13E+00	-4.53E-01	2.63E-01	1.58E+00	-4.02E-01	1.53E+00
0.328	9.84E+01	4.41E-02	-5.28E-03	2.14E+00	-4.55E-01	2.63E-01	1.58E+00	-4.02E-01	1.53E+00
0.33	9.90E+01	4.41E-02	-5.28E-03	2.14E+00	-4.56E-01	2.63E-01	1.59E+00	-4.02E-01	1.53E+00
0.332	9.96E+01	4.41E-02	-5.28E-03	2.14E+00	-4.55E-01	2.63E-01	1.59E+00	-4.02E-01	1.53E+00
0.334	1.00E+02	4.41E-02	-5.28E-03	2.14E+00	-4.55E-01	2.63E-01	1.59E+00	-4.02E-01	1.53E+00
0.336	1.01E+02	4.41E-02	-5.28E-03	2.14E+00	-4.55E-01	2.63E-01	1.59E+00	-4.02E-01	1.53E+00
0.338	1.01E+02	4.41E-02	-5.27E-03	2.13E+00	-4.54E-01	2.63E-01	1.58E+00	-4.01E-01	1.53E+00
0.34	1.02E+02	4.41E-02	-5.27E-03	2.14E+00	-4.54E-01	2.62E-01	1.58E+00	-4.03E-01	1.53E+00
0.342	1.03E+02	4.41E-02	-5.27E-03	2.13E+00	-4.55E-01	2.63E-01	1.58E+00	-4.01E-01	1.53E+00
0.344	1.03E+02	4.41E-02	-5.27E-03	2.13E+00	-4.51E-01	2.61E-01	1.58E+00	-4.03E-01	1.53E+00
0.346	1.04E+02	4.41E-02	-5.27E-03	2.13E+00	-4.53E-01	2.63E-01	1.58E+00	-4.01E-01	1.53E+00
0.348	1.04E+02	4.41E-02	-5.27E-03	2.14E+00	-4.53E-01	2.63E-01	1.58E+00	-4.02E-01	1.53E+00
0.35	1.05E+02	4.41E-02	-5.27E-03	2.13E+00	-4.53E-01	2.62E-01	1.58E+00	-4.02E-01	1.53E+00
0.352	1.06E+02	4.41E-02	-5.27E-03	2.13E+00	-4.54E-01	2.63E-01	1.58E+00	-4.02E-01	1.53E+00
0.354	1.06E+02	4.41E-02	-5.27E-03	2.14E+00	-4.55E-01	2.63E-01	1.58E+00	-4.02E-01	1.53E+00
0.356	1.07E+02	4.41E-02	-5.27E-03	2.14E+00	-4.54E-01	2.63E-01	1.59E+00	-4.03E-01	1.53E+00
0.358	1.07E+02	4.41E-02	-5.27E-03	2.13E+00	-4.53E-01	2.63E-01	1.58E+00	-4.02E-01	1.53E+00
0.36	1.08E+02	4.41E-02	-5.27E-03	2.13E+00	-4.52E-01	2.62E-01	1.58E+00	-4.03E-01	1.53E+00
0.362	1.09E+02	4.41E-02	-5.27E-03	2.13E+00	-4.53E-01	2.63E-01	1.58E+00	-4.02E-01	1.53E+00
0.364	1.09E+02	4.41E-02	-5.27E-03	2.14E+00	-4.53E-01	2.62E-01	1.58E+00	-4.02E-01	1.53E+00
0.366	1.10E+02	4.41E-02	-5.27E-03	2.13E+00	-4.52E-01	2.62E-01	1.58E+00	-4.02E-01	1.53E+00
0.368	1.10E+02	4.41E-02	-5.27E-03	2.14E+00	-4.56E-01	2.63E-01	1.58E+00	-4.01E-01	1.53E+00

(Portions deleted for brevity)

## E. NuMAD Files

### E.1. NuMAD Hydrofoil Input Files - fx77\_02349\_01\_xy

<reference>ref. fx\_77, </reference>

<coords>

1.000000 0.0000  
0.997987 -0.004898  
0.991965 -0.004787  
0.981981 -0.004820  
0.968117 -0.005200  
0.950484 -0.006015  
0.929224 -0.007350  
0.904508 -0.009344  
0.876536 -0.012049  
0.845531 -0.015566  
0.811745 -0.020058  
0.775449 -0.025486  
0.736934 -0.031868  
0.696513 -0.039280  
0.654508 -0.047602  
0.611260 -0.056139  
0.567117 -0.063046  
0.522432 -0.068014  
0.477568 -0.070953  
0.432883 -0.072598  
0.388740 -0.073210

0.345491 -0.072705  
0.303487 -0.071205  
0.263066 -0.069004  
0.224552 -0.066143  
0.188255 -0.062381  
0.154469 -0.058059  
0.123464 -0.053444  
0.095492 -0.047989  
0.070776 -0.042003  
0.049516 -0.036072  
0.031883 -0.029562  
0.018019 -0.022478  
0.008035 -0.015299  
0.002013 -0.006934  
0.000000 0.000000  
0.002013 0.020833  
0.008035 0.035972  
0.018019 0.051300  
0.031883 0.067540  
0.049516 0.083550  
0.070776 0.099524  
0.095492 0.115203  
0.123464 0.129362  
0.154469 0.141606  
0.188255 0.152101  
0.224552 0.160033  
0.263066 0.164681  
0.303487 0.165898  
0.345491 0.163158  
0.388740 0.156034  
0.432883 0.145918  
0.477568 0.134809  
0.522432 0.123089  
0.567117 0.111113  
0.611260 0.099577  
0.654508 0.088171  
0.696513 0.076993  
0.736934 0.066416  
0.775449 0.056577  
0.811745 0.047504  
0.845531 0.039299  
0.876536 0.032069  
0.904508 0.025652  
0.929224 0.020136  
0.950484 0.015515  
0.968117 0.011799  
0.981981 0.008892  
0.991965 0.006825  
0.997987 0.005452  
</coords>

## E.2. NuMAD Hydrofoil Input Files - fx77\_01442\_15\_xy

<reference>ref. fx\_77, </reference>  
<coords>  
1.000000 0.000000  
0.997987 -0.001046  
0.991965 -0.002054  
0.981981 -0.003413  
0.968117 -0.005274  
0.950484 -0.007390  
0.929224 -0.009440  
0.904508 -0.011264  
0.876536 -0.012940  
0.845531 -0.014520  
0.811745 -0.016023  
0.775449 -0.017381  
0.736934 -0.018726

0.696513 -0.019990  
0.654508 -0.021096  
0.611260 -0.022170  
0.567117 -0.023208  
0.522432 -0.024113  
0.477568 -0.024987  
0.432883 -0.025852  
0.388740 -0.026462  
0.345491 -0.026922  
0.303487 -0.027467  
0.263066 -0.027622  
0.224552 -0.027572  
0.188255 -0.027477  
0.154469 -0.026999  
0.123464 -0.026188  
0.095492 -0.025151  
0.070776 -0.023797  
0.049516 -0.021861  
0.031883 -0.019518  
0.018019 -0.016965  
0.008035 -0.012893  
0.002013 -0.006684  
0.000000 0.000000  
0.002013 0.007113  
0.008035 0.017200  
0.018019 0.029050  
0.031883 0.041700  
0.049516 0.054655  
0.070776 0.067617  
0.095492 0.079697  
0.123464 0.090760  
0.154469 0.100275  
0.188255 0.107653  
0.224552 0.112868  
0.263066 0.115979  
0.303487 0.116420  
0.345491 0.112918  
0.388740 0.107141  
0.432883 0.099796  
0.477568 0.091671  
0.522432 0.083222  
0.567117 0.074694  
0.611260 0.066253  
0.654508 0.058075  
0.696513 0.050388  
0.736934 0.043102  
0.775449 0.036368  
0.811745 0.030245  
0.845531 0.024655  
0.876536 0.019609  
0.904508 0.015019  
0.929224 0.010768  
0.950484 0.007183  
0.968117 0.004342  
0.981981 0.002445  
0.991965 0.001390  
0.997987 0.000834  
</coords>

### E.3. NuMAD Materials Files – MatDBsi.TXT

```
<material>  
  <type>orthotropic</type>  
  <name>QQ1_VU90079</name>  
  <reference></reference>  
  <ex>1.380e+010</ex>
```

```

<ey>1.180e+010</ey>
<ez>1.180e+010</ez>
<gxy>5.000e+009</gxy>
<gyz>5.000e+009</gyz>
<gxz>5.000e+009</gxz>
<prxy>0.25</prxy>
<pryz>0.25</pryz>
<prxz>0.25</prxz>
<dens>1626.00</dens>
</material>
<material>
  <type>orthotropic</type>
  <name>QQ1_U14EU920</name>
  <reference></reference>
  <ex>3.840e+010</ex>
  <ey>1.200e+010</ey>
  <ez>1.200e+010</ez>
  <gxy>5.000e+009</gxy>
  <gyz>5.000e+009</gyz>
  <gxz>5.000e+009</gxz>
  <prxy>0.25</prxy>
  <pryz>0.25</pryz>
  <prxz>0.25</prxz>
  <dens>1690.00</dens>
</material>
<material>
  <type>orthotropic</type>
  <name>QQ1_VU90079_35</name>
  <reference></reference>
  <ex>4.830e+011</ex>
  <ey>1.180e+011</ey>
  <ez>1.180e+011</ez>
  <gxy>5.000e+010</gxy>
  <gyz>5.000e+010</gyz>
  <gxz>5.000e+010</gxz>
  <prxy>0.25</prxy>
  <pryz>0.25</pryz>
  <prxz>0.25</prxz>
  <dens>5.691e+004</dens>
</material>
<material>
  <type>orthotropic</type>
  <name>QQ1_U14EU920_35</name>
  <reference>QQ1_U14EU920_35= QQ1_U14EU920 x 35</reference>
  <ex>1.344e+012</ex>
  <ey>4.200e+011</ey>
  <ez>4.200e+011</ez>
  <gxy>1.750e+011</gxy>
  <gyz>1.750e+011</gyz>
  <gxz>1.750e+011</gxz>
  <prxy>0.25</prxy>
  <pryz>0.25</pryz>
  <prxz>0.25</prxz>
  <dens>5.915e+004</dens>
</material>
<material>
  <type>orthotropic</type>
  <name>QQ1_VU90079_20</name>
  <reference></reference>
  <ex>2.760e+011</ex>
  <ey>2.360e+011</ey>
  <ez>2.360e+011</ez>
  <gxy>1.000e+011</gxy>
  <gyz>1.000e+011</gyz>
  <gxz>1.000e+011</gxz>
  <prxy>0.25</prxy>
  <pryz>0.25</pryz>
  <prxz>0.25</prxz>

```

```

    <dens>3.252e+004</dens>
  </material>
  <material>
    <type>orthotropic</type>
    <name>QQ1_U14EU920_20</name>
    <reference></reference>
    <ex>7.680e+011</ex>
    <ey>2.400e+011</ey>
    <ez>2.400e+011</ez>
    <gxy>1.000e+011</gxy>
    <gyz>1.000e+011</gyz>
    <gxz>1.000e+011</gxz>
    <prxy>0.25</prxy>
    <pryz>0.25</pryz>
    <prxz>0.25</prxz>
    <dens>3.380e+004</dens>
  </material>
  <material>
    <type>orthotropic</type>
    <name>QQ1_VU90079_10</name>
    <reference>QQ1_VU90079_1/10</reference>
    <ex>1.380e+011</ex>
    <ey>1.180e+011</ey>
    <ez>1.180e+011</ez>
    <gxy>5.000e+010</gxy>
    <gyz>5.000e+010</gyz>
    <gxz>5.000e+010</gxz>
    <prxy>0.25</prxy>
    <pryz>0.25</pryz>
    <prxz>0.25</prxz>
    <dens>1.626e+004</dens>
  </material>
  <material>
    <type>orthotropic</type>
    <name>QQ1_U14EU920_10</name>
    <reference></reference>
    <ex>3.840e+011</ex>
    <ey>1.200e+011</ey>
    <ez>1.200e+011</ez>
    <gxy>5.000e+010</gxy>
    <gyz>5.000e+010</gyz>
    <gxz>5.000e+010</gxz>
    <prxy>0.27</prxy>
    <pryz>0.27</pryz>
    <prxz>0.27</prxz>
    <dens>1.690e+004</dens>
  </material>
  <material>
    <type>composite</type>
    <name>QQ1_1</name>
    <reference></reference>
    <thicknessType>Constant</thicknessType>
    <uniqueLayers>3</uniqueLayers>
    <symmetryType>odd</symmetryType>
    <layer>
      <layerName>QQ1_VU90079</layerName>
      <thicknessA>0.000511</thicknessA>
      <thicknessB>0.000511</thicknessB>
      <theta>45</theta>
    </layer>
    <layer>
      <layerName>QQ1_VU90079</layerName>
      <thicknessA>0.000511</thicknessA>
      <thicknessB>0.000511</thicknessB>
      <theta>-45</theta>
    </layer>
    <layer>
      <layerName>QQ1_U14EU920</layerName>

```

```

    <thicknessA>0.00205</thicknessA>
    <thicknessB>0.00205</thicknessB>
    <theta>0</theta>
  </layer>
</material>
<material>
  <type>composite</type>
  <name>QQ1_1_10</name>
  <reference></reference>
  <thicknessType>Constant</thicknessType>
  <uniqueLayers>3</uniqueLayers>
  <symmetryType>odd</symmetryType>
  <layer>
    <layerName>QQ1_VU90079_10</layerName>
    <thicknessA>0.0000511</thicknessA>
    <thicknessB>0.0000511</thicknessB>
    <theta>45</theta>
  </layer>
  <layer>
    <layerName>QQ1_VU90079_10</layerName>
    <thicknessA>0.0000511</thicknessA>
    <thicknessB>0.0000511</thicknessB>
    <theta>-45</theta>
  </layer>
  <layer>
    <layerName>QQ1_U14EU920_10</layerName>
    <thicknessA>0.000205</thicknessA>
    <thicknessB>0.000205</thicknessB>
    <theta>0</theta>
  </layer>
</material>
<material>
  <type>composite</type>
  <name>QQ1_2</name>
  <reference></reference>
  <thicknessType>Constant</thicknessType>
  <uniqueLayers>5</uniqueLayers>
  <symmetryType>even</symmetryType>
  <layer>
    <layerName>QQ1_VU90079</layerName>
    <thicknessA>0.000511</thicknessA>
    <thicknessB>0.000511</thicknessB>
    <theta>45</theta>
  </layer>
  <layer>
    <layerName>QQ1_VU90079</layerName>
    <thicknessA>0.000511</thicknessA>
    <thicknessB>0.000511</thicknessB>
    <theta>-45</theta>
  </layer>
  <layer>
    <layerName>QQ1_U14EU920</layerName>
    <thicknessA>0.00205</thicknessA>
    <thicknessB>0.00205</thicknessB>
    <theta>0</theta>
  </layer>
  <layer>
    <layerName>QQ1_VU90079</layerName>
    <thicknessA>0.000511</thicknessA>
    <thicknessB>0.000511</thicknessB>
    <theta>-45</theta>
  </layer>
  <layer>
    <layerName>QQ1_VU90079</layerName>
    <thicknessA>0.000511</thicknessA>
    <thicknessB>0.000511</thicknessB>
    <theta>45</theta>
  </layer>

```



```

</material>
<material>
  <type>composite</type>
  <name>QQ1_2_20</name>
  <reference></reference>
  <thicknessType>Constant</thicknessType>
  <uniqueLayers>5</uniqueLayers>
  <symmetryType>even</symmetryType>
  <layer>
    <layerName>QQ1_U90079_20</layerName>
    <thicknessA>0.0000256</thicknessA>
    <thicknessB>0.0000256</thicknessB>
    <theta>45</theta>
  </layer>
  <layer>
    <layerName>QQ1_U90079_20</layerName>
    <thicknessA>0.0000256</thicknessA>
    <thicknessB>0.0000256</thicknessB>
    <theta>-45</theta>
  </layer>
  <layer>
    <layerName>QQ1_U14EU920_20</layerName>
    <thicknessA>0.0001025</thicknessA>
    <thicknessB>0.0001025</thicknessB>
    <theta>0</theta>
  </layer>
  <layer>
    <layerName>QQ1_U90079_20</layerName>
    <thicknessA>0.0000256</thicknessA>
    <thicknessB>0.0000256</thicknessB>
    <theta>-45</theta>
  </layer>
  <layer>
    <layerName>QQ1_U90079_20</layerName>
    <thicknessA>0.0000256</thicknessA>
    <thicknessB>0.0000256</thicknessB>
    <theta>45</theta>
  </layer>
</material>
<material>
  <type>composite</type>
  <name>QQ1_3</name>
  <reference></reference>
  <thicknessType>Constant</thicknessType>
  <uniqueLayers>8</uniqueLayers>
  <symmetryType>odd</symmetryType>
  <layer>
    <layerName>QQ1_VU90079</layerName>
    <thicknessA>0.000511</thicknessA>
    <thicknessB>0.000511</thicknessB>
    <theta>45</theta>
  </layer>
  <layer>
    <layerName>QQ1_VU90079</layerName>
    <thicknessA>0.000511</thicknessA>
    <thicknessB>0.000511</thicknessB>
    <theta>-45</theta>
  </layer>
  <layer>
    <layerName>QQ1_U14EU920</layerName>
    <thicknessA>0.00205</thicknessA>
    <thicknessB>0.00205</thicknessB>
    <theta>0.0</theta>
  </layer>
  <layer>
    <layerName>QQ1_VU90079</layerName>
    <thicknessA>0.000511</thicknessA>
    <thicknessB>0.000511</thicknessB>
  </layer>

```

```

    <theta>-45</theta>
  </layer>
  <layer>
    <layerName>QQ1_VU90079</layerName>
    <thicknessA>0.000511</thicknessA>
    <thicknessB>0.000511</thicknessB>
    <theta>45</theta>
  </layer>
  <layer>
    <layerName>QQ1_VU90079</layerName>
    <thicknessA>0.000511</thicknessA>
    <thicknessB>0.000511</thicknessB>
    <theta>45</theta>
  </layer>
  <layer>
    <layerName>QQ1_VU90079</layerName>
    <thicknessA>0.000511</thicknessA>
    <thicknessB>0.000511</thicknessB>
    <theta>-45</theta>
  </layer>
  <layer>
    <layerName>QQ1_U14EU920</layerName>
    <thicknessA>0.00205</thicknessA>
    <thicknessB>0.00205</thicknessB>
    <theta>0</theta>
  </layer>
</material>
<material>
  <type>composite</type>
  <name>QQ1_35</name>
  <reference></reference>
  <thicknessType>Constant</thicknessType>
  <uniqueLayers>8</uniqueLayers>
  <symmetryType>odd</symmetryType>
  <layer>
    <layerName>QQ1_VU90079_35</layerName>
    <thicknessA>0.0000146</thicknessA>
    <thicknessB>0.0000146</thicknessB>
    <theta>45</theta>
  </layer>
  <layer>
    <layerName>QQ1_VU90079_35</layerName>
    <thicknessA>0.0000146</thicknessA>
    <thicknessB>0.0000146</thicknessB>
    <theta>-45</theta>
  </layer>
  <layer>
    <layerName>QQ1_U14EU920_35</layerName>
    <thicknessA>0.0000584</thicknessA>
    <thicknessB>0.0000584</thicknessB>
    <theta>0.0</theta>
  </layer>
  <layer>
    <layerName>QQ1_VU90079_35</layerName>
    <thicknessA>0.0000146</thicknessA>
    <thicknessB>0.0000146</thicknessB>
    <theta>-45</theta>
  </layer>
  <layer>
    <layerName>QQ1_VU90079_35</layerName>
    <thicknessA>0.0000146</thicknessA>
    <thicknessB>0.0000146</thicknessB>
    <theta>45</theta>
  </layer>
  <layer>
    <layerName>QQ1_VU90079_35</layerName>
    <thicknessA>0.0000146</thicknessA>
    <thicknessB>0.0000146</thicknessB>

```

```

    <theta>45</theta>
  </layer>
</layer>
<layer>
  <layerName>QQ1_VU90079_35</layerName>
  <thicknessA>0.0000146</thicknessA>
  <thicknessB>0.0000146</thicknessB>
  <theta>-45</theta>
</layer>
<layer>
  <layerName>QQ1_U14EU920_35</layerName>
  <thicknessA>0.0000584</thicknessA>
  <thicknessB>0.0000584</thicknessB>
  <theta>0.0</theta>
</layer>
</material>

```

## E.4. NuMAD Output Blade Properties Files – BPE2FAST.dat

```

----- FAST INDIVIDUAL BLADE FILE -----
FAST blade file generated by BPE from NuMAD project:
C:/FAU/NREL/NuMAD/PhD_QQ1_1a_Ansys/fau_fxBlade_QQ1_3a_ansys on 06/11/2013
----- BLADE PARAMETERS -----

```

```

27  NBlInpSt  - Number of blade input stations (-)
FALSE  CalcBMode  - Calculate blade mode shapes internally {T: ignore mode shapes from below, F: use mode
shapes from below} [CURRENTLY IGNORED] (flag)
3.0  BldFlDmp1  - Blade flap mode #1 structural damping in percent of critical (%)
3.0  BldFlDmp2  - Blade flap mode #2 structural damping in percent of critical (%)
5.0  BldEdDmp1  - Blade edge mode #1 structural damping in percent of critical (%)

```

```

----- BLADE ADJUSTMENT FACTORS -----
1  F1StTunr1  - Blade flapwise modal stiffness tuner, 1st mode (-)
1  F1StTunr2  - Blade flapwise modal stiffness tuner, 2nd mode (-)
1  AdjBlMs  - Factor to adjust blade mass density (-)
1  AdjFlSt  - Factor to adjust blade flap stiffness (-)
1  AdjEdSt  - Factor to adjust blade edge stiffness (-)

```

```

----- DISTRIBUTED BLADE PROPERTIES -----
BlFract  AeroCent  StrcTwst  BMassDen  FlpStff  EdgStff  GJStff  EASStff  Alpha
(-)      (-)      (deg)      (kg/m)      (Nm^2)      (Nm^2)      (Nm^2)      (N)      (-)
0         0.25      25.2379   5.66667    141885     1.8325e+6   0  0  0
0.00805802 0.25      26.6262   7          106619     1.28312e+6  0  0  0
0.020145  0.25      28.7085   9          53720     459051      0  0  0
0.0318292 0.25      25.3568   7.89474    49234.8    311928      0  0  0
0.0507655 0.25      23.4021   7.85714    38126.5    243136      0  0  0
0.0769541 0.25      19.1369   5.94595    36234.1    233520      0  0  0
0.109992  0.25      15.3652   5.55556    29376.6    246813      0  0  0
0.149476  0.25      14.7422   5.28302    27170.1    281102      0  0  0
0.194601  0.25      13.1342   4.91525    21306.8    232718      0  0  0
0.244561  0.25      11.0263   4.61538    16537.6    233048      0  0  0
0.29855  0.25      9.41346   4.34783    12133.2    211216      0  0  0
0.355761  0.25      7.91365   4.10959    8584.89    179231      0  0  0
0.415794  0.25      6.62505   3.81579    5511.78    147163      0  0  0
0.477438  0.25      5.74368   2.98701    3330.57    114311      0  0  0
0.539081  0.25      4.72765   2.63158    2292.74    92686.2     0  0  0
0.600322  0.25      3.92154   2.5         1711.72    76567.4     0  0  0
0.660355  0.25      3.24897   2.32877    1270.78    62903.7     0  0  0
0.717566  0.25      2.50213   2.17391    932.496    50375       0  0  0
0.771555  0.25      1.83508   1.53846    691.533    39752.4     0  0  0
0.821515  0.25      1.25153   1.52542    539.204    33348.7     0  0  0
0.86664  0.25      0.72927   1.32075    437.919    29318.2     0  0  0
0.906124  0.25      0.16996   1.33333    365.259    26263.1     0  0  0
0.939162  0.25      -0.228375 1.35135    313.122    23911.1     0  0  0
0.965351  0.25      -1.04977  1.42857    292.359    23183       0  0  0
0.984287  0.25      -0.0725284 1.05263    276.594    21956.3     0  0  0
0.995971  0.25      11.883    1          230.749    3655.31     0  0  0
1         0.25      16.0055   0.981851   214.94     3655.31     0  0  0

```

```

----- BLADE MODE SHAPES -----
0.3159  BldFl1Sh2 - Flap mode 1, coeff of x^2

```

-0.5205 BldF11Sh3 - , coeff of x^3  
2.032 BldF11Sh4 - , coeff of x^4  
0.0447 BldF11Sh5 - , coeff of x^5  
-0.8721 BldF11Sh6 - , coeff of x^6  
-0.6937 BldF12Sh2 - Flap mode 2, coeff of x^2  
23.0531 BldF12Sh3 - , coeff of x^3  
-102.546 BldF12Sh4 - , coeff of x^4  
136.2782 BldF12Sh5 - , coeff of x^5  
-55.0916 BldF12Sh6 - , coeff of x^6  
2.7708 BldEdgSh2 - Edge mode 1, coeff of x^2  
-2.8102 BldEdgSh3 - , coeff of x^3  
3.3825 BldEdgSh4 - , coeff of x^4  
-4.5049 BldEdgSh5 - , coeff of x^5  
2.1619 BldEdgSh6 - , coeff of x^6

## REFERENCES

1. Asseff, N.S. 2009. Design and Finite Element Analysis of Ocean Current Turbine Blade, MS Thesis, Florida Atlantic University.
2. Asseff, N.S. and Mahfuz, H. 2009. Design and Finite Element Analysis of an Ocean Current Turbine Blade. OCEANS '09, October 26-29, 2009, Biloxi, Mississippi, ISBN:978-1-4244-4960-6.
3. Batten, W.M.J. A.S. Bahaj, A.F. Molland, J.R. Chaplin, 2006. Hydrodynamics of marine current turbines. Renewable Energy 31, 2006
4. Baek, S., Cho, S., Joo, W. 2008. Fatigue Life Prediction Based on Rainflow Cycle Counting Method for the End Beam of a Freight Car Bogie. International Journal of Automotive Technology, Vol 9, pp. 95-101.
5. Bir, G.S. 2005. User's Guide to PreComp (Pre-Processor for Computing Composite Blade Properties). NREL/TP-500-38926. Golden, CO: National Renewable Energy Laboratory
6. Bir, G.S. 2005. User's Guide to BModes; Software for Computing Rotating Beam Coupled Modes, NREL TP-500-38976, Golden, Colorado: National Renewable Energy Laboratory. Florida Department of Transportation, Structures Design Guidelines, 2004.

7. Bir, G.S., Lawson, Michael J., and Li, Ye. 2011. Structural Design of a Horizontal-Axis Tidal Current Turbine Composite Blade. ASME 30th International Conference on Ocean, Offshore, and Arctic Engineering Rotterdam, The Netherlands.
8. Buhl, Jr. M.L.; Wright; A.D.; Pierce, K.G. 2001. FAST\_AD Code Verification: A Comparison to ADAMS. The 20th ASME Wind Energ.
9. Burton, Tony. 2001. Wind Energy Handbook. John Wiley & Sons, New York, NY.
10. Buhl, Jr. M.L. 2002. Installing NWTC Design Codes on PCs Running Windows NT®." National Renewable Energy Laboratory, <http://wind.nrel.gov/designcodes/papers/setup.pdf>. Last modified Dec. 22, 2000; NREL/EP-500-29384. Golden, Colorado.
11. Daniel L. Laird, Brian R. Resor. 2009. NuMAD User's Manual. Wind Energy Technology, Sandia National Laboratories.
12. Department of the Interior. 2006. Technology White Paper on Ocean Current Energy Potential on the U.S. Outer Continental Shelf.
13. DOE & MSU. 2010. DOE / MSU Composite Material Fatigue Database. March 31, 2010, Version 19.0.
14. DET NORSKE VERITAS. 2011. Modeling and Analysis OF Marine Operations. Offshore Standard, 2011.
15. F. R. Driscoll, G. M. Alsenas, P. P. Beaujean, Shirley Ravenna, Jason Raveling, Erick Busold, and Caitlin Slezycki, 2008. A 20 KW Open Ocean

- Current Test Turbine", Center for Ocean Energy Technology, Florida Atlantic University.
16. Germanischer Lloyd. 2005. Guideline for the Certification of Ocean Energy Converters Part 1: Ocean Current Turbines. Hamburg, Germany.
  17. Germanischer Lloyd WindEnergie. 2005. Guideline for the Certification of Offshore Wind Turbines. Hamburg, Germany.
  18. Hansen, Craig. 2007. NWTC Design Codes. <http://wind.nrel.gov/designcodes/preprocessors/airfoilprep/> National Renewable Energy Laboratory, Golden, CO.
  19. HyperSizer. 2010. HyperSizer Composite Wind Blade Software. [http://hypersizer.com/download.php?type=pdf&file=HyperSizer\\_for\\_Composite\\_Wind\\_Blade\\_Design\\_-\\_Brochure.pdf](http://hypersizer.com/download.php?type=pdf&file=HyperSizer_for_Composite_Wind_Blade_Design_-_Brochure.pdf).
  20. Jonkman, J.M. 2003. Modeling of the UAE Wind Turbine for Refinement of FAST\_AD. M.S. Thesis, Colorado State University: Department of Mechanical Engineering.
  21. Jonkman, J. and Cotrell, J. 2003. Demonstration of the Ability of RCAS to Model Wind Turbines. National Renewable Energy Laboratory, Golden, CO., NREL/TP-500-34632.
  22. Jonkman, J.M., Buhl Jr., M.L. 2005. FAST User's Guide, NREL/EL-500-29798. Golden, Colorado: National Renewable Energy Laboratory.
  23. Jonkman, J. Butterfield, S., Musial, W., and Scott, G. 2009. Definition of a 5-MW Reference Wind Turbine for Offshore System Development, NREL

Technical Report, NREL/TP- 500-38060.

24. Jonkman, J.M.; Buhl, Jr. M.L. 2004. New Development's for the NWTC's FAST Aeroelastic HAWT Simulator. The 23rd ASME Wind Energy Symposium, Reno, Nevada, January 5–8, 2004. NREL/CP-500-35077. Golden, Colorado: National Renewable Energy Laboratory.
25. Jonkman, J.M., & Buhl Jr., M.L. 2012. TurSim User's Guide, NREL/TP-500-39797. National Renewable Energy Laboratory, Golden, Colorado.
26. James L. Tangler, 2000. The Evolution of Rotor and Blade Design. Presented at the American Wind Energy Association WindPower.
27. Laino, D.J., & Hansen, A.C. 2002. User's Guide to the Wind Turbine Dynamics Computer Software AeroDyn. Salt Lake City, Utah.
28. Laird, Daniel L., & Resor, Brian R. 2009. NuMAD User's Manual. Wind Energy Technology, Sandia National Laboratories.
29. Locke, James & Valencia, Ulyses. 2004. Design Studies for Twist-Coupled Wind Turbine Blades. Sandia National Laboratories, Report SAND2004-0522.
30. Mahfuz, H., & Akram, M.W. 2011. Life Prediction of Composite Turbine Blades under Random Ocean Current and Velocity Shear. In: OCEANS'11 Conference, Santander, Spain.
31. Miner, M.A. 1945. Cumulative Damage in Fatigue. J. Appl. Mech., vol. 12, Trans. ASME, pp. A159-A164.
32. Maniaci, David C., & Li, Ye. 2012. Investigating the Influence of the Added



- Mass Effect to Marine Hydrokinetic Horizontal-Axis Turbines Using a General Dynamic Wake Wind Turbine Code. NREL/JA-5000-54403, National Renewable Energy Laboratory, Golden, Colorado.
33. Manjock, A. 2005. Evaluation Report: Design Codes FAST and ADAMS® for Load Calculations of Onshore Wind Turbines. Report No. 72042. Humburg Germany: Germanischer Lloyd WindEnergie GmbH, May 26, 2005.
34. Moriarty, P.J.& Hansen, A.C. 2005. AeroDyn Theory Manual. National Renewable Energy Laboratory, Golden, Colorado
35. Pierson, Seth Hunter. 2009. Composite Rotor Design for a Hydrokinetic Turbine. University of Tennessee Honors Thesis Projects.
36. Sale, Danny C. 2010. HARP\_Opt User's Guide. [http://wind.nrel.gov/designcodes/simulators/HARP\\_Opt](http://wind.nrel.gov/designcodes/simulators/HARP_Opt). National Renewable Energy Laboratory, Golden, CO.
37. Sutherland, H. J. 1999. On the Fatigue Analysis of Wind Turbines. SAND99-0089, Sandia National Laboratories, June 1999.
38. U.S. Census Bureau. 2005. Interim Projections of the Total Population for the United States: April 1, 2000 to July 1, 2030.
39. VanZwieten Jr., James H., Oster, Carey M., & Duerr, Alana E.S. 2011. Design and Analysis of a Rotor Blade Optimized for Extracting Energy from the Florida Current. In: OMAE2011 Conference. Rotterdam, Netherlands.

40. Michael Borghi, Fumbi Kolawole, Sathya Gangadharan, William Engblom, James VanZwieten, Gabriel Alsenas, William Baxley, and Shirley Ravenna. 2012. IEEE.
41. OceanWorld. 2004. [http://oceanworld.tamu.edu/resources/ocng\\_textbook/chapter09/chapter09\\_01.htm](http://oceanworld.tamu.edu/resources/ocng_textbook/chapter09/chapter09_01.htm). Ocean World, NASA/JPL and the Texas A&M Department of Oceanography.
42. Wilson, R.E., Walker, S.N., & Heh, P. 1999. Technical and User's Manual for the FAST\_AD Advanced Dynamics Code. OSU/NREL Report 99-01. Corvallis, Oregon: Oregon State University, May 1999.
43. Zhou, F., Mahfuz, H., Alsenas, G., & Hanson, H. 2013. Static and Fatigue Analysis of Composite Turbine Blades under Random Ocean Current Loading. Marine Technology Society Journal, Volume 47, Number 2, March/April 2013, pp. 59-69.